Low-valent group 14 metal containing ligands: versatile building blocks for the synthesis of transition metal complexes

Dissertation

Zur Erlangung des Grades
des Doktors der Naturwissenschaften
der Naturwissenschaftlich-Technischen Fakultät III
Chemie, Pharmazie, Bio- und Werkstoffwissenschaften
der Universität des Saarlandes

Von

Antoine Laurent

Saarbrücken

2007

Tag des Kolloqiums:	18.06.2007
Dekan:	Prof. Dr. Kaspar Hegetschweiler
Vorsitzender:	Prof. Dr. Uli Kazmaier
Berichterstatter:	Prof. Dr. Michael Veith
	Prof. Dr. Dr. h.c. Theophil Eicher
Akad. Mitarbeiter:	Dr. Holger Kohlmann

Die vorliegende Arbeit entstand in der Zeit vom November 2002 bis März 2007 in der Anorganischen Chemie der Universität des Saarlandes in Saarbrücken unter Anleitung von Herrn Prof. Dr. Michael Veith.

Ein besonderer Dank gilt meinem verehrten Doktorvater, Herrn Prof. Dr. Michael Veith, für die interessante Themenstellung, die stete Diskussionsbereitschaft und die großzügige Unterstützung während der Durchführung der Arbeit.

Allen Mitgliedern AK Veith sowie allen Angestellten des Instituts für Anorganische Chemie, die auf verschiedenste Weise zum Gelingen dieser Arbeit beigetragen haben, sei an dieser Stelle herzlich gedankt.

Herrn Dr. Markus Ehses bin ich besonders dankbar für die wertvollen Ratschläge, die Diskussionsbereitschaft, sowie für seine Geduld.

Herrn Dr. Volker Huch danke ich für die Durchführung der Röntgenanalysen.

Weiterhin danke ich Herrn Dr. Michael Zimmer für die Aufnahme der NMR-Spektren am 400er.

Frau Helga Feuerhake gilt mein Dank für die Durchführung der Elementaranalysen.

Für die gute Arbeitsatmosphäre bedanke ich mich herzlich bei meinen jetzigen und ehemaligen Kollegen vom Labor 290, hier besonders bei Herrn Dr. Markus Ehses, Herrn Amadou Latyr Ndiaye, Herrn Nicolas Auvray und Frau Anusch Shariatmadari für ihre Freundschaft und ihre Unterstützung in jeglicher Hinsicht.

Aber auch bei Frau Dipl. Ing. Eva Sow, meiner Familie, und meinen Freunden, auch wenn sie wenig mit der eigentlichen chemischen Arbeit zu tun haben, möchte ich mich bedanken, da sie mir den nötigen Rückhalt gegeben haben.

Table of contents

Table of abbreviations

BM	Bohr magneton
COD	1,5-cyclooctadiene
CVD	Chemical Vapour Deposition
El	element
Et	ethyl
et al.	and others (latin: et alii or et alteri)
*i*Pr	*iso*-propyl
IR	infrared
L	ligand
M	metal
Me	methyl
nbd	norbornadiene
Nep	neopentyl
NMR	Nuclear Magnetic Resonance
Ph	phenyl
ppm	10^{-6} parts per million
*t*Bu	tertiary butyl
tert	tertiary
THF / thf	tetrahydrofuran / ~ as ligand
UV-Vis	ultra violet-visible spectroscopy

Table of compounds

Zusammenfassung auf Deutsch

Die vorliegende Arbeit beschäftigt sich mit niederwertigen Metallkomplexen der Gruppe 14, die als Liganden in der Synthese von Übergangsmetallkomplexen benutzt worden sind.

Im ersten Teil wurden Untersuchungen über die Koordinationsweise von Natrium-*bis*[tris(*tert*-butoxy)germanat, -stannat, und -plumbat mit Nickel(II)-Halogeniden durchgeführt. Während die Natriumalkoxygermanate und -plumbate mit den Nickelhalogeniden ausschließlich zu Verbindungen des Typs $Ni_2El_2(OtBu)_8$ (mit El = Ge und Pb) reagieren, gibt es bei den Stannaten die Möglichkeit die Verbindung des Typs $NiSn_2(OtBu)_6$ darzustellen. Eisencarbonyl-Fragmente lassen sich an die endständigen Germanium- und Zinn-Atome anhängen. Die niederwertigen Elemente der Gruppe 14 wirken hierbei als Lewis-Basen gegenüber den nullwertigen Übergangsmetall-Atomen. Es entstehen eindimensionale Anordnungen von Metall-Atomen mit der allgemeinen Formel $[\{(CO)_4Fe\}_2\{Ni_2El_2(OtBu)_8\}]$ (mit El = Ge, Sn), die magnetische Eigenschaften besitzen. Ihre magnetischen Momente wurden nach der Evans Methode gemessen.

Durch Alkoholyse des cyclischen *bis*(amido)stannylens $Sn(NtBu)_2SiMe_2$ konnte das Alkoxystannylen $Sn(OiPr)_2$ dargestellt, spektroskopisch und kristallstrukturanalytisch untersucht werden. Die Verbindung liegt als lineares Polymer $[Sn(\mu\text{-}OiPr)_2]_\infty$ mit verbrückenden O*i*Pr vor. Die strukturelle Integrität dieser Metallalkoxydekette wurde durch die Reaktion mit Dieisennonacarbonyl gestört und eine molekulare Verbindung der Formel $[Sn\{(\mu\text{-}OiPr)_2Sn(OiPr)Fe(CO)_4\}_2]$ selektiv erhalten und vollständig charakterisiert.

Der Gegenstand des zweiten Teils der Arbeit war hauptsächlich die Untersuchung der Verhalten eines nullwertigen Nickel-Komplexes $Ni[Sn(NtBu)_2Si(CH_3)_2]_4$ gegenüber Alkoholen. Die vollständige Eliminierung der Amido-Reste am Stannylen-Liganden konnte nur unter Zersetzung des Komplexes erzielt werden. Wurde das Ausgangmaterial $Ni[Sn(NtBu)_2Si(CH_3)_2]_4$ mit Methanol umgesetzt, führt die Reaktion zu einer nahezu quantitativen und formalen 1,2-Addition des Methanols. Die zwei Stickstoffatome des Stannylens wirken als Lewis-Basen und fangen das Proton des

Methanols ab, während das Methanolat am Zinn koordiniert, das als Lewis-Säure Zentrum fungiert.

Weiterhin wurde das Ausgangmaterial $Ni[Sn(N\mathit{t}Bu)_2Si(CH_3)_2]_4$ mit *iso*-Propanol umgesetzt. In diesem Fall konnte keine Additionsreaktion des Alkohols festgestellt werden. Die Reaktion führt zu einer Oxydation des Ausgangmaterials. Der Komplex konnte in sehr kleiner Menge isoliert und kristallstrukturanalytisch untersucht werden. Die Verbindung weist paramagnetisches Verhalten auf, das spektroskopisch nach Evans Methode quantifiziert wurde.

In Rahmen dieses Studiums über die Reaktivität von verschiedenen Nickel(0)-Komplexen, wurde ein neues Nickeltetracarbonyl-Homologes, $Ni[Ge(N\mathit{t}Bu)_2Si(CH_3)_2]_4$, hergestellt und vollständig charakterisiert. Es konnte weiterhin spektroskopisch gezeigt werden, dass einer der vier Germylen-Liganden durch ein Stannylen $Sn(N\mathit{t}Bu)_2SiMe_2$ ersetzt werden kann.

Abstract

The present work focuses on the synthesis of new transition metal-low-valent group 14 metal complexes.

The first part is devoted to the synthesis of nickel(II) complexes displaying low-valent group 14 metal alkoxides as ligand. While the sodium alkoxigermanate and -plumbate react with nickel(II) chloride to lead to the formation of compounds of the general formula $Ni_2El_2(O\mathit{t}Bu)_8$ (with El = Ge, Pb), the sodium alkoxistannate offers the possibility to form the following complex: $NiSn_2(O\mathit{t}Bu)_6$. These mixed metal alkoxides could have been structurally characterised. They display two low-valent group 14 metallic elements, which can be involved, as Lewis-bases towards zero-valent transition metal complexes, in further coordination reactions. Reacted with nonacarbonyl diiron, these mixed metal alkoxides allow the formation of hetero-trimetallic complexes. The arrangement of the metallic elements in these compounds occurs in a one-dimensional fashion as demonstrated for $[\{(CO)_4Fe\}_2\{Ni_2El_2(O\mathit{t}Bu)_8\}]$ (with El = Ge, Sn). The presence of nickel(II) centres in tetrahedral coordinations provide to the complexes paramagnetic properties, which have been quantified according to the Evans method.

An alcoholysis reaction was performed with *iso*-propanol on the cyclic *bis*(amido)stannylene $Sn(N\mathit{t}Bu)_2SiMe_2$. The obtained compound could have been spectroscopically as well as structurally characterised. It revealed a polymeric arrangement of the general formula $[Sn(\mu\text{-}O\mathit{i}Pr)_2]_\infty$. The reaction with nonacarbonyl diiron destroys the structural integrity of the polymeric tin(II) alkoxide to lead selectively to the formation of a molecular compound: $[Sn\{(\mu\text{-}O\mathit{i}Pr)_2Sn(O\mathit{i}Pr)Fe(CO)_4\}_2]$. This complex could have been fully characterised.

The second part of this work deals mainly with a study of the reactivity of the tetrakis-*bis*(amido)stannylene containing nickel(0) complex $Ni[Sn(N\mathit{t}Bu)_2Si(CH_3)_2]_4$ towards different alcohols. A complete alcoholysis reaction, in which the metallic skeleton of the starting compound is remained intact, under elimination of the amido residues could not have been performed. If methanol is allowed to react with $Ni[Sn(N\mathit{t}Bu)_2Si(CH_3)_2]_4$, a formal 1,2-addition of the methanol takes place. The proton is trapped by one of the two nitrogen atoms of each cyclic stannylene ligand,

while the methanolate fragment acts as a base adduct on the Lewis acid tin centre. The obtained complex $Ni[Sn(OCH_3)(N\textit{t}Bu)\{N(H)\textit{t}Bu\}Si(CH_3)_2]_4$ could have been isolated in good yield and fully characterised. If the starting complex is reacted with *iso*-propanol, no addition occurs but a product resulting from an oxidation of the nickel centre of the following formula $Ni[(Sn(N\textit{t}Bu)_2SiMe)_2\mu\text{-}O\textit{i}Pr]_2$ is isolated in weak yield. According to its crystal structure, the complex exhibits magnetic properties, which were quantified according to the Evans method.

Still within the scope of researches about the reactivity of nickel(0) centred complexes, the synthesis of a new nickel tetracarbonyl-homologue $Ni[Ge(N\textit{t}Bu)_2Si(CH_3)_2]_4$ was performed. Moreover, spectroscopic investigations evidenced that the selective replacement of one germylene ligand by one stannylene $Sn(N\textit{t}Bu)_2Si(CH_3)_2$ unit is feasible.

Chapter 1

Introduction and aim of the work

1.1 Introduction

One of the greatest milestones in the man's technological development could be considered as the discovery, around 3500 BC, that copper, easily smelted but rather soft, could be made harder and stronger by alloying with tin. This augured the advent of the bronze. The earliest mention of tin occurs in the Old Testament, in the Book of Numbers (31:22) and is mentioned as a metal of value under the name of *Bedil*: "Only the gold, and the silver, the brass, the tin and the lead".

Compounds of tin are dated back to the time of the Copts of Egypt, who reportedly used basic tin citrate in dye preparation. Modern tin chemistry appears to start in 1605 with the experiments of Libavius. He described a fuming liquid, which he called *liquor argenti vivi sublimati or spiritus argenti vivi sublimati* prepared by distillation from a mixture of tin or tin amalgam and mercuric chloride. The liquid, obviously tin(IV) chloride, was referred to as *spiritus fumans Libavii*. The first organotin compound, diethyltin diiodide, was prepared by Frankland in 1849: the tin chemistry really began at this date. More than one century later, the progresses in chemistry allowed the isolation and the unambiguous characterisation of the first monomeric bivalent tin compound.[1] The chemistry of monomeric bivalent tin compounds, usually referred to as stannylenes (IUPAC nomenclature *stannanediyls*), are of considerable interest as they can be considered as carbene analogues.[2,3] Similar to the term "carbene" for CR_2 moieties, the MXY entities (where M is a group 14 metal, X and Y are σ-bonded 7 valence electrons groups) will be called "germylenes", "stannylenes", "plumbylenes" and considered as neutral species with the formal oxidation state +2 at the respective main group metal element. With a ground state configuration of ns^2np^2 (where n = 4 for germanium, n = 5 for tin and n = 6 for lead), the metal centre can formally behave as an amphoteric species, since it owns

simultaneously a lone-pair of electron and a vacant orbital. Germylenes, stannylenes or plumbylenes use their p electrons in covalent bonding and the remaining two electrons, constituting the lone-pair, can be used to form an adduct with a Lewis acid and thus, are considered as σ-donors. These metallic centres display also low-lying empty p orbitals, which are of suitable symmetry and orientation for π-bonding. Thus, germylenes, stannylenes or plumbylenes are typically excellent π-acceptors. As shown in figure 1, there are several hybridization geometries for these species.[4]

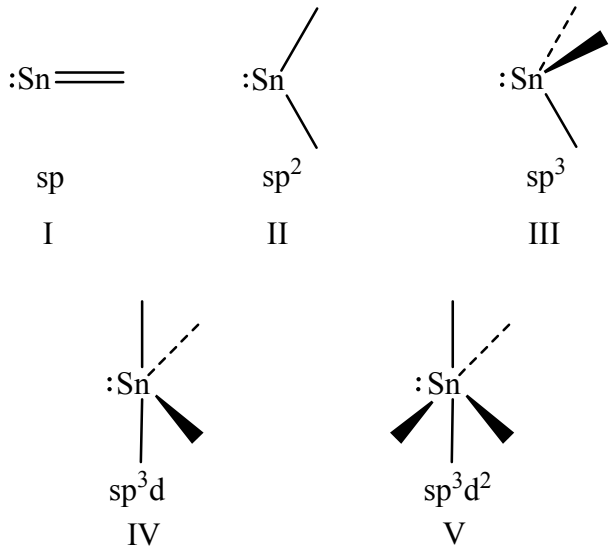

Figure 1: Hybridisation geometry for stannylenes.

Of these, the second, third and fourth are the most important, the first and fifth are very uncommon.[5]

Their uncommon electronic features render the bivalent group 14 metallic elements very interesting in the field of coordination chemistry. It began ostensibly in 1971 with the work of Marks,[6] 7 years after the first report about carbene complexes by Fischer *et. al.*[7] Nevertheless, in 1957, Hieber, the father of the metal carbonyl chemistry, reported an iron-tin complex of the formula $[(t\text{Bu})_2\text{SnFe(CO)}_4]$.[8] The known transition metal complexes displaying a group 14 metallic element in the oxidation state II as ligand can be described as shown in figure 2.

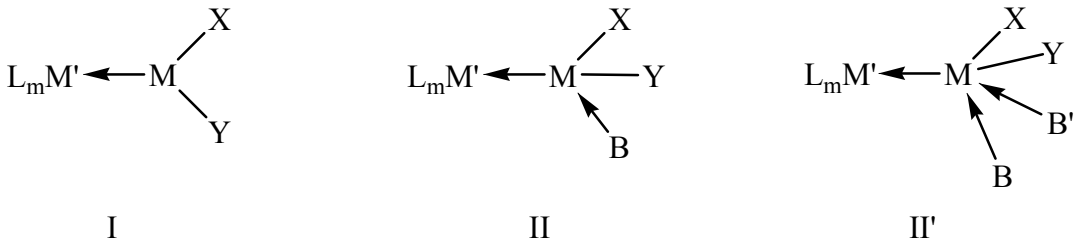

I II II'

Figure 2: Different structures of simple (I) and base-stabilised complexes (II and II') where M stands for a group 14 metal, M' stands for a transition metal, L_m represents a set of ligands and B (and B') stands for a neutral Lewis base molecule such as THF or pyridine.

These different arrangements summarize roughly the main properties of a bivalent group 14 metal ligand: a neutral fragment behaving as a Lewis acid towards base adducts and behaving as a Lewis base through its lone pair towards transition metals. Several synthetic routes have been developed (salt elimination,[9] oxidative addition,[10] oxidative elimination,[11] insertion,[12] transmetallation[13]…), resulting in a very large number of transition metal complexes, in which germylenes, stannylenes or plumbylenes are involved as ligands. Nevertheless, and despite the fact that organometallic chemistry offers a number of reactive sources of nickel, very few complexes containing nickel-group 14 metal bonds are known. An explanation is furnished by Holt *et. al.* as they predict that "nickel-tin chemistry is expected to be characterised primarily by the extreme lability of the attached ligands. As a result, it may be that thermodynamically, the nickel-tin bond is stable, but not kinetically accessible".[14] Indeed, to the best of our knowledge, no zero-valent nickel compound displaying a homoleptic set of low-valent group 14 metal alkoxide ligand is reported in the literature to date. However, heterobimetallic alkoxides are currently widely used: due to their good solubility, high volatility and low decomposition temperatures they provide variable and designable sources of precursors to ceramic materials.[15-18] Moreover, the interesting potential of nickel-tin bimetallic systems has already been demonstrated in the field of heterogeneous catalysis[19-21] or in the materials science, with the use for example of nickel-tin alloys as deposit on anodes in lithium-ion batteries.[22]

1.2 Aim of the work

The present work focuses on the synthesis of new nickel-low-valent group 14 metal complexes.

First, in order to continue the work initiated by Veith *et. al.*,[23] studies concerning the synthesis and reactivity of one-dimensionally and discretely arranged metallic chains displaying nickel(II) atoms and low-valent group 14 metal alkoxides will be reported. The reactivity of these complexes, in particular the ability of the low-valent element situated in the terminal position of the metallic chain to coordinate further metallic fragments will also be explored.

In a second part, investigations on the reactivity of different zero-valent nickel-amido stannylene complexes towards alcohols will be reported. In order to achieve the synthesis of new nickel-alkoxy stannylene complexes, the work will focus on alcoholysis reactions, in which the metallic skeleton of the starting material would remain intact under elimination of the amino substituent.

Chapter 2

State of the art

2.1 Low-valent group 14 metals in ligands for zero-valent nickel complexes

Nickel tetracarbonyl was discovered in 1890 by Mond, Langer and Quincke.[24] The synthesis was achieved by the reaction of carbon monoxide with nickel powder at atmospheric pressure and temperatures below 100 °C. It is the first example of a transition metal complex with a formally zero-valent metal.

The ability of carbonyl fragments to furnish electrons through its lone pair is known to be insufficient to explain the formation of four nickel-carbon σ-bonds. Thus, the Ni-C bond consists of a σ-bond formed by overlap of a filled carbon σ-orbital with a vacant σ-orbital on nickel and a π-bond formed by overlap of a filled dπ nickel orbital with an empty pπ antibonding orbital on carbon monoxide. This bonding mode may be described as being synergic: the feeding of metal electrons into carbon monoxyde orbitals will tend to increase the σ-donor ability of the latter while at the same time, the donation of electrons from carbon to the metal along the σ-bond renders the carbon monoxide more positive and ready to accept electrons from the metal into its π-orbital. This has been evidenced by infrared spectroscopy. Indeed, the absorption frequency of the carbonyl fragment can be considered as a function of the degree of π-bonding to give a structure such as Ni=C=O where a 3d electron pair of the nickel is donated to a 2p orbital of the carbon.[25,26]

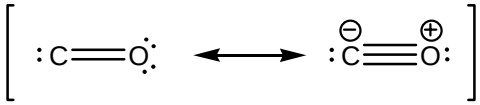

Figure 13: Resonance forms of the carbonyl group.

One can extend this representation to the other elements of the group 14 and consider the fragments Si=E, Ge=E, Sn=E and Pb=E (where E is a 6 electrons fragment) as being isoelectronic with the C=O group. This consideration allows paralleling group 14 metal ligands ElR_2 (with El = Ge, Sn, pb) with carbonyl units. Indeed, M. Veith *et. al.* reported the synthesis of the first binary nickel stannylene complex as follow: "a stable analogue of nickel tetracarbonyl".[27] The stability of this complex is mainly dependent on the π-electron accepting strength of the stannylene ligand.

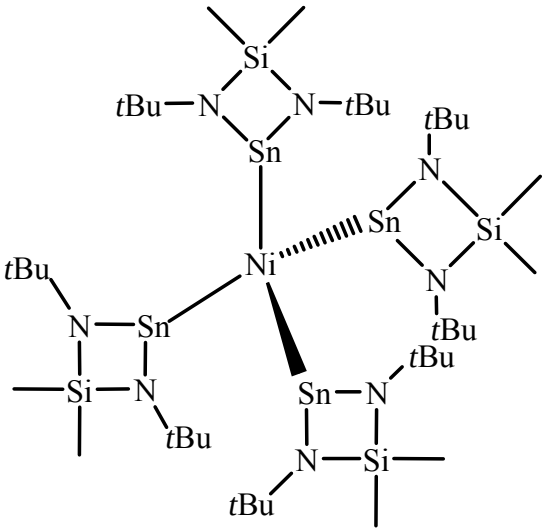

Figure 14: First binary nickel stannylene complex.[27]

M. Lappert and co-workers reported a few years earlier the synthesises of the first homoleptic stannylene complexes of zero-valent platinum(0) and palladium(0).[28-31] The extent of multiple bonding between transition metals and the group 14 elements, and the consequences of this bonding mode with respect to the reactivity has been of intense interest for the last decades. Nevertheless, reports on unambiguously characterised homoleptic nickel-group 14 tricoordinated elements are still scarce.[32] As mentioned earlier, M. Veith *et. al.* reported the synthesis of the first binary nickel stannylene complex $Ni[Sn(NtBu)_2Si(CH_3)_2]_4$ followed a few years later by J. Schneider and co-workers, who performed the synthesis of two other binary zero-valent nickel stannylene complexes: $Ni[Sn\{CH(SiMe)_3\}_2]_4$ and $Ni[Sn\{C_6HtBu\text{-}2\text{-}Me_3\text{-}3,\ 4,\ 5\}_2]_4$.[33] These synthesises could have been achieved with the use of an unconventional metal vapor method[34-36] to generate "solvated metal atoms", in other terms: high reactive zero-valent nickel sources.

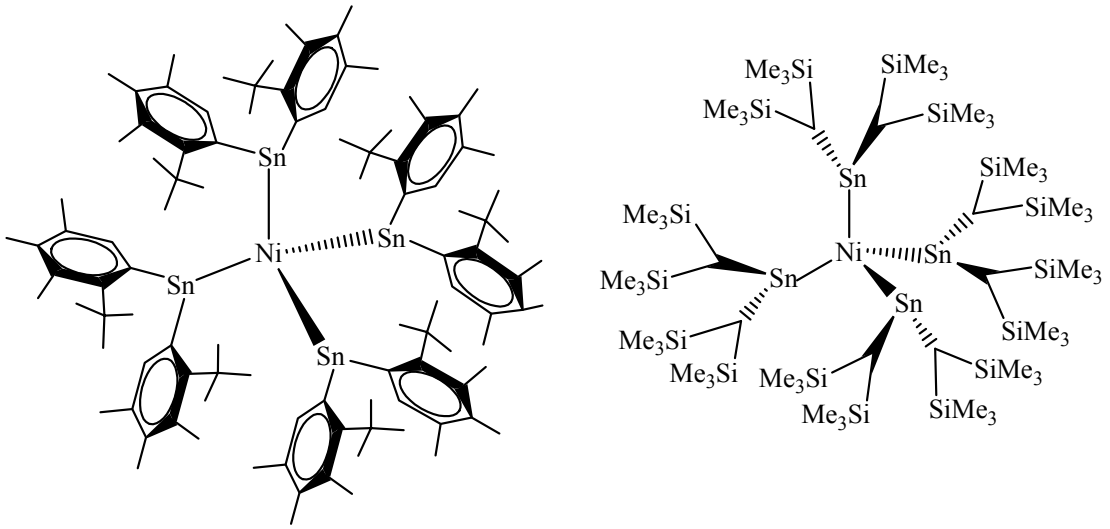

Figure 15: Homoleptic zero-valent nickel stannylene complexes [$Ni(SnR_2)_4$] [where R = (CH(SiMe)3)and (C_6H*t*Bu-2-Me_3-3, 4, 5)].

Research efforts have also been focused on the synthesis of heteroleptic zero-valent nickel stannylene complexes like the mono-stannylene nickel complex $Ni[\{C_2H_4\}_2\{Sn(CH(SiMe)_3)_2\}]$[37] obtained from the reaction of [$Ni(C_2H_4)_3$], the most reactive source of zero-valent nickel conventionally available, with the so-called Lappert stannylene $Sn\{CH(SiMe)_3\}_2$,[38] or the dimeric compound $[Ni(CO)_3Sn(O$*t*$Bu)_2]_2$ reported by M. Grenz and W. du Mont.[39]

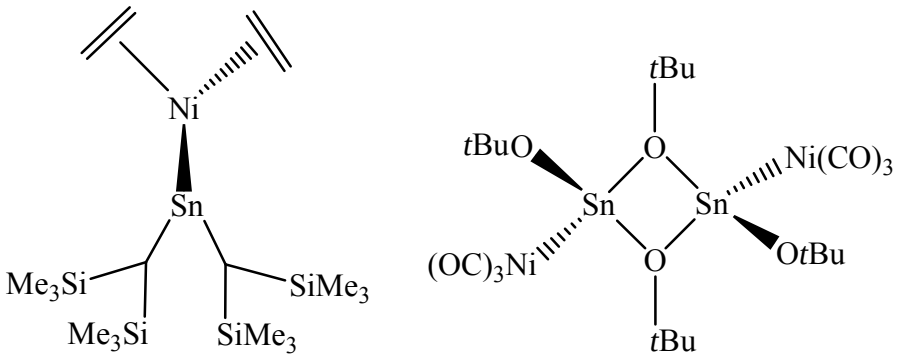

Figure 16: Heteroleptic zero-valent nickel stannylene complexes.

More recently, the research efforts have been focused on the lighter elements of the group 14. The pioneer works realised by A. Arduengo and co-workers, amongst other, permitted to isolate and characterise the first stable carbenes and silylenes.[40-42] These progresses propelled the synthesises of new divalent germanium compounds able as well, due to their high ligating properties, to stabilise zero-valent nickel centres. The equation 1 shows how the first fully characterised binary nickel tetragermylene

complex was achieved.[43] A previous reported homoleptic nickel germylene compound could not have been structurally characterised.[21] Structurally characterised zero-valent binary nickel germylene complexes are limited to the following heteroleptic compounds: $L_2Ni(CO)_2$ (L = (*t*BuNCH$_2$CH$_2$N*t*Bu)Ge),[44] the mono(germylene) species $LNi(PPh_3)_2$ (L = Ge[N(SiMe$_3$)$_2$]$_2$ or Ge(2,4,6-(CF$_3$)$_3$C$_6$H$_2$)$_2$)[45,46] and [{(*t*BuO)(μ-O*t*Bu)}GeNi(CO)$_3$]$_2$.[47]

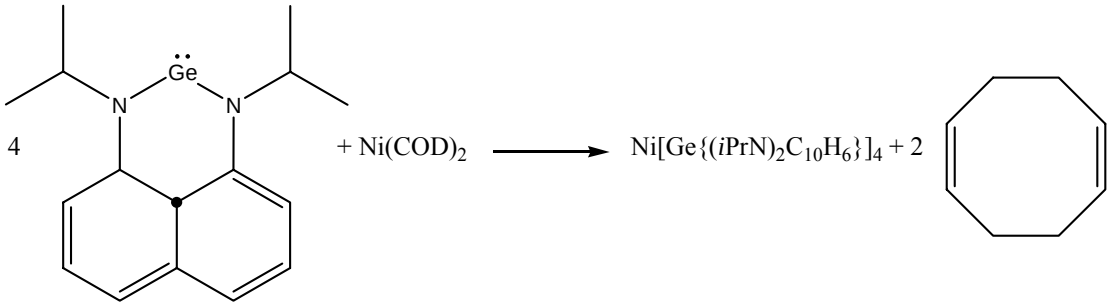

(Eq 1)

Starting from the bis(μ-σ-stannediyl)dinickel butterfly cluster [{{(SiMe$_3$)$_2$CH}$_2$Sn-Ni(η^5-Cp)}$_2$] achieved according to the equation 2, J. Schneider *et. al.* performed a surprising treatment with water resulting in the cleavage of a Ni-Sn bond and the opening of the cluster cage to yield to a trinuclear compound displaying an hydroxo bridging group as depicted in figure 17.[48]

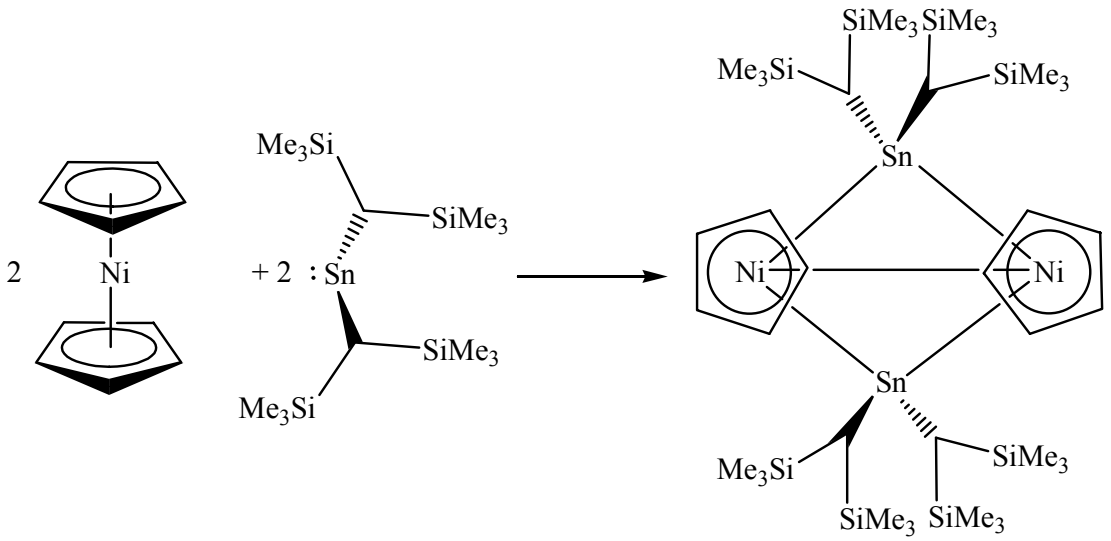

(Eq 2)

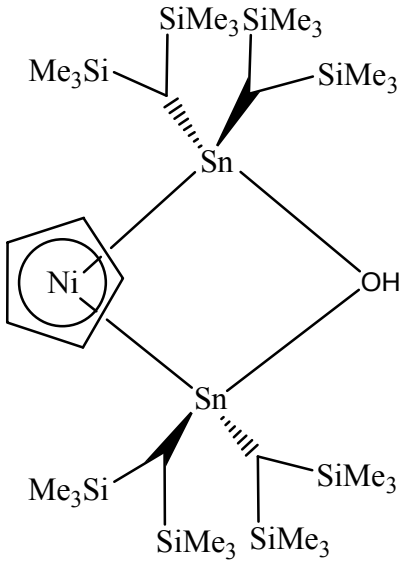

Figure 17: Trinuclear complex $[(\eta^5\text{-Cp})Ni\{Sn(CH(SiMe_3)_2\}_2OH]$.

This compound constitutes one of the very few examples of complex displaying connectivity between nickel and tin atoms and a bridging hydroxo group. Nevertheless, this could not have been structurally characterised due to the poor quality of the obtained crystals.

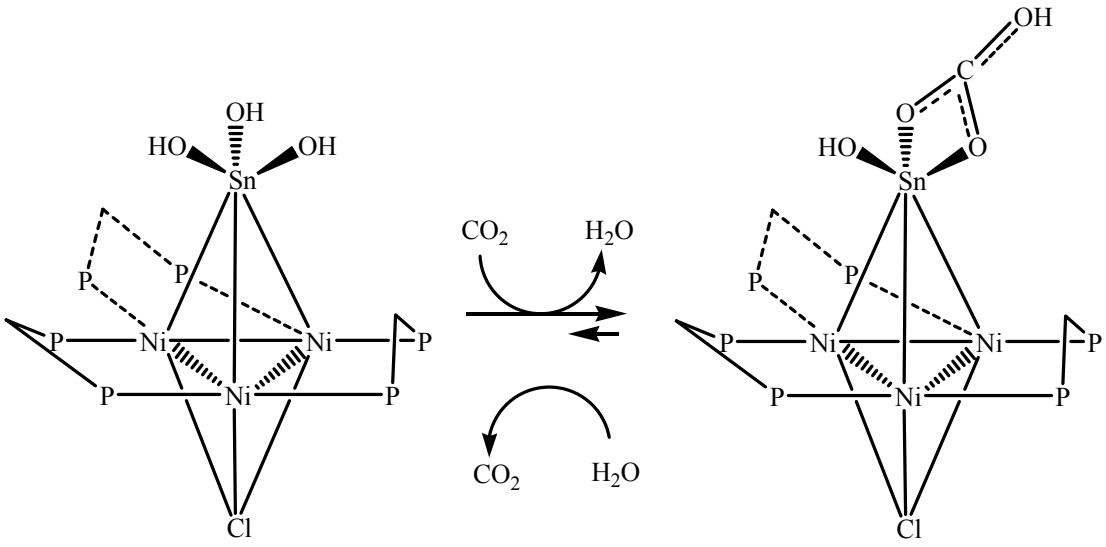

(Eq 3)

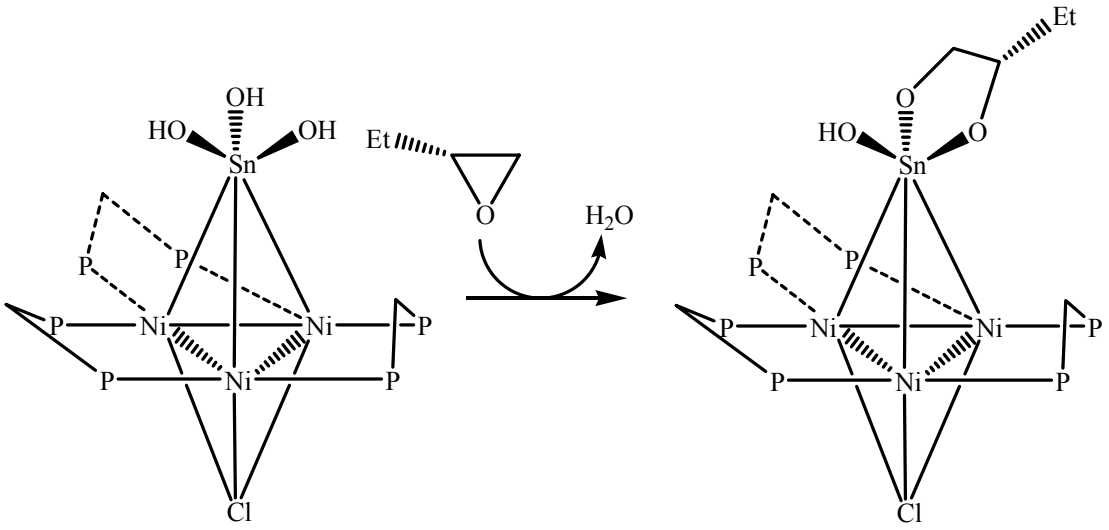

(Eq 4)

C. Kubiak and E. Simón-Manson reported a trinuclear nickel cluster presenting a μ_3-trihydroxystannyl group. This tin(IV) centre exhibits nucleophilic addition to carbon dioxide and epoxides to form, according to the equations 3 and 4, the η^2-carbonate complex and the 1,2 diolate cluster, respectively (see equations 3 and 4).[49] These two clusters are the only reported compounds displaying a nickel-tin-alkoxide rest connectivity.

Chapter 3

Low-valent group 14 metal alkoxides of transition metals

3.1 Synthesis of $NiSn_2(OtBu)_6$ 1

An analogue synthetic approach as the one reported by M. Veith *et al.*[23] to prepare germanate or plumbate of divalent transition metals was chosen. According to the equation 1, one equivalent of dried nickel bromide[50] was reacted with freshly sublimated (or re-crystallised) sodium stannate $Na_2Sn_2(OtBu)_6$ **15**.[51]

$$\underset{\mathbf{15}}{Na_2Sn_2(OtBu)_6} + NiBr_2 \longrightarrow \underset{\mathbf{1}}{NiSn_2(OtBu)_6} + 2\ NaBr\downarrow \qquad \text{(Eq 1)}$$

A colour change of the suspension from orange to blue was observed after 30 minutes, which indicates a change of coordination and geometry at the nickel atom from bromide substituents to *tert*-butoxide groups.[52-54] The reaction may be described as a salt-exchange, the formation of sodium bromide being the driving force of the reaction. As reported by Mehrotra *et al.* amongst others, the very slow kinetics of the reaction may be attributed to the weak solubility of the dried nickel bromide in toluene. Despite 48 hours of stirring at 120°C, the conversion into the desired product is not complete. Indeed, the yield could not have been better as 42 %. In very similar systems, this problem of solubility is overcome with the addition of a small amount of pyridine (approximately 10 % in volume.) in the reaction mixture.[55] The complex **1** could also have been isolated as a side product according an other synthetic procedure. The initial intention of the reaction was to perform an alcoholysis reaction on the following nickel tetrastannylene complex: $Ni[Sn(NtBu)_2Si(CH_3)_2]_4$ **14** as shown in equation 2:

$Ni[Sn(NtBu)_2Si(CH_3)_2]_4 + 8\ tBuOH \not\longrightarrow Ni[Sn(OtBu)_2]_4 + 4\ (HNtBu)_2Si(CH_3)_2$

14 **25** (Eq 2)

After three days in refluxing benzene, the reaction mixture became slightly blue and a lot of decomposition products were observed. The sublimation of the crude (70°C, 10^{-2} bar) provided 7% of a crystalline blue solid identified as being the complex **1**. This synthetic approach permitted to highlight the interesting volatile properties of the complex.

3.2 Spectral properties of $NiSn_2(OtBu)_6$ 1

In tetrahedral fields, the outer electronic configuration of nickel(II) complexes is $e^4t_2^4$ and the splitting of the free ion terms becomes that shown in figure 1.

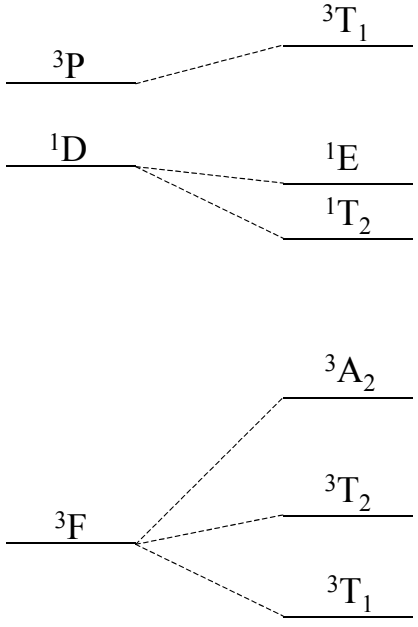

Figure 1: Energies of triplet terms for tetrahedral nickel(II) complexes.

Three allowed spin transitions are expected from the $^3T_1$ ground state. In general, the spectra show a very broad band in the 15000 cm^{-1} region containing the $^3T_1 \rightarrow {}^3T_1(P)$ transition with weaker bands on either side of this transition being assigned to spin-forbidden bands. The near infrared band around 7000 cm^{-1} is assigned to $^3T_1 \rightarrow {}^3A_2$

transition, the lowest energy band, corresponding to the $^3T_1 \rightarrow {}^3T_2$ transition, is not frequently observed.[115]

The complex **1** $NiSn_2(OtBu)_6$ has been investigated by UV-Vis spectroscopy analysis. The obtained spectrum recorded in toluene is depicted in figure 2.

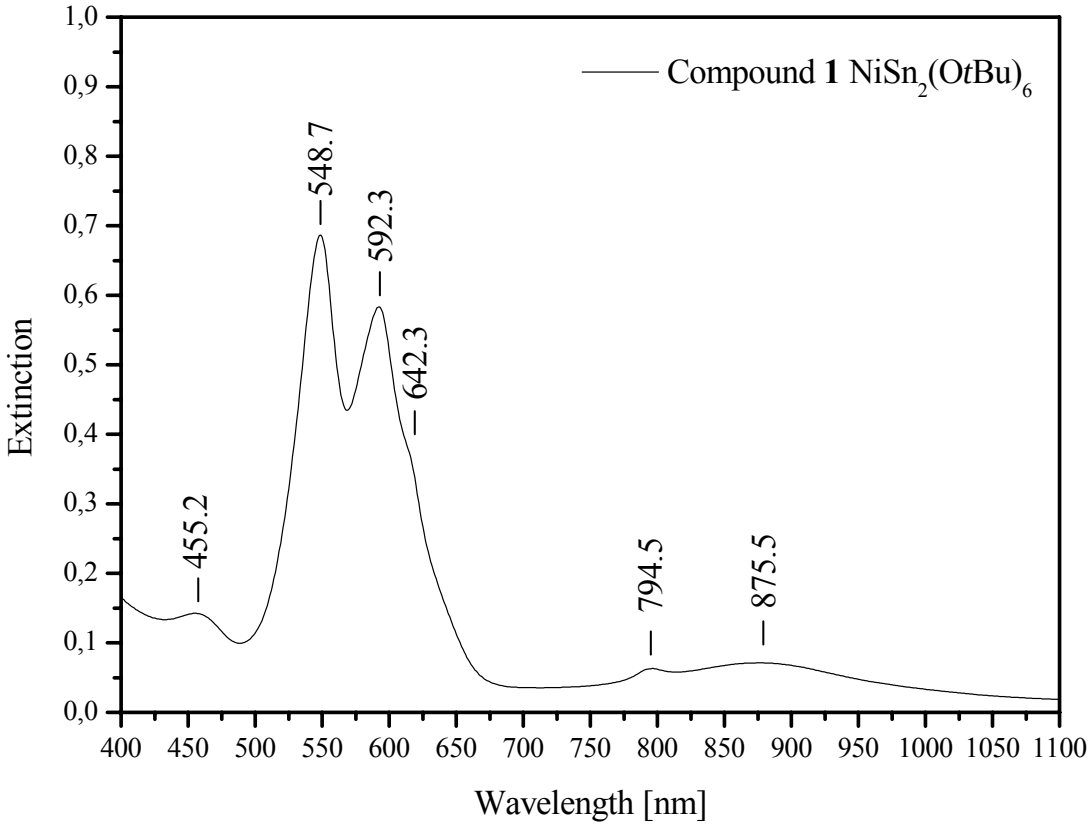

Figure 2: UV-Vis solution spectrum of the compound **1** $NiSn_2(OtBu)_6$.

From a qualitative point of view, the comparison of the recorded spectrum with other previous reports dealing with nickel(II) complexes[56,126,127] allows to form the assumption that the compound **1** is tetrahedrally surrounded.

As the splitting of the different d orbitals is smaller in a tetrahedral crystal field as in an octahedral one ($\Delta_t \approx 4/9\Delta_o$), the absorption bands corresponding to a tetrahedral complex are displaced to the smaller wave numbers. As a result, the υ_3 transition [$^3T_1 \rightarrow {}^3T_1(P)$] appears in the visible region. Moreover, the spin-orbit interaction splits up the $^3T_1(P)$ term in four terms (Γ_3, Γ_5, Γ_4, Γ_1).[128,129] This is the reason why the υ_3 transition appears as two absorption bands at 548.7 nm (18225 cm^{-1}) and 592.3 nm (16883 cm^{-1}), respectively. Two weaker absorption bands have to be noticed: the first one, a relative sharp band at 455.2 nm (21968 cm^{-1}) and the second: a very broad

band at 794.5 nm (12587 cm^{-1}). According to Mehrotra *et al.*, these two absorption bands may be assigned to electronic transitions corresponding to an octahedral coordination at the nickel centre.[130] This latter assumption would signify that an equilibrium phenomenon is taking place between a tetrahedral and an octahedral coordination. Different literature reports dealing with nickel alkoxides have already described similar systems[130,131] but to the best of our knowledge, this kind of equilibrium has never been evidenced for nickel-tin complexes. Nevertheless, considerations about the molecular crystal structure (see chapter 3.3.1.) could provide an explanation for this unusual coordination mode.

The initial assumption that the central nickel atom displays a tetrahedral environment is confirmed in chapter 3.3.1. This geometry confers to the compound magnetic properties (see the crystal field splitting diagrams for nickel(II) in different crystal fields in chapter 5.1.2). The paramagnetic behaviour of the complex has been quantified according to the Evans method (see chapter 5.2).

3.3 Crystal structure determination of $NiSn_2(O\mathit{t}Bu)_6$ 1

Crystals of $NiSn_2(O\mathit{t}Bu)_6$ **1** were obtained from a concentrated toluene solution placed at -10°C. An appropriate crystal was isolated and anchored at a cryo-loop. From the determination and the refinement of the unit cell dimensions arose the space group $P2_1/n$ in a monoclinic crystal system. The position of each atom, except the hydrogen atoms, was anisotropically refined. Hydrogen atoms were refined as rigid groups with the attached carbon atoms in ideal positions. The R-value is 6.33 %. In table 1 are reported the crystal data and the structure refinement for the compound and in table 2 are reported some selected bond lengths and angles of interest.

Table 1: Crystal data and structure refinement for shelxs2028.

Identification code	shelxs2028
Empirical formula	C24 H54 Ni O6 Sn2
Formula weight	734.76
Temperature	293(2) K

Wavelength	0.71073 Å	
Crystal system	Monoclinic	
Space group	$P2_1/n$	
Unit cell dimensions	a = 16.386(3) Å	α= 90°
	b = 11.889(2) Å	β= 113.73(3)°
	c = 19.136(4) Å	γ = 90°
Volume	3412.8(11) $Å^3$	
Z	4	
Density (calculated)	1.430 Mg/m^3	
Absorption coefficient	2.027 mm^{-1}	
F(000)	1496	
Crystal size	0.4 x 0.25 x 0.2 mm^3	
Theta range for data collection	2.07 to 24.01°.	
Index ranges	-18<=h<=18, -13<=k<=13, -21<=l<=21	
Reflections collected	20470	
Independent reflections	5211 [R(int) = 0.1586]	
Completeness to theta = 24.01°	97.1 %	
Absorption correction	Numerical	
Refinement method	Full-matrix least-squares on F^2	
Data / restraints / parameters	5211 / 0 / 298	
Goodness-of-fit on F^2	1.095	
Final R indices [I>2sigma(I)]	R1 = 0.0633, wR2 = 0.1556	
R indices (all data)	R1 = 0.0712, wR2 = 0.1622	
Largest diff. peak and hole	1.825 and -1.289 $e.Å^{-3}$	

Table 2: Selected bond lengths [Å] and angles [°] for shelxs2028.

Sn(2)-O(6)	2.009(6)	Sn(1)-O(2)	2.143(4)
Sn(2)-O(3)	2.142(5)	Ni(1)-O(4)	1.943(5)
Sn(2)-O(4)	2.145(5)	Ni(1)-O(3)	1.952(5)
Sn(1)-O(5)	2.003(5)	Ni(1)-O(2)	1.966(5)
Sn(1)-O(1)	2.130(5)	Ni(1)-O(1)	1.968(5)

O(6)-Sn(2)-O(3)	91.9(2)	O(3)-Ni(1)-O(2)	123.0(2)
O(6)-Sn(2)-O(4)	90.4(2)	O(4)-Ni(1)-O(1)	130.4(2)
O(3)-Sn(2)-O(4)	71.9(2)	O(3)-Ni(1)-O(1)	125.9(2)
O(5)-Sn(1)-O(1)	91.7(2)	O(2)-Ni(1)-O(1)	80.1(2)
O(5)-Sn(1)-O(2)	92.1(2)	Ni(1)-O(1)-Sn(1)	103.6(2)
O(1)-Sn(1)-O(2)	72.6(2)	Ni(1)-O(2)-Sn(1)	103.2(2)
O(4)-Ni(1)-O(3)	80.5(2)	Ni(1)-O(3)-Sn(2)	103.5(2)
O(4)-Ni(1)-O(2)	123.5(2)	Ni(1)-O(4)-Sn(2)	103.7(2)

3.3.1 Discussion of the molecular structure of $NiSn_2(OtBu)_6$ 1

A single crystal X-ray analysis of $NiSn_2(OtBu)_6$ **1** was carried out for unequivocal identification of the structure as shown in figure 3.

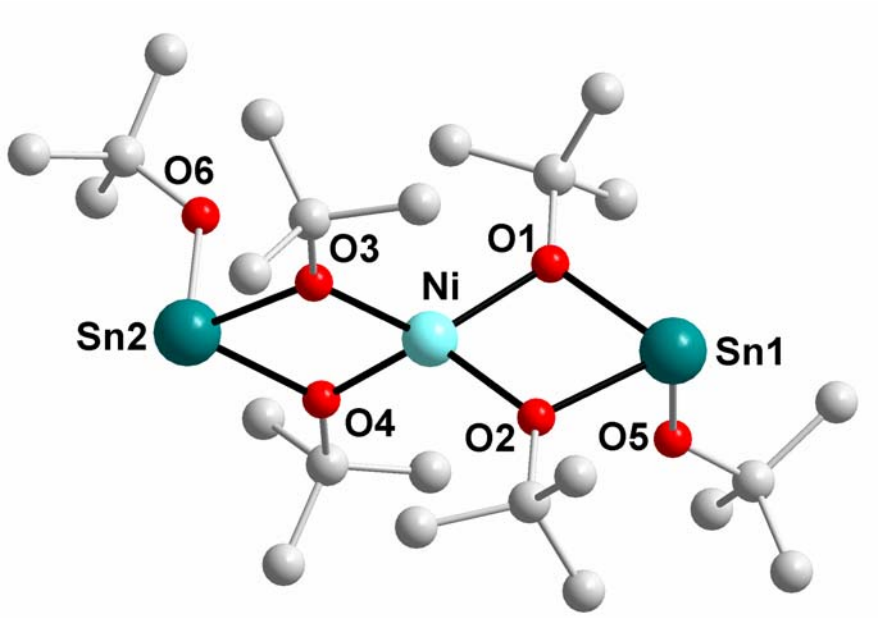

Figure 3: X-ray molecular structure of $NiSn_2(OtBu)_6$ **1**. Hydrogen atoms are omitted for clarity and carbon atoms are not labelled.

The molecular structure consists of two planar four-membered rings (Sum of angles = 359.46(1)°) oriented in a perpendicular manner to each other with the central spirocyclic nickel atom being almost tetrahedrally surrounded by two chelating stannates $[Sn(OtBu)_3]^-$. The three metallic atoms are arranged linearly (Sn(1)-Ni-Sn(2) = 178.35(1)°). The NiO_4^- tetrahedron is distorted: In the case of a perfect tetrahedron, the Sn(1)-Ni-Sn(2) axis would be an S_4 axis but the chelating effect of the two bidentate stannates ligands causes an elongation of the tetrahedron along the same axis. As a result, both angles O(1)-Ni-O(2) and O(3)-Ni-O(4) are 80.06(1)°and 80.51(1)°, respectively, instead of 109.5° that would be expected for a perfect tetrahedron. This effect has already been observed in a lot of similar spirocyclic-compounds.[23] As shown in figure 4, the two exocyclic *tert*-butoxide groups on the tin atoms are almost perpendicular to the planes formed by the two four-membered rings (Ni-Sn(2)-O(6) = 88.56(1)° and O(6)-Sn(2)-O(3) = 91.93(1)°) and thus, also

perpendicular to each other. The two low-valent tin atoms are situated on the axial sites of trigonal pyramids. The values of the angles Ni-Sn(2)-O(6) = 88.56(1)°, O(1)-Sn(1)-O(2) = 72.60(1)°, O(1)-Sn(1)-O(5) = 91.65(1)°, O(2)-Sn(1)-O(5) = 92.15(1)° show that the tin atoms tend to be sp^3 hybridised.

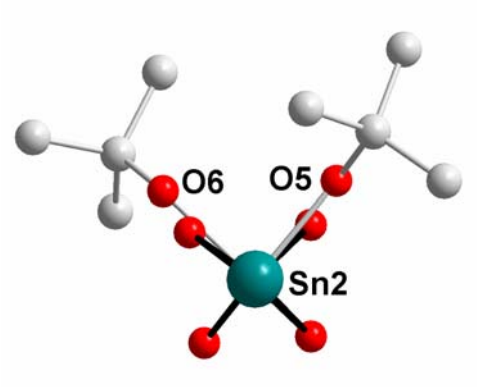

Figure 4: Projection of the ground structure along the Sn(2)-Ni-Sn(1) axis. Hydrogen atoms and all carbon atoms except the terminal *tert*-butoxide groups are omitted for clarity.

As far as the bond lengths are concerned, the average of the Ni-O bond lengths is 1.96(2) Å and is in the range of one can expect for a tetrahedral nickel(II) complex displaying alkoxide substituents.[23,56-58]

In regard to the tin-oxygen bond lengths, the *exo*cyclic Sn-O bond [Sn(1)-O(5)] measures 2.01(1) Å and the *endo*cyclic Sn-O bonds show an average length of 2.140(7) Å. The average Ni···Sn distance is 3.220(2) Å. This value is very close to those measured for the dinickel stannate complex $Ni_2Sn_2(O\mathit{t}Bu)_8$ **21**, which exhibits a Ni···Sn distance of 3.211(1) Å.

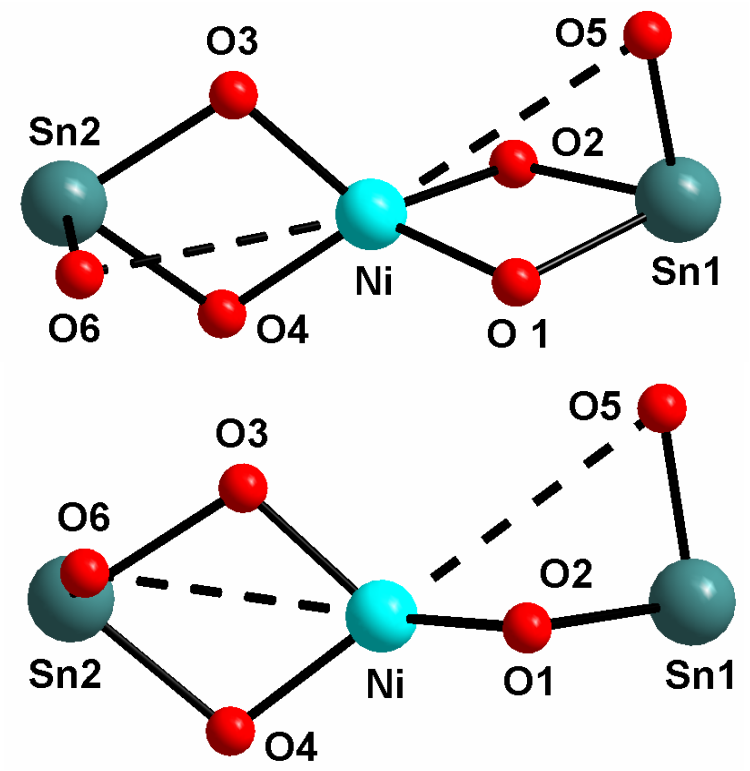

Figure 5: Simplified representations of the compound **1** $NiSn_2(OtBu)_6$ in different orientations. O(5)-Ni and O(6)-Ni bonds have been artificially added. Hydrogen and carbon atoms are omitted for clarity.

The figure 5 represents simplified views of the compound **1** $NiSn_2(OtBu)_6$, where the organic part of the molecule has been hidden. Moreover, both bonds Ni-O(5) and Ni-O(6), which do not exist in the crystal structure and figured by dots, have been added to highlight an higher coordination number of the nickel centre. It appears clearly, that one cannot define an octahedral coordination and it seems like a trigonal anti-prismatic coordination matches more with the observed structure. Nevertheless, none of this description has to be taken as borderline. The assumption made in regard to the obtained UV-Vis spectrum of **1** concerning an equilibrium phenomenon between the tetrahedral environment and a six-coordinate nickel centre (see chapter 3.2.) is reinforced by the orientation of the terminal alkoxide residues (figured here only by the oxygen atoms O(5) and O(6), respectively). Indeed, it appears clearly, that the both oxygen atoms O(5) and O(6) are oriented in the direction of the nickel centre. The slight folding of the four membered ring Ni-O(1)-Sn(1)-O(2) contributes also to bring the terminal oxygen atom O(5) cloth to the nickel centre (O(5)-Ni = 3.584 Å).

3.4 Synthesis of $Ni_2Pb_2(OtBu)_8$ 2

A previous study showed that no reaction was observed between sodium plumbate and nickel chloride after many days in refluxing toluene.[59] Our first attempts were realised according to the previously established procedure.[23] To a toluene solution of sodium plumbate were added one or two equivalents of nickel halide (nickel chloride or nickel bromide have been tested). The suspension was stirred at least two days in refluxing toluene.

$$\underset{\textbf{17}}{Na_2Pb_2(OtBu)_6} + NiBr_2 \not\longrightarrow NiPb_2(OtBu)_6 + 2\ NaBr\downarrow \qquad \text{(Eq 3)}$$

As shown in equation 3, if one equivalent of nickel halide was added, no nickel plumbate was obtained but the starting sodium plumbate was isolated almost quantitatively as well as an amorphous and insoluble blue solid, identified as being $[Ni(OtBu)_2]_n$. This would first signify that the nickel halide might react in this case with the "NaO*t*Bu" moiety of the sodium plumbate and second, that the plumbate anion is not reactive enough to break the polymeric chains of $[Ni(OtBu)_2]_n$.
The second attempt was realised according the equation 4.

$$4\ \underset{\textbf{17}}{Na_2Pb_2(OtBu)_6} + 6\ NiBr_2 \longrightarrow 3\ \underset{\textbf{2}}{Ni_2Pb_2(OtBu)_8} + 8\ NaBr\downarrow + 2\ SnCl_2\downarrow \qquad \text{(Eq 4)}$$

This reaction depends greatly on the solvents used. The reaction was first performed in toluene to give an amorphous and insoluble blue substance considered as being $[Ni(OtBu)_2]_n$ as well as sodium bromide. After filtration of these solids, an NMR sample was prepared from the solution and no trace of the starting material could have been identified, which may signify that the nickel halide has react with the "NaO*t*Bu" moiety of all the starting sodium plumbate.
The addition of a small amount of pyridine (approximately 10 % in volume) permitted to overcome these difficulties and to isolate the desired complex in 31 %. The relative weak yield may be improved by the addition of a larger amount of pyridine or by a longer reaction time.

The nickel plumbate complex exhibits magnetic properties. Its magnetic susceptibility in solution has been determined according to the Evans method and is given in chapter 5.2.

3.5 Crystal structure determination of $Ni_2Pb_2(OtBu)_8$ 2

Crystals of $Ni_2Pb_2(OtBu)_8$ **2** were obtained from a concentrated toluene/pyridine solution 10:1 placed at -10°C. An appropriate crystal was isolated and anchored at a cryo-loop. From the determination and the refinement of the unit cell dimensions arose the space group $P2_1/n$ in a monoclinic crystal system. The position of each atom, except the hydrogen atoms, was anisotropicaly refined. Hydrogen atoms were refined as rigid groups with the attached carbon atoms in ideal positions. The R-value is 11.18 %. This high value is due to the poor quality of the measured crystal. This is reflected by the high internal R-value: 0.1416. A large number of literature reports describe complexes owning this type of crystal structure,[60-62] which often show disorders. It mainly concerns the "periphery" of the molecule (the organic part of the complex), whereas the different measured electron densities corresponding to the metallic core of the molecule can be unambiguously assigned. Thus, one can assume, that central metallic part of the complex matches with the reality. In table 3 are reported the crystal data and the structure refinement for the compound and in table 4 are reported some selected bond lengths and angles of interest.

Table 3: Crystal data and structure refinement for sh2361.

Identification code	sh2361
Empirical formula	C32 H72 Ni2 O8 Pb2
Formula weight	1116.70
Temperature	103(2) K
Wavelength	0.71073 Å
Crystal system	Monoclinic
Space group	$P2_1/n$
Unit cell dimensions	a = 9.742(4) Å α= 90°

	b = 14.803(7) Å β= 97.61(2)°
	c = 14.717(6) Å γ = 90°
Volume	2103.7(16) Å^3
Z	2
Density (calculated)	1.763 Mg/m^3
Absorption coefficient	8.900 mm^{-1}
F(000)	1096
Crystal size	0.2 x 0.25 x 0.43 mm^3
Theta range for data collection	1.96 to 23.96°.
Index ranges	-8<=h<=10, -16<=k<=16, -16<=l<=15
Reflections collected	12464
Independent reflections	3024 [R(int) = 0.1416]
Completeness to theta = 23.96°	92.2 %
Absorption correction	Semi-empirical from equivalents
Refinement method	Full-matrix least-squares on F^2
Data / restraints / parameters	3024 / 0 / 211
Goodness-of-fit on F^2	1.454
Final R indices [I>2sigma(I)]	R1 = 0.1118, wR2 = 0.2314
R indices (all data)	R1 = 0.1567, wR2 = 0.2477
Largest diff. peak and hole	3.708 and -4.624 e.Å^{-3}

Table 4: Selected bond lengths [Å] and angles [°] for sh2361.

Pb-O(3)	2.13(2)	O(3)-Pb-O(2)	87.3(6)
Pb-O(2)	2.23(1)	O(3)-Pb-O(1)	86.9(6)
Pb-O(1)	2.23(2)	O(2)-Pb-O(1)	69.8(5)
Pb-Ni	3.29(3)	O(3)-Pb-Ni	80.2(4)
Ni-O(4)#1	1.94(1)	O(2)-Pb-Ni	35.7(4)
Ni-O(1)	1.94(1)	O(1)-Pb-Ni	35.1(3)
Ni-O(4)	1.97(1)	O(4)#1-Ni-O(1)	127.0(6)
Ni-O(2)	1.97(1)	O(4)#1-Ni-O(4)	78.6(7)
O(4)-Ni#1	1.94(1)	O(1)-Ni-O(4)	125.9(6)

O(4)#1-Ni-O(2)	128.1(6)	Ni-O(1)-Pb	103.6(6)
O(1)-Ni-O(2)	81.4(6)	C(5)-O(2)-Ni	131.6(1)
O(4)-Ni-O(2)	122.5(6)	C(5)-O(2)-Pb	125.4(1)
O(4)#1-Ni-Pb	151.3(4)	Ni-O(2)-Pb	103.0(6)
O(1)-Ni-Pb	41.3(5)	C(9)-O(3)-Pb	125.9(2)
O(4)-Ni-Pb	130.2(4)	C(13)-O(4)-Ni#	1129.8(1)
O(2)-Ni-Pb	41.3(4)	C(13)-O(4)-Ni	128.8(1)
C(1)-O(1)-Ni	134.5(2)	Ni#1-O(4)-Ni	101.4(7)
C(1)-O(1)-Pb	121.8(1)		

3.5.1 Discussion of the molecular crystal structure of $Ni_2Pb_2(O\mathit{t}Bu)_8$ 2

A single crystal X-ray analysis allowed the unequivocal identification of the molecular structure of $Ni_2Pb_2(O\mathit{t}Bu)_8$ **2** as depicted in figure 6. The molecule displays an inversion centre situated in the centre of the Ni_2O_2 four-membered ring. Similar crystal structures with lighter homologues of lead (nickel germanate and nickel stannate) have already been reported by M. Veith *et al.*[23] They all show similar features.

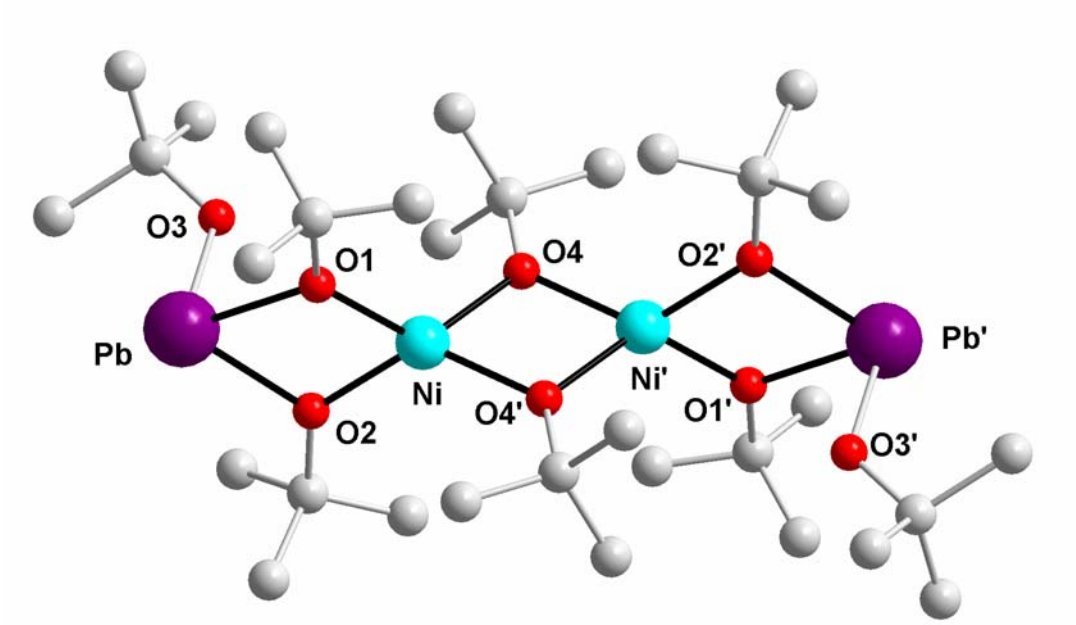

Figure 6: X-ray molecular structure of $Ni_2Pb_2(O\mathit{t}Bu)_8$ **2**. Hydrogen atoms are omitted for clarity and carbon atoms are not labelled.

In this compound, the transition metals are situated in fourfold coordination sites, which can be described as spiro-metallic centres in distorted oxygen tetrahedrons. The metal chain is elongated by the formal insertion of one $Ni(O\mathit{t}Bu)_2$ unit with respect to $NiSn_2(O\mathit{t}Bu)_6$. As discussed with the crystal structure of $NiSn_2(O\mathit{t}Bu)_6$ **1**, this may be explained by the chelating effect of the plumbate units $[Pb(O\mathit{t}Bu)_3]^-$, which contributes to the elongation of the tetrahedron along the S_4 axis (O(1)-Ni-

O(2) = 81.48(1)°, O(4)-Ni-O(4') = 78.6(7)°, O(4)-Ni-O(1) = 125.91(2)°, O(2)-Ni-O(4') = 128.16(2)°, O(1)-Ni-O(4') = 127.0(6)°, O(2)-Ni-O(4) = 122.51(1)°) instead of the 109.50° that would be expected for a perfect tetrahedron). The arrangement of the metallic atoms deviates from linearity (Pb-Ni-Ni' = 169.14(1)°) presumably due to intra-molecular hinder. This metallic array is linked together by bridging alkoxide groups and the three four-membered rings are arranged in a perpendicular fashion. Each lead atom is situated on the axial site of a distorted trigonal pyramid. In an alternative description, each lead atom would be situated in the centre of a tetrahedron with three oxygen atoms and one stereochemically active lone pair of electron at the corners of the polyhedron. *Tert*-butoxide groups in *trans* configuration terminate the compound. The angle Ni-Pb-O(3) is around 80.18(1)°. It is noteworthy, that this value increases drastically when the size of the low-valent element decreases. Indeed, similar compounds containing tin and germanium as low-valent element show angles of 85.64(1)° and 92.51°, respectively.[23]

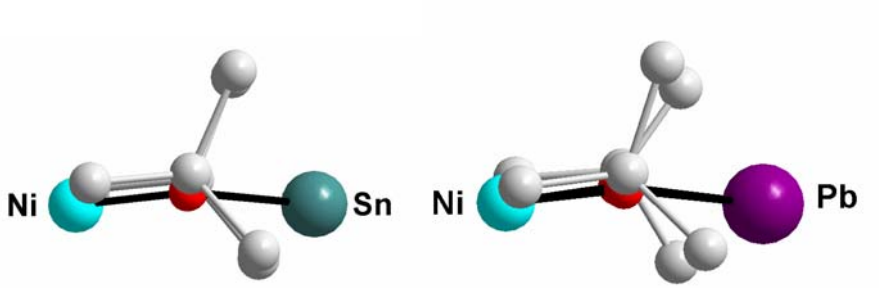

Figure 7: Projection of the four membered-rings of $Ni_2Sn_2(OtBu)_8$[23] and $Ni_2Pb_2(OtBu)_8$ along the C-O bonds axis.

As shown in figure 7, *endo*cyclic bridging *tert*-butoxide groups are arranged not exactly in the same manner according to the nature of the low-valent element. Whereas in the nickel-tin compound the *tert*-butoxide groups are almost perfectly eclipsed (torsion angle = 1.82(3)°), they are stronger rotated against each other (torsion angle = 11.73(2)°) in the nickel-lead complex. In the central four membered-ring, *tert*-butoxide groups are oriented in a staggered fashion (torsion angle = 59.99(2)°).

In table 5, selected bond lengths and distances for the three homologues complexes are compared.

Compound	Ni-O[a]	Ni-O[b]	El(II)-O[b]	El(II)-O[c]	Ni···Ni	Ni···El(II)
$Ni_2Ge_2(OtBu)_8$	1.947(1)	1.946(2)	1.954(3)	1.834(1)	2.994(1)	3.058(1)
$Ni_2Sn_2(OtBu)_8$	1.937(4)	1.965(8)	2.11(4)	2.00(4)	3.01(4)	3.21(4)
$Ni_2Pb_2(OtBu)_8$	1.954(1)	1.96(1)	2.232(9)	2.13(2)	3.03(1)	3.288(3)

Table 5: Selected bond lengths and distances [Å] of compound **21, 22** and **2**. a : oxygen atoms between two transition metals. b: oxygen atoms between Ni and El(II). c: oxygen atoms of terminal alkoxide groups.

3.6 Synthesis of $[\{(CO)_4Fe\}_2\{Ni_2Sn_2(OtBu)_8\}]$ 3

As shown in figure 8, the starting material $Ni_2Sn_2(OtBu)_8$ **21** displays two low-valent tin atoms situated on the axial sites of trigonal pyramids. This predisposes it to further complexation reactions with transition metal carbonyls.

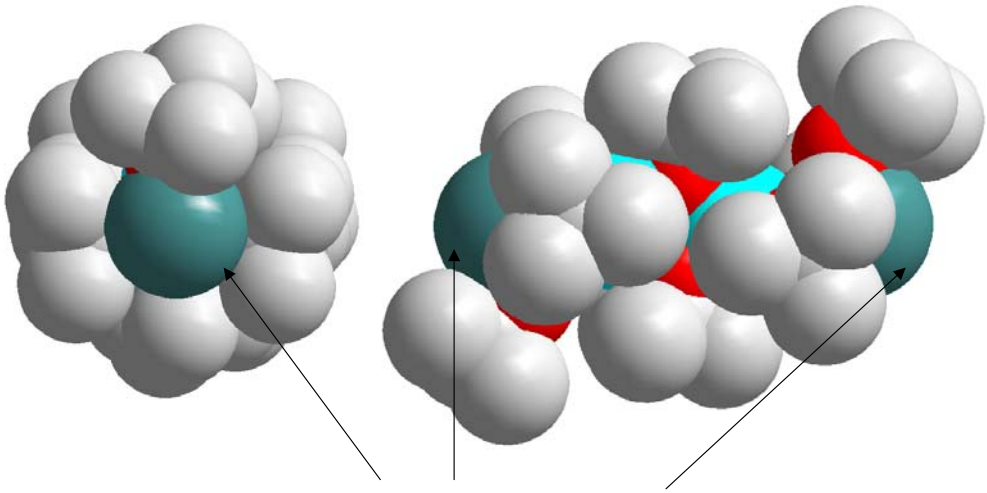

Figure 8: Space filling representations in axial and longitudinal views of $Ni_2Sn_2(OtBu)_8$ **21**.

The nickel stannate complex was react with two equivalents of nonacarbonyl diiron according the equation 5.

$$Ni_2Sn_2(OtBu)_8 + 2\ Fe_2(CO)_9 \longrightarrow [\{(CO)_4Fe\}_2\{Ni_2Sn_2(OtBu)_8\}] + 2\ Fe(CO)_5$$

21 **3** (Eq 5)

The formation of the targeted product could have been followed by infrared spectroscopy. While the vibrational bands of nonacarbonyl diiron decreased, the characteristic IR signature of a pentacoordinated complex $(CO)_4M$-L (with L in axial position, due to the C_{3v} symmetry, one should expect 3 vibration bands: two bands A_1 and one band E) appeared: υ [cm^{-1}] = 1938 (vs), 1970 (m) and 2044 (s). Concomitantly, the formation of dodecacarbonyl triiron coloured the solution in dark green and could have been observed as well by infrared spectroscopy.
As well as its uncoordinated homologue, the complex shows magnetic properties. The magnetic susceptibility of the complex has been quantified according to the Evans method (see chapter 5.2).

3.7 Crystal structure determination of $[\{(CO)_4Fe\}_2\{Ni_2Sn_2(OtBu)_8\}]$ 3

Crystals of $[\{(CO)_4Fe\}_2\{Ni_2Sn_2(OtBu)_8\}]$ **3** were obtained from a concentrated hexane/THF 1:1 solution placed at -10°C. An appropriate crystal was isolated and anchored at a cryo-loop. From the determination and the refinement of the unit cell dimensions arose the space group P-1 in a triclinic crystal system. The position of each atom, except the hydrogen atoms, was anisotropicaly refined. Hydrogen atoms were refined as rigid groups with the attached carbon atoms in ideal positions. The R-value is 4.19 %. In table 6 are reported the crystal data and the structure refinement for the compound and in table 7 are reported some selected bond lengths and angles of interest.

Table 6: Crystal data and structure refinement for sh2218.

Identification code	sh2218	
Empirical formula	C40 H72 Fe2 Ni2 O16 Sn2	
Formula weight	1275.48	
Temperature	103(2) K	
Wavelength	0.71073 Å	
Crystal system	Triclinic	
Space group	P-1	
Unit cell dimensions	a = 10.6720(5) Å	α= 86.907(2)°
	b = 10.8659(5) Å	β= 88.002(2)°
	c = 23.6521(11) Å	γ = 80.176(2)°
Volume	2697.6(2) $Å^3$	
Z	2	
Density (calculated)	1.570 Mg/m^3	
Absorption coefficient	2.177 mm^{-1}	
F(000)	1296	
Crystal size	0.25 x 0.1 x 0.05 mm^3	
Theta range for data collection	1.73 to 33.02°.	
Index ranges	-16<=h<=16, -16<=k<=16, -36<=l<=36	
Reflections collected	86330	
Independent reflections	20135 [R(int) = 0.0407]	
Completeness to theta = 33.02°	98.8 %	
Absorption correction	None	
Refinement method	Full-matrix least-squares on F^2	
Data / restraints / parameters	20135 / 0 / 583	
Goodness-of-fit on F^2	1.212	
Final R indices [I>2sigma(I)]	R1 = 0.0419, wR2 = 0.0997	
R indices (all data)	R1 = 0.0516, wR2 = 0.1051	
Largest diff. peak and hole	2.733 and -1.314 e.$Å^{-3}$	

Table 7: Selected bond lengths [Å] and angles [°] for sh2218.

Sn(1)-O(4)	1.965(2)	O(1)-Sn(1)-O(2)	74.27(8)
Sn(1)-O(1)	2.049(2)	O(4)-Sn(1)-Fe(1)	136.03(6)
Sn(1)-O(2)	2.055(2)	O(1)-Sn(1)-Fe(1)	120.46(5)
Sn(1)-Fe(1)	2.4754(5)	O(2)-Sn(1)-Fe(1)	120.43(6)
Ni(1)-O(3)	1.943(2)	O(3)-Ni(1)-O(1)	125.34(8)
Ni(1)-O(1)	1.981 (2)	O(3)-Ni(1)-O(2)	125.40(8)
Ni(1)-O(2)	1.981(2)	O(1)-Ni(1)-O(2)	77.40(8)
Fe(1)-C(20)	1.776(3)	C(20)-Fe(1)-Sn(1)	173.24(1)
Fe(1)-C(18)	1.786(3)	C(18)-Fe(1)-Sn(1)	90.1(1)
Fe(1)-C(19)	1.793(3)	C(19)-Fe(1)-Sn(1)	84.5(1)
Fe(1)-C(17)	1.797(3)	C(17)-Fe(1)-Sn(1)	91.03(1)
Sn(2)-O(12)	1.958(2)	O(12)-Sn(2)-O(9)	92.99(9)
Sn(2)-O(9)	2.052(2)	O(12)-Sn(2)-O(10)	95.8(1)
Sn(2)-O(10)	2.054(2)	O(9)-Sn(2)-O(10)	74.37(8)
Sn(2)-Fe(2)	2.4700(5)	O(12)-Sn(2)-Fe(2)	131.38(7)
Ni(2)-O(11)	1.942(2)	O(9)-Sn(2)-Fe(2)	124.44(6)
Ni(2)-O(9)	1.982(2)	O(10)-Sn(2)-Fe(2)	121.58(6)
Ni(2)-O(10)	1.986(2)	O(11)-Ni(2)-O(9)	125.41(9)
Fe(2)-C(40)	1.780(3)	O(11)-Ni(2)-O(10)	123.96(9)
Fe(2)-C(37)	1.784(3)	O(9)-Ni(2)-O(10)	77.45(8)
Fe(2)-C(38)	1.795(3)	Ni(1)-O(1)-Sn(1)	103.09(8)
Fe(2)-C(39)	1.795(3)	Ni(1)-O(2)-Sn(1)	102.87(9)
O(4)-Sn(1)-O(1)	93.52(9)	Ni(2)-O(9)-Sn(2)	103.04(8)
O(4)-Sn(1)-O(2)	93.66(8)	Ni(2)-O(10)-Sn(2)	102.82(9)

3.7.1 Discussion of the molecular crystal structure of [{(CO)$_4$Fe}$_2${Ni$_2$Sn$_2$(O*t*Bu)$_8$}] 3

A single crystal X-ray analysis allowed the unequivocal identification of the molecular structure of [{(CO)$_4$Fe}$_2${Ni$_2$Sn$_2$(O*t*Bu)$_8$}] **3** as shown in figure 9. The molecule crystallises in the triclinic space group P-1. The crystallographic inversion centre is located in the centre of the Ni-O(3)-Ni'-O(3') four membered-ring. An analogous compound of the formula [{(CO)$_4$Fe}$_2${Co$_2$Sn$_2$(O*t*Bu)$_8$}] was reported by M. Veith *et al*.[23] Both show not only the same crystal space group but are also isotypic. In table 8, their space groups and unit cell dimensions are reported for comparison.

Compound	Space group	a/Å	b/ Å	c/ Å	α/ °	β/°	γ/°
23	P-1	10.786	11.029	24.017	87.04	87.94	79.45
3	P-1	10.620	10.866	23.652	86.91	88.00	80.18

Table 8: Space groups and unit cell dimensions of [{(CO)$_4$Fe}$_2${Co$_2$Sn$_2$(O*t*Bu)$_8$}] **23** and [{(CO)$_4$Fe}$_2${Ni$_2$Sn$_2$(O*t*Bu)$_8$}] **3**.

In this complex, six metal atoms are arranged in one dimension. The central transition metals are in fourfold coordination sites, which can be described as spiro metallic centres in distorted oxygen tetrahedrons elongated along the metal-metal axis.[63] Four of the six metallic elements are linked together by bridging alkoxide groups and the resulting three four-membered rings are oriented in a perpendicular fashion. Both iron-carbonyl units terminate the array and are oriented in *trans* to each other.

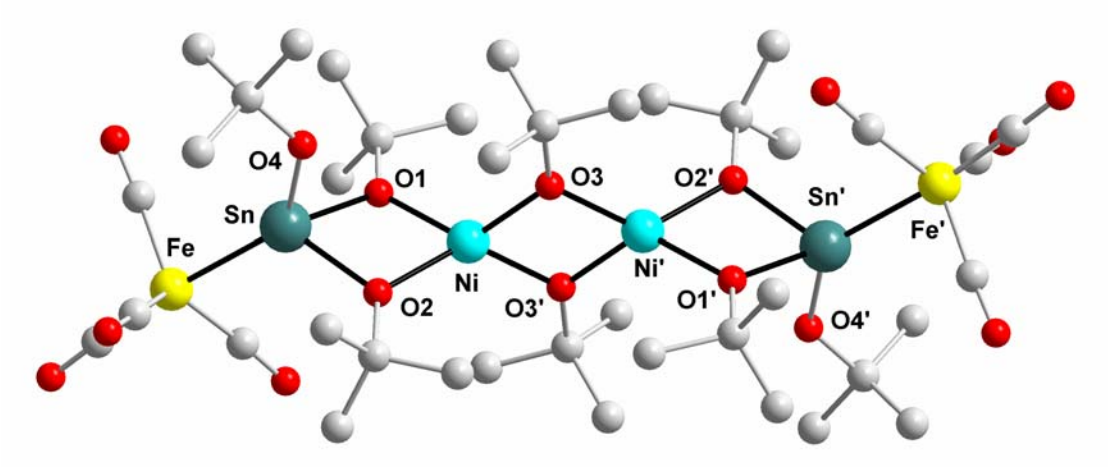

Figure 9: X-ray molecular structures of [{$(CO)_4Fe$}$_2${Ni_2Sn_2(O*t*Bu)$_8$}] **3**. Hydrogen atoms are omitted for clarity and carbon atoms are not labelled.

The four metal atoms constituting the core of the molecule are not oriented in a straight linear manner. Both Sn-Ni-Ni' and Ni-Ni'-Sn' angles are around 169.14°. It is interesting to notice that the linearity of the core metal atoms in the starting compound is more pronounced: Sn-Ni-Ni' and Ni-Ni'-Sn' show angles of 171.02°. The same observation is true for the planarity of the Sn-O(1)-Ni-O(2) four-membered-ring: planarity decreases through complexation with iron. Indeed, the sum of angles of the *endo*cyclic angles of the Sn-O(1)-Ni-O(2) four-membered ring for the iron-containing complex is around 357.64(2)° whereas the same measurement for the non coordinated complex gives 358.45°. It means that through complexation, the compound tends to fold slightly up.

In the projection along the C-O-O-C axis of the bridging *tert*-butoxide groups, it becomes obvious that in the central Ni_2O_2 ring, the methyl groups are staggered, whereas in the outer Sn_2O_2 rings, they are eclipsed presumably due to packing effects.

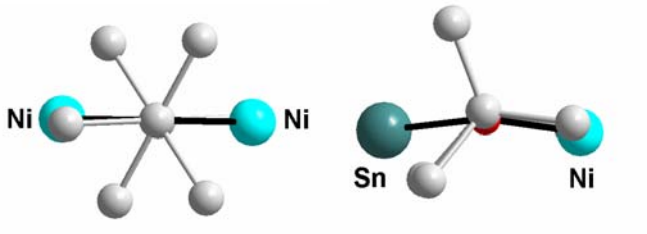

Figure 10: Projection of the four membered-rings along the C-O-O-C axis of the bridging *tert*-butoxide groups.

*Exo*cyclic *tert*-butoxide groups coordinated at the tin atoms are in a *trans* fashion to each other and, like in other compounds where a stannylene moiety is coordinated to a transition metal,[64] they are almost orthogonal to the metallic axis (Ni-Sn-O(4) = 87.47°). Measurement of the Ni/Sn-Fe angle provides a value of 136.54°, which is also typical for a low-valent tin atom in this configuration.[65]

A further comparison with the previously seen Co/Sn-Fe complex **23** delivers a surprising information: indeed, although the nickel atom has a smaller atomic radius than cobalt, the metal···metal distance in the compound is slightly larger for the Ni/Sn-Fe complex **3** (Ni···Ni = 3.013(4) Å) than for the Co/Sn-Fe complex (Co···Co = 2.977(3) Å). This observation is not valid anymore for the respective Ni···Sn and Co···Sn distances (Ni···Sn = 3.157(2) Å and Co···Sn = 3.165(1) Å). In regard to the Ni-O and Co-O bond lengths, both Ni-O(3) [and Ni-O(3')] and Ni-O(1) [and Ni-O(2)] are slightly shorter than those of the cobalt containing complex: Ni-O(3) = 1.943(2) Å, Co-O = 1.950(5) Å and Ni-O(2) = 1.981(2) Å, while Co-O = 2.005(5) Å.

The Sn-Fe bond lengths are 2.473(2) Å, which is in the range of one can expect for iron complexes with stannylene ligands.[65] As expected, the iron-carbon bonds show a slight *trans* effect due to the coordination of the low-valent tin atom: despite its axial position, the *trans* metal-carbon bond is shorter than the cis ones (*trans*-Fe-C = 1.767(1) Å, average value for the *cis*-Fe-C bonds: 1.785(1) Å). The coordination of the stannylene unit in the axial position denotes a strong σ-donor but a weak π-acceptor character.[66-68]

3.8 Synthesis of $[\{(CO)_4Fe\}_2\{Ni_2Ge_2(O\mathit{t}Bu)_8\}]$ 4

The synthesis of $[\{(CO)_4Fe\}_2\{Ni_2Ge_2(O\mathit{t}Bu)_8\}]$ **4** was achieved according the same procedure as the one described in chapter 3.6. As mentioned previously by M. Veith *et. al.*, and contrary to $Ni_2Sn_2(O\mathit{t}Bu)_8$, the starting nickel germanate complex **22** could have been obtained only in limited quantity.[23] The yield of the reaction could never be better than 30 %. The next step, which permitted to lead to the synthesis of the targeted complex, was realised straightforward as depicted in equation 6.

$Ni_2Ge_2(OtBu)_8 + 2\ Fe_2(CO)_9 \longrightarrow [\{(CO)_4Fe\}_2\{Ni_2Ge_2(OtBu)_8\}] + 2\ Fe(CO)_5$

22 **4** (Eq 6)

Two equivalents of nonacarbonyl diiron were reacted with the nickel germanate complex **22** at room temperature. The infrared monitoring of the reaction showed the simultaneous disappearance of the starting nonacarbonyl diiron and the appearance of the typical infrared pattern of tetracarbonyl fragment displaying an approximate C_{3v} symmetry.

The complex exhibits magnetic properties. The magnetic susceptibility in solution of **4** has been quantified according to the Evans method (see chapter 5.2).

3.9 Crystal structure determination of $[\{(CO)_4Fe\}_2\{Ni_2Ge_2(OtBu)_8\}]$ 4

Crystals of were $[\{(CO)_4Fe\}_2\{Ni_2Ge_2(OtBu)_8\}]$ **4** obtained from a concentrated hexane/THF 1:1 solution placed at -10°C. An appropriate crystal was isolated and anchored at a cryo-loop. From the determination and the refinement of the unit cell dimensions arose the space group $P2_1/n$ in a monoclinic crystal system. The position of each atom, except the hydrogen atoms, was anisotropicaly refined. Hydrogen atoms were refined as rigid groups with the attached carbon atoms in ideal positions. The R-value is 4.70 %. In table 9 are reported the crystal data and the structure refinement for the compound and in table 10 are reported some selected bond lengths and angles of interest.

Table 9: Crystal data and structure refinement for sh2262.

Identification code	sh2262
Empirical formula	C54 H94 Fe2 Ge2 Ni2 O18
Formula weight	1405.59
Temperature	103(2) K
Wavelength	0.71073 Å
Crystal system	Monoclinic

Space group	$P2_1/n$	
Unit cell dimensions	a = 9.8146(12) Å	α= 90°
	b = 20.943(3) Å	β= 93.092(7)°
	c = 15.6380(19) Å	γ = 90°
Volume	3209.7(7) $Å^3$	
Z	2	
Density (calculated)	1.454 Mg/m^3	
Absorption coefficient	2.003 mm^{-1}	
F(000)	1468	
Crystal size	0.45 x 0.33 x 0.1 mm^3	
Theta range for data collection	1.63 to 29.54°.	
Index ranges	-13<=h<=13, -28<=k<=27, -19<=l<=21	
Reflections collected	39642	
Independent reflections	8902 [R(int) = 0.0465]	
Completeness to theta = 29.54°	99.1 %	
Absorption correction	None	
Refinement method	Full-matrix least-squares on F^2	
Data / restraints / parameters	8902 / 0 / 328	
Goodness-of-fit on F^2	1.087	
Final R indices [I>2sigma(I)]	R1 = 0.0470, wR2 = 0.1172	
R indices (all data)	R1 = 0.0769, wR2 = 0.1381	
Largest diff. peak and hole	1.461 and -0.777 $e.Å^{-3}$	

Table 10: Selected bond lengths [Å] and angles [°] for sh2262.

Fe-C(20)	1.785(4)	Ge-O(2)	1.876(2)
Fe-C(17)	1.786(4)	Ni-O(1)	1.944(2)
Fe-C(19)	1.789(4)	Ni-O(3)	1.988(2)
Fe-C(18)	1.804(4)	Ni-O(2)	1.989(2)
Fe-Ge	2.3253(6)	O(4)-Ge-O(3)	97.5(1)
Ge-O(4)	1.776(2)	O(4)-Ge-O(2)	97.2(1)
Ge-O(3)	1.871(2)	O(3)-Ge-O(2)	79.5(1)

O(4)-Ge-Fe	129.23(8)	O(1)-Ni-O(2)	125.9(1)
O(3)-Ge-Fe	119.87(7)	O(3)-Ni-O(2)	74.13(9)
O(2)-Ge-Fe	120.87(7)	Ge-O(2)-Ni	101.8(1)
O(1)-Ni-O(3)	124.6(1)	Ge-O(3)-Ni	102.0(1)

3.9.1 Discussion of the molecular structure of $[\{(CO)_4Fe\}_2\{Ni_2Ge_2(OtBu)_8\}]$ 4

A single crystal X-ray analysis of $[\{(CO)_4Fe\}_2\{Ni_2Ge_2(OtBu)_8\}]$ **4** was carried out for unequivocal identification of the structure as shown in figure 11.

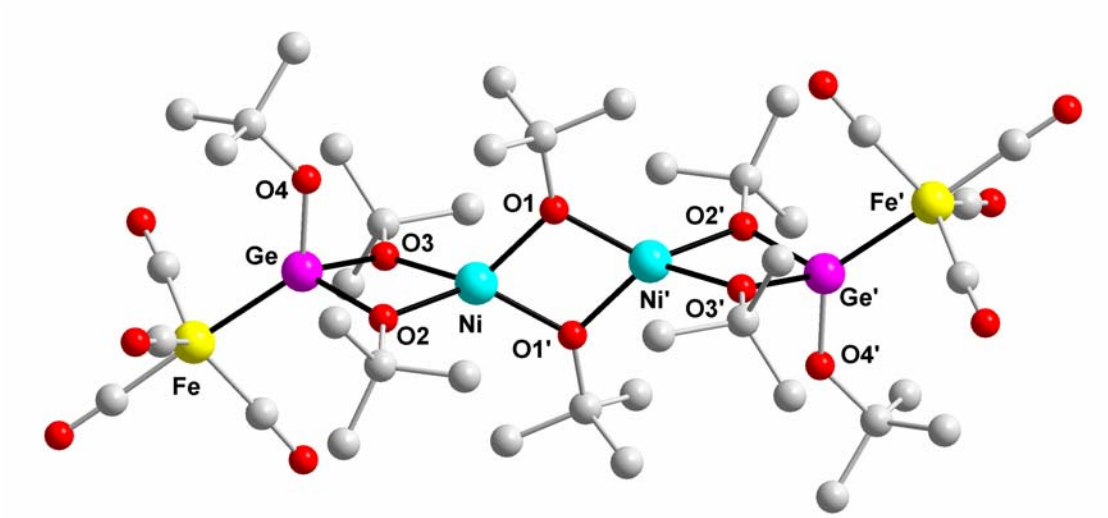

Figure 11: X-ray molecular structure of $[\{(CO)_4Fe\}_2\{Ni_2Ge_2(OtBu)_8\}]$ **4**. Hydrogen atoms are omitted for clarity and carbon atoms are not labelled.

This compound is closely related to its tin homologue despite its different space group. The difference arises most probably from the co-crystallisation of two molecules of solvent per unit cell (not shown here), which cause a different packing. The complex crystallises in the monoclinic space group $P2_1/n$. This does not signify that the molecule owns more symmetry than its tin homologue but that the packing itself is more symmetrical. Once again, the framework consists in a one-dimensional arrangement of six metallic elements. The four central metallic elements are held together by bridging alkoxide groups forming three four-membered rings oriented in a perpendicular fashion. The nickel atoms are almost tetrahedrally surrounded by a chelating germanate units $[Ge(OtBu)_3]^-$ and nickel bridging *tert*-butoxide groups. Both iron-carbonyl units are oriented *trans* to each other and their respective carbonyl groups are also staggered to each other.

Another comparison with the previously described compound **3** permits to observe, that through complexation with the iron carbonyl fragment, the germanium complex tends to fold stronger up than its tin homologue does. Indeed, the sum of angles of the Ge-O(2)-Ni-O(3) four-membered ring gives 357.54(2)° (Nickel-germanate complex with no iron coordinated: 359.62(2)°) and the measurement of the Ge-Ni-Ni' angle gives a value of 167.71° (Nickel-germanate complex with no iron coordinated: 173.24°). Due to the smaller atomic radius of germanium, the O(2)-Ge-O(3) angle is less acute than for its tin homologue: 79.54(10)° (O-Sn-O = 74.20°) A qualitative explanation may be: being smaller, germanium has "to open its arm broader", than tin. In table 11 are reported some selected bond lengths and distances of compounds **3, 4** and **23** for comparison. All distances are very close to each other, except those with involvement of the main group element: Ge-O, Ge-Fe and Ni···Ge are significantly shorter than their tin analogue (The nickel···germanium distance is slightly smaller than for the other compounds. It may be explain by the folding of the four-membered ring, which occurs and brings together both atoms in space.).
As observed for the tin homologue, the iron-carbon bonds show a *trans* influence due to the coordination of the low-valent germanium atom: despite its axial position, the *trans* metal-carbon bond is shorter than the *cis* ones. Nevertheless, the influence of the germylene moiety seems to be slightly weaker than this observed with tin: *trans*-Fe-C = 1.785(3) Å, average bond lengths: *cis*-Fe-C = 1.793(2) Å.
The shortening of the M-El(II) bonding when going from M/Sn-Fe (M = Co, Ni) to Ni/Ge-Fe (0.15 Å) reflects the difference in the valence radii of coordinated Sn(II) and Ge(II). Nevertheless, it seems like this trend of bond lengths shortening may be due to other aspects, developed in the chapter 3.10.

3.10 Simplified model of molecular orbitals related to the crystal structures of the compounds 2, 3 and 4

All the compounds **2**, **3**, and **4** display the same type of structural arrangement. In each case, the crystal structure determination delivers for the central nickel atoms a tetrahedral environment. Noteworthy, a characteristic distortion is observed in each case: the tetrahedrons show all a significant elongation along the S_4 axis. The average

value of the O-Ni-O angles can furnish a rate of the deformation. Indeed, the expected value for a perfect tetrahedron is 109.5°, while the nickel stannate complex $Ni_2Sn_2(OtBu)_8$ **21** shows an average angle of 78.31°, the nickel germanate $Ni_2Ge_2(OtBu)_8$ **11** exhibits an average value of 78.09° (This value has to be considered very carefully: the co-crystallisation phenomenon may influence drastically the packing of the molecule and thus, modify considerably the bond angles.) and the nickel plumbate complex $Ni_2Pb_2(OtBu)_8$ **2** shows an average O-Ni-O angle of 80.01°. The elongation of the tetrahedron occurs along the metallic axis of the molecule (along the axis formed by the El(II)-Ni-Ni-El(II) axis with El(II) = Ge, Sn, Pb). One will consider arbitrary this axis as being the z axis. In the graph 1, the degeneration of the d orbitals (e_g and t_{2g} levels, respectively) is reported as a function of the O-Ni-O angle, for a tetrahedral arrangement (O-Ni-O = 109.5°) as well as for a linear arrangement (O-Ni-O = 0°).[138,139]

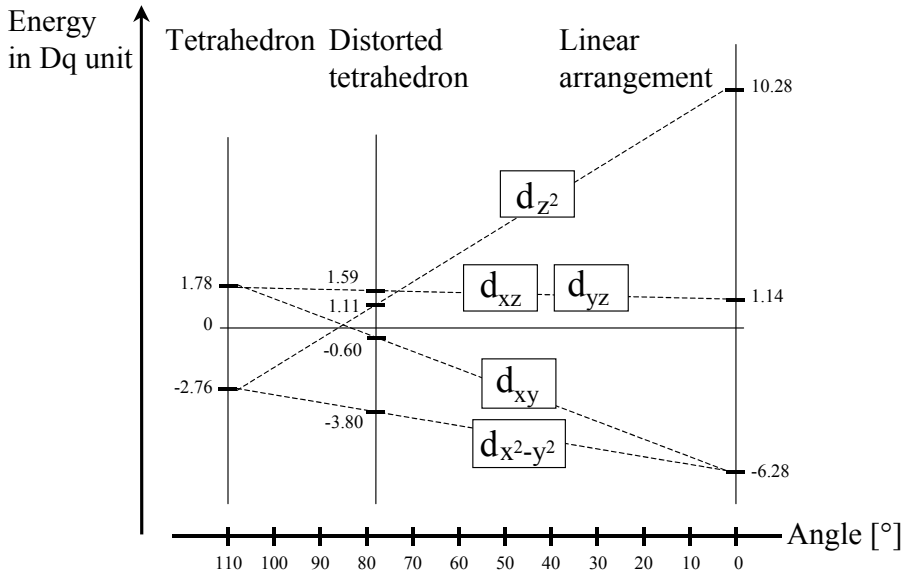

Figure 12: Dq energy values for tetrahedral and linear coordinations used as clues for the distorted tetrahedron coordination mode as a function of the value exhibited by the O-Ni-O angle in compounds of the type $[\{(CO)_4Fe\}_2\{Ni_2El_2(OtBu)_8\}]$ (with El = Sn, Ge).

If one vary the value of the O-Ni-O angle between the tetrahedral and the linear arrangement, the energy level of the degenerated e_g and t_{2g} orbitals will also vary. This very simplified and pure qualitative model of the molecular orbitals permits to level the degenerated d orbitals for the distorted tetrahedral arrangement, that one

have to deal with. According to this model, and for an angle of 77.46° (average value of the O-Ni-O angles calculated for the compounds **3** and **4**), the orbitals are ranged as follow: $d_{x^2-y^2} < d_{xy} < d_{z^2} < d_{xz} = d_{yz}$. Moreover, thanks to this model, one can observe that these high-spin nickel(II) complexes (d^8 outer electron configuration), have all their d_{z^2} orbital doubly occupied (figure 13).

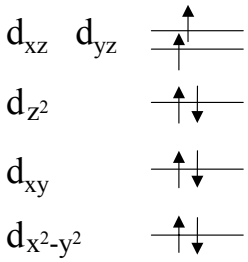

Figure 13: Degeneration and occupation of the d orbitals in a distorted tetrahedral nickel(II) complex.

Starting from this point, it is now possible to explain some trends and deviations observed in bond lengths of different complexes. For example, if one consider both complexes $Co_2Sn_2(O\textit{t}Bu)_8$ and $Ni_2Sn_2(O\textit{t}Bu)_8$,[23] the Co-O bonds are slightly larger than the Ni-O bonds. It can be explained by the fact that the nickel atom, which has a smaller atom radius, forms smaller bonds than the cobalt atom. Logically, one should expect the same trend for the Co···Co and Ni···Ni distances but this is not the case. Indeed, as the Co···Co distance is about 2.986 Å, the Ni···Ni distance measures 3.009 Å.

The simplified model of molecular orbitals above-mentioned may explain this deviation. The nickel complex $Ni_2Sn_2(O\textit{t}Bu)_8$ **21** with its d^8 outer electron configuration fills its d_{z^2} orbital with two electrons. The cobalt(II) complex displays a d^7 outer electron configuration. It means that the d_{z^2} orbital is in the case occupied by a single electron. If one compare now the experimentally measured bond lengths with the qualitative model of molecular orbitals, one observes that the repulsion between the two metallic atoms, which occurs along the metallic axis of the molecule, seems to be a function of the occupation of the d_{z^2} orbital. The same trend is observed for the iron-coordinated complexes **3** and **4** compared to the complex **23**. The distance Ni···Ni is almost constant, despite the change in the nature of the low-valent element in both complexes **3** and **4**, while the same measurement for the complex $[\{(CO)_4Fe\}_2\{Co_2Sn_2(O\textit{t}Bu)_8\}]$ **23** shows a much smaller Co···Co distance: 2.977 Å.

If one compare the compound **3** [{(CO)$_4$Fe}$_2${Ni$_2$Sn$_2$(O*t*Bu)$_8$}] with the compound **4** [{(CO)$_4$Fe}$_2${Ni$_2$Ge$_2$(O*t*Bu)$_8$}], the change of the low-valent metallic element, from tin to germanium induces also a diminution of the distance between the transition metal and the low-valent metallic element. This may be attributed to the higher electronegativity of the germanium.

The coordination with the iron-carbonyl fragment affects also the Ni···Ni distances (table 12). It seems like the iron centre withdraw some electronic density from the Ni···Ni system as the distance between the two transition metal atoms increases with the complexation (from 2.994 Å for Ni$_2$Ge$_2$(O*t*Bu)$_8$ to 3.012 Å for [{(CO)$_4$Fe}$_2${Ni$_2$Ge$_2$(O*t*Bu)$_8$}] and from 3.009 Å for Ni$_2$Sn$_2$(O*t*Bu)$_8$ to 3.013 Å for [{(CO)$_4$Fe}$_2${Ni$_2$Sn$_2$(O*t*Bu)$_8$}]. An opposite trend occurs for the Ni···Sn and Ni···Ge distances. The coordination with iron gives rise to an elongation of the Ni-O bond lengths, while the Ni···Sn and Ni···Ge distances decrease drastically. This may be due to a change in the general geometry of the molecule, in particular, to the folding up of the Ni-O-Sn-O four membered ring (Ni-O-Ge-O, respectively).

	Co/Sn-Fe **23**	Ni/Sn-Fe **3**	Ni/Ge-Fe **4**
M-O^a	1.950(5)	1.936(3)	1.933(4)
M-O^b	2.005(5)	1.980(3)	1.989(2)
El(II)-O^c	1.957(7)	1.963(2)	1.776(4)
El(II)-O^b	2.057(10)	2.052(3)	1.873(3)
El(II)-Fe	2.480(1)	2.475(2)	2.325(4)
M···M’	2.977(3)	3.013(4)	3.012(1)
M···El(II)	3.165(1)	3.157(4)	3.001

Table 11: Selected bond lengths and distances [Å] of compounds **3**, **4**, and **23** (M = Co, Ni; El(II) = Ge, Sn). O^a stands for oxygen atoms between two transition metals. O^b stands for oxygen atoms between M and El(II). O^c represents oxygen atoms of terminal alkoxide groups.

	Ni/Ge	Ni/Sn	Ni/Pb	Ni/Ge-Fe	Ni/Sn-Fe
Ni-O[a]	1.947(1)	1.937(5)	1.955(7)	1.933(4)	1.936(3)
Ni-O[b]	1.946(2)	1.964(5)	1.957(7)	1.989(2)	1.980(3)
Ni···Ni'	2.994(1)	3.009(1)	3.026(1)	3.012(1)	3.013(4)
Ni···El(II)	3.058(1)	3.211(1)	3.288(1)	3.001	3.157(4)

Table 12: Selected bond lengths and distances [Å] of compounds **11**, **21**, and **2**, **3** and **4** (El(II) = Ge, Sn). O[a] stands for oxygen atoms between two nickel atoms. O[b] stands for oxygen atoms between Ni and El(II).

3.11 Reaction between $Na_2Ge_2(OtBu)_6$ 16 and $NiBr_2$

An analogue synthetic approach as the one described in chapter 3.1 has been applied to achieve the synthesis of a new nickel germanate of type $NiGe_2(OtBu)_6$. According to the equation 7, sodium germanate was reacted with nickel bromide in the same stoechiometry but the reaction did not yield to the expected product.

$$Na_2Ge_2(OtBu)_6 + NiBr_2 \quad \not\longrightarrow \quad NiGe_2(OtBu)_6 + 2\ NaBr\downarrow \qquad \text{(Eq 7)}$$

16

After approximately 30 minutes, the reaction mixture turned from orange to blue, which indicates a change in the geometry and in the coordination of the nickel centre from bromide substituents to *tert*-butoxide groups. After 48 hours of stirring in refluxing toluene, the classical treatment was applied: filtration of the sodium bromine salt and crystallisation of the targeted product from the concentrated mother liquor. Surprisingly, the X-ray analysis of the obtained crystals revealed the formation of co-crystals of separated molecules in good yield (up to 60 %). Until now, no mechanism could have been determined for the formation of these co-crystals.

3.12 Crystal structure determination of $[Ni_2Ge_2(OtBu)_8]$ and $[Na_2Ge_2(OtBu)_6]$ 11

Crystals of $[\{Ni_2Ge_2(OtBu)_8][Na_2Ge_2(OtBu)_6\}]$ **11** were obtained from a concentrated toluene solution placed at -10°C. An appropriate crystal was isolated and anchored at a cryo-loop. From the determination and the refinement of the unit cell dimensions arose the space group $P2_1$ in a monoclinic crystal system. The position of each atom, except the hydrogen atoms, was anisotropicaly refined. Hydrogen atoms were refined as rigid groups with the attached carbon atoms in ideal positions. The R- Value is 5.34 %. In table 13 are reported the crystal data and the structure refinement for the compound and in table 14 are reported some selected bond lengths and angles of interest.

Table 13: Crystal data and structure refinement for sh2261.

Identification code	sh2261	
Empirical formula	C28 H63 Ge2 Na Ni O7	
Formula weight	738.66	
Temperature	203(2) K	
Wavelength	0.71073 Å	
Crystal system	Monoclinic	
Space group	$P2_1$	
Unit cell dimensions	a = 9.4667(7) Å	α= 90°
	b = 15.6903(12) Å	β= 93.040(4)°
	c = 25.7362(19) Å	γ = 90°
Volume	3817.4(5) $Å^3$	
Z	4	
Density (calculated)	1.285 Mg/m^3	
Absorption coefficient	2.099 mm^{-1}	
F(000)	1560	
Crystal size	0.22 x 0.4 x 0.56 mm^3	
Theta range for data collection	0.79 to 24.18°.	

Index ranges	-10<=h<=10, -17<=k<=17, -29<=l<=29
Reflections collected	33158
Independent reflections	11966 [R(int) = 0.0736]
Completeness to theta = 24.18°	99.2 %
Absorption correction	Empirical
Refinement method	Full-matrix least-squares on F^2
Data / restraints / parameters	11966 / 1 / 745
Goodness-of-fit on F^2	1.002
Final R indices [I>2sigma(I)]	R1 = 0.0534, wR2 = 0.1139
R indices (all data)	R1 = 0.0838, wR2 = 0.1270
Absolute structure parameter	0.00
Largest diff. peak and hole	1.968 and -0.514 e.Å^{-3}

Table 14: Selected bond lengths [Å] and angles [°] for sh2261.

Ge(1)-O(7)	1.823(6)	Ni(1)-O(3)	1.937(5)
Ge(1)-O(1)	1.952(5)	Ni(1)-O(1)	1.946(5)
Ge(1)-O(2)	1.958(5)	Ni(1)-O(4)	1.946(5)
Ge(2)-O(8)	1.835(6)	Ni(1)-Ni(2)	2.993(1)
Ge(2)-O(5)	1.944(5)	Ni(2)-O(3)	1.943(5)
Ge(2)-O(6)	1.956(5)	Ni(2)-O(4)	1.947(5)
Ge(3)-O(14)	1.885(5)	Ni(2)-O(6)	1.949(5)
Ge(3)-O(13)	1.887(5)	Ni(2)-O(5)	1.965(5)
Ge(3)-O(12)	1.927(6)	Na(1)-O(11)	2.241(6)
Ge(3)-Na(1)	3.264(3)	Na(1)-O(13)	2.253(6)
Ge(3)-Na(2)	3.306(3)	Na(1)-O(12)	2.370(6)
Ge(4)-O(11)	1.878(5)	Na(1)-O(10)	2.401(6)
Ge(4)-O(9)	1.883(6)	Na(1)-Na(2)	2.982(4)
Ge(4)-O(10)	1.920(5)	Na(2)-O(9)	2.219(6)
Ge(4)-Na(2)	3.263(3)	Na(2)-O(14)	2.242(6)
Ge(4)-Na(1)	3.286(3)	Na(2)-O(10)	2.363(6)
Ni(1)-O(2)	1.933(5)	Na(2)-O(12)	2.402(6)

O(7)-Ge(1)-O(1)	94.2(3)	O(1)-Ni(1)-Ni(2)	141.2(2)
O(7)-Ge(1)-O(2)	93.4(2)	O(4)-Ni(1)-Ni(2)	39.8(2)
O(1)-Ge(1)-O(2)	76.0(2)	O(3)-Ni(2)-O(4)	79.2(2)
O(8)-Ge(2)-O(5)	94.5(2)	O(3)-Ni(2)-O(6)	123.5(2)
O(8)-Ge(2)-O(6)	91.4(2)	O(4)-Ni(2)-O(6)	131.7(2)
O(5)-Ge(2)-O(6)	76.9(2)	O(3)-Ni(2)-O(5)	123.3(2)
O(14)-Ge(3)-O(13)	95.2(2)	O(4)-Ni(2)-O(5)	129.8(2)
O(14)-Ge(3)-O(12)	85.9(2)	O(6)-Ni(2)-O(5)	76.6(2)
O(13)-Ge(3)-O(12)	87.2(3)	O(3)-Ni(2)-Ni(1)	39.4(2)
O(14)-Ge(3)-Na(1)	84.5(2)	O(4)-Ni(2)-Ni(1)	39.7(2)
O(13)-Ge(3)-Na(1)	42.1(2)	O(6)-Ni(2)-Ni(1)	142.6(2)
O(12)-Ge(3)-Na(1)	45.9(2)	O(5)-Ni(2)-Ni(1)	140.0(2)
O(14)-Ge(3)-Na(2)	40.7(2)	O(11)-Na(1)-O(13)	175.0(2)
O(13)-Ge(3)-Na(2)	86.3(2)	O(11)-Na(1)-O(12)	106.6(2)
O(12)-Ge(3)-Na(2)	45.9(2)	O(13)-Na(1)-O(12)	69.3(2)
Na(1)-Ge(3)-Na(2)	53.98(7)	O(11)-Na(1)-O(10)	68.4(2)
O(11)-Ge(4)-O(9)	95.0(2)	O(13)-Na(1)-O(10)	109.3(2)
O(11)-Ge(4)-O(10)	86.9(2)	O(12)-Na(1)-O(10)	102.5(2)
O(9)-Ge(4)-O(10)	85.9(2)	O(11)-Na(1)-Na(2)	86.4(2)
O(11)-Ge(4)-Na(2)	84.8(2)	O(13)-Na(1)-Na(2)	88.8(2)
O(9)-Ge(4)-Na(2)	41.0(2)	O(12)-Na(1)-Na(2)	51.8(2)
O(10)-Ge(4)-Na(2)	45.7(2)	O(10)-Na(1)-Na(2)	50.7(2)
O(11)-Ge(4)-Na(1)	41.1(2)	O(11)-Na(1)-Ge(3)	141.3(2)
O(9)-Ge(4)-Na(1)	85.7(2)	O(13)-Na(1)-Ge(3)	34.7(2)
O(10)-Ge(4)-Na(1)	46.3(2)	O(12)-Na(1)-Ge(3)	35.7(2)
Na(2)-Ge(4)-Na(1)	54.17(7)	O(10)-Na(1)-Ge(3)	104.8(2)
O(2)-Ni(1)-O(3)	130.0(2)	Na(2)-Na(1)-Ge(3)	63.73(8)
O(2)-Ni(1)-O(1)	76.7(2)	O(11)-Na(1)-Ge(4)	33.4(1)
O(3)-Ni(1)-O(1)	129.1(2)	O(13)-Na(1)-Ge(4)	143.6(2)
O(2)-Ni(1)-O(4)	125.1(2)	O(12)-Na(1)-Ge(4)	103.9(2)
O(3)-Ni(1)-O(4)	79.3(2)	O(10)-Na(1)-Ge(4)	35.3(1)
O(1)-Ni(1)-O(4)	124.0(2)	Na(2)-Na(1)-Ge(4)	62.53(8)
O(2)-Ni(1)-Ni(2)	141.8(2)	Ge(3)-Na(1)-Ge(4)	126.3(1)
O(3)-Ni(1)-Ni(2)	39.6(1)	O(9)-Na(2)-O(14)	174.4(2)

O(9)-Na(2)-O(10)	68.8(2)	C(17)-O(5)-Ge(2)	124.5(5)
O(14)-Na(2)-O(10)	108.0(2)	C(17)-O(5)-Ni(2)	131.6(5)
O(9)-Na(2)-O(12)	108.0(2)	Ge(2)-O(5)-Ni(2)	102.9(2)
O(14)-Na(2)-O(12)	67.9(2)	C(21)-O(6)-Ni(2)	132.6(5)
O(10)-Na(2)-O(12)	102.7(2)	C(21)-O(6)-Ge(2)	123.7(5)
O(9)-Na(2)-Na(1)	88.3(2)	Ni(2)-O(6)-Ge(2)	103.1(2)
O(14)-Na(2)-Na(1)	86.2(2)	C(25)-O(7)-Ge(1)	124.6(7)
O(10)-Na(2)-Na(1)	51.8(2)	C(29)-O(8)-Ge(2)	124.8(5)
O(12)-Na(2)-Na(1)	50.8(2)	C(33)-O(9)-Ge(4)	122.1(5)
O(9)-Na(2)-Ge(4)	33.9(2)	C(33)-O(9)-Na(2)	126.6(5)
O(14)-Na(2)-Ge(4)	142.1(2)	Ge(4)-O(9)-Na(2)	105.1(3)
O(10)-Na(2)-Ge(4)	35.6(1)	C(37)-O(10)-Ge(4)	119.6(5)
O(12)-Na(2)-Ge(4)	103.8(2)	C(37)-O(10)-Na(2)	131.1(5)
Na(1)-Na(2)-Ge(4)	63.31(8)	Ge(4)-O(10)-Na(2)	98.7(2)
O(9)-Na(2)-Ge(3)	142.6(2)	C(37)-O(10)-Na(1)	121.0(5)
O(14)-Na(2)-Ge(3)	33.2(1)	Ge(4)-O(10)-Na(1)	98.4(2)
O(10)-Na(2)-Ge(3)	104.5(2)	Na(2)-O(10)-Na(1)	77.5(2)
O(12)-Na(2)-Ge(3)	35.2(1)	C(41)-O(11)-Ge(4)	124.8(5)
Na(1)-Na(2)-Ge(3)	62.29(8)	C(41)-O(11)-Na(1)	124.8(4)
Ge(4)-Na(2)-Ge(3)	125.59(9)	Ge(4)-O(11)-Na(1)	105.5(2)
C(1)-O(1)-Ni(1)	131.4(4)	C(45)-O(12)-Ge(3)	118.9(5)
C(1)-O(1)-Ge(1)	124.3(4)	C(45)-O(12)-Na(1)	130.7(5)
Ni(1)-O(1)-Ge(1)	103.4(2)	Ge(3)-O(12)-Na(1)	98.3(2)
C(5)-O(2)-Ni(1)	133.3(5)	C(45)-O(12)-Na(2)	122.5(5)
C(5)-O(2)-Ge(1)	123.0(4)	Ge(3)-O(12)-Na(2)	99.0(2)
Ni(1)-O(2)-Ge(1)	103.6(2)	Na(1)-O(12)-Na(2)	77.3(2)
C(13)-O(3)-Ni(1)	132.0(4)	C(49)-O(13)-Ge(3)	122.0(5)
C(13)-O(3)-Ni(2)	127.0(5)	C(49)-O(13)-Na(1)	126.8(5)
Ni(1)-O(3)-Ni(2)	101.0(2)	Ge(3)-O(13)-Na(1)	103.7(3)
C(9)-O(4)-Ni(1)	127.2(5)	C(53)-O(14)-Ge(3)	124.5(4)
C(9)-O(4)-Ni(2)	132.2(5)	C(53)-O(14)-Na(2)	126.6(4)
Ni(1)-O(4)-Ni(2)	100.5(2)	Ge(3)-O(14)-Na(2)	106.2(2)

3.12.1 Discussion of the molecular crystal structure of $[Na_2Ge_2(OtBu)_6]$ 11

An X-ray analysis of the single crystals obtained in Chapter 3.9 revealed the formation of co-crystals of separated molecules $[Ni_2Ge_2(OtBu)_8]$ and $[Na_2Ge_2(OtBu)_6]$ (closest intermolecular distance is 3.899(4) Å between two carbon atoms (Hydrogen are omitted in the measurement). The molecular structure of $[Ni_2Ge_2(OtBu)_8]$ and $[Na_2Ge_2(OtBu)_6]$ is depicted in figure 14.

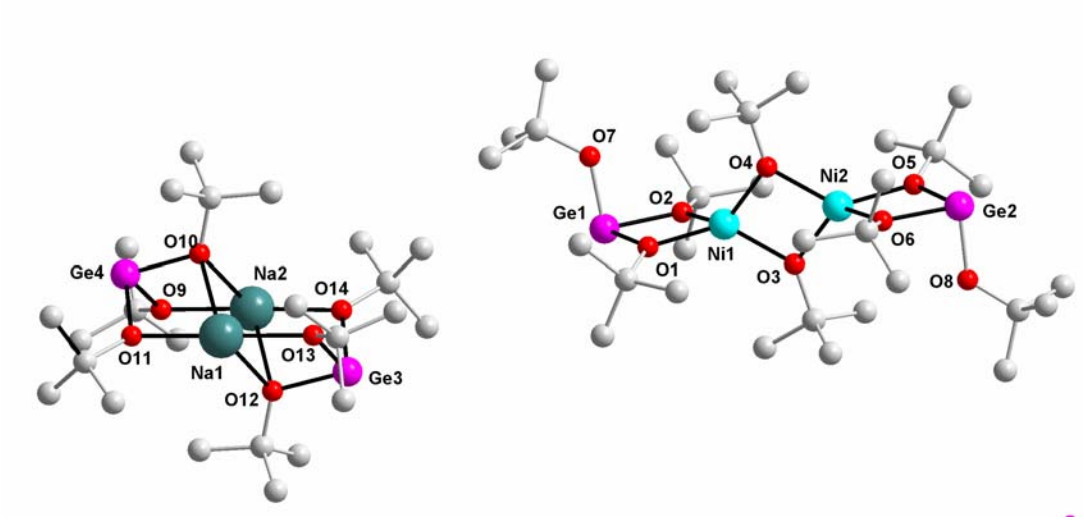

Figure 14: X-Ray molecular structure of $[Ni_2Ge_2(OtBu)_8]$ and $[Na_2Ge_2(OtBu)_6]$. Hydrogen atoms are omitted for clarity and carbon atoms are not labelled.

The two molecular compounds were already reported separately.[23,51] Thus, the following discussion will mainly focus on the deviations in the co-crystal. The main features of the structures are the same in both environments. Regarding the sodium germanate moiety, the complex consists in a centro symmetrical dimer and has amongst others similar structure analogous to those of the $Sn_2Li_2(OtBu)_6$[69] and $Pb_2Li_2(OCH(CF_3)_2)_6$ complexes.[70] It is characterised by the presence of the $Ge_2Na_2O_6$ framework consisting of two *seco*-norcubane $Ge_2Na_2O_3$ units, sharing a Na_2O_2 four membered-ring with sodium atoms in the spiro positions. The inversion centre of the molecule is located in the centre of the four-membered ring Na_2O_2. A lot of compounds providing the same composition: $M^I_2M^{II}_2(OR)_6$ have already been reported, which show all similar arrangement.[71-73] Both sodium atoms are

coordinated in a "teeter-totter" fashion like e.g. SF_4.[74] Two types of *tert*-butoxide bridging groups have to be considered here: doubly (μ_2) and triply (μ_3) bridging Na/Ge bonds show lengths of 1.865(1) Å and 1.918(1) Å, respectively. According to the Gillepsie rules, the germanium atoms in the GeO_3 fragments have a distorted tetrahedral coordination with the lone pair of electron occupying one of the coordination sites (AB_3X coordination mode). The metrical data for this moiety are consistent with the literature.[51] Bond lengths of the central four membered-ring are in the range of Na-O = 2.378(4) Å. In table 15, selected bond lengths and angles of the single compound as well as the complex taking part in the co-crystallisation phenomenon are compared

	Single $Na_2Ge_2(OtBu)_6$ **16**	Co-crystal $Na_2Ge_2(OtBu)_6$ **11**
d[Na(1)-O(10)] [Å]	2.398	2.391(2)
d[Ge(4)-O(11)] [Å]	1.894	1.865(1)
d[Ge(4)-O(10)] [Å]	1.904	1.918(1)
Na(1)-O(10)-Na(2) [°]	76.71	77.5(2)
Ge(4)-O(11)-Na(1) [°]	104.36	105.5(2)
Ge(4)-O(10)-Na(1) [°]	99.30	98.4(2)
O(10)-Na(1)-O(12) [°]	103.29	102.5(2)

Table 15: Selected bond lengths and angles for $Na_2Ge_2(OtBu)_6$ **16** and co-crystal $Na_2Ge_2(OtBu)_6$ **11**.

3.12.2 Discussion of the molecular crystal structure of $[Ni_2Ge_2(O\mathit{t}Bu)_8]$ 11

As far as the nickel-germanate unit is concerned, the compound is structurally very closely related with its single homologue **22**. Unfortunately, no suitable crystal of the single nickel germanate were ever obtained to allow an X-ray structure analysis. For this reason, we will consider, that only very weak space filling effects may participate to slightly distort the compound. As its heavier homologues (nickel stannate[23] and nickel plumbate), the main framework consists in a spiro-cyclic arrangement of metallic elements oriented in a perpendicular fashion to each other and held together by bridging *tert*-butoxide groups. All metrical data are consistent with its homologues. Nevertheless, a geometrical aspect, directly connected to the size of the low-valent element, differs from the both other homologues: the value of the angle formed by the two *endo*-cyclic oxygen atoms and the low-valent element in the four membered-ring increases drastically when the size of the low-valent element decreases. In this complex, a measurement of this angle provides 76.04° whereas the tin and lead homologues show angles of 72.12(2)° and 69.82(1)°, respectively.

3.13 Reactions between $Ni_2Sn_2(O\mathit{t}Bu)_8$ 21 and group 6 metal carbonyl complexes

3.13.1 Photolytic activation

Different synthetic strategies have been applied to achieve the formation of complexes displaying a direct bond between a group 6 metal carbonyl and the tin atom of the starting material $Ni_2Sn_2(O\mathit{t}Bu)_8$ **21**. The photolysis approach introduced by Strohmeier[75,76] was widely used in transition metal chemistry[77-79] to produce transition metal carbonyl complexes of ns^2-elements. This can be accomplished as outlined in equations 8 and 9:

$$[M(CO)_6] \xrightarrow[THF]{h\upsilon} [M(CO)_5(thf)] \quad \text{(Eq 8)}$$

$$n\,[M(CO)_5(thf)] + Ni_2Sn_2(O\mathit{t}Bu)_8 \rightarrow [\{M(CO)_5\}_n\{Ni_2Sn_2(O\mathit{t}Bu)_8\}] \quad \text{(Eq 9)}$$

With M = Cr, Mo, W and n = 1 or 2.

The infrared monitoring of the irradiation reaction permits to observe until 95 % of conversion from the starting material into the pentacarbonyl-THF adduct moiety. Then the simultaneous disappearance of the transition specie [M(CO)5(thf)] (decreasing of a very small vibrational band at 2072 cm^{-1} for $[Cr(CO)_5(thf)]$) and the anchoring of a new fragment at the pentacarbonyl metal centre [M(CO)5] (appearance of a new band at 2052 cm^{-1} still for a chrome centre) was evidenced by infrared. Very similar infrared patterns of the carbonyl-stretching region as those for pentacarbonyl fragments owning an approximate C_{4v} symmetry were obtained. [80,81] It may signify that the photogenerated [M(CO)5(thf)] specie may react to yield the desired compound. Nevertheless, after approximately one hour of stirring, and despite the fact that the reaction was not complete, the reaction mixture has always become cloudy. This may be interpreted by disproportionation phenomena of the pentacarbonyl fragment to lead to the formation of different $[M(CO)_n]$ (n = 3, 4) moieties. In their turn, these species may interact with the starting complex $Ni_2Sn_2(O\mathit{t}Bu)_8$ **21.** Until now, it was neither possible to determine a chemical composition of these compounds nor to isolate any product.

Surprisingly, a previous work concerning the complexation reactions of different stannates of alkaline earth metal with the group 6 metal carbonyls showed that through the photolysis way, no mono-coordinated complex was isolable.[82] These results are contradict by the study of M. Ehses, on very similar systems, who showed that the synthesis of the dicoordinated complexes of the type $[\{M(CO)_5\}_2\{Sn(\mu\text{-}O\mathit{t}Bu)(O\mathit{t}Bu)\}_2]$ could only be stepwise performed.[64] This tends to show, that no general rule can be formulated concerning the reactivity of this kind of complex and that only the experimental work can give insight into their behaviour.

3.13.2 Thermally induced substitution

Contrary to the reaction of $Ni_2Sn_2(OtBu)_8$ **21** with nonacarbonyl diiron, which works at room temperature, no reaction was observed at room temperature between $Ni_2Sn_2(OtBu)_8$ **21** and any of the group 6 metal carbonyl complexes (equation 10). Even after 3 days in refluxing toluene, no evidence of the formation of a pentacarbonyl fragment could have been obtained. Instead, a large part of the starting nickel complex decomposed while the metal hexacarbonyl complexes could have been recrystallised and unambiguously identified.

$$Ni_2Sn_2(OtBu)_8 + n\ M(CO)_6 \not\longrightarrow [\{M(CO)_5\}_n\{Ni_2Sn_2(OtBu)_8\}] + n\ CO\uparrow \quad \text{(Eq 10)}$$

21

With M = Cr, Mo, W; n = 1 or 2.

However, a previous study showed, that the use of a very large excess of metal carbonyl and long reaction times (80°C, 5-7 days) could induce the carbonyl substitution.[82] According to these results, the starting nickel complex $Ni_2Sn_2(OtBu)_8$ **21** was reacted with 10 equivalents of metal hexacarbonyl and placed at 70-80°C for 7 days. No reaction could have been evidenced, instead, the starting material decomposed and the metal hexacarbonyl complexes could have been recrystallised in an almost quantitative way. Other attempts were realised to reduce the reaction time: even at 120°C for two days, no reaction at the metal carbonyl centre occurred.

3.14 Reaction between $Ni_2Sn_2(OtBu)_8$ 21 and $[\{(CO)_4Fe\}_2\{Ni_2Sn_2(OtBu)_8\}]$ 3

An alternative method to create new complexes displaying a one-dimensional arrangement of metallic elements was to react the diiron coordinated complex **3** with its uncoordinated homologue **21**. Nevertheless, the infrared monitoring of the reaction

revealed that the displacement of a carbonyl group by the complex $Ni_2Sn_2(OtBu)_8$ **21** was not feasible (equation 11).

$$Ni_2Sn_2(OtBu)_8 + [\{(CO)_4Fe\}_2\{Ni_2Sn_2(OtBu)_8\}] \not\longrightarrow [\{Ni_2Sn_2(OtBu)_8\}\{(CO)_3Fe\}\{Ni_2Sn_2(OtBu)_8\}\{(CO)_4Fe\}] + CO\uparrow \quad \text{(Eq 11)}$$

Instead, a very probably reaction of conmutation took place to achieve the formation of the monocoordinated complex according to the equation 12.

$$Ni_2Sn_2(OtBu)_8 + [\{(CO)_4Fe\}_2\{Ni_2Sn_2(OtBu)_8\}] \longrightarrow 2\,[\{(CO)_4Fe\}\{Ni_2Sn_2(OtBu)_8\}] \quad \text{(Eq 12)}$$

Until now, it was neither possible to determine an exact chemical composition of these compounds nor to isolate any product.

3.15 Reaction between $NiSn_2(OtBu)_6$ 1 and $[M(CO)_4(nbd)]$

Different attempts aiming to elongate the metallic sequence of the complex $NiSn_2(OtBu)_6$ **1** were realised with the use of a "diactivated" metal carbonyl complex. According to an established procedure, chromium or molybdenum hexacarbonyl were reacted with norbornadiene (nbd) to form a *cis*-substituted tetracarbonyl complex of the general formula $[M(CO)_4(nbd)]$.[83] This complex was then allowed to react with the nickel complex $NiSn_2(OtBu)_6$ **1**.

The norbornadiene displacement requires high temperature and long reaction time. The use of solvents containing aromatic systems such as benzene or toluene is to be avoided as they interfere in the reaction mechanism. Therefore a solvent of type benzene F having a high boiling point and no π-system is appropriate. This method permits to create molecules displaying *cis* or *trans* arrangements at the transition metal centre and having a local symmetry of either C_{2v} or D_{4h}, respectively.

The reactions between $NiSn_2(OtBu)_6$ **1** and $[M(CO)_4(nbd)]$ were carried out according to an established procedure.[84] Two equivalents of the complex

$NiSn_2(OtBu)_6$ **1** were reacted with $[M(CO)_4(nbd)]$ in benzene F for 24 hours at 80°C. As shown in equation 13, no selective displacement of the norbornadiene ligand was observed.

$$2\ NiSn_2(OtBu)_6 + [M(CO)_4(nbd)] \not\longrightarrow [(CO)_4M\{NiSn_2(OtBu)_6\}_2] + nbd \quad \text{(Eq 13)}$$

With M = Cr, Mo.

Surprisingly, an unexpected tin-molybdenum complex could have been isolated from the crude. The weak yield (under 10 %) indicates that it is a side product. Until now, no reaction mechanism could have been found for the formation of this complex.

3.16 Crystal structure determination of $[\{Mo_2(\mu\text{-}O)_2\}(\mu_3\text{-}O)_2\{Sn_3(\mu\text{-}OtBu)_5\}_2]$ 7

Crystals of **7** were obtained from a concentrated petroleum ether solution placed at -10°C. An appropriate crystal was isolated and anchored at a cryo-loop. From the determination and the refinement of the unit cell dimensions arose the space group $P2_1/n$ in a monoclinic crystal system. The position of each atom, except the hydrogen atoms, was anisotropicaly refined. Hydrogen atoms were refined as rigid groups with the attached carbon atoms in ideal positions. The R-value is 10.99 %. This relative high value is due to the presence of residual electron densities, which do not match with the elaborated model. These residual electron densities could not have been unambiguously assigned to atoms to build a structure, which would make a sense from a chemical point of view. In table 16 are reported the crystal data and the structure refinement for the compound and in table 17 are reported some selected bond lengths and angles of interest.

Table 16: Crystal data and structure refinement for sh2256.

Identification code	sh2256
Empirical formula	C40 H90 Mo2 O16 Sn6

Formula weight	1731.14	
Temperature	103(2) K	
Wavelength	0.71073 Å	
Crystal system	Monoclinic	
Space group	$P2_1/n$	
Unit cell dimensions	a = 10.2169(6) Å	α= 90°.
	b = 26.9659(16) Å	β= 10.298(3)°.
	c = 11.7063(8) Å	γ = 90°.
Volume	3024.9(3) $Å^3$	
Z	2	
Density (calculated)	1.901 Mg/m^3	
Absorption coefficient	2.889 mm^{-1}	
F(000)	1684	
Crystal size	0.2 x 0.3 x 0.45 mm^3	
Theta range for data collection	1.51 to 29.63°.	
Index ranges	-14<=h<=13, -37<=k<=35, -16<=l<=15	
Reflections collected	36193	
Independent reflections	8476 [R(int) = 0.0598]	
Completeness to theta = 29.63°	99.3 %	
Absorption correction	Multi scan	
Refinement method	Full-matrix least-squares on F^2	
Data / restraints / parameters	8476 / 0 / 305	
Goodness-of-fit on F^2	1.131	
Final R indices [I>2sigma(I)]	R1 = 0.1099, wR2 = 0.2804	
R indices (all data)	R1 = 0.1325, wR2 = 0.2940	
Extinction coefficient	0.00020(8)	
Largest diff. peak and hole	7.403 and -2.890 $e.Å^{-3}$	

Table 17: Selected bond lengths [Å] and angles [°] for sh2256.

Sn(1)-O(1)	2.23(1)	O(3)-Sn(2)-O(6)	96.2(5)
Sn(1)-O(5)	2.32(1)	O(1)-Sn(3)-O(2)	78.7(4)
Sn(1)-O(2)	2.34(1)	O(1)-Sn(3)-O(6)	75.6(4)
Sn(1)-O(4)	2.35(1)	O(2)-Sn(3)-O(6)	91.4(5)
Sn(1)-O(3)	2.41(1)	O(7)-Mo-O(8)#1	100.2(5)
Sn(2)-O(1)	2.10(1)	O(7)-Mo-O(8)	99.1(5)
Sn(2)-O(3)	2.11(1)	O(8)#1-Mo-O(8)	97.3(4)
Sn(2)-O(6)	2.19(1)	O(7)-Mo-O(4)	100.9(5)
Sn(3)-O(1)	2.09(1)	O(8)#1-Mo-O(4)	91.4(5)
Sn(3)-O(2)	2.11(1)	O(8)-Mo-O(4)	156.4(5)
Sn(3)-O(6)	2.23(1)	O(7)-Mo-O(5)	99.5(5)
Mo-O(7)	1.71(1)	O(8)#1-Mo-O(5)	158.9(5)
Mo-O(8)#1	1.94(1)	O(8)-Mo-O(5)	86.7(4)
Mo-O(8)	1.98(1)	O(4)-Mo-O(5)	77.7(5)
Mo-O(4)	2.06(1)	O(7)-Mo-O(1)	168.0(5)
Mo-O(5)	2.13(1)	O(8)#1-Mo-O(1)	91.1(4)
Mo-O(1)	2.26(1)	O(8)-Mo-O(1)	83.1(4)
Mo-Mo#1	2.584(3)	O(4)-Mo-O(1)	74.8(4)
O(8)-Mo#1	1.94(1)	O(5)-Mo-O(1)	68.8(4)
O(1)-Sn(1)-O(5)	66.2(4)	O(7)-Mo-Mo#1	104.7(4)
O(1)-Sn(1)-O(2)	71.1(4)	O(8)#1-Mo-Mo#1	49.3(3)
O(5)-Sn(1)-O(2)	79.7(4)	O(8)-Mo-Mo#1	48.1(3)
O(1)-Sn(1)-O(4)	70.1(4)	O(4)-Mo-Mo#1	136.0(4)
O(5)-Sn(1)-O(4)	68.7(4)	O(5)-Mo-Mo#1	131.0(3)
O(2)-Sn(1)-O(4)	137.2(4)	O(1)-Mo-Mo#1	85.6(3)
O(1)-Sn(1)-O(3)	68.6(4)	Sn(3)-O(1)-Sn(2)	107.7(5)
O(5)-Sn(1)-O(3)	134.7(4)	Sn(3)-O(1)-Sn(1)	105.3(4)
O(2)-Sn(1)-O(3)	86.7(4)	Sn(2)-O(1)-Sn(1)	110.5(5)
O(4)-Sn(1)-O(3)	95.4(4)	Sn(3)-O(1)-Mo	110.4(5)
O(1)-Sn(2)-O(3)	76.8(4)	Sn(2)-O(1)-Mo	125.9(5)
O(1)-Sn(2)-O(6)	76.3(5)	Sn(1)-O(1)-Mo	94.8(4)

C(1)-O(2)-Sn(3)	130.2(1)	Mo-O(4)-Sn(1)	96.5(5)
C(1)-O(2)-Sn(1)	128.3(1)	C(13)-O(5)-Mo	126.6(1)
Sn(3)-O(2)-Sn(1)	100.7(5)	C(13)-O(5)-Sn(1)	127.5(1)
C(5)-O(3)-Sn(2)	125.0(1	Mo-O(5)-Sn(1)	95.5(4)
C(5)-O(3)-Sn(1)	130.8(1)	C(17)-O(6)-Sn(2)	124.7(1)
Sn(2)-O(3)-Sn(1)	103.4(5)	C(17)-O(6)-Sn(3)	128.7(1)
C(9)-O(4)-Mo	131.9(1)	Sn(2)-O(6)-Sn(3)	99.6(5)
C(9)-O(4)-Sn(1)	130.0(1)	Mo#1-O(8)-Mo	82.7(4)

Symmetry transformations used to generate equivalent atoms:

#1 -x+2,-y,-z

3.16.1 Discussion of the molecular crystal structure of $[\{Mo_2(\mu\text{-}O)_2\}(\mu_3\text{-}O)_2\{Sn_3(\mu\text{-}O\mathit{t}Bu)_5\}_2]$ 7

A single crystal X-ray analysis of **7** was carried out for unequivocal identification of the structure as depicted in figure 15.

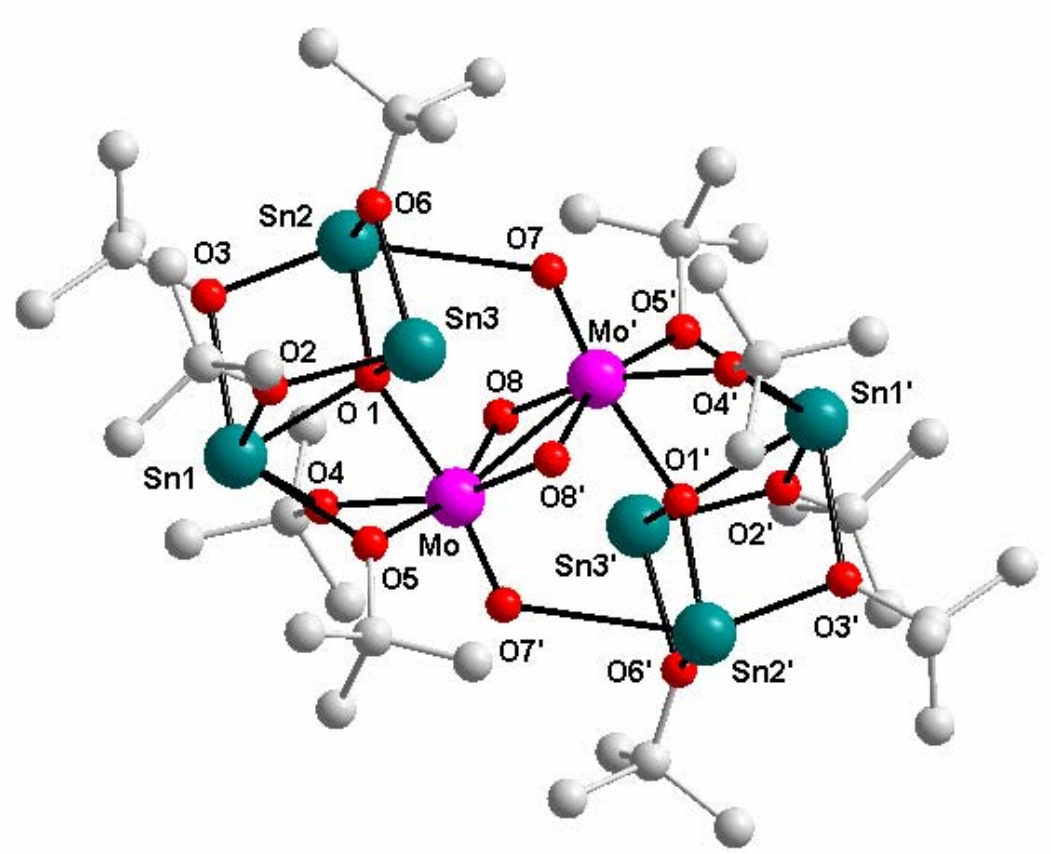

Figure 15: X-ray molecular structure of **7**. Hydrogen atoms are omitted for clarity and carbon atoms are not labelled.

The inversion centre is situated in the middle of the Mo-Mo' bond. Both of the molybdenum atoms are situated in slightly distorted octahedral coordination sites (see figure 16), which bond an Sn_3O_4 norcubane unit, respectively. Bond lengths and angles are consistent with this description: Mo-O(8) = 1.98(1) Å, Mo-O(8') = 1.94(1) Å, Mo-O(4) = 2.06(1) Å, Mo-O(5) = 2.13(1) Å correspond to the bonds situated in the equatorial plane.

In regard to the axial bonds, the measurement provides very different lengths. This may be explained by the double bond character of the Mo-O(7) bond. Mo-O(1) shows a length of 2.278(2) Å , which is in accord with its axial situation instead of Mo-O(7), which measures only 1.708(2) Å and thus, reveals a nature of double bond.

In regard to the composition and the structure of the complex, it seems like one have to deal with molybdenum atoms in the oxidation state (V). Moreover, a di μ-oxo bridge, is a well-known structural motif in molybdenum(V) compounds.[132,133] The distance Mo-Mo' is about 2.584(3) Å, nevertheless, the relation bond length-bond strength does not allow here to conclude unambiguously about the nature of the bonding between the two molybdenum atoms, specially in their high oxidation state. The uncommonly long bond length Sn(2)-O(7) (Sn(2)-O(7) = 2.865 Å) may be explained by the delocalisation of an electron pair of O(7) to stabilise the tin centre and may confirm the double bond character of the Mo-O(7) bond. The different bond angles around the molybdenum centres are also consistent with the description of an octahedral coordination. Indeed, all O-Mo-O angles contained in the equatorial plane show values close to the expected 90°: O(8)-Mo-O(8') = 97.3(4)°, O(4)-Mo-O(5) = 77.7(5)°, O(8)-Mo-O(5) = 86.7(4)°, O(8')-Mo-O(4) = 91.4(5)°. In regard to the axial sites, the O(7')-Mo-O(1) angle shows a value of 168.0(5)°.

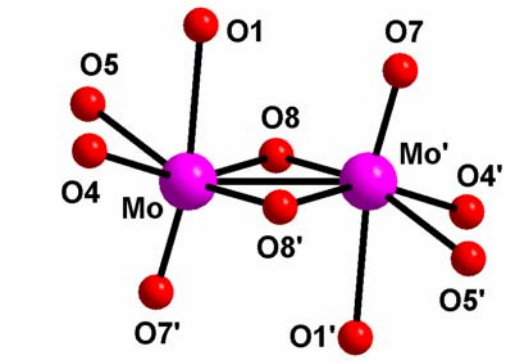

Figure 16: Distorted hexagonal coordination geometry of the central molybdenum atoms of **7**

The rest of the molecule consists in two Sn_3O_4 norcubane units bonded to the central metallic core by a corner [O(1) and O(1')] and two *tert*-butoxide bridging groups (O(4)-*tert*-butyl and O(5)-*tert*-butyl). Both of the norcubane units are built by three Sn_2O_2 motifs. O(1) and O(1') atoms, which are bonding the norcubane units to the

central part of the compound, show tetrahedral coordinations: O(1)-Sn(2) = 2.10(1) Å, O(1)-Sn(3) = 2.09(1) Å, O(1)-Sn(1) = 2.23(1) Å and O(1)-Mo = 2.26(1) Å The Sn-O bond lengths within the norcubane units are all in the same range: Sn(3)-O(2) = 2.11(1) Å, Sn(1)-O(2) = 2.34(1) Å, Sn(3)-O(6) = 2.23(1) Å, Sn(2)-O(6) = 2.19(1) Å, Sn(1)-O(3) = 2.41(1) Å, Sn(2)-O(3) = 2.11(1) Å.

3.17 Synthesis of $[Sn(\mu\text{-}O\textit{i}Pr)_2]_\infty$ 5

In a typical alcoholysis reaction, the stannylene $Sn(N\textit{t}Bu)_2Si(CH_3)_2$ **12**[85] was reacted with freshly distilled *iso*-propanol. The ligand exchange took place in an exothermic reaction and the NMR monitoring of the reaction revealed that the displacement of the amido ligands is almost complete, the free diamine $(NH\textit{t}Bu)_2Si(CH_3)_2$ being the sole byproduct (equation 14).

$$\underset{\mathbf{12}}{n\ Sn(N\textit{t}Bu)_2Si(CH_3)_2} + 2n\ HO\textit{i}Pr \longrightarrow \underset{\mathbf{5}}{[Sn(\mu\text{-}O\textit{i}Pr)_2]_n} + n\ \underset{\mathbf{25}}{(NH\textit{t}Bu)_2Si(CH_3)_2} \quad \text{(Eq 14)}$$

The ^{1}H-NMR and ^{13}C-NMR solution spectra support the formation of a single product. Nevertheless, variable temperature ^{119}NMR solution spectra show a considerable dependence of the chemical shift and the line width towards the temperature (Figure 17). A reversible drift of 15 ppm of the signal is occurring going from 293 K to 363 K.

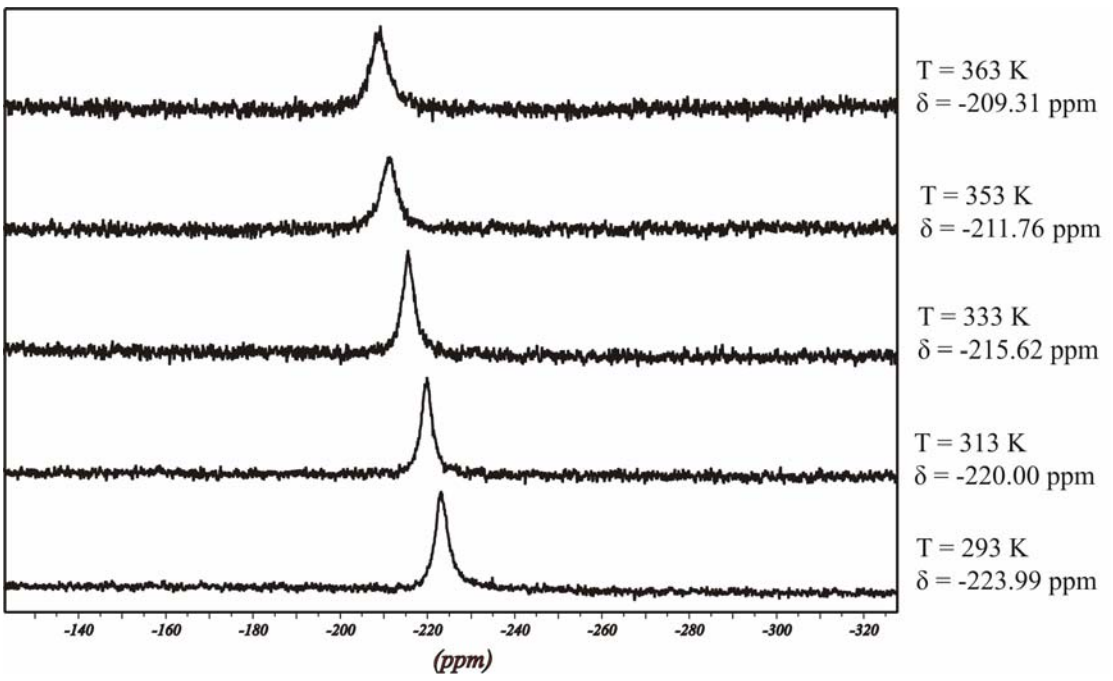

Figure 17: Temperature variable ^{119}Sn NMR solution spectra of **5** recorded between 293 K and 363 K (d_8 toluene).

On the graph 2 is represented the chemical shift as a function of the temperature. As can be seen, the drift of the resonance band follows a linear function: $y = ax + b$ (where $a = 0.18$; $b = -271.23$).

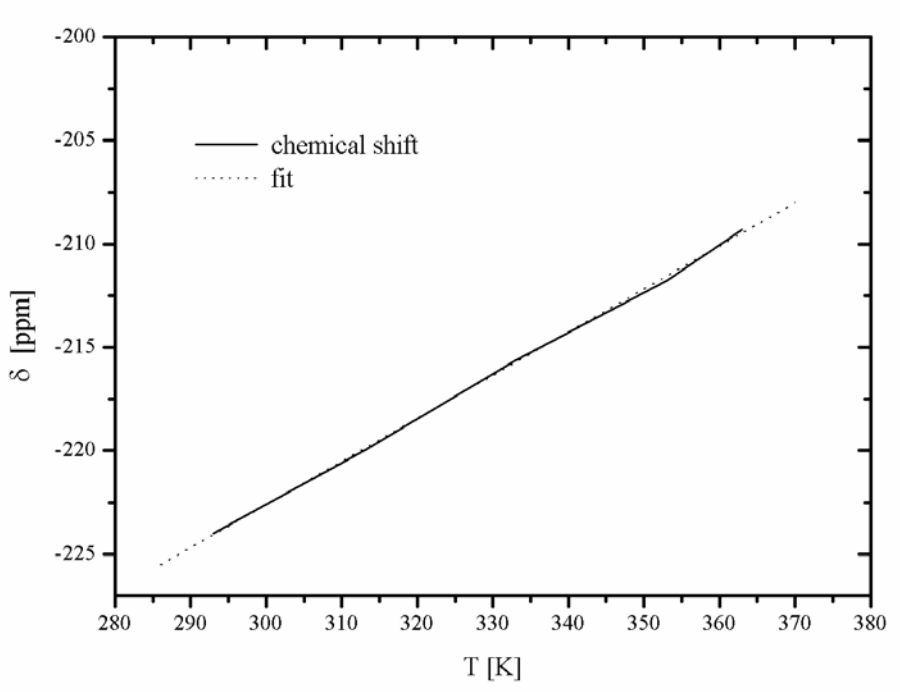

Graph 2: Chemical shift of the resonance band of **5** as a linear function of the temperature.

A more diluted probe was realised to study the behaviour of the compound at lower temperature. As can be seen on figure 18, the same trend is observed. The chemical shift of the resonance band as well as the line width show a pronounced dependence towards temperature.

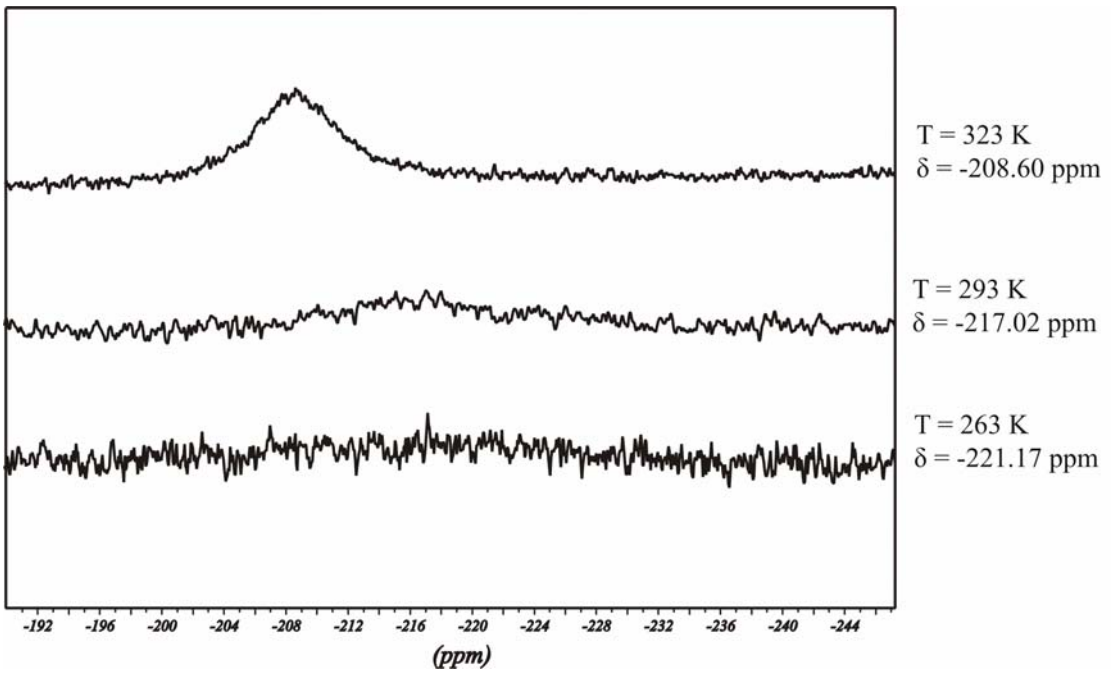

Figure 18: Temperature variable ^{119}Sn NMR solution spectra of **5** recorded between 263 K and 323 K (d_8 toluene).

The chemical shift is going from -221.17 ppm to -208.60 ppm, while the temperature is going from 263 K to 323 K. As expected, the observed trend is the same at low temperature as well as at high temperature. This denotes notable changes in the geometry and in the coordination number around the tin nuclei.

As can be seen on the graph 3, the chemical shift of the signal can be described once again as a linear function of the temperature ($y = ax + b$ where $a = 0.22$; $b = -275.2$). The coefficient a, measured at low temperature, is noteworthy close to the one measured at higher temperature.

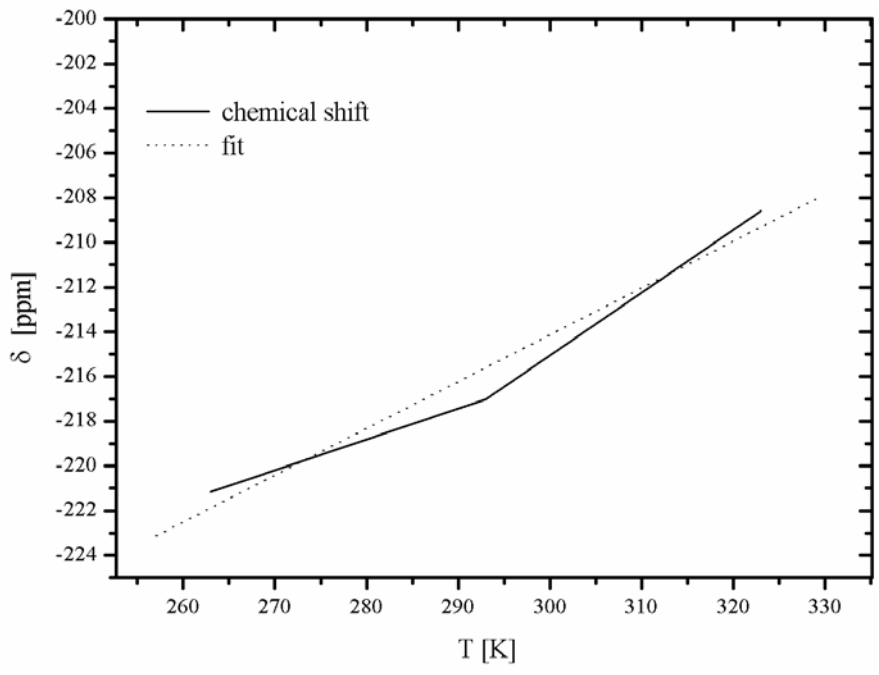

Graph 3: Chemical shift of the resonance band of **5** as a function of the temperature.

As explained in the next chapter, the *iso*-propoxystannylene **5** displays a polymeric structure. Thus, the dependence of the chemical shift towards the temperature may result from a change in the degree of oligomerisation of the compound. At low temperature, the complex may have a large polymeric character, which requires a statistically large number of four-coordinated tin atoms and thus, implicates an upfield drift. On the other hand, at higher temperature, the polymeric integrity of the complex is broken and a lot of smaller oligomeric species are formed. Statistically, a larger number of three-coordinated tin atoms are present and thus, a displacement of the resonance band in the low-field region is observed.

A measurement of a very diluted probe and of a concentrated probe at the same temperature permitted to confirm this assumption. Indeed, at 293 K, the concentrated probe provided a signal at -224 ppm, whereas the diluted probe exhibits a resonance band at -217 ppm. As the degree of oligomerisation in a concentrated medium is higher than in a lower concentrated one, the chemical shift of the tin nuclei may be expected in a higher-field region for a concentrated sample than for a low concentrated sample.

3.18 Crystal structure determination of $[Sn(\mu\text{-}O\textit{i}Pr)_2]_\infty$ 5

Crystals of $[Sn(\mu\text{-}O\textit{i}Pr)_2]_\infty$ **5** were obtained from a concentrated toluene solution placed at -10°C. An appropriate crystal was isolated and anchored at a cryo-loop. From the determination and the refinement of the unit cell dimensions arose the space group $P2_1/c$ in a monoclinic crystal system. The position of each atom, except the hydrogen atoms, was anisotropicaly refined. Hydrogen atoms were refined as rigid groups with the attached carbon atoms in ideal positions. The R-value is 2.01 %. In table 18 are reported the crystal data and the structure refinement for the compound and in table 19 are reported some selected bond lengths and angles of interest.

Table 18: Crystal data and structure refinement for sh2171a.

Identification code	sh2171a	
Empirical formula	C12 H28 O4 Sn2	
Formula weight	473.72	
Temperature	293(2) K	
Wavelength	0.71073 Å	
Crystal system	Monoclinic	
Space group	$P2_1/c$	
Unit cell dimensions	a = 17.823(4) Å	α= 90°
	b = 7.855(2) Å	β= 99.85(3)°
	c = 6.3440(10) Å	γ = 90°
Volume	875.1(3) $Å^3$	
Z	2	
Density (calculated)	1.798 Mg/m^3	
Absorption coefficient	2.858 mm^{-1}	
F(000)	464	
Crystal size	0.793 x 0.302 x 0.278 mm^3	
Theta range for data collection	2.84 to 31.50°.	
Index ranges	-26<=h<=26, -11<=k<=11, -9<=l<=9	
Reflections collected	13163	
Independent reflections	2898 [R(int) = 0.0226]	

Completeness to theta = 31.50°	99.5 %
Absorption correction	Multi scan
Refinement method	Full-matrix least-squares on F^2
Data / restraints / parameters	2898 / 0 / 86
Goodness-of-fit on F^2	1.103
Final R indices [I>2sigma(I)]	R1 = 0.0201, wR2 = 0.0509
R indices (all data)	R1 = 0.0215, wR2 = 0.0519
Largest diff. peak and hole	0.920 and -1.468 e.Å^{-3}

Table 19: Selected bond lengths [Å] and angles [°] for sh2171a.

Sn(1)-O(1)	2.139(1)	O(2)#1-Sn(1)-O(1)#1	70.17(5)
Sn(1)-O(2)#1	2.148(1)	O(2)-Sn(1)-O(1)#1	158.41(5)
Sn(1)-O(2)	2.369(1)	C(1)-O(1)-Sn(1)	123.1(1)
Sn(1)-O(1)#1	2.452(1)	C(1)-O(1)-Sn(1)#2	125.1(1)
O(1)-Sn(1)#2	2.452(1)	Sn(1)-O(1)-Sn(1)#2	107.34(5)
O(2)-Sn(1)#2	2.148(1)	C(4)-O(2)-Sn(1)#2	124.9(1)
O(1)-Sn(1)-O(2)#1	93.59(6)	C(4)-O(2)-Sn(1)	120.6(1)
O(1)-Sn(1)-O(2)	71.99(5)	Sn(1)#2-O(2)-Sn(1)	110.05(5)
O(2)#1-Sn(1)-O(2)	93.43(4)		
O(1)-Sn(1)-O(1)#1	94.48(4)		

3.18.1 Discussion of the molecular crystal structure of $[Sn(\mu\text{-}O\textit{i}Pr)_2]_\infty$ 5

A single crystal X-ray analysis of $[Sn(\mu\text{-}O\textit{i}Pr)_2]_\infty$ **5** was carried out for unequivocal identification of the molecular structure as shown in figure 19.

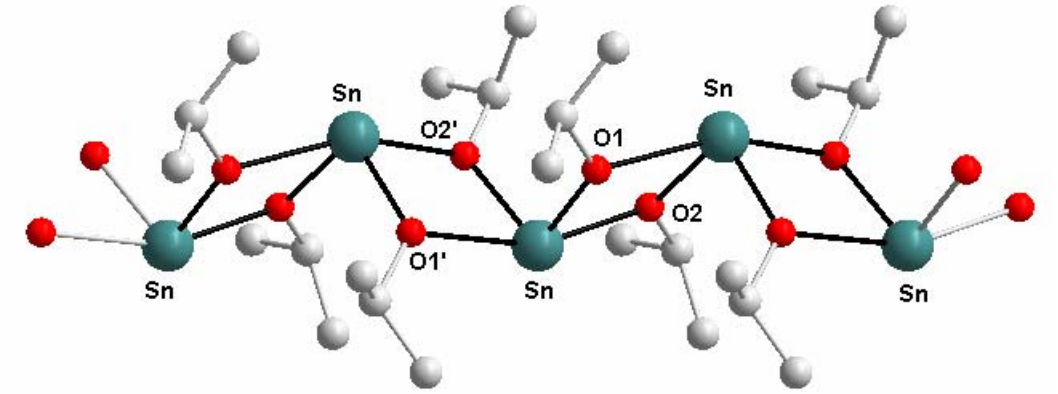

Figure 19: X-ray crystal structure of $[Sn(\mu\text{-}O\textit{i}Pr)_2]_\infty$ **5**. Hydrogen atoms are omitted for clarity and carbon atoms are not labelled.

Each metal centre is coordinated by four O*i*Pr bridging ligands, forming a zig-zag chain. It fits well in a series of tin(II) alkoxides with different steric demands of the residues on oxygen.

The methyl and linear homologues precipitate as amorphous solids for which various studies suggest a polymeric structure. Neopentyl derivative crystallises in polymeric chains of equal $Sn(OR)_2$ units: the Sn-O distances are all in the same range (2.15 Å). Increasing steric bulk splits the polymeric chains into dimers (R = *t*Bu) and monomers (R = $OC_6H_2(CH_3)$-4-*t*Bu_2-2,6). In that series of compounds, $[Sn(\mu\text{-}O\textit{i}Pr)_2]_\infty$ **5** is situated between the neopentyl and *t*Bu derivatives: the two different classes of Sn-O bond lengths suggest that monomeric units (d(Sn-O) = 2.139(1) Å; 2.148(1) Å) are linked together by weaker contacts (d(Sn-O) = 2.369(1) Å; 2.452(1) Å) to build polymeric chains.

From the data available, it can be deduced that for alkylic residues, the steric hindrance of the α-carbon atom is determining the degree of oligomerisation. For aromatic residues, the bulk of the *ortho* substituents is decisive. In that respect, it is

interesting to note that dithiophene residues on tin(II) are able to form an equilibrium between monomers and dimers in coordinating solvents.[86]

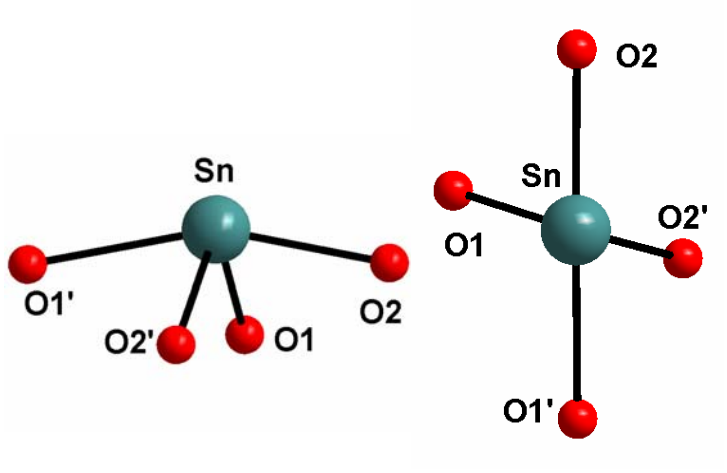

Figure 20: Coordination geometry at the tin(II) centre for $[Sn(\mu\text{-}O\textit{i}Pr)_2]_\infty$ **5**.

According to T. J. Boyle *et al.*, who reported a polymeric tin(II) alkoxide with neopentoxide ligands of the general formula $[Sn(\mu ONep)_2]_\infty$,[87] if the free electron pair of each Sn(II) metal centre is considered in the overall geometry (i.e. stereochemically active), a trigonal bipyramidal arrangement is observed with the free electron pair located in one of the equatorial sites. Nevertheless, this description requires typical angles values which are not verified here: O(1)-Sn-O(2') = 93.59(6)° (instead of 90° that one would expect), O(2)-Sn-O(2') = 93.43(4)° (90° would be expected), O(2)-Sn-O(1') = 158.41(5)° (180° would be expected), O(2')-Sn-O(1') = 70.17(5)° (instead of 90°), O(1)-Sn-O(2) = 71.99(5)° (instead of 90°) and O(1)-Sn-O(1') = 94.48(4)° (instead of 90°). With regard to the figure 20, it appears that the coordination mode might be described as a distorted square bipyramidal where two corners would be missing like SF_4. The equatorial plane O(1')-Sn-O(2) deviates severely from orthogonality in regard to the axial axis.

Within the bond lengths, the Sn-O bonds constituting the core of the polymer are more or less constant in the case of $[Sn(\mu ONep)_2]_\infty$ (largest difference is about 0.289 Å), whereas in the case of $[Sn(\mu\text{-}O\textit{i}Pr)_2]_\infty$ **5**, the Sn-O bonds are more strongly influenced by the ligands around and can be divided in two different groups: the short ones Sn-O(2') = 2.148(1) Å and Sn-O(1) = 2.139(1) Å correspond to the bonds situated in the equatorial plane and the long ones: Sn-O(2) = 2.369(1) Å and Sn-O(1') = 2.52(3) Å, which correspond to the axial bonds. This species may be described as a polymer where each monomer is strongly influenced by its

neighbouring units and may represent the intermediary state between the dimeric compound [Sn(μ-O*t*Bu)(O*t*Bu)]$_2$ **13**[88] where any polymerisation is prohibited by the steric hindrance of the *tert*-butoxide groups and [Sn(μONep)$_2$]$_\infty$ where polymerisation is allowed. The distance between two tin atoms is about 3.684 Å. and the angle Sn-Sn-Sn is around 118.85°.

The data for this compound are consistent with literature reports on tin alkoxy compounds.[89-92]

3.19 Synthesis of [Sn{(μ-O*i*Pr)$_2$Sn(O*i*Pr)Fe(CO)$_4$}$_2$] 6

The polymeric chain [Sn(μ-O*i*Pr)$_2$]$_\infty$ **5** was allowed to react with nonacarbonyl diiron. The aim of this experiment was to study the behaviour of the polymeric chain towards a transition metal carbonyl fragment. Different reaction pathways were intended. Would the polymeric chain remain its structural integrity and allow the coordination of iron carbonyl fragments at the same time? Would the coordination reaction destroy the polymeric architecture of the starting compound and lead to discrete molecular units? And in this case, how do these molecular fragments can be stabilised? As shown in equation 15, the reaction was first performed with a stoechiometry 1:1

$$[Sn(\mu\text{-}O\textit{i}Pr)_2]_n + n\ Fe_2(CO)_9 \longrightarrow [Sn\{(\mu\text{-}O\textit{i}Pr)_2Sn(O\textit{i}Pr)Fe(CO)_4\}_2] + n\ Fe(CO)_5$$

5 **6** (Eq 15)

The ^{119}Sn NMR monitoring of the reaction revealed the formation of two new resonance bands at +97 ppm and -550 ppm with a relative intensity 2 for 1,which supports the proposed equation. The ^{13}C NMR solution spectrum shows only two resonance bands in the carbonyl region. This indicates that the rotation around the transition metal-tin bond is unhindered. Moreover, the observed ^{13}C deshielding is in agreement with the expected π-backbonding[93] and matches to other reported tin-tetracarbonyl iron fragments displaying a C_{3V} symmetry.[94]

3.20 Crystal structure determination of [Sn{(μ-O*i*Pr)$_2$Sn(O*i*Pr)Fe(CO)$_4$}$_2$] 6

Crystals of [Sn{(μ-O*i*Pr)$_2$Sn(O*i*Pr)Fe(CO)$_4$}$_2$] **6** were obtained from a concentrated toluene solution placed at -10°C. An appropriate crystal was isolated and anchored at a cryo-loop. From the determination and the refinement of the unit cell dimensions arose the space group P2$_1$/n in a monoclinic crystal system. The position of each atom, except the hydrogen atoms, was anisotropicaly refined. Hydrogen atoms were refined as rigid groups with the attached carbon atoms in ideal positions. The R-value is 2.37 %. In table 20 are reported the crystal data and the structure refinement for the compound and in table 21 are reported some selected bond lengths and angles of interest.

Table 20: Crystal data and structure refinement for sh2388.

Identification code	sh2388	
Empirical formula	C26 H42 Fe2 O14 Sn3	
Formula weight	1046.37	
Temperature	103(2) K	
Wavelength	0.71073 Å	
Crystal system	Monoclinic	
Space group	P2$_1$/n	
Unit cell dimensions	a = 13.4599(6) Å	α= 90°
	b = 16.2430(7) Å	β=103.866(2)°
	c = 18.0443(8) Å	γ= 90°
Volume	3830.0(3) Å^3	
Z	4	
Density (calculated)	1.815 Mg/m^3	
Absorption coefficient	2.725 mm^{-1}	
F(000)	2048	
Crystal size	0.6 x 0.48 x 0.2 mm^3	
Theta range for data collection	1.71 to 32.50°.	

Index ranges	-18<=h<=20, -21<=k<=24, -27<=l<=27
Reflections collected	101285
Independent reflections	13875 [R(int) = 0.0504]
Completeness to theta = 32.50°	100.0 %
Absorption correction	Empirical
Refinement method	Full-matrix least-squares on F^2
Data / restraints / parameters	13875 / 0 / 418
Goodness-of-fit on F^2	1.195
Final R indices [I>2sigma(I)]	R1 = 0.0266, wR2 = 0.0570
R indices (all data)	R1 = 0.0375, wR2 = 0.0677
Largest diff. peak and hole	2.172 and -0.958 e.Å^{-3}

Table 21: Selected bond lengths [Å] and angles [°] for sh2388.

Sn(1)-O(5)	1.958(2)	Fe(2)-C(25)	1.791(3)
Sn(1)-O(2)	2.041(2)	Fe(2)-C(23)	1.796(3)
Sn(1)-O(1)	2.063(2)	O(5)-Sn(1)-O(2)	98.42(7)
Sn(1)-Fe(1)	2.4477(4)	O(5)-Sn(1)-O(1)	97.17(7)
Sn(2)-O(4)	2.164(2)	O(2)-Sn(1)-O(1)	76.90(6)
Sn(2)-O(1)	2.175(2)	O(5)-Sn(1)-Fe(1)	125.21(5)
Sn(2)-O(3)	2.317(2)	O(2)-Sn(1)-Fe(1)	119.71(5)
Sn(2)-O(2)	2.326(2)	O(1)-Sn(1)-Fe(1)	127.09(5)
Sn(3)-O(6)	1.959(2)	O(4)-Sn(2)-O(1)	89.53(6)
Sn(3)-O(3)	2.044(2)	O(4)-Sn(2)-O(3)	69.37(6)
Sn(3)-O(4)	2.074(2)	O(1)-Sn(2)-O(3)	86.04(6)
Sn(3)-Fe(2)	2.4526(4)	O(4)-Sn(2)-O(2)	86.06(6)
Fe(1)-C(22)	1.772(3)	O(1)-Sn(2)-O(2)	69.00(6)
Fe(1)-C(19)	1.788(3)	O(3)-Sn(2)-O(2)	145.23(6)
Fe(1)-C(20)	1.796(3)	O(6)-Sn(3)-O(3)	95.96(7)
Fe(1)-C(21)	1.797(3)	O(6)-Sn(3)-O(4)	97.81(7)
Fe(2)-C(26)	1.773(3)	O(3)-Sn(3)-O(4)	76.64(7)
Fe(2)-C(24)	1.786(3)	O(6)-Sn(3)-Fe(2)	135.64(5)

O(3)-Sn(3)-Fe(2)	113.95(5)	Sn(1)-O(2)-Sn(2)	104.58(7)
O(4)-Sn(3)-Fe(2)	119.79(5)	Sn(3)-O(3)-Sn(2)	104.38(7)
Sn(1)-O(1)-Sn(2)	109.36(7)	Sn(3)-O(4)-Sn(2)	108.97(7)

3.20.1 Discussion of the molecular crystal structure of [Sn{(μ-O*i*Pr)$_2$Sn(O*i*Pr)Fe(CO)$_4$}$_2$] 6

A single crystal X-ray analysis of [Sn{(μ-O*i*Pr)$_2$Sn(O*i*Pr)Fe(CO)$_4$}$_2$] **6** was carried out for unequivocal identification of the structure as depicted in figure 21.

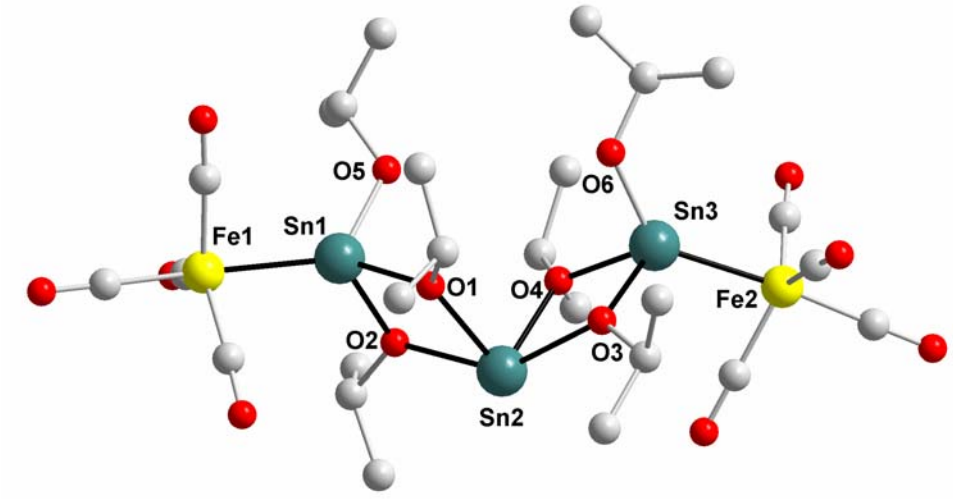

Figure 21: X-ray molecular structure of [Sn{(μ-O*i*Pr)$_2$Sn(O*i*Pr)Fe(CO)$_4$}$_2$] **6**. Hydrogen atoms are omitted for clarity and carbon atoms are not labelled.

In regard to [Sn(μ-O*i*Pr)$_2$]$_\infty$ **5**, used as starting material, the polymeric interlinking has been broken to provide a metallic arrangement where formally three stannylene units remained together are coordinated on each side by a tertracarbonyl-iron moiety. One can recognise in the spatial organisation of the trimer-stannylene structure the former fashion of the stannylene chain. The central tin atom constitutes an example among very few of a tin(II) species coordinated by four oxygen atoms. It is situated in a very distorted coordination site. If the free electron pair of the tin centre is considered in the overall geometry (i.e. stereochemically active), one may describe the coordination fashion as tetragonal pyramid where the tin atom would be localised in the centre of the pyramid. Nevertheless, this description requires that all tin-oxygen bond lengths

are equal and this is not the case. Furthermore, distortions in the supposed rhomboid ground of the pyramid are too important to allow this description. An other point of view, also in regard to the free electron pair of the tin centre would depict the coordination site as a very distorted trigonal bipyramid arrangement with the free electron pair located in one of the equatorial sites. Nevertheless, this description supposes that O(1)-Sn(2)-O(4) angle contained in the equatorial plan shows a value of approximately 120°. Now, measurement of this angle gives only 89.53(6)°. Furthermore, the O(2)-Sn(2)-O(3) angle shows a value of 145.23(6)° (instead of the 180 °that would normally be expected). Bond lengths provide nevertheless consistent values with this description. Thus, bonds situated in equatorial plan, which are supposed to be shorter than those in axial positions, are effectively shorter: Sn(2)-O(1) and Sn(2)-O(4) show lengths of 2.175(2) Å and 2.163(2) Å, respectively to compare with the supposed axial bonds: Sn(2)-O(2) = 2.326(2) Å and Sn(2)-O(3) = 2.316(2) Å. Finally, one may also describe the coordination of the central tin atom as a slightly distorted "teeter-totter" arrangement like e.g. SF_4.

As expected, the coordination of the two carbonyl-iron fragments induces a slight folding of the complex. Thus, the distance between Sn(1) and Sn(3) is around 5.508(1) Å, whereas the same measurement with the non-coordinated complex gives 6.344(1) Å.

Sn_2O_2 rings are planar but do not form perfect rhombus, since the Sn(1)-O(1) and Sn(2)-O(2) bonds are not identical (Sn(1)-O(1) = 2.064 Å and Sn(2)-O(2) = 2.326 Å). This slight shrinkage of the adjacent bonds when a tin(II) centre is coordinated to a transition metal was already reported[95] and is a well-established phenomenon. It can be explained by an electron transfer to the transition metal. Due to steric hindrance, one of the tertiary carbon atoms belonging to the bridging *iso*-propoxide groups is not coplanar with the Sn_2O_2 rings. Coordination geometry around the iron atom is trigonal bipyramidal with the $Fe(CO)_4$ fragment being at a distance of 2.450(2) Å to the tin centre. This value is rather shorter than in other Sn-Fe complexes involving a tertra coordinate tin atom.[96] This indicates a strong Fe-Sn interaction, the stannylene ligand behaving a strong σ-donor and a weak π-acceptor character.

Dealing with carbonyl-iron fragments, one can observe, as expected, a *trans* influence caused by the stannylene ligand: the *trans* bond is shorter ($Fe\text{-}C_{trans}$ = 1.773(1) Å) than the *cis* ones ($Fe\text{-}C_{cis}$ = 1.794(1) Å). Fe(1)-Sn(1)-Sn(2) angle is in the range of 136.67°, this value is consistent with other literature reports. Terminal *iso*-propoxide

goups are not oriented in a perpendicular fashion to the Sn_2O_2 rings: O(5)-Sn(1)-Sn(2) = 97.98°.

Starting from the well-known $[Sn(\mu\text{-O}t\text{Bu})(\text{O}t\text{Bu})]_2$ **13** dimeric species,[88] P. Braunstein *et al*. have described a very close complexation reaction where each tin atom is coordinated by a tetracarbonyl-iron moiety.[65] In analogy with this result, the obtained compound can be formally described as a supplementary non-coordinated stannylene inserted in a dicoordinated dimeric species.

To our knowledge, this is the first species providing a well-defined one-dimensional arrangement of tin(II) atoms coordinated on each side by a transition metal carbonyl. The only compound owning three stannylene units and coordinated by a transition metal was reported by T. J. Boyle *et al.* in 2002 and showed a cyclic arrangement.[97]

Chapter 4

Low-valent group 14 metals in ligands for zero-valent nickel complexes

4.1 Synthesis of Ni[Ge(N*t*Bu)$_2$Si(CH$_3$)$_2$]$_4$ 8

Like carbenes, sylilenes and stannylenes, germylenes are isolobal (isoelectronic) with phosphines and may function as ligand to transition metal complexes. A few years ago, M. Veith *et. al*. reported the synthesis of the first binary stannylene complex of the first transition series and therefore showed that this type of ligand is suitable to stabilise nickel(0) centres.[27] The equation 1 shows the synthetic approach applied to achieve the synthesis of the following complex Ni[Ge(N*t*Bu)$_2$Si(CH$_3$)$_2$]$_4$ **8**.

$$Ni(cod)_2 + 4\ Ge(NtBu)_2Si(CH_3)_2 \longrightarrow \underset{\mathbf{8}}{Ni[Ge(NtBu)_2Si(CH_3)_2]_4} + 2\ cod \qquad \text{(Eq 1)}$$

When monitored by ^{1}H NMR spectroscopy, the reaction between Ge(N*t*Bu)$_2$Si(CH$_3$)$_2$ and Ni(cod)$_2$ in a ration 4:1 appeared to be complete and free 1,5-cyclooctadiene was the sole byproduct. The NMR spectroscopic characterisation supports the formation of an homoleptic germanium containing nickel(0) complex. To our knowledge, there is only one previously reported homoleptic germanium containing nickel complex, which has been spectroscopically as well as structurally characterised.[98] Structurally characterised germylene containing nickel complexes are limited to the bis(germylene) complex L$_2$Ni(CO)$_2$ (L = (*t*BuNCH$_2$CH$_2$N*t*Bu)Ge),[99] the mono(germylene) species LNi(PPh$_3$)$_2$ (L = Ge[N(SiMe$_3$)$_2$]$_2$ or Ge(2,4,6-(CF$_3$)$_3$C$_6$H$_2$)$_2$)[100,101] and [{(*t*BuO)(μ-O*t*Bu)}GeNi(CO)$_3$]$_2$.[47]

4.2 Crystal structure determination of $Ni[Ge(NtBu)_2Si(CH_3)_2]_4$ 8

Crystals of $Ni[Ge(NtBu)_2Si(CH_3)_2]_4$ **8** were obtained from a concentrated toluene solution placed at -10°C. An appropriate crystal was isolated and anchored at a cryo-loop. From the determination and the refinement of the unit cell dimensions arose the space group P2/c in a monoclinic crystal system. The position of each atom, except the hydrogen atoms, was anisotropicaly refined. Hydrogen atoms were refined as rigid groups with the attached carbon atoms in ideal positions. The R-value is 3.55 %. In table 1 are reported the crystal data and the structure refinement for the compound and in table 2 are reported some selected bond lengths and angles of interest.

Table 1: Crystal data and structure refinement for sh2152a.

Identification code	sh2152a	
Empirical formula	C40 H96 Ge4 N8 Ni Si4	
Formula weight	1150.68	
Temperature	293(2) K	
Wavelength	0.71073 Å	
Crystal system	Monoclinic	
Space group	P2/c	
Unit cell dimensions	a = 40.342(8) Å	α= 90°
	b = 13.351(3) Å	β= 90.01(3)°
	c = 22.723(5) Å	γ = 90°
Volume	12239(5) $Å^3$	
Z	8	
Density (calculated)	1.249 Mg/m^3	
Absorption coefficient	2.354 mm^{-1}	
F(000)	4832	
Crystal size	0.8 x 0.49 x 0.36 mm^3	

Theta range for data collection	1.51 to 30.51°.
Index ranges	-56<=h<=56, -18<=k<=18, -32<=l<=31
Reflections collected	158806
Independent reflections	36589 [R(int) = 0.0354]
Completeness to theta = 30.51°	97.9 %
Absorption correction	Multiscan
Refinement method	Full-matrix least-squares on F^2
Data / restraints / parameters	36589 / 0 / 1122
Goodness-of-fit on F^2	1.081
Final R indices [I>2sigma(I)]	R1 = 0.0355, wR2 = 0.0754
R indices (all data)	R1 = 0.0490, wR2 = 0.0797
Largest diff. peak and hole	1.112 and -0.819 e.Å^{-3}

Table 2: Bond lengths [Å] and angles [°] for sh2152a.

Ni(1)-Ge(2)	2.2483(5)	Ge(4)-N(8)	1.873(2)
Ni(1)-Ge(2)#1	2.2483(5)	Ge(4)-N(7)	1.893(2)
Ni(1)-Ge(1)	2.2673(4)	Ge(4)-Si(4)	2.6709(8)
Ni(1)-Ge(1)#1	2.2675(4)	Ge(5)-N(10)	1.883(2)
Ge(1)-N(2)	1.880(2)	Ge(5)-N(9)	1.884(2)
Ge(1)-N(1)	1.897(2)	Ge(5)-Si(5)	2.6871(8)
Ge(1)-Si(1)	2.6901(8)	Ge(6)-N(12)	1.867(2)
Ge(2)-N(4)	1.865(2)	Ge(6)-N(11)	1.885(2)
Ge(2)-N(3)	1.890(2)	Ge(6)-Si(6)	2.6599(8)
Ge(2)-Si(2)	2.6784(8)	Ni(3)-Ge(8)	2.2411(5)
Ni(2)-Ge(6)	2.2317(5)	Ni(3)-Ge(8)#2	2.2412(5)
Ni(2)-Ge(4)	2.2433(5)	Ni(3)-Ge(7)#2	2.2552(5)
Ni(2)-Ge(3)	2.2625(5)	Ni(3)-Ge(7)	2.2553(5)
Ni(2)-Ge(5)	2.2635(5)	Ge(7)-N(13)	1.876(2)
Ge(3)-N(5)	1.881(2)	Ge(7)-N(14)	1.891(2)
Ge(3)-N(6)	1.886(2)	Ge(7)-Si(7)	2.6782(8)
Ge(3)-Si(3)	2.6868(7)	Ge(8)-N(15)	1.867(2)

Ge(8)-N(16)	1.895(2)	N(10)-Ge(5)-Si(5)	40.48(6)
Ge(8)-Si(8)	2.6714(8)	N(9)-Ge(5)-Si(5)	40.24(6)
Ge(2)-Ni(1)-Ge(2)#1	97.72(3)	Ni(2)-Ge(5)-Si(5)	167.97(2)
Ge(2)-Ni(1)-Ge(1)	106.32(2)	N(12)-Ge(6)-N(11)	82.5(1)
Ge(2)#1-Ni(1)-Ge(1)	125.55(2)	N(12)-Ge(6)-Ni(2)	141.80(7)
Ge(2)-Ni(1)-Ge(1)#1	125.55(2)	N(11)-Ge(6)-Ni(2)	135.49(7)
Ge(2)#1-Ni(1)-Ge(1)#1	106.32(2)	N(12)-Ge(6)-Si(6)	41.15(8)
Ge(1)-Ni(1)-Ge(1)#1	98.09(2)	N(11)-Ge(6)-Si(6)	41.34(7)
Ge(6)-Ni(2)-Ge(4)	97.06(2)	Ni(2)-Ge(6)-Si(6)	175.87(2)
Ge(6)-Ni(2)-Ge(3)	108.28(3)	Ge(8)-Ni(3)-Ge(8)#2	95.65(3)
Ge(4)-Ni(2)-Ge(3)	123.53(2)	Ge(8)-Ni(3)-Ge(7)#2	124.06(2)
Ge(6)-Ni(2)-Ge(5)	121.57(2)	Ge(8)#2-Ni(3)-Ge(7)#2	108.14(2)
Ge(4)-Ni(2)-Ge(5)	109.17(2)	Ge(8)-Ni(3)-Ge(7)	108.14(2)
Ge(3)-Ni(2)-Ge(5)	99.10(2)	Ge(8)#2-Ni(3)-Ge(7)	124.05(2)
N(5)-Ge(3)-Ni(2)	136.44(5)	Ge(7)#2-Ni(3)-Ge(7)	99.08(2)
N(6)-Ge(3)-Ni(2)	140.92(6)	N(13)-Ge(7)-N(14)	81.23(9)
N(5)-Ge(3)-Si(3)	40.35(5)	N(13)-Ge(7)-Ni(3)	136.29(7)
N(6)-Ge(3)-Si(3)	40.66(6)	N(14)-Ge(7)-Ni(3)	141.37(6)
Ni(2)-Ge(3)-Si(3)	172.13(2)	N(13)-Ge(7)-Si(7)	40.58(7)
N(8)-Ge(4)-N(7)	81.73(8)	N(14)-Ge(7)-Si(7)	40.77(6)
N(8)-Ge(4)-Ni(2)	144.75(6)	Ni(3)-Ge(7)-Si(7)	174.38(2)
N(7)-Ge(4)-Ni(2)	133.37(6)	N(15)-Ge(8)-N(16)	81.47(9)
N(8)-Ge(4)-Si(4)	40.97(6)	N(15)-Ge(8)-Ni(3)	144.23(7)
N(7)-Ge(4)-Si(4)	40.79(6)	N(16)-Ge(8)-Ni(3)	133.69(6)
Ni(2)-Ge(4)-Si(4)	174.01(2)	N(15)-Ge(8)-Si(8)	40.93(7)
N(10)-Ge(5)-N(9)	80.70(8)	N(16)-Ge(8)-Si(8)	40.55(7)
N(10)-Ge(5)-Ni(2)	140.92(6)	Ni(3)-Ge(8)-Si(8)	172.29(2)
N(9)-Ge(5)-Ni(2)	136.09(6)		

Symmetry transformations used to generate equivalent atoms:

#1 -x+1,y,-z+1/2 #2 -x,y,-z+1/2

4.2.1 Discussion of the molecular structure of Ni[Ge(N*t*Bu)$_2$Si(CH$_3$)$_2$]$_4$ 8

A single crystal X-ray analysis of Ni[Ge(N*t*Bu)$_2$Si(CH$_3$)$_2$]$_4$ **8** was carried out for unequivocal identification of the structure as shown in figure 1.

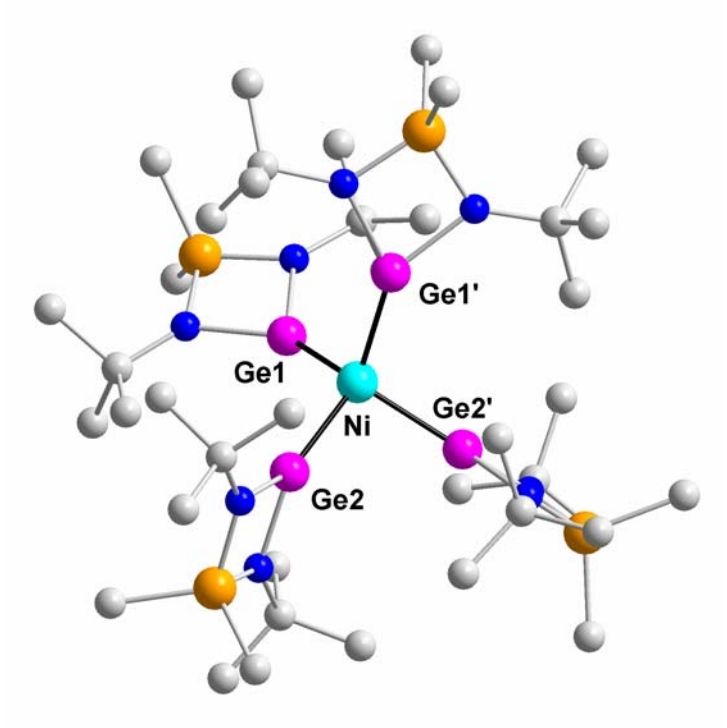

Figure 1: X-ray molecular structure of Ni[Ge(N*t*Bu)$_2$Si(CH$_3$)$_2$]$_4$ **8**. Hydrogen atoms are omitted for clarity and carbon, nitrogen and silicon atoms are not labelled.

The central nickel atom is almost tetrahedrally surrounded by four *bis*(amido)germylene ligands. The planes formed by the *bis*(amido)germylene four-membered rings are screwed with respect to each other, but as the two-fold axes of the GeN$_2$Si cycles do not exactly match with the three-fold axes of a regular tetrahedron, there are sever distortions of the tetrahedral symmetry, as can be seen from the bond angles. Thus, the smallest Ge-Ni-Ge angle measures 97.06(2)° [Ge(2)-Ni-Ge(2')] while the largest of these angles is 125.55(2)° [Ge(1)-Ni-Ge(2')]. In contrast, the Ni-Ge bond lengths are almost constant: average length is 2.258(6) Å. As reported by M. Veith *et al.* dealing with the tin(II) derivative, the homoleptic nickel tetra-*bis*(amino)stannylene complex **14**, this Ni-Ge bond length is considerably smaller than the sum of the covalent radii of nickel and germanium (2.37 Å). This shortening

may signify a "double-bond character, and may imply d(π) → p(π) back-donation in the metal-metal interaction."[27] This interpretation is moreover reinforced by the unusual deep red colour of the compound in the solid state as well as in solution, especially when bearing in mind that complexes of the nominal composition NiL_4 having ligands without significant intraligand π conjugation like PR_3 are usually colourless or light yellow.[102] In regard to the germylene moieties, the bond lengths and angles do not differ significantly from those in the non-coordinated molecule.[103] The *bis*(amido)germylene four-membered rings are perfectly planar. The measurement of the N-Ge-N angle gives 81.54(2)° and the bond distance Ge-N is around 1.88(2) Å.

4.3 Reactions between Ni[Ge(N*t*Bu)$_2$Si(CH$_3$)$_2$]$_4$ 8 and Sn(N*t*Bu)$_2$Si(CH$_3$)$_2$ 12

To our knowledge, no zero-valent nickel complex displaying stannylene and germylene ligands is reported in the literature. Therefore, the nickel tetrakis(bis)amidogermylene **8** was in a preliminary attempt reacted with a very large excess of the cyclic bis-amidostannylene Sn(N*t*Bu)$_2$Si(CH$_3$)$_2$ **12** to attest that the displacement of a germylene ligand is feasible by the stannylene. The ^{119}Sn NMR monitoring of the reaction is a convenient tool to get more insight into the reactivity of the starting complex towards an other low-valent group 14 metal ligand.

^{119}Sn NMR solution spectrum of the zero-valent nickel tetrakis(bis)amidostannylene complex Ni[Sn(N*t*Bu)$_2$Si(CH$_3$)$_2$]$_4$ **14** furnishes a broad resonance band at +696 ppm (Figure 2).

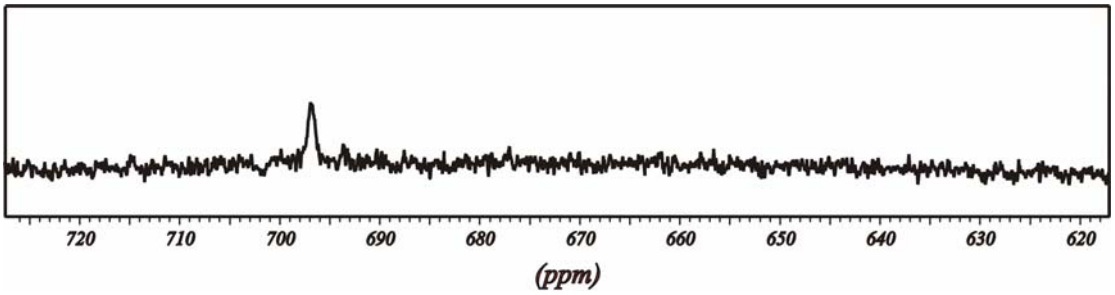

Figure 2: ^{119}Sn NMR solution spectrum of Ni[Sn(N*t*Bu)$_2$Si(CH$_3$)$_2$]$_4$ **14**.

After 12 hours stirring at room temperature, a sample was taken from the crude. As expected, the recorded spectrum (depicted in figure 3) showed the typical very broad resonance band of the free stannylene **12** at +637 ppm (this may be explained first by the neighbouring of the two nitrogen atoms: ^{14}N has a spin of 1 and consequently displays a quadrupole moment and second by the short relaxation time of the tin atom due to its chemical shift anisotropy). Interestingly, the appearance of two new resonance bands at +645 ppm and +658 ppm may let suppose that a partial displacement of the starting ligand has taken place. The new pattern of the ^{119}Sn NMR spectrum may result from the successive replacements of one and then two germylene ligands by the stannylene **12**. The later interpretation supports the fact that no dissociation phenomenon (equation 2) of the four coordinate nickel(0) complex is taking place.

$$Ni(L)_4 \rightleftharpoons Ni(L)_3 + L \qquad \text{(Eq 2)}$$

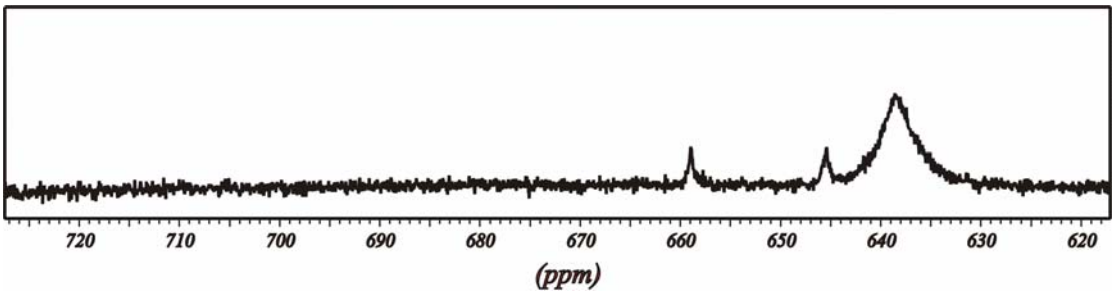

Figure 3: ^{119}Sn NMR solution spectrum of Ni[Ge(N*t*Bu)$_2$Si(CH$_3$)$_2$]$_4$ **8** reacted with an excess of stannylene Sn(N*t*Bu)$_2$Si(CH$_3$)$_2$ **12**.

As the initial assumption, that the replacement of a germylene ligand by a stannylene is achievable, was verified, a further attempt to replace selectively one germylene by a stannylene was performed. Therefore, the zero-valent nickel tetrakis(bis)amidogermylene complex Ni[Ge(N*t*Bu)$_2$Si(CH$_3$)$_2$]$_4$ **8** was allowed to react

with one equivalent of stannylene **12**. The NMR monitoring of the reaction provided the spectrum depicted in figure 4.

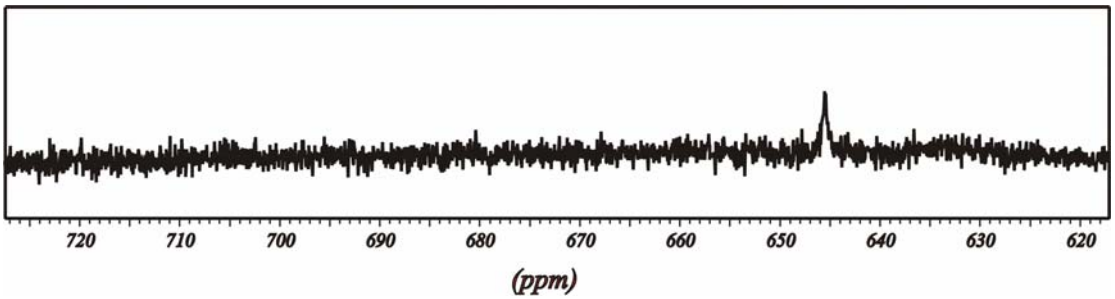

Figure 4: ^{119}Sn NMR solution spectrum of Ni[Ge(N*t*Bu)$_2$Si(CH$_3$)$_2$]$_4$ **8** reacted with one equivalent of stannylene Sn(N*t*Bu)$_2$Si(CH$_3$)$_2$ **12**.

As shown in figure 4, after 15 hours of stirring at room temperature, no resonance band of the free stannylene is observable. On the other hand, the same resonance band as described earlier appeared at +645 ppm. This confirms the initial assumption of a replacement of the germylene ligands by the stannylene. ^{1}H and ^{13}C NMR investigations of the mother liquor support the idea of a selective displacement of a germylene by a stannylene unit. As depicted in figure 5, the ^{1}H NMR of the crude exhibits two main signals at 1.48 ppm and 0.43 ppm, closely accompanied by two smaller signals at 1.47 ppm and 0.42 ppm, respectively. According to their chemical shifts, these main resonance bands can be assigned to the starting complex Ni[Ge(N*t*Bu)$_2$Si(CH$_3$)$_2$]$_4$ **8** and the two smaller ones to a stannylene unit. The integrations of these four signals match almost perfectly with three coordinated germylene ligands and one coordinated stannylene (The main signals exhibit integrations of 54 and 18 protons, respectively. It corresponds to 6 *tert*-butyl groups and 6 methyl groups displayed by three germylene ligands, while the smaller resonance bands show 18 and 6 protons, which is exactly the count of proton of one stannylene.). In the case of a stoechiometric displacement of one germylene ligand by one stannylene, one should expect to find the signals corresponding to one free germylene unit in the crude: the signals at 1.17 ppm and 0.34 ppm correspond to the free germylene.[103]

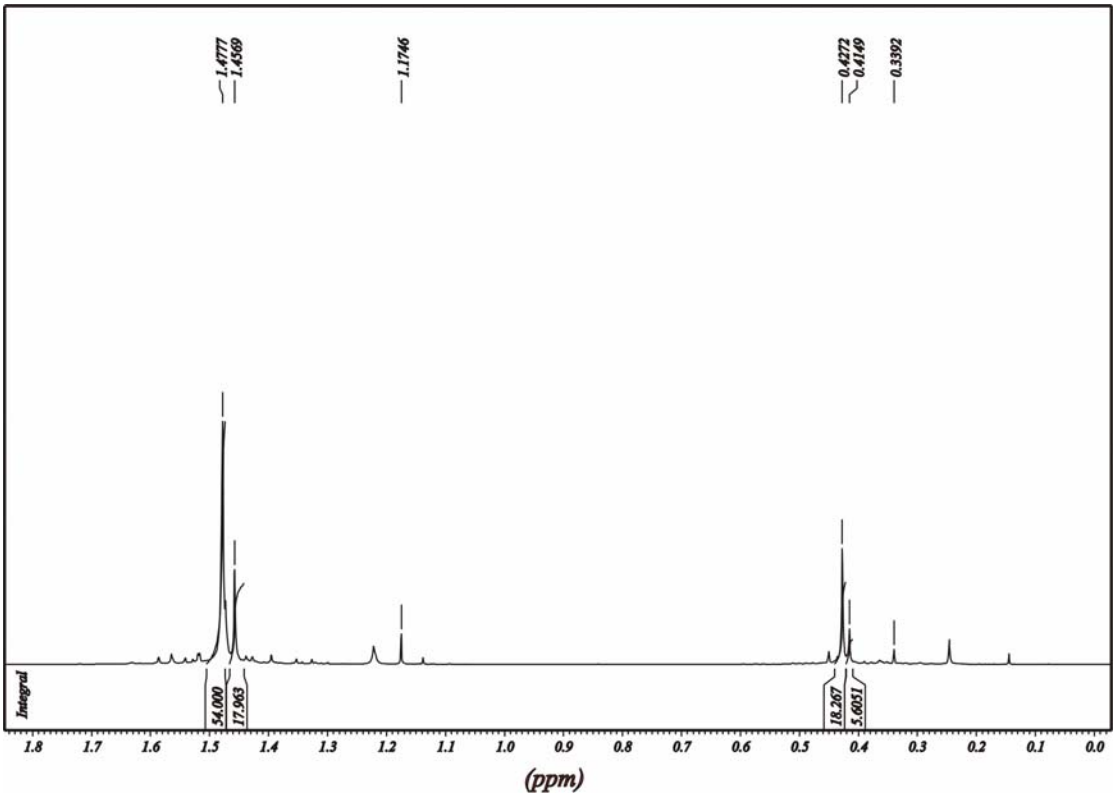

Figure 5: ^{1}H NMR solution spectrum of Ni[Ge(N*t*Bu)$_2$Si(CH$_3$)$_2$]$_4$ **8** reacted with one equivalent of stannylene Sn(N*t*Bu)$_2$Si(CH$_3$)$_2$ **12**.

The recording of a ^{13}C NMR solution spectrum taken from the crude (presented in figure 6) should provide 3 sets of signals: one set for the three coordinated germylene ligands, one set for one coordinated stannylene ligand and finally, one set corresponding to one free germylene. The main signals correspond to the three coordinated germylene ligands. An enlargement of these resonance bands allows to see, that each signal displays an other signal very closely. These signals are assigned to the second set of resonance bands: the coordinated stannylene, which exhibits logically very similar chemical shifts to those of the coordinated germylene ligands. In regard to the free germylene, one could not distinguish unambiguously its resonance bands from other minority byproducts.

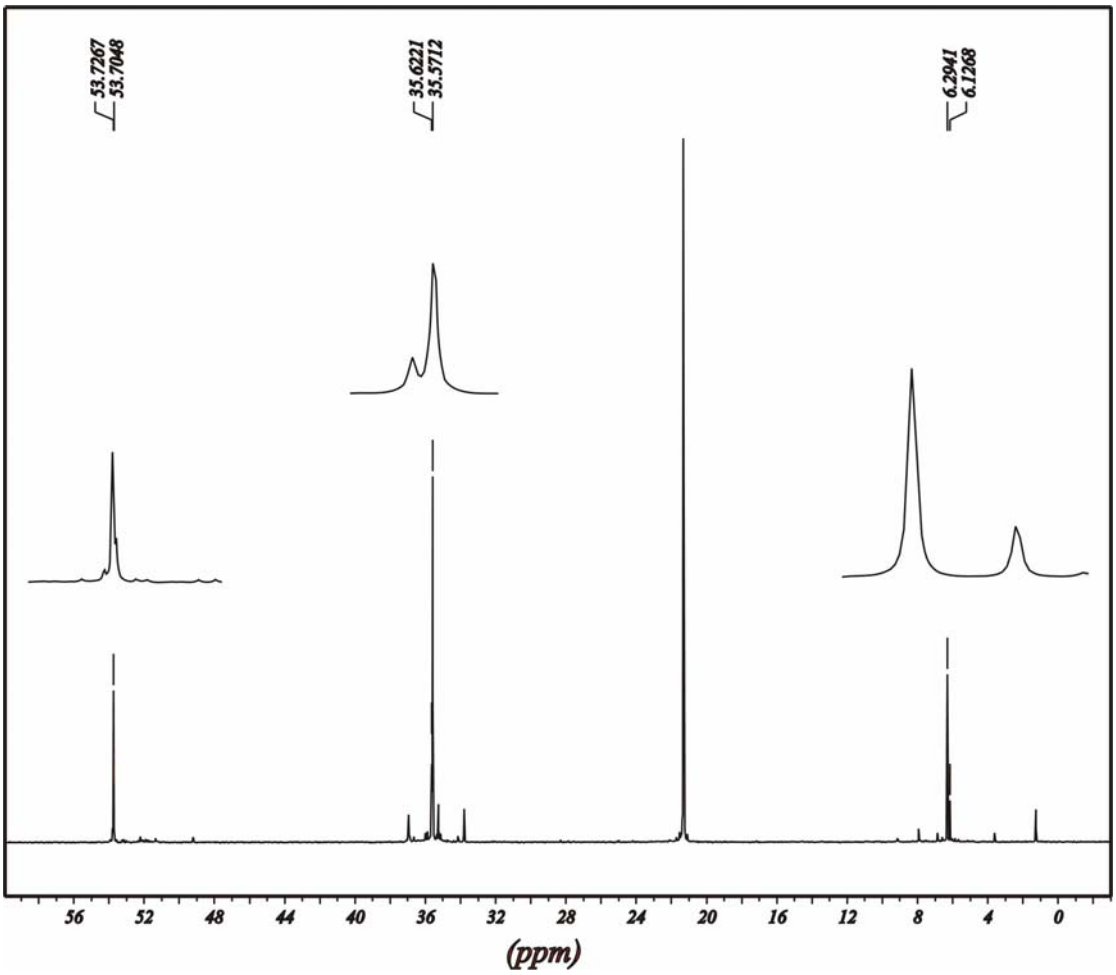

Figure 6: ^{13}C NMR solution spectrum of Ni[Ge(N*t*Bu)$_2$Si(CH$_3$)$_2$]$_4$ **8** reacted with one equivalent of stannylene Sn(N*t*Bu)$_2$Si(CH$_3$)$_2$ **12**. The main signal corresponds to toluene.

According to the NMR investigations, one may assume that the reaction between the compound **8** Ni[Ge(N*t*Bu)$_2$Si(CH$_3$)$_2$]$_4$ and the stannylene **12** Sn(N*t*Bu)$_2$Si(CH$_3$)$_2$ leads to the formation of an heteroleptic nickel(0) complex displaying three germylene units and one stannylene ligand of the general formula Ni[{Ge(N*t*Bu)$_2$Si(CH$_3$)$_2$}$_3${Sn(N*t*Bu)$_2$Si(CH$_3$)$_2$}].

4.4 Crystal Structure determination of Ni[{Ge(N*t*Bu)$_2$Si(CH$_3$)$_2$}$_3${Sn(N*t*Bu)$_2$Si(CH$_3$)$_2$}]

Crystals of Ni[{Ge(N*t*Bu)$_2$Si(CH$_3$)$_2$}$_3${Sn(N*t*Bu)$_2$Si(CH$_3$)$_2$}] were obtained from a concentrated toluene solution placed at -10°C. An appropriate crystal was isolated and anchored at a cryo-loop. From the determination and the refinement of the unit cell dimensions arose the space group P2/c in a monoclinic crystal system. The unit cell dimensions could have been determined and show a very slight compression of the unit cell compared to the values obtained from the X-ray crystal analysis of the compound **8** Ni[Ge(N*t*Bu)$_2$Si(CH$_3$)$_2$]$_4$ (see table 3).

Unit cell dimensions	Ni[{Ge(N*t*Bu)$_2$Si(CH$_3$)$_2$}$_3${Sn(N*t*Bu)$_2$Si(CH$_3$)$_2$}]	Ni[Ge(N*t*Bu)$_2$Si(CH$_3$)$_2$]$_4$
a [Å]	39.802(1)	40.342(8)
b [Å]	13.236(5)	13.351(3)
c [Å]	22.541(8)	22.723(5)
Volume [Å^3]	11876(7)	12239(5)

Table 3: Unit cell dimensions of compound **8** Ni[Ge(N*t*Bu)$_2$Si(CH$_3$)$_2$]$_4$ and Ni[{Ge(N*t*Bu)$_2$Si(CH$_3$)$_2$}$_3${Sn(N*t*Bu)$_2$Si(CH$_3$)$_2$}].

The refinement of the structure could not have been performed and thus, no exact crystal structure of the obtained compound could have been determined. Indeed, the electronic density corresponding to the tin atom seems to be too diffuse to assign the tin atom at a given position in the cell. This may be attributed to the fact that the crystallisation process has taken place without a favoured direction for the tin atom.

4.5 Synthesis of

$Ni[Sn(OCH_3)(N\mathit{t}Bu)\{N(H)\mathit{t}Bu\}Si(CH_3)_2]_4$ 9-H

To the best of our knowledge, no literature report deals with subvalent nickel complexes displaying homoleptic sets of tin(II) alkoxide ligands. Therefore, different attempts were realised to perform the complete alcoholysis of the nickel tetrakis(bis)amidostannylene complex $Ni[Sn(N\mathit{t}Bu)_2Si(CH_3)_2]_4$ **14**.

The reaction was performed in a non-polar solvent (hexane) and during the addition, the solution turned from dark red to yellow almost instantaneously. The obtained complex is noteworthy less soluble than the starting compound: an amorphous solid was observed at the bottom of the flask after 30 minutes stirring.

$$Ni[Sn(N\mathit{t}Bu)_2Si(CH_3)_2]_4 + 8\ CH_3OH \longrightarrow Ni[Sn(OCH_3)(N\mathit{t}Bu)\{N(H)\mathit{t}Bu\}Si(CH_3)_2]_4 + 4\ CH_3OH$$

14 **9-H** (Eq 3)

As depicted in equation 3, no alcoholysis reaction occurs during the reaction. The methanolate ligand acts formally as base adduct on the Lewis acid tin centre, while the proton is trapped by one of the two nitrogen atoms in the ring. As a result, the former symmetrical four-membered ring loses the C_2 symmetry axis situated along the axis formed by the silicon atom and the tin atom. This could have been evidenced by ^1H NMR spectroscopy as well as ^{13}C NMR spectroscopy. Indeed, as shown in figure 7, the two resonance bands displayed by the starting complex $Ni[Sn(N\mathit{t}Bu)_2Si(CH_3)_2]_4$ **14** corresponding to the methyl groups and the *tert*-butyl groups, respectively are splitted in two to provide two sets of resonance bands for the methyl groups on the silicon atom as well as for the *tert*-butyl groups.

In order to evidence unambiguously the presence of a proton trapped by the nitrogen atoms of the stannylene four-membered ring, the same experiment was performed with deuterated methanol CH_3OD. The same procedure as before was applied. After a few minutes, the mother liquor had turned from dark red to yellow with the appearance of an amorphous yellow solid at the bottom of the flask. The ^1H NMR investigation of the mother liquor furnished the spectrum depicted in figure 7'. Both

methyl groups attached at the silicon and *tert*-butyl groups attached at the nitrogen atoms show the expected splitting in two. This indicates indirectly the presence of the deuterium atom since the mirror plan contained in the stannylene four-membered ring is destroyed.

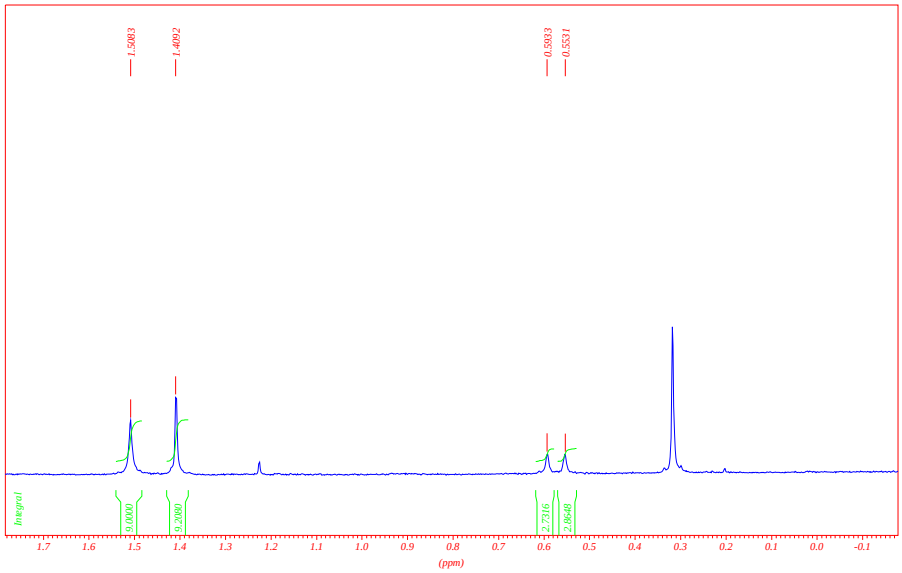

Figure 7: ^{1}H NMR solution spectrum of Ni[Sn(OCH$_3$)(N*t*Bu){N(H)*t*Bu}Si(CH$_3$)$_2$]$_4$ **9-H**.

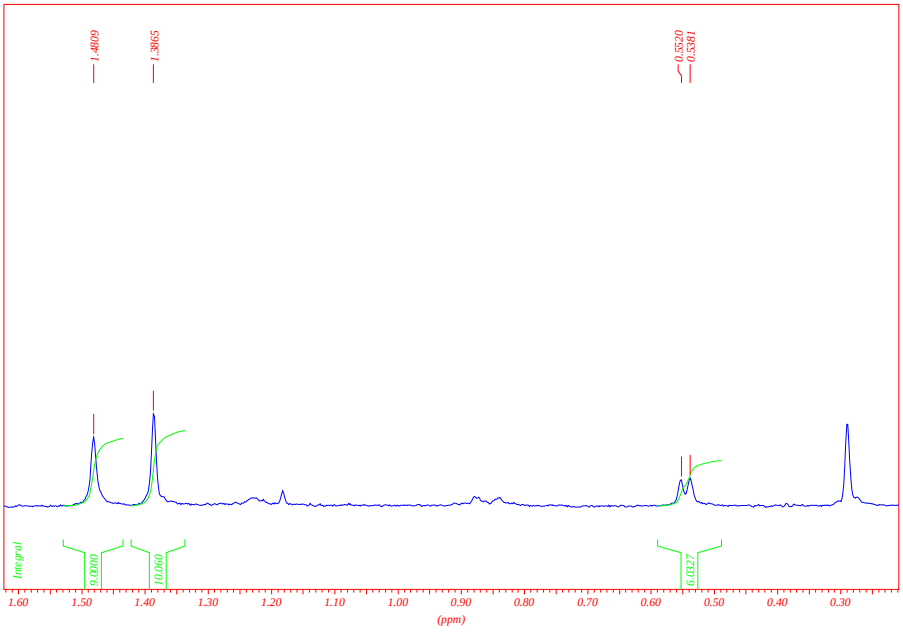

Figure 7': ^{1}H NMR solution spectrum of Ni[Sn(OCH$_3$)(N*t*Bu){N(D)*t*Bu}Si(CH$_3$)$_2$]$_4$ **9-D**.

The figure 8 presents an other part of the same ^{1}H NMR solution spectrum. It shows the resonance bands of the methanolate adduct at δ = 3.99 ppm and the broad signal in the low-field region (δ = 5.84 ppm) corresponds to the proton trapped by one of the nitrogen atom in the stannylene unit. The ^{1}H NMR investigation of the deuterated compound Ni[Sn(OCH$_3$)(N*t*Bu){N(D)*t*Bu}Si(CH$_3$)$_2$]$_4$ **9-D** depicted in figure 8' shows now an important difference with those of the protonated complex: The broad resonance band corresponding to the N-H group previously observed is now vanished.

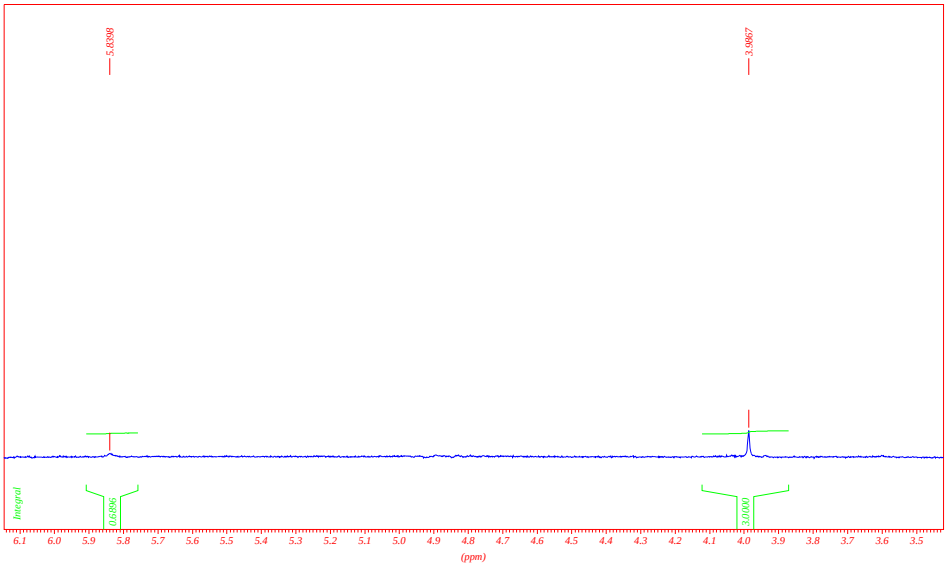

Figure 8: ^{1}H NMR solution spectrum of Ni[Sn(OCH$_3$)(N*t*Bu){N(H)*t*Bu}Si(CH$_3$)$_2$]$_4$ **9-H**.

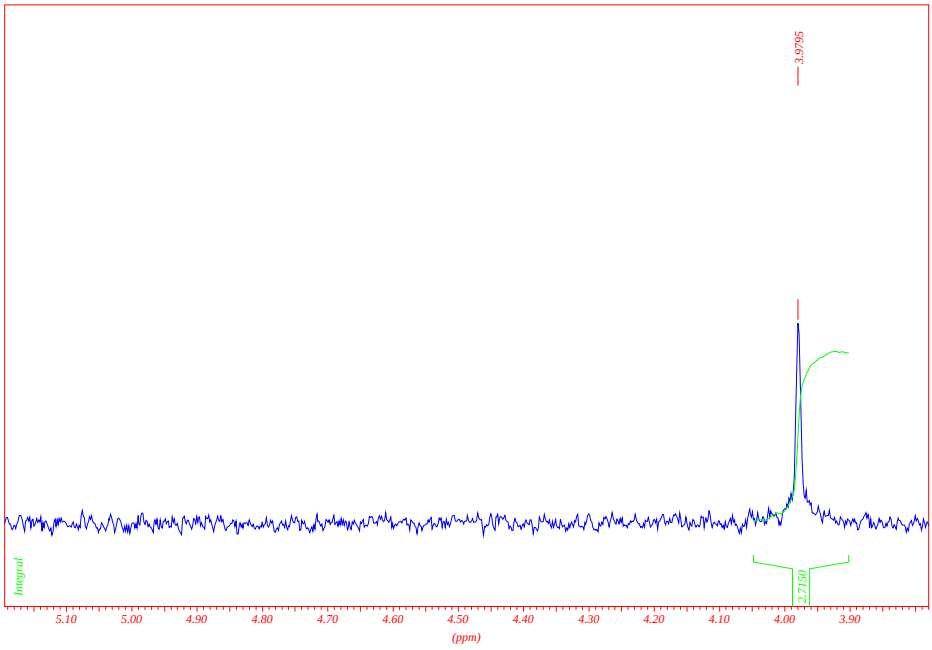

Figure 8': ^{1}H NMR solution spectrum of Ni[Sn(OCH$_3$)(N*t*Bu){N(D)*t*Bu}Si(CH$_3$)$_2$]$_4$ **9-D**.

The figure 9 gives an overview of the ^{13}C NMR solution spectrum of the compound $Ni[Sn(OCH_3)(NtBu)\{N(H)tBu\}Si(CH_3)_2]_4$ **9-H**. The splitting in two of each of the methyl and *tert*-butyl resonance bands of the stannylene four-membered ring is still to be observed.

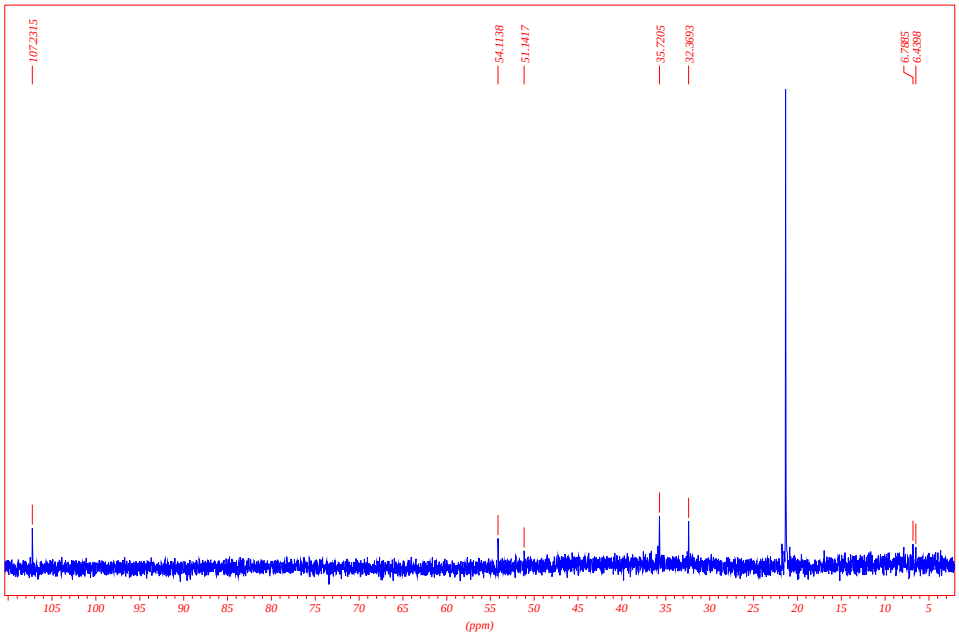

Figure 9: ^{13}C NMR solution spectrum of $Ni[Sn(OCH_3)(NtBu)\{N(H)tBu\}Si(CH_3)_2]_4$ **9-H**. The strongest resonance band at δ = 21.3 ppm corresponds to toluene.

^{119}Sn NMR solution spectrum, which is a sensitive probe for the chemical environment of tin nuclei, shows also significant changes in line width and in chemical shift. The starting material exhibits a broad resonance at +696 ppm (because of the paramagnetic contribution of the ligand: $\pi \rightarrow \pi^*$ transition is energetically small and the probability that an unpaired electron can reach the π^* orbital exists) while the obtained complex shows a sharp resonance at +48 ppm. This large upfield drift outlines the base coordination of the methanolate fragment at the tin centre.[104]

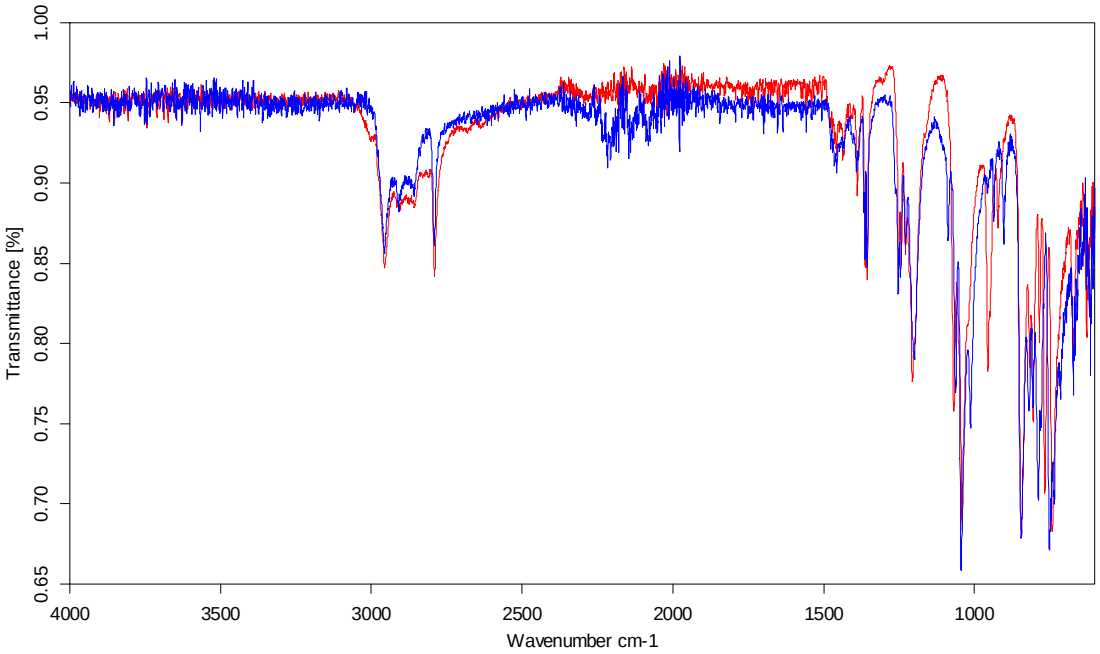

Figure 10: IR spectra of the complexes Ni[Sn(OCH$_3$)(N*t*Bu){N(H)*t*Bu}Si(CH$_3$)$_2$]$_4$ **9-H** in red and Ni[Sn(OCH$_3$)(N*t*Bu){N(D)*t*Bu}Si(CH$_3$)$_2$]$_4$ **9-D** in blue.

The IR investigation of both compounds Ni[Sn(OCH$_3$)(N*t*Bu){N(H)*t*Bu}Si(CH$_3$)$_2$]$_4$ **9-H** and Ni[Sn(OCH$_3$)(N*t*Bu){N(D)*t*Bu}Si(CH$_3$)$_2$]$_4$ **9-D** did not permit to confirm unequivocally the presence of the proton trapped by one of the nitrogen atoms. This type of $\upsilon_{N\text{-}H}$ stretching vibration band is known to provide generally weak and broad resonance bands so that they are often overlooked.[134] Moreover, and as shown in chapter 4.5.1., the presence of this proton allows the formation of an hydrogen bond between the N-H fragment of one stannylene and the oxygen atom of one methanolate adduct situated on a further ligand. It is also well-known, that hydrogen bonding contributes drastically to lower and broaden the frequencies of the N-H vibrations.[135,136] Thus, no signal could have been unambiguously assigned to the $\upsilon_{N\text{-}H}$ stretching vibration band. Both IR spectra of the **9-H** and **9-D** complexes are displayed in figure 10. The fingerprint region is very similar for both of the spectra. Nevertheless, a very broad signal provided by the complex Ni[Sn(OCH$_3$)(N*t*Bu){N(H)*t*Bu}Si(CH$_3$)$_2$]$_4$ **9-H** emerges from the superposition of the two spectra at approximately 2900 cm^{-1}. Different literature reports have mentioned the presence of this type of N-H stretching vibration in the same region.[137] One may assume, that it corresponds to the $\upsilon_{N\text{-}H}$ stretching vibration band. Starting from this assumption, and thanks to the model of the simple harmonic oscillator, it is possible to

find where the vibration frequency (and consequently the wavenumber) of the $\upsilon_{N\text{-}D}$ stretching vibration band is supposed to be located:

$$\upsilon = \frac{1}{2\pi} \cdot \sqrt{\frac{k}{\mu}} \qquad \text{k: spring constant and } \mu\text{: reduced masse, } \mu = \frac{m_1 \cdot m_2}{m_1 + m_2}$$

In the case of an isotopic exchange, the spring constant stays unchanged so that the formula provides the following ratio:

$$\frac{\upsilon_1}{\upsilon_2} = \frac{\upsilon_{NH}}{\upsilon_{ND}} = \sqrt{\frac{2}{1} \cdot \frac{14+1}{14+2}} = \sqrt{2.\frac{15}{16}} = 1.369$$

$$\upsilon_{ND} = \frac{\upsilon_{NH} \cdot \upsilon_2}{\upsilon_1} = \frac{2900}{1.369}$$

$$\upsilon_{N\text{-}D} = 2118.3 \text{ cm}^{-1}$$

The $\upsilon_{N\text{-}D}$ stretching vibration band should be expected to emerge at about 2118.3 cm^{-1}. As shown in figure 10, the complex $Ni[Sn(OCH_3)(N\textit{t}Bu)\{N(D)\textit{t}Bu\}Si(CH_3)_2]_4$ **9-D** deviates from its protonated homologue in this region. This point, added with the evidences provided by the NMR spectroscopy allows to conclude to the presence of a proton trapped by one of the nitrogen atoms.

4.6 Crystal structure determination of $Ni[Sn(OCH_3)(N\textit{t}Bu)\{N(H)\textit{t}Bu\}Si(CH_3)_2]_4$ 9-H

Crystals of $Ni[Sn(OCH_3)(N\textit{t}Bu)\{N(H)\textit{t}Bu\}Si(CH_3)_2]_4$ **9-H** were obtained from a concentrated hexane solution placed at -10°C. An appropriate crystal was isolated and anchored at a cryo-loop. From the determination and the refinement of the unit cell dimensions arose the space group $P4_2/n$ in a tetragonal crystal system. The position of each atom, except the hydrogen atoms, was anisotropicaly refined. Hydrogen atoms were refined as rigid groups with the attached carbon atoms in ideal positions. The R-

value is 3.17 %. In table 4 are reported the crystal data and the structure refinement for the compound and in table 5 are reported some selected bond lengths and angles of interest.

Table 4: Crystal data and structure refinement for sh614.

Identification code	sh614	
Empirical formula	C44 H112 N8 Ni O4 Si4 Sn4	
Formula weight	1463.25	
Temperature	293(2) K	
Wavelength	0.71073 Å	
Crystal system	Tetragonal	
Space group	$P4_2/n$	
Unit cell dimensions	a = 17.235(9) Å	α= 90°
	b = 17.235(9) Å	β= 90°
	c = 11.253(6) Å	γ = 90°
Volume	3343(3) $Å^3$	
Z	2	
Density (calculated)	1.454 Mg/m^3	
Absorption coefficient	1.862 mm^{-1}	
F(000)	1496	
Crystal size	0.45 x 0.30 x 0.25 mm^3	
Theta range for data collection	1.67 to 22.50°.	
Index ranges	0<=h<=18, 0<=k<=18, 0<=l<=6	
Reflections collected	1624	
Independent reflections	1521 [R(int) = 0.0244]	
Completeness to theta = 22.50°	69.5 %	
Absorption correction	Empirical	
Refinement method	Full-matrix least-squares on F^2	
Data / restraints / parameters	1521 / 0 / 137	
Goodness-of-fit on F^2	0.947	
Final R indices [I>2sigma(I)]	R1 = 0.0317, wR2 = 0.1024	

R indices (all data)	R1 = 0.0438, wR2 = 0.1117
Largest diff. peak and hole	0.514 and -0.476 e.Å^{-3}

Table 5: Selected bond lengths [Å] and angles [°] for sh614.

Sn-O	2.043(4)	O-Sn-N(1)	98.4(2)
Sn-N(2)	2.076(7)	N(2)-Sn-N(1)	69.5(3)
Sn-N(1)	2.370(5)	O-Sn-Ni	114.0(1)
Sn-Ni	2.415(1)	N(2)-Sn-Ni	145.0(2)
Sn-Si	2.996(2)	N(1)-Sn-Ni	114.5(1)
Ni-Sn#1	2.415(1)	Sn-Ni-Sn#1	100.58(2)
Ni-Sn#2	2.415(1)	Sn-Ni-Sn#2	129.27(4)
Ni-Sn#3	2.415(1)	Sn#1-Ni-Sn#2	100.58(2)
Si-N(2)	1.677(7)	Sn-Ni-Sn#3	100.58(2)
Si-N(1)	1.796(6)	Sn#1-Ni-Sn#3	129.27(4)
O-Sn-N(2)	99.0(2)	Sn#2-Ni-Sn#3	100.57(2)

4.6.1 Discussion of the molecular structure of Ni[Sn(OCH$_3$)(N*t*Bu){N(H)*t*Bu}Si(CH$_3$)$_2$]$_4$ 9-H

A single crystal X-ray analysis of Ni[Sn(OCH$_3$)(N*t*Bu){N(H)*t*Bu}Si(CH$_3$)$_2$]$_4$ **9-H** was carried out for unequivocal identification of the structure as depicted in figure 11.

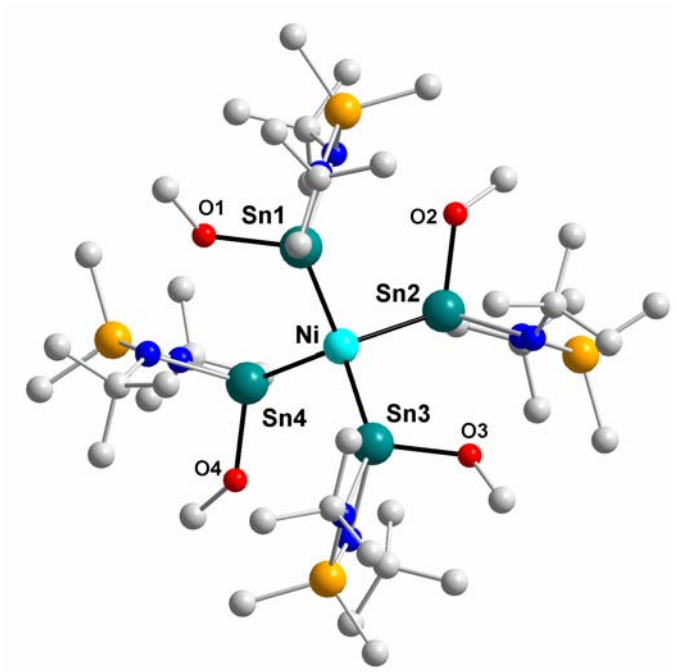

Figure 11: X-ray molecular structure of Ni[Sn(OCH$_3$)(N*t*Bu){N(H)*t*Bu}Si(CH$_3$)$_2$]$_4$ **9-H**. Hydrogen atoms are omitted for clarity and carbon, nitrogen and silicon atoms are not labelled.

The complex owns an S_4 crystal point symmetry. Compared to compounds **8** and **14**, the complex may be understood as a four-fold adduct of methanol across one Sn-N bond in each ligand. Coordinated to the tin atom, one methanolate base increases the coordination number of the tin to four. The remaining proton has been trapped by one of the two basic nitrogen atoms in the ring.

The planes formed by the Sn-N_2-Si four-membered rings are slightly screwed with respect to each other. Due to the coordination of the methanolate adduct on the tin atom, the two-fold axes of the Sn-N_2-Si cycles do not perfectly match with the three-fold axes of a regular tetrahedron. Because of the steric encumbrance of the ligands, the tetrahedron centre shows a strong distortion. Thus, Sn-Ni-Sn angles are varying

between 100.57(2)° and 129.27(4)° instead of 109.5° expected for a perfect tetrahedron.

Within the bond lengths, an elongation of the nickel-tin bonds occurs in comparison with the starting material, due to the increasing coordination number of the tin atom (in the starting material: Ni-Sn = 2.394 Å and Ni-Sn = 2.415(1) Å in this complex). Moreover, the trapping of the hydrogen atom by one of the nitrogen atom in the four membered-ring provides a loss of symmetry of the *bis*(amido)stannylene ligand. Indeed, as shown in figure 12 a) and b), one nitrogen atom remains its trigonal planar coordination (N(2) is sp^2 hybridised) and the other, which is trapping the hydrogen atom, shows a more tetrahedral coordination (N(1) is sp^3 hybridised). It results in different bond lengths for the Sn-N(1) bond and for the Sn-N(2) bond, respectively. Thus, the covalent bond N(2)-Sn(1) is around 2.076(7) Å whereas the dative bond N(1)-Sn(1) shows a length of 2.370(5) Å. The deviation from planarity of the *tert*-butyl group attached at the N(1) nitrogen atom corroborates the presence of an hydrogen atom [see figure 12 b)]. A further observation permits to identify an oxygen···nitrogen hydrogen bond (O···N = 2.889(1) Å) between a methanolate group and a nitrogen atom of a neighbouring *bis*(amido)stannylene ligand **12**. The general geometry of the complex as well as the presence of the hydrogen bond suggests an unusual addition mechanism of the methanol units. In a classical addition mechanism on a stannylene moiety, the obtained product is generally in *cis* configuration.[105] In contrast, this complex presents four stannylene units where the addition seems to have occurred in a *trans* fashion. This might be explained by the following interpretation: the methanolate would approach of the Lewis acid tin(II) centre and in the same time the proton would be trapped by the basic centre formed by the two nitrogen atoms of a neighbouring stannylene unit. This mechanism might be designated as interligand addition.

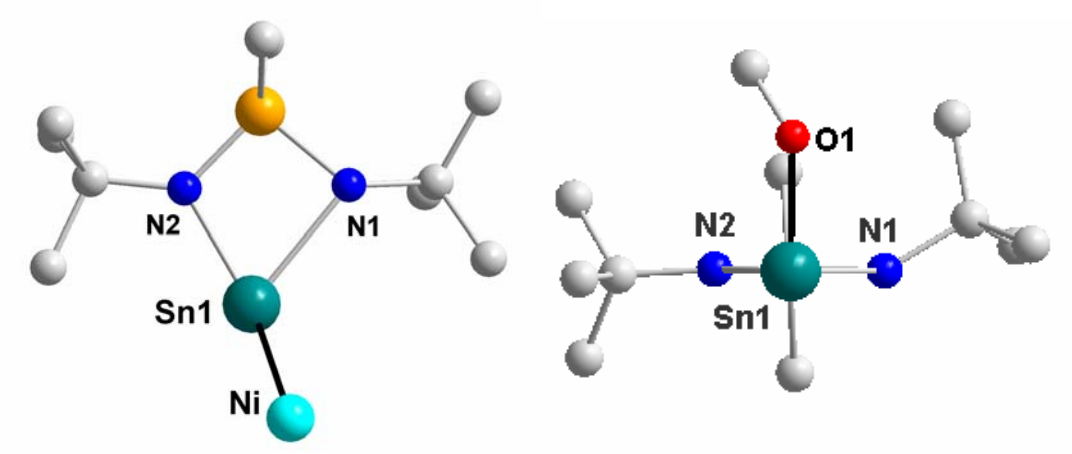

a) b)

Figure 12: Different bonding situation for the sp^2 N(2) and the sp^3 N(1) due to the trapped hydrogen atom. The methanolate group has been omitted for clarity in a).

4.7 Reactions between Ni[Sn(N*t*Bu)$_2$Si(CH$_3$)$_2$]$_4$ 14 and ethyl alcohol

Repeated attempts were realised to achieve the alcoholysis of the starting nickel complex **14** with ethanol. The same procedure as the one described in chapter 4.5 was applied: to a stirred toluene solution of Ni[Sn(N*t*Bu)$_2$Si(CH$_3$)$_2$]$_4$ **14**, ethanol was slowly added. During the addition of ethanol, the solution turned suddenly from dark red to yellow and then to brown. Interpretation of ^{1}H NMR and ^{13}C NMR solution spectra measured after 2 hours of stirring could not provide more insight into the mechanism of the reaction. The same procedure was repeated in order to stop the reaction when it becomes yellow and to isolate the observed transition state. As expected, the solution turned suddenly from dark red to yellow during the addition. The addition was immediately stopped and an ice bath was set up to cold down the solution and stop the reaction. As observed previously for the reaction with methanol, an amorphous solid fell down at the bottom of the flask. Different attempts to solubilise this solid were realised: a very large volume of hexane or toluene could not redissolve the product without decomposition and a slight warming up of the suspension gave rise to the formation of a brown oily solution. ^{1}H NMR as well as ^{13}C NMR solution spectra gave the same pattern as those observed for a complete

addition. This may signify that a very small energy input may be sufficient to allow the observed and high reactive intermediate to evolve until a more stable compound.
This observed thermochromic behaviour might be attributable to a change of coordination polyhedron at the nickel atom. Transformations of this type have been unequivocally demonstrated in other classes of compounds.[106] This may also be attributed to a change in the oxidation state of the nickel centre.
Until now, it was neither possible to determine an exact chemical composition of these compounds nor to isolate any product.
The same procedure was applied in a more polar solvent: dichloromethane. ^{119}Sn NMR revealed that the reaction is not selective and lead to the formation of different products. X-ray crystal structure analysis evidenced unambiguously the formation of *tert*-butyl ammonium chloride. This permits to establish that the nitrogen-tin bonds of the starting material are broken and that the solvent participates to the reaction. Nevertheless, although the reaction works very differently according to the used solvent, its role in the reaction mechanism remains unclear.

4.8 Reaction between $Ni[Sn(NtBu)_2Si(CH_3)_2]_4$ 14 and *iso*-propyl alcohol

A previous work was realised concerning the reaction between the starting tetrakis(bis)amidostannylene nickel complex $Ni[Sn(NtBu)_2Si(CH_3)_2]_4$ **14** and *iso*-propanol.[107] It showed that a complex structure was obtained from this reaction. Surprisingly, five tin atoms are coordinated to the central nickel atom in a very distorted trigonal bipyramidal arrangement. As depicted in figure 13, Sn(2) and Sn(3) still display an unchanged $[Me_2Si(NtBu)_2]$ ligand, while in a further ligand, an hydrogen atom has been trapped by one of the nitrogen belonging to the ring. Sn(1) and Sn(3) are connected together by an *iso*-propoxide group. The latter tin atoms: Sn(4) and Sn(5) display exclusively *iso*-propoxide ligands. This indicates that the alcoholysis reaction took place for certain ligands, while other have remained intact their initial structure. To the question: why the Ni(0) centre is coordinated by five stannylene ligands, M. Veith proposed an original explanation.[107] Starting from crystallographic considerations, which will not be presented here, he proposed to

describe the compound as a "classical" nickel(0) complex displaying four ligands in an almost tetrahedral environment, where a [Sn(O*i*Pr)$_2$] fragment would have been inserted between two ligands in such a way that two oxygen atoms [O(2) and O(3)] would coordinate to different tin centres [Sn(2) and Sn(5)]. The filled d_{z^2} orbital of the nickel centre would coordinate the tin atom, which would use its empty p_z orbital as acceptor ($d\pi \rightarrow p\pi$ bonding).

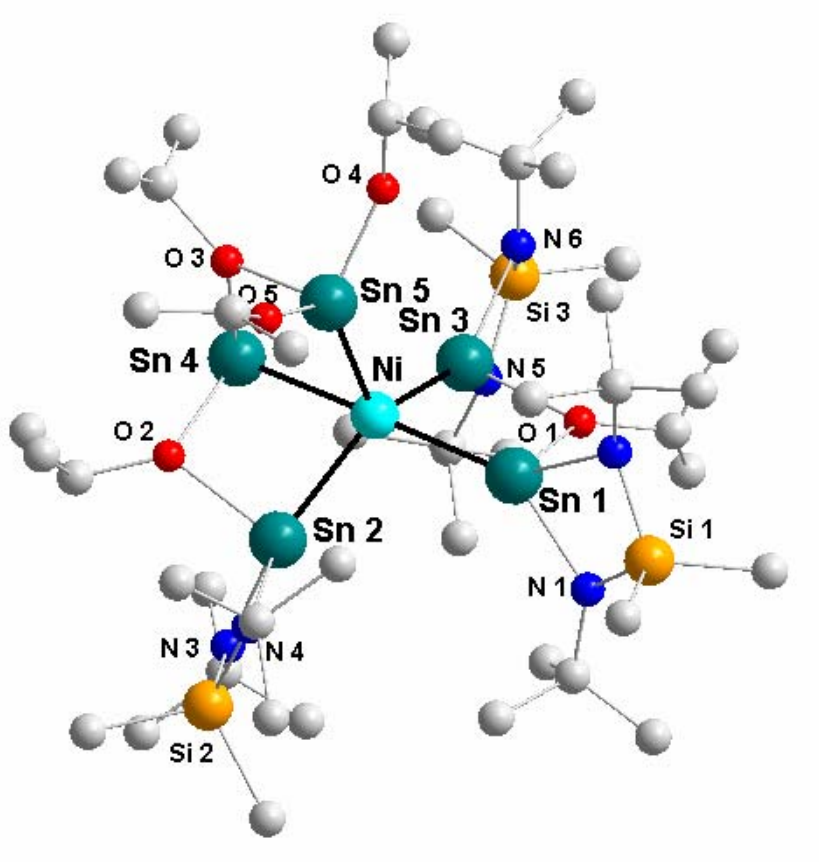

Figure 13: X-ray crystal structure of [{Me$_2$Si(N*t*Bu)$_2$Sn}$_2${Me$_2$Si(N*t*Bu)(NH*t*Bu)Sn(O*i*Pr)}{(O*i*Pr)$_2$Sn}$_2$Ni]. Hydrogen atoms are omitted for clarity and carbon atoms are not labelled.

Surprisingly, the same experiment gave us a very different result. As can be seen in equation 4, *iso*-propyl alcohol reacts with the starting tetrakis(bis)amidostannylene-nickel complex Ni[Sn(N*t*Bu)$_2$Si(CH$_3$)$_2$]$_4$ **14** in such a way that a diadduct is formed (see equation 3). Each *iso*-propylate fragment is bridging two stannylene units.

$Ni[Sn(NtBu)_2Si(CH_3)_2]_4 + 8\ iPrOH \longrightarrow Ni[(Sn(NtBu)_2SiMe_2)_2\mu\text{-}OiPr]_2 + H_2 + 6\ iPrOH$

14 **10** (Eq 4)

As shown in equation 4, dihydrogen is formed during the reaction. This point is of a special interest because it lets suppose, that an oxidation of the nickel centre is taking place. Indeed, the starting complex $Ni[Sn(NtBu)_2Si(CH_3)_2]_4$ **14** displays a nickel centre in the zero oxidation state, while the obtained compound $Ni[(Sn(NtBu)_2SiMe_2)_2\mu\text{-}OiPr]_2$ **10** is a nickel(II) complex. In the chapter 4.5., an attempt to perform an alcoholysis reaction of the starting complex $Ni[Sn(NtBu)_2Si(CH_3)_2]_4$ **14** with methanol has been described (see equation 3). As evidenced by spectroscopic methods (IR and NMR spectroscopy) and by the X-ray crystal structure analysis, the proton of the methanol is trapped by one of the nitrogen atoms of the four-membered ring, while the methanolate fragment acts as a Lewis base towards the Lewis acid tin centre. The reaction with *iso*-propanol seems to work very differently since the obtained product results from an oxidation. This is supported by the spectroscopic investigations of the complex $Ni[(Sn(NtBu)_2SiMe_2)_2\mu\text{-}OiPr]_2$ **10**. The IR investigation of the complex **10** could not permit to observe any N-H vibration band. Moreover [and as evidenced for the complex **9-H** (see chapter 4.5.)], the presence of a proton at one of the two nitrogen atoms in the four-membered ring destroys the mirror plan contained in each ligand and thus, the resonance bands of the methyl groups attached at the silicon atom and those of the *tert*-butyl groups are splitted in two in ^{1}H NMR as well as ^{13}C NMR spectra. This has not been observed for the compound $Ni[(Sn(NtBu)_2SiMe_2)_2\mu\text{-}OiPr]_2$ **10**.

From a mechanistic point of view, the probability that two *iso*-propylate fragments react simultaneously with the starting complex is very low. Instead, it seems much more probable, that the reaction consists in a successive addition of a first and then a second *iso*-propylate moiety. This point lets suppose, that as the first *iso*-propylate fragment has just reacted, the nickel centre would display the formal oxidation state (I).

^{119}Sn NMR solution spectrum shows a broad resonance band at -398 ppm. Compared to the starting complex $Ni[Sn(NtBu)_2Si(CH_3)_2]_4$ **14**, which exhibits a resonance band at +696 ppm, the upfield drift may be seem to be large. Nevertheless, different

conjugated effects may work together to explain this drift. The first qualitative explanation is that the *iso*-propylate adduct increases the coordination number of the tin centre and provides electron density to it and consequently, tends to displace the resonance band in the high field region. Secondly, the presence of the *iso*-propylate group renders negligible the paramagnetic contribution of the four ligands (due to a very small energy difference of the $\pi \rightarrow \pi^*$ transition in the starting complex as well as in the free stannylene **12**), which is known to contribute very strongly in the deshielding of the ^{119}Sn nuclei.[108,109] Finally, the π-allyl system formed by the possible delocalisation of electrons between the two nitrogen atoms and *via* the tin atom in each of the four ligands of the starting material is disturbed by the presence of the *iso*-propylate adduct.

The versatile behaviour of the nickel complex towards alcohols is one more time demonstrated here. The reproducibility of the different synthesises remains limited and until now, neither a systematic mechanism nor a general trend could have been found to explain and foresee the nature of the obtained products.

4.9 Crystal structure determination of Ni[(Sn(N*t*Bu)$_2$SiMe$_2$)$_2$μ-O*i*Pr]$_2$ 10

Crystals of Ni[(Sn(N*t*Bu)$_2$SiMe$_2$)$_2$μ-O*i*Pr]$_2$ **10** were obtained from a concentrated hexane solution placed at -10°C. An appropriate crystal was isolated and anchored at a cryo-loop. From the determination and the refinement of the unit cell dimensions arose the space group I2 in a monoclinic crystal system. The position of each atom, except the hydrogen atoms, was anisotropicaly refined. Hydrogen atoms were refined as rigid groups with the attached carbon atoms in ideal positions. The R-value is 4.90 %. In table 6 are reported the crystal data and the structure refinement for the compound and in table 7 are reported some selected bond lengths and angles of interest.

Table 6: Crystal data and structure refinement for sh2313.

Identification code	sh2313	
Empirical formula	C46 H110 N8 Ni O2 Si4 Sn4	
Formula weight	1453.25	
Temperature	103(2) K	
Wavelength	0.71073 Å	
Crystal system	Monoclinic	
Space group	I2	
Unit cell dimensions	a = 16.195(3) Å	α = 90°
	b = 10.774(2) Å	β= 94.774(13)°
	c = 18.863(4) Å	γ = 90°
Volume	3279.6(11) $Å^3$	
Z	2	
Density (calculated)	1.472 Mg/m^3	
Absorption coefficient	1.895 mm^{-1}	
F(000)	1484	
Crystal size	0.2 x 0.3 x 0.42 mm^3	
Theta range for data collection	1.59 to 28.84°.	
Index ranges	-21<=h<=21, -14<=k<=14, -25<=l<=25	
Reflections collected	38281	
Independent reflections	8499 [R(int) = 0.0539]	
Completeness to theta = 28.84°	99.5 %	
Absorption correction	Empirical	
Refinement method	Full-matrix least-squares on F^2	
Data / restraints / parameters	8499 / 1 / 313	
Goodness-of-fit on F^2	1.282	
Final R indices [I>2sigma(I)]	R1 = 0.0444, wR2 = 0.1099	
R indices (all data)	R1 = 0.0490, wR2 = 0.1126	
Absolute structure parameter	0.23(3)	
Largest diff. peak and hole	3.988 and -2.717 e.$Å^{-3}$	

Table 7: Selected bond lengths [Å] and angles [°] for sh2313.

Ni(1)-Sn(2)	2.4533(6)	Sn(2)-N(3)	2.052(5)
Ni(1)-Sn(2)#1	2.4533(6)	Sn(2)-O(1)	2.208(4)
Ni(1)-Sn(1)#1	2.4571(6)	Sn(2)-Ni(1)-Sn(2)#1	172.06(5)
Ni(1)-Sn(1)	2.4572(6)	Sn(2)-Ni(1)-Sn(1)#1	98.38(2)
Sn(1)-N(1)	2.044(5)	Sn(2)#1-Ni(1)-Sn(1)#	182.13(2)
Sn(1)-N(2)	2.055(5)	Sn(2)-Ni(1)-Sn(1)	82.1 (3)
Sn(1)-O(1)	2.214(4)	Sn(2)#1-Ni(1)-Sn(1)	98.38(2)
Sn(1)-Si(1)	2.816(2)	Sn(1)#1-Ni(1)-Sn(1)	172.63(5)
Sn(1)-Sn(2)	3.2259(7)	Sn(2)-O(1)-Sn(1)	93.7(2)
Sn(2)-N(4)	2.050(5)		

4.9.1 Discussion of the molecular crystal structure of Ni[(Sn(N*t*Bu)$_2$SiMe$_2$)$_2$μ-O*i*Pr]$_2$ 10

A single crystal X-ray analysis of Ni[(Sn(N*t*Bu)$_2$SiMe$_2$)$_2$μ-O*i*Pr]$_2$ **10** was carried out for unequivocal identification of the structure as depicted in figure 14.

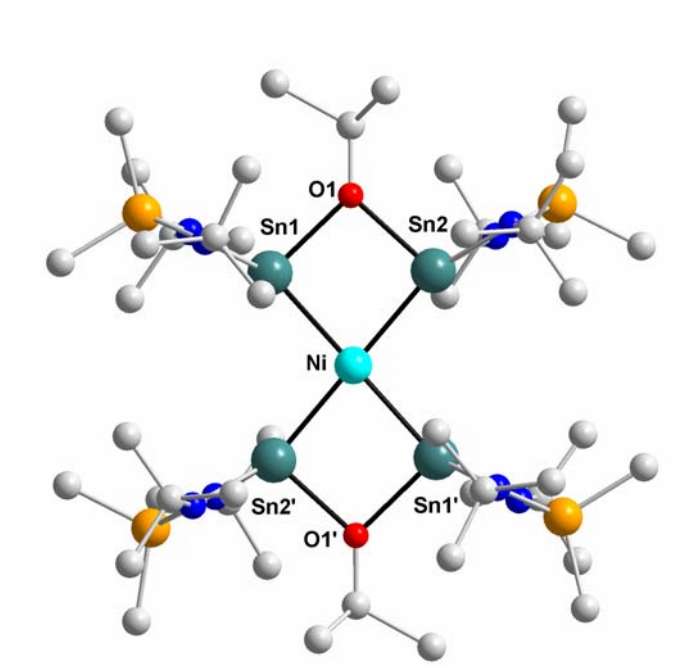

Figure 14: X-ray molecular structure of Ni[(Sn(N*t*Bu)$_2$SiMe$_2$)$_2$μ-O*i*Pr]$_2$ **10**. Hydrogen atoms are omitted for clarity and carbon, nitrogen and silicon atoms are not labelled.

The metal atoms in this compound form an almost planar NiSn$_4$ cross with nickel in the centre. One can measure the deviation from the ideal value of 180° with the both angles: Sn(1)-Ni-Sn(1') = 172.64(1)° and Sn(2)-Ni-Sn(2') = 172.06(1)°. The transition metal occupies the central site and two *iso*-propylate groups are inserted between two tin atoms forming a nearly symmetrical Sn-O-Sn bridge (Sn-O-Sn = 93.63(1)°, Sn(1)-O(1) = 2.216(2) Å and Sn(2)-O(1) = 2.208(2) Å). With respect to the NiSn$_2$O squares, each stannylene moiety is oriented in a perpendicular fashion. The change in coordination geometry of the central nickel atom between the starting material and the obtained compound explains the change in the formal oxidation state. From a formal Ni(0) (d^{10}) in the starting complex **14**, the nickel atom has the

oxidation state (II) (d^8) in the obtained compound **10**. This oxidation reaction is supported by IR spectroscopy as well as by NMR spectroscopy (see chapter 4.8.). A comparison of the X-ray crystal structures obtained for the complexes $Ni[Sn(OCH_3)(NtBu)\{N(H)tBu\}Si(CH_3)_2]_4$ **9-H** and $Ni[(Sn(NtBu)_2SiMe_2)_2\mu\text{-}OiPr]_2$ **10** corroborates this latter assumption. In the figure 15 are represented the planes formed by the stannylene's four-membered rings along the tin-silicon axis for the complexes **9-H** and **10**, a) and b), respectively.

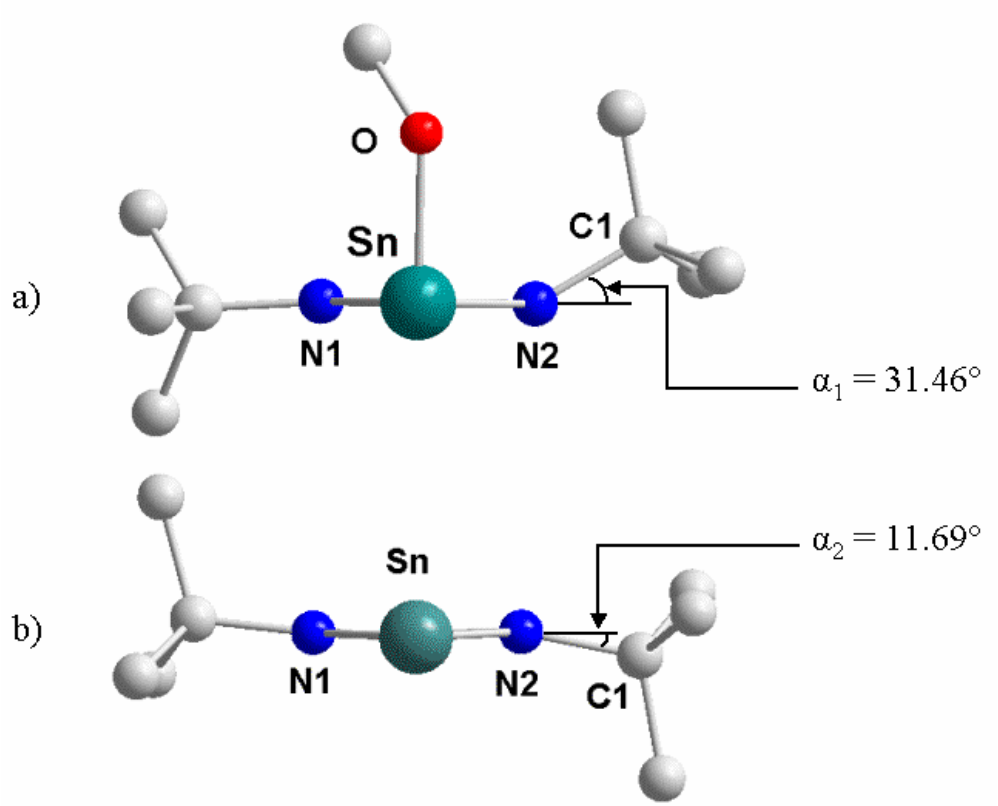

Figure 15: View along the Sn-Si axes of the stannylene ligands for the compounds $Ni[Sn(OCH_3)(NtBu)\{N(H)tBu\}Si(CH_3)_2]_4$ **9-H** and $Ni[(Sn(NtBu)_2SiMe_2)_2\mu\text{-}OiPr]_2$ **10**, a) and b), respectively.

The first observation, that can be made from this view is following: in the complex $Ni[Sn(OCH_3)(NtBu)\{N(H)tBu\}Si(CH_3)_2]_4$ **9-H** [figure 15 a)], one *tert*-butyl group deviates strongly from the plane formed by the four-membered ring. It corresponds to the *tert*-butyl group attached to the nitrogen atom N(2), which has trapped the hydrogen and whose geometry tends to be sp^3. The other *tert*-butyl group deviates only slightly from the plane. The nitrogen atom N(1) is still displays a trigonal planar geometry (sp^2 hybridised). At the contrary, and as can be seen on the figure 15 b), the

deviation from planarity for both of the *tert*-butyl groups in the compound **10** is equivalent. It means, that this deformation may not be due to a chemical factor (The presence of two hydrogen atoms does not make sense in a chemical point of view, and the presence of one hydrogen atom would provide an asymmetrical deformation.) but to packing effects. Moreover, the deviation itself is much more larger for the compound $Ni[Sn(OCH_3)(N\textit{t}Bu)\{N(H)\textit{t}Bu\}Si(CH_3)_2]_4$ **9-H** that for the compound $Ni[(Sn(N\textit{t}Bu)_2SiMe_2)_2\mu\text{-}O\textit{i}Pr]_2$ **10** ($\alpha_1 = 31.46°$ and $\alpha_2 = 11.69°$, respectively). It confirms that the compound **9-H** displays a proton at one nitrogen atom of each of its ligands, while the complex **10** results from an oxidation and does not present any protonated nitrogen atom on one of its ligands.

On the basis of the molecular crystal structure of **10**, two interpretations may be available to describe the complex: either a Ni^{2+} coordinated by two $[(Me_2Si(N\textit{t}Bu)_2Sn)_2(\mu\text{-}O\textit{i}Pr)]^-$ anions or a $(Me_2Si(N\textit{t}Bu)_2Sn)_4Ni^{2+}$ cation with two further *iso*-propylate moieties as counter-anion. Of course, any of these descriptions has to be taken as borderline cases and the charge separation into anions and cations is purely formal. A very few transition metal complexes of this type are reported in the literature. Veith *et al.* reported a similar compound where two bridging bromine atoms are located in the positions of the *iso*-propylate groups as can be seen in figure 16.[110]

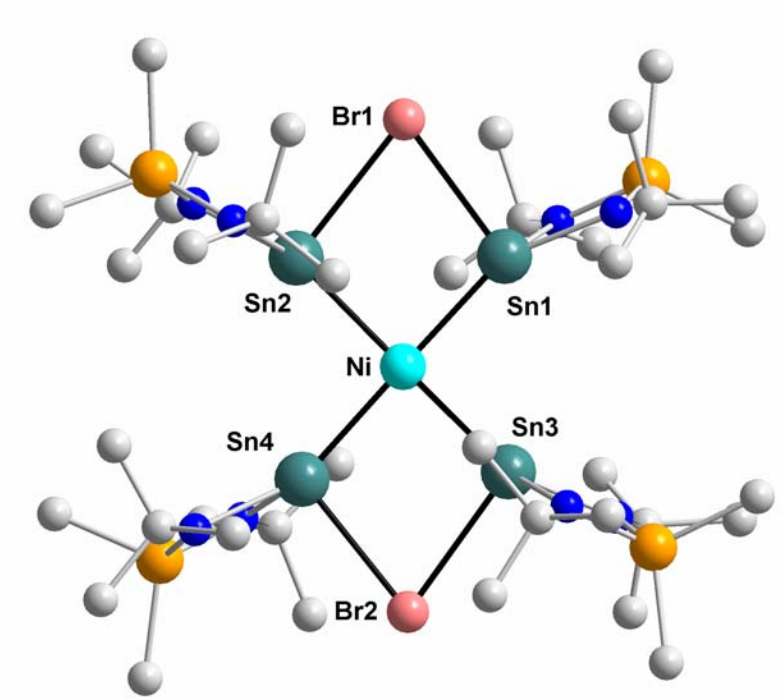

Figure 16: X-ray molecular structure of $[(Sn(NtBu)_2SiMe_2)_2\mu\text{-}Br]_2Ni$. Hydrogen atoms are omitted for clarity and carbon, nitrogen and silicon atoms are not labelled.

According to the general geometry of the compound, and in particular to the weak deviation from planarity of the nickel's coordination, it seems logical to consider the complex as only slightly paramagnetic and still more weakly paramagnetic than its bromine homologue. In figure 17 the respective deviations from planarity of both complexes $Ni[(Sn(NtBu)_2SiMe_2)_2\mu\text{-}OiPr]_2$ **10** and $[(Sn(NtBu)_2SiMe_2)_2\mu\text{-}Br]_2Ni$ are depicted. The magnetic behaviour of **10** has been studied and the magnetic susceptibility of the complex has been quantified according to the Evans method (see chapter 5.2).

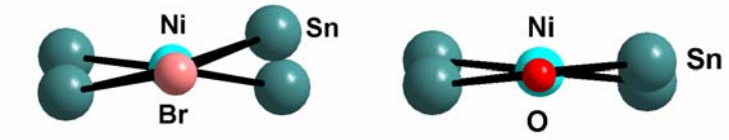

Figure 17: Comparison of the deviation from planarity for both complexes $[(Sn(NtBu)_2SiMe_2)_2\mu\text{-}Br]_2Ni$ and $Ni[(Sn(NtBu)_2SiMe_2)_2\mu\text{-}OiPr]_2$ **10**.

In regard to the bond lengths, it is to notice that due to the increasing coordination number at the tin atom, the nickel-tin bonds are longer than in the starting material:

Ni-Sn = 2.455(5) Å [Ni-Sn = 2.394 Å in the homoleptic nickel tetrakis-*bis*(amido)stannylene complex **14**].

In table 8 are reported some selected bond lengths and bond angles of **10** and $[(Sn(NtBu)_2SiMe_2)_2\mu\text{-}Br]_2Ni$ for comparison.

	$Ni\text{-}Sn_4\text{-}OiPr_2$ **10**	$Ni\text{-}Sn_4\text{-}Br_2$
Ni-Sn [Å]	2.455(7)	2.463(5)
Sn-X [Å]	2.212(2)	2.806(5)
Sn-N [Å]	2.05(3)	2.02(2)
Sn···Sn [Å]	3.23(2)	3.420(5)
Sn(1)-Ni-Sn(2) [°]	82.13(1)	87.7(1)
Sn(1)-Ni-Sn(1') [°]	172.64(1)	163.7(2)
Sn(2)-Ni-Sn(2') [°]	172.06(1)	162.9(2)
Sn-X-Sn [°]	93.63(1)	75.3(3)

Table 8: Selected bond lengths and angles for $[(Sn(NtBu)_2SiMe_2)_2\mu\text{-}Br]_2Ni$ and **10** (with X = O*i*Pr, Br).

4.10 Reactions between [CpNi{Sn(N*t*Bu)$_2$Si(CH$_3$)$_2$}$_2${μ-Cp}] 24 and different alcohols

As reported by M. Veith *et. al.* the reaction between the paramagnetic 20-electrons complex nickelocene [NiCp$_2$] with the bis(amido)stannylene Sn(N*t*Bu)$_2$Si(CH$_3$)$_2$ **12** gives rise to the formation of an 18-electrons sandwich complex **24** of the formula [CpNi{Sn(N*t*Bu)$_2$Si(CH$_3$)$_2$}$_2${μ-Cp}].[111] Repeated attempts to achieve an alcoholysis reaction without breaking the structural integrity of the starting complex were realised. As shown in equation 5, the nickel-tin bonds of starting complex **24** are cleaved by the addition an alcohol even in mild conditions.

[CpNi{Sn(N*t*Bu)$_2$Si(CH$_3$)$_2$}$_2${μ-Cp}] + 4 ROH

$\longrightarrow$ [NiCp$_2$] + 2 (NH*t*Bu)$_2$Si(CH$_3$)$_2$ + 2 "Sn(OR)$_2$"

24 **25** (Eq 5)

With R = Me, Et, *i*Pr, *t*Bu

^{119}Sn NMR solution spectra revealed the formation of the respective alkoxy stannylene. ^{1}H NMR and ^{13}C NMR showed the free diamine as byproduct. [NiCp$_2$] could have been unambiguously identified by recrystallisation or sublimation of the crude.

Chapter 5

Magnetic properties of the complexes 1, 2, 3, 4 and 10

5.1 Theoretical background

5.1.1 Magnetic moment and magnetic susceptibility

Electrons carry a negative electrical charge and produce a magnetic field as they move through space. A magnetic field is produced whenever an electrical charge is in motion. The strength of this field is called the magnetic moment.

When a substance (dissolved in a solvent or in the solid state) is placed within a magnetic field, the magnetic forces of the substance's electrons will be affected. In most atoms, electrons occur in pairs. Each electron in a pair spins in the opposite direction. So when electrons are paired together, their opposite spins cause their magnetic fields to cancel each other. Therefore, no net magnetic field exists. Alternately, substances with some unpaired electrons will have a net magnetic field and will react more to an external field. Most materials can be classified as ferromagnetic, diamagnetic or paramagnetic.

Diamagnetic substances have a very weak and negative susceptibility to magnetic fields. Diamagnetic materials are slightly repelled by a magnetic field and the material does not retain the magnetic properties when the external field is removed. Diamagnetic materials are substances with all paired electrons and, therefore, no permanent net magnetic moment per atom. Diamagnetic properties arise from the realignment of the electron orbits under the influence of an external magnetic field. Most elements in the periodic table, including copper, silver, and gold, are diamagnetic.

Paramagnetic substances have a small and positive susceptibility to magnetic fields. These materials are slightly attracted by a magnetic field and the material does not retain the magnetic properties when the external field is removed. Paramagnetic properties are due to the presence of some unpaired electrons and from the realignment of the electron orbits caused by the external magnetic field. Paramagnetic materials include magnesium, molybdenum, lithium, and tantalum.
Ferromagnetic substances have a large and positive susceptibility to an external magnetic field. They exhibit a strong attraction to magnetic fields and are able to retain their magnetic properties after the external field has been removed. Ferromagnetic materials have some unpaired electrons so their atoms have a net magnetic moment. Iron, nickel, and cobalt are examples of ferromagnetic materials.

The value that summarizes the magnetic properties of a substance is the magnetic susceptibility and is denoted χ. According to the different situations or measurement methods, one can deal with three different forms of the magnetic susceptibility:

χ_m: mass susceptibility
χ_V: volume susceptibility with $\chi_V = \rho . \chi_m$ (Eq 1)
χ_M: molar susceptibility with $\chi_M = M . \chi_m$ (Eq 2)

As far as the molecular properties are concerned, χ_M has to be used. In a general manner, the molar susceptibility can be defined as follow:

$\chi_M = \chi_M(dia) + \chi_M(para)$
$< 0 \qquad > 0$
$\neq f(T) \qquad = f(1/T)$

Type	χ_M [$cm^{-3}.mol^{-1}$]	Temperature dependence
Dia	-(1 to 500). 10^{-6}	Independent
Para	+(0 to 1). 10^{-2}	1/T
Ferro	+(10 to 10^6)	Complex $\chi \uparrow$, T $\downarrow$
Antiferro	+(0 to 1). 10^{-2}	Complex $\chi \uparrow$, T $\uparrow$

Table 1: The different types of magnetism.

Consider a liquid sample constituted by a set of identical molecules dissolved in a solvent (the eventual magnetic properties of the solvent are neglected), each one having a magnetic moment μ free to orient in any direction. An external magnetic field will coerce an alignment of these moments. Nevertheless, the thermic motion will hinder this alignment. The following equations (equations 3 and 4), known as the Curie's law, give an expression of the magnetic moment μ as a function of the magnetic susceptibility χ:

$$\chi_M = \frac{\mu^2.N_a}{3kT} \qquad \text{(Eq 3)}$$

$$\mu = \frac{\sqrt{3RT.\chi_M}}{N_a} = 2.828\ \sqrt{\chi_M.T} \qquad \text{(Eq 4)}$$

5.1.2 Magnetic properties of nickel(II) complexes

The nickel(II) ion has a $3d^8$ outer electron configuration, which gives rise to the triplet and singlet terms (in order of increasing energy) ^3F, ^1D, ^3P, ^1G, ^1S. The crystal field diagrams for this ion in tetrahedral, octahedral and tetragonal fields are shown in figure 1. It can be readily seen from these diagrams that in octahedral and in slightly tetragonally distorted octahedral fields, two unpaired electrons are present. The ground state makes no orbital contribution to the magnetic moment so that these moments are expected to be not greatly different from the "spin only" moment (2.83 BM[112,113]). In tetrahedral field, again, two unpaired electrons are present, but there is now orbital contribution to the magnetic moment through the equivalence and

degeneracy of the incompletely filled t_2 orbitals. Magnetic moments are thus expected to be larger than the spin only value and typically lie in the range 3.2-4.4 BM.[114,115]

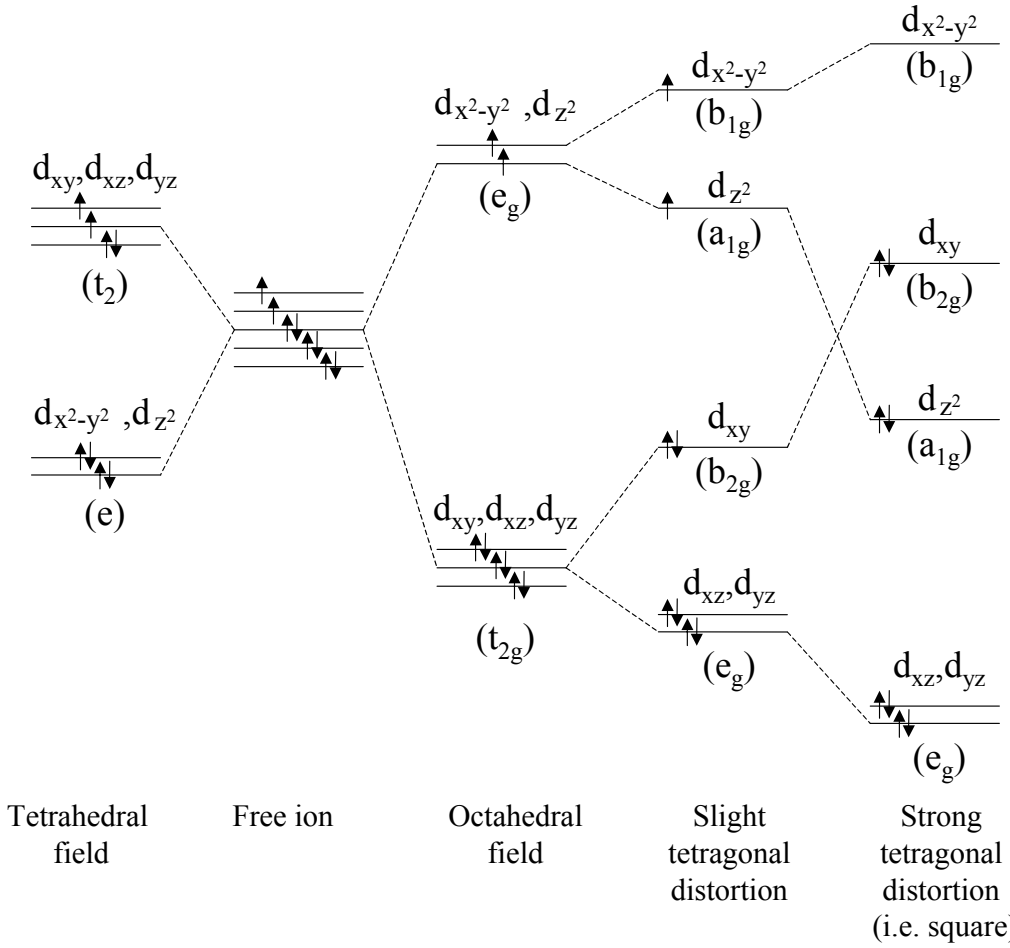

Figure 1: Crystal field splitting diagrams for nickel(II) in different crystal field.

5.1.3 Evans method

In the present work, magnetic moments μ of different nickel complexes are determined in solution according to a spectroscopic method called Evans method.[116] In a classical NMR measurement, the chemical shifts of hydrogen or carbon atoms of a given molecule depend of the susceptibility of the medium. In presence of a compound having magnetic properties, the resonance frequencies of the solvent are shifted in comparison with an external standard (the pure solvent) according to the following equations (Equations 5 and 6):

$$\frac{\Delta H}{H} = \frac{\Delta \upsilon}{\upsilon} = \frac{2\pi}{3} \Delta\chi \qquad \text{(Eq 5)}$$

$$\frac{\Delta H}{H} = \frac{\Delta \upsilon}{\upsilon} = \frac{4\pi}{3}\Delta\chi \qquad \text{(Eq 6)}$$

H: Magnetic field

$\Delta\chi$: Difference of the volume susceptibility between the solution and the solvent

$\Delta\upsilon$: Difference of chemical shift (Hz)

υ: Spectrometer frequency (Hz)

$\frac{2\pi}{3}$: Form factor of a cylindrical sample (NMR sample) if the sample is perpendicularly oriented to the magnetic field.

$\frac{4\pi}{3}$: Form factor of a cylindrical sample (NMR sample) if the sample is oriented in a parallel fashion to the magnetic field

Then, the Evans formula (equation 7) permits to obtain the mass susceptibility of the dissolved paramagnetic compound χ_m (here with the factor $\frac{4\pi}{3}$):

$$\chi_m = \frac{3\Delta\upsilon}{4\pi\upsilon m} + \chi_0 + \frac{\chi_0(d_0 - d_s)}{m} \qquad \text{(Eq 7)}$$

m: Concentration of the compound in $g.ml^{-1}$

χ_0 : Mass susceptibility of the solvent

d_0: Density of the solvent

d_s: Density of the solution

The introduction of the mass susceptibility in the equation 2 allows the calculation of the molar susceptibility:

$\chi_M = M.\ \chi_m$

The magnetic moment can be now easily calculated through the use of the Curie's law (equation 4):

$$\mu = \frac{\sqrt{3RT.\chi_M}}{N_a} = 2.828\ \sqrt{\chi_M.T}$$

As far as tetrahedral nickel(II) complexes are concerned, their experimental moments lie within the range of 3.2-4.4 BM[115] and are dependent upon temperature. If the

ligand field departs from tetrahedral symmetry or if electron delocalisation occurs, then the magnetic moment becomes closer to the spin only value, and shows less variation with the temperature.

5.2 Experimental determination of the magnetic susceptibility of the complexes 1, 2, 3, 4 and 10

The determination of the magnetic susceptibility of the complexes **1**, **2**, **3**, **4** and **10** was carried out according to the previously described Evans method. The analysis of the complex $NiSn_2(OtBu)_6$ **1**, revealed a magnetic susceptibility of 3.98 BM. This value almost matches with what one should expect from a nickel atom displaying two unpaired electrons. The magnetic susceptibility exhibited by the dinickel homologue $Ni_2Sn_2(OtBu)_8$ **21**, is 4.40 BM.[23] The comparison of these values suggests that the electrons of one metallic ion may have spin orientations opposite to those of the other, and so the electrons appear to be spin-paired. Normally, this arises in covalent electron pair bond formation, but here the two nickel(II) ions are not directly bonded to each other. Rather they are indirectly coupled through the bridging alkoxide groups. The oxygen atom is sp^2 hybridised, with a p orbital displaying a strong lone pair character. This phenomenon is called "superexchange"[117-119] or "anti-ferromagnetic coupling" of electrons.[120,121] It is entirely analogous to the coupling of nuclear spins.[122]

In figure 2, a simplified model is proposed to explain the weak magnetic susceptibility obtained for the complexes $Ni_2Sn_2(OtBu)_8$ **21**, $[\{(CO)_4Fe\}_2\{Ni_2Sn_2(OtBu)_8\}]$ **3**, and $[\{(CO)_4Fe\}_2\{Ni_2Ge_2(OtBu)_8\}]$ **4**.

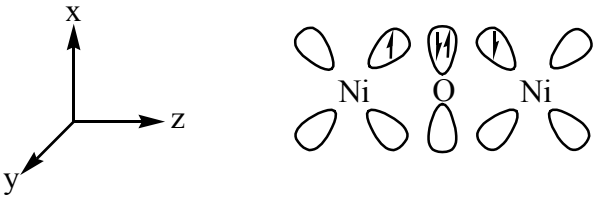

Figure 2: Combination of two nickel (d_{xz}) orbitals and one oxygen (p_x) orbital forming an anti-ferromagnetic coupling.

The measurement of the magnetic susceptibility of the nickel plumbate $Ni_2Pb_2(OtBu)_8$ **2** gave a value of 4.32 BM. This value confirms the previously reported presumption that the ligand does not participate significantly to the magnetic behavior of the complex. Indeed, the lighter nickel germanate homologue presents a magnetic susceptibility of 4.51 BM and the nickel stannate shows a value of 4.40. This may signify that the nature and the geometry of the central core of the complex is the most determining factor, which decides of the main magnetic character of the complex.

The compounds $[\{(CO)_4Fe\}_2\{Ni_2Sn_2(OtBu)_8\}]$ **3** and $[\{(CO)_4Fe\}_2\{Ni_2Ge_2(OtBu)_8\}]$ **4** were also the subjects of a quantitative analysis. They show a value of 4.11 BM and 4.26 BM, respectively. As expected, the magnetic susceptibility for these two complexes is slightly weaker than those measured for the non-coordinated complexes. This matches with the initial assumption that the "peripheric" metallic atoms do not significantly interfere with the central dinickel core of the compound. From a qualitative point of view, it seems like the iron carbonyl moieties may withdraw some electron density from the centre of the complex and thus, contribute to decrease slightly the magnetic susceptibility.

Analysis of the structural data revealed important contributions of the electronic environments of the central nickel atoms to the Ni···Ni and Ni···El distances (with El = Ge, Sn). The qualitative model of molecular orbitals described in the chapter 3.10. has been used to explain these features.

Finally, it seems like each nickel atom of the compounds **2**, **3** and **4** can influence its neighbor through a direct "contact" or through a superexchange phenomenon via the alkoxide bridging groups.

The compound **10** $Ni[(Sn(NtBu)_2SiMe_2)_2\mu\text{-}OiPr]_2$ exhibits a slight magnetic behavior. This property could have been predicted by the analysis of the crystal structure. As shown in chapter 4.9.1., the square formed by the central core of the molecule: $Ni\text{-}Sn_4$ deviates slightly from planarity. As a result, and as shown in chapter 5.1.2., this induces a very weak magnetic effect, which has been quantified according to the Evans method. The measurement showed a value of 0.1 BM, which is in accord with one can expect from the literature.[110]

Chapter 6

Summary and outlook

The present work focuses on the synthesis of new nickel complexes displaying low-valent group 14 metals as ligand. The work was divided in two parts: In a first part, investigations falling under the continuation of the work initiated by Veith *et. al.*,[23] concerning the synthesis and reactivity of one-dimensionally and discretely arranged metallic chains displaying nickel(II) atoms and low-valent group 14 metallic elements held together by bridging alkoxide groups is investigated. The reactivity of these complexes, in particular the ability of the low-valent element situated in the terminal position of the metallic chain to coordinate further metallic fragments was also explored.

The second part deals with the investigations on the reactivity of two zero-valent nickel-amido stannylene complexes ($Ni[Sn(NtBu)_2Si(CH_3)_2]_4$ **14** and $[CpNi\{Sn(NtBu)_2Si(CH_3)_2\}_2\{\mu\text{-}Cp\}]$ **24**) towards alcohols and tends to demonstrate how a small metallic centre such as nickel can be stabilised by group 14 bivalent metallic ligands.

After the synthesises of the nickel germanate $Ni_2Ge_2(OtBu)_8$ **22** and the nickel stannate $Ni_2Sn_2(OtBu)_8$ **21** performed earlier, the synthesis of the heaviest homologue of the group $Ni_2Pb_2(OtBu)_8$ **2** was also achieved.

A very similar procedure was carried out to perform the synthesis of a new spiro nickel stannate $NiSn_2(OtBu)_6$ **1**. This promising complex differs from the previously reported homologues because of its good volatility.

All these compounds display a low-valent metallic element situated in the

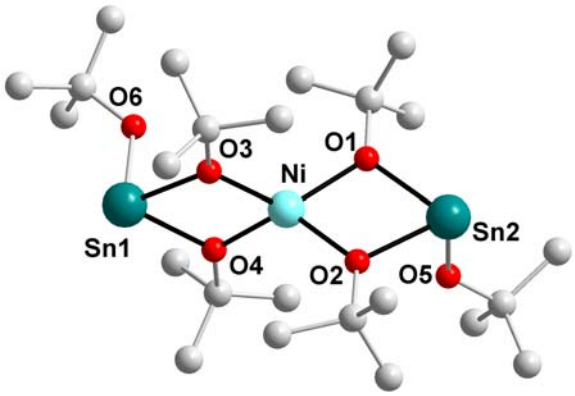

Figure 1: $NiSn_2(OtBu)_6$ **1**.

terminal position of the metallic chain. These metallic centres are all situated in the axial site of a trigonal pyramid and thus, are of suitable orientation for a complexation with further metallic units.

The researches were focused on the reactivity of $Ni_2Sn_2(OtBu)_8$ **21** towards different metal carbonyl fragments. Different procedures were applied: group 6 metal carbonyls were photolytically activated and allowed to react with **21**. The infrared monitoring of the reactions evidenced the formation of new tin-metal bonds but until now, it was neither possible to determine an exact chemical composition of these compounds nor to isolate any product. It appeared, that nonacarbonyl diiron provided better results, since reacted with **21** or **22**, the linear trimetallic chains $[\{(CO)_4Fe\}_2\{Ni_2Sn_2(OtBu)_8\}]$ **3** and $[\{(CO)_4Fe\}_2\{Ni_2Ge_2(OtBu)_8\}]$ **4** (Figure2) could have been obtained in acceptable yields.

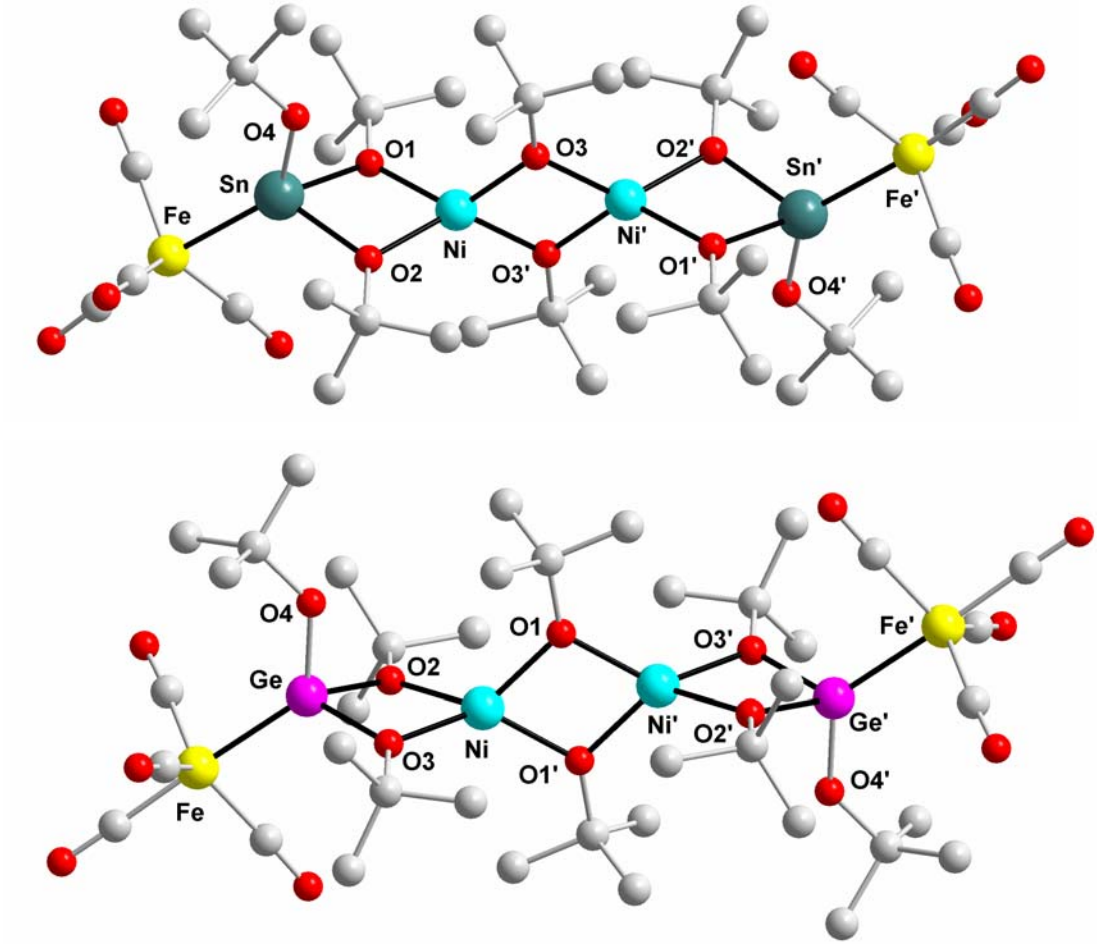

Figure 2: $[\{(CO)_4Fe\}_2\{Ni_2Sn_2(OtBu)_8\}]$ **3** and $[\{(CO)_4Fe\}_2\{Ni_2Ge_2(OtBu)_8\}]$ **4**.

All these complexes exhibit magnetic properties. A quantitative analysis of the magnetic susceptibility in solution was performed by each of these compounds. It

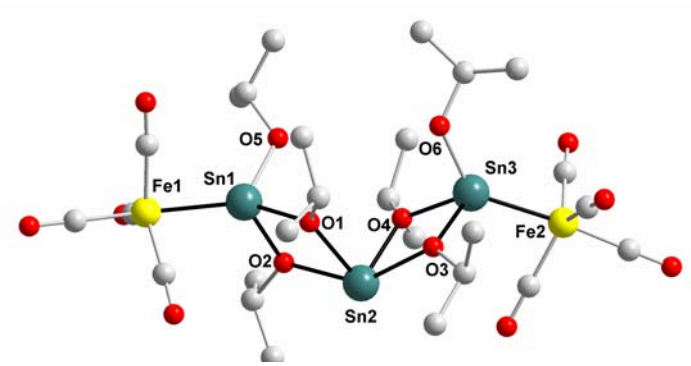

Figure 3: [Sn{(μ-O*i*Pr)$_2$Sn(O*i*Pr)Fe(CO)$_4$}$_2$] **6**.

revealed that the magnetic behaviour of these complexes is determined by the central dinickel core of the compounds. The initial assumption, that the "peripheric" metal atoms do not seem to interfere significantly with the central dinickel moiety have been verified. The complex **6**, which can also be described as a bent chain of metallic atoms, was obtained from the reaction of nonacarbonyl diiron with [Sn(μ-O*i*Pr)$_2$]$_\infty$ **5**. It was shown, that the the starting polymer **5** was cleaved to yield selectively to a bimetallic arrangement (Figure 3).

The second part of the work was focused on the study of nickel(0)-tin(II) systems. In order to achieve the synthesis of alkoxy stannylene containing nickel(0) complexes, investigations on the reactivity of the amido stannylene-nickel complex **14** towards alcohols were carried out. The main trend, that could have been established, is the very high lability of the stannylene ligand. It appeared, that this chemistry is greatly determined by kinetics aspects. Despite the fact that no selective elimination of the amido residues could have been performed, alkoxy ligands could have been coordinated at the tin centre without decomposition of the starting complex.

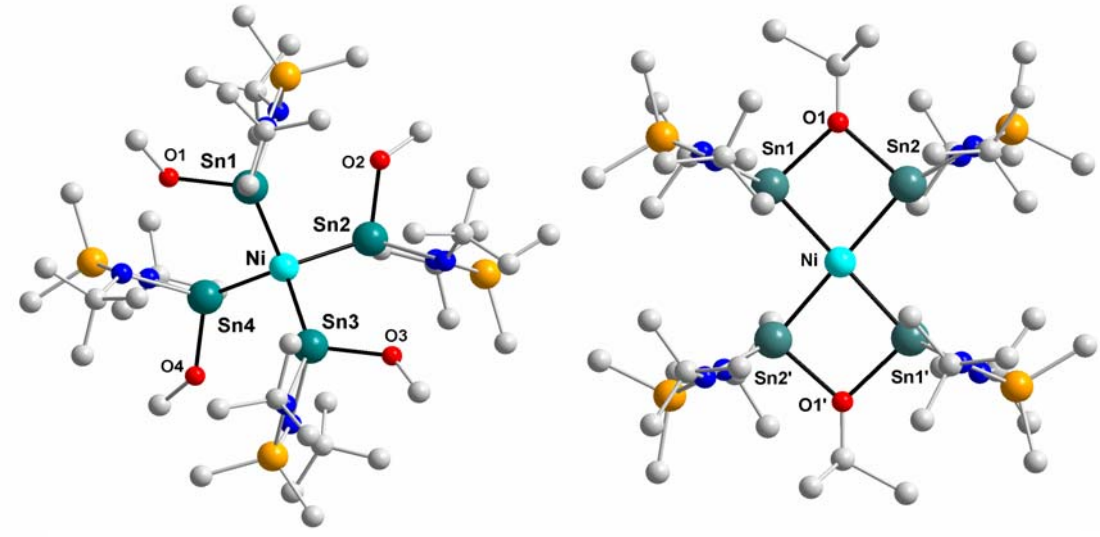

Figure 4: Ni[Sn(OCH$_3$)(N*t*Bu){N(H)*t*Bu}Si(CH$_3$)$_2$]$_4$ **9-H** and Ni[(Sn(N*t*Bu)$_2$SiMe$_2$)$_2$μ-O*i*Pr]$_2$ **10**.

Two new zero-valent nickel-stannylene complexes could have been isolated and unambiguously characterised. The compounds **9-H** and **10** constitute two scarce examples of structurally characterised molecular compounds displaying a nickel-tin(II)-oxygen connectivity. Nevertheless, while the complex **9-H** or its deuterated homologue **9-D** still display a nickel(0) centre, the complex **10**, with its nickel(II) centre, results from an oxidation reaction. This point underlines the very versatile behaviour of the starting amidostannylene-nickel complex **21** towards alcohols.
The synthesis of $Ni[Ge(NtBu)_2Si(CH_3)_2]_4$ **8**, a new zero-valent nickel-germylene complex, allows also the same type of alcoholysis reactions to occur and consequently, represents a promising compound. A study about the ligating properties of the germylene unit towards a stannylene ligand has been reported. Despite the lack of crystallographic evidences, it appears almost sure that the replacement of a germylene ligand by a stannylene is feasible. The reaction leads to the isolation of a new heteroleptic germylene-stannylene-nickel(0) complex. To the best of our knowledge, no complex of this type have been reported until now.

Both types of complexes, Ni(II)-Sn(II) one-dimensionally arranged systems or Ni(0)-Sn(II) centered molecules, constitute potential precursors of interest. Compounds **1**, **2**, **3** and **4** or designable complexes of this type have already proven their quality as ceramic precursors. To go more ahead into the understanding of their magnetic properties, an analysis in the solid state may be required.
Further investigations on a potential catalytic activity of the presented zero-valent nickel-stannylene or germylene complexes may also constitute an interesting field of research.

Chapter 7

Experimental part

7.1 General techniques

All reactions were carried out under inert dinitrogen atmosphere in a modified "Stockschen vacuum apparatus". The necessary vacuum was obtained with a rotary vane pump of the Vacuumbrand company (model R75, 5.4 m^3/h, $4x10^{-4}$ mbar). The solvents (THF, pentane, hexane, toluene, benzene) were distilled from sodium and kept under nitrogen.

7.2 Elemental analysis

Analytical data were measured on an all-automatic CHN-900 Elemental Analysator from LECO *Corporation*, by Mss. Helga Feuerhake (Anorganische Chemie, Saarbrücken). Calculations of theoretical molar masses were done with relative atomic masses IUPAC 2001.
Some samples (Compound **1**, **2**, **3**, **8**) repeatedly showed a considerably lower content of cabon and hydrogen than calculated. This may be due in part to carbide formation during the combustion and high sensitivity of the compounds.

7.3 Spectroscopic methods

7.3.1 Nuclear Magnetic Resonance

The NMR spectra were recorded on Bruker 200 NMR ACF and ACP spectrometers. Samples were prepared with appropriate solvent and approximately 5 Vol.% C_6D_6 used as lock solvent. Chemical shifts are given according to the δ-scale in ppm. The

reference corresponds to the signal of benzene ($\delta(^1H, C_6D_5H)$ = 7.15 ppm, $\delta(^{13}C)$ = 128.0 ppm). Coupling constants ^nJ are given in Herz (Hz). To characterise the spin multiplicity, abbreviation are used: s = singlet, d = doublet, t = triplet, q = quartet, m = multiplet.

Core	Measurement frequency (MHz)
^1H	200.1
^{13}C	50.3
^{119}Sn	74.6

Table 1: Measurement frequency used for NMR samples.

7.3.2 Infrared

The solution IR spectra were recorded in KBr cuvettes on a BioRad FTS 165. The designation of the bands was done with subjective appreciation: vs (very strong), s (strong), m (medium), w (weak), br (broad).

7.3.3 Ultraviolet-visible

The electronic transition spectra were measured in liquid media on a SP8-100 spectrometer from Pye Unicam.

7.4 Crystallographic analysis

X-Ray crystallography was performed with a STOE IPDS diffractometer with Kα radiation (λ = 0.71073 Δ). Structures were solved by direct methods and refined by full-matrix least-square methods on F^2 with SHELX-97. Hydrogen atoms were refined as rigid groups with the attached carbon atoms. Drawings were made with Diamond2.1.

7.5 Synthesis of the starting materials

The following compounds were prepared according to well-established procedures. Excepting elemental analyses, which were not systematically proceeding, they were fully characterised.

Compound	Reference
$(CH_3)_2Si(NHtBu)_2$	[123]
$Sn(NtBu)_2SiMe_2$	[109]
$[Sn(\mu\text{-}OtBu)(OtBu)]_2$	[88]
$Ni[Sn(NtBu)_2Si(CH_3)_2]_4$	[61]
$[NaSn(OtBu)_3]_2$	[51]
$[NaGe(OtBu)_3]_2$	[51]
$[NaPb(OtBu)_3]_2$	[51]
$Li[N(Si(CH_3)_3)_2]$	[124]
$Ge(N(Si(CH_3)_3)_2$	[125]
$Pb(N(Si(CH_3)_3)_2$	[125]
$Ni_2Sn_2(OtBu)_8$	[23]
$Ni_2Ge_2(OtBu)_8$	[23]

Table 2: Bibliographical references of starting materials.

7.6 Synthesis of $NiSn_2(OtBu)_6$ 1

$NiCl_2$ (0.49 g, 3.78 mmol) was added in a solution of $[NaSn(OtBu)_3]_2$ (2.46 g, 3.41 mmol) in toluene. The suspension was refluxed during 2 days, during which the colour turned to violet. After filtration of NaCl, the solvent was removed under reduced pressure until a solid starts to form at the glass wall. The solution was kept at –10 °C over 2 days and very fine blue violet needles were isolated (1.13 g, 42 %).
This complex was also prepared according to a second way of synthesis, nevertheless, it appeared that it was only a byproduct:

Tert-butyl alcohol (0.20 ml, 2.10 mmol) was slowly added to a stirred solution of $Ni[Sn(NtBu)_2Si(CH_3)_2]_4$ (0.35 g, 0.26 mmol) in toluene at 0 °C. The solution turned instantaneously black. After 1 hour stirring, the solvent was removed *in vacuo* and the black residue was sublimed under reduced pressure (55 °C, 10^{-2} mbar). A violet solid was obtained in a very weak yield (13.3 mg, 7 %).

Characterisation:
Formula: $C_{24}H_{54}O_6Sn_2Ni$
Molecular weight (calculated): 734.33 g/mol
UV (toluene): λ [nm] = 455.2; 548.7; 592.3; 642.3; 794.5; 875.5
ε [$dm^3.mol^{-1}.cm^{-1}$] = 0.143; 0.687; 0.583; 0.063; 0.071
Elemental analysis:

	C	H	N
Found [%]	33.77	6.51	0.08
Calculated [%]	39.23	7.41	0.00

7.7 Synthesis of $Ni_2Pb_2(OtBu)_8$ 2

$NiBr_2$ (0.76 g, 3.46 mmol) was added to $[NaPb(OtBu)_3]_2$ (3.11 g, 3.46 mmol) dissolved in a toluene / pyridine 5:1 mixture. The suspension was refluxed during 12 hours, during which the colour turned to violet. After filtration of NaBr, the solvent was removed under reduced pressure until a solid starts to form at the glass wall. The solution was kept at -10 °C over 2 days and very fine blue violet needles were isolated (1.19 g, 31 %).

Characterisation:
Formula: $C_{32}H_{72}O_8Pb_2Ni_2$
Molecular weight (calculated): 1116.10 g/mol
Elemental analysis:

	C	H	N
Found [%]	32.70	6.42	0.05
Calculated [%]	34.42	6.50	0.00

7.8 Synthesis of $[\{(CO)_4Fe\}_2\{Ni_2Sn_2(OtBu)_8\}]$ 3

$Fe_2(CO)_9$ (0.32 g, 0.88 mmol) was directly added as solid in a toluene solution (25 ml) of $Ni_2Sn_2(OtBu)_8$ (0.41 g, 0.44 mmol). The suspension was allowed to stir 15 h at room temperature. After removal of the solvent, a brown solid was extracted with hexane, re-dissolved in a THF / *n*-hexane 1:1 mixture, concentrated and kept at -10 °C. Micro violet needles were isolated (0.25 g, 44 %).

Characterisation:
Formula: $C_{40}H_{72}O_{16}Sn_2Ni_2Fe_2$
Molecular weight (calculated): 1274.88 g/mol
IR: υ [cm^{-1}] = 1938 (vs), 1970 (m), 2044 (s)

Elemental analysis:

	C	H	N
Found [%]	32.88	5.26	-0.23
Calculated [%]	37.69	5.65	0.00

7.9 Synthesis of [{(CO)$_4$Fe}$_2${Ni$_2$Ge$_2$(O*t*Bu)$_8$}] 4

$Fe_2(CO)_9$ (0.16 g, 0.44 mmol) was directly added as a solid in a toluene solution (25 ml) of $Ni_2Ge_2(O$*t*$Bu)_8$ (0.14 g, 0.22 mmol). The suspension was allowed to stir 12 hours at room temperature. After removal of the solvent, a brown solid was extracted with hexane, re-dissolved in a THF / *n*-hexane 1:1 mixture, concentrated and kept at -10 °C. Micro violet needles were isolated (0.16 g, 62 %).

Characterisation:
Formula: $C_{40}H_{72}O_{16}Ge_2Ni_2Fe_2$
Molecular weight (calculated): 1182.68 g/mol
IR: υ [cm^{-1}] = 1939 (vs), 1968 (m), 2037 (s)
Elemental analysis:

	C	H	N
Found [%]	40.96	6.35	0.12
Calculated [%]	40.62	6.09	0.00

7.10 Synthesis of $[Sn(\mu\text{-}O\textit{i}Pr)_2]_\infty$ 5

To a magnetically stirred solution of $Sn(N^tBu)_2SiMe_2$ (4.53 g, 14.20 mmol) in toluene (15 ml), 2-propanol (2.14 ml, 28.4 mmol) was slowly added. The initially red solution lost instantaneously its coloration. After 30 minutes, the solution had become completely colourless and was reduced *in vacuo*. The white residue was sublimated under reduced pressure (60 °C, 10^{-2} mbar) to give a white crystalline solid (2.92 g, 87 %).

Characterisation:

Formula: $C_6H_{14}O_2Sn$ calculated for a monomer.

Molecular weight (calculated): 236.69 g/mol

^{1}H-NMR (C_6D_6, 200.1MHz)

δ [ppm] = 1.53 (6H, d, $C(C\mathbf{H}_3)_2$)

2.26 (1H, sep, $C\mathbf{H}(CH_3)_2$)

$^{13}C\{^1H\}$-NMR (C_6D_6, 50.3MHz)

δ [ppm] = 28.42 ($C(\mathbf{C}H_3)_2$)

65.69 ($\mathbf{C}H(CH_3)_2$)

$^{119}Sn\{^1H\}$-NMR (C_6D_6, 74.6MHz)

δ [ppm] = -209.87

Elemental analysis:

	C	H	N
Found [%]	28.74	5.12	0.02
Calculated [%]	30.42	5.96	0.00

7.11 Synthesis of [Sn{(μ-O*i*Pr)$_2$Sn(O*i*Pr)Fe(CO)$_4$}$_2$] 6

$Fe_2(CO)_9$ (1.51 g, 4.14 mmol) was added to a magnetically stirred solution of [Sn(μ-O*i*Pr)$_2$]$_\infty$ (0.98 g, 4.14 mmol). The suspension was stirred at room temperature until the complete dissolution of $Fe_2(CO)_9$, and the reaction was monitored by IR-spectroscopy. After 24 hours, the solvent was removed under reduced pressure and the residue was washed three times with toluene to extract fully $Fe(CO)_5$. The residue was dissolved in toluene and slowly re-concentrated under reduced pressure until a solid starts to form at the glass wall. The solution was kept at -10 °C and after one night, well-developed orange crystals were isolated (2.40 g, 56 %).

Characterisation:

Formula: $C_{26}H_{42}O_{14}Sn_3Fe_2$

Molecular weight (calculated): 1046.04 g/mol

^{1}H-NMR (C_6D_6, 200.1MHz)

δ [ppm] = 1.27 (6H, d, CH(C**H**$_3$)$_2$)

4.59 (1H, sep, C**H**(CH$_3$)$_2$)

^{13}C{^{1}H}-NMR (C_6D_6, 50.3MHz)

δ [ppm] = 27.32 (CH(**C**H$_3$)$_2$)

68.95 (**C**H(CH$_3$)$_2$)

210.48 (CO *trans* to Sn)

213.32 (CO *cis* to Sn)

^{119}Sn{^{1}H}-NMR (C_6D_6, 74.6MHz)

δ [ppm] = -550.60; 97.49

IR: υ [cm^{-1}] = 1946 (vs), 1973 (m), 2049 (s)

Elemental analysis:

	C	H	N
Found [%]	30.24	4.55	-0.16
Calculated [%]	29.85	4.02	0.00

7.12 Synthesis of $Ni[Ge(NtBu)_2Si(CH_3)_2]_4$ 8

The established procedure for the synthesis of $Ni[Sn(NtBu)_2Si(CH_3)_2]_4$ was reproduced. Only the ligand was changed: To a magnetically stirred solution of $Ni(cod)_2$ (0.82 g, 2.98 mmol) in toluene (50 ml) at -78 °C, $Ge(NtBu)_2Si(CH_3)_2$ (3.25 g, 11.92 mmol) was slowly added. The initially yellow solution darkened on warming and became deep red at -30 °C. Following stirring at room temperature for 3 h, the solution was filtered and reduced in volume to 20 ml. After one night at -10 °C, well developed, red plate crystals (3.08 g, 2.68 mmol) were isolated in a 90 % yield.

Characterisation:
Formula: $C_{40}H_{96}N_8Si_4Ge_4Ni$
Molecular weight (calculated): 1149.89 g/mol

^{1}H-NMR (C_6D_6, 200.1MHz)

δ [ppm] = 0.44 (3H, s, SiMe)
1.49 (9H, s, $C(CH_3)_3$)

$^{13}C\{^1H\}$-NMR (C_6D_6, 50.3MHz)

δ [ppm] = 6.32 (SiMe)
35.61 ($C(\mathbf{C}H_3)_3$)
53.78 ($\mathbf{C}(CH_3)_3$)

Elemental analysis:

	C	H	N
Found [%]	38.61	9.62	9.02
Calculated [%]	41.78	8.35	9.74

7.13 Synthesis of $Ni[Sn(OCH_3)(NtBu)\{N(H)tBu\}Si(CH_3)_2]_4$ 9-H

CH_3OH (0.04 ml, 1.02 mmol) freshly distilled from CaH_2 was slowly added to a stirred solution of $Ni[Sn(NtBu)_2Si(CH_3)_2]_4$ (0.17g, 0.13mmol) in *n*-hexane. The mixture turned instantaneously from dark red to yellow. After a reaction time of 90 minutes, volatiles were removed under reduced pressure until a solid starts to form at the glass wall. The solution was kept at -10 °C over 5 days and very sensitive fine yellow needles were isolated (0.11 g, 62 %).
The synthesis of the complex **9-D** was achieved according to the same experimental procedure.

Characterisation:
Formula: $C_{44}H_{112}N_8NiO_4Si_4Sn_4$
Molecular weight (calculated): 1463.29 g/mol
^{1}H-NMR (C_6D_6, 200.1MHz)

δ [ppm] = 0.55 (3H, s, SiMe)
0.59 (3H, s, SiMe)
1.41 (9H, s, $C(CH_3)_3$)
1.51 (9H, s, $C(CH_3)_3$)
3.99 (3H, s, OMe)
5.84 (1H, s, NH)

$^{13}C\{^1H\}$-NMR (C_6D_6, 50.3MHz)

δ [ppm] = 6.44 (SiMe)
6.79 (SiMe)
32.37 ($C(\mathbf{C}H_3)_3$)
35.72 ($C(\mathbf{C}H_3)_3$)
51.14 ($\mathbf{C}(CH_3)_3$)
54.11 ($\mathbf{C}(CH_3)_3$)
107.23 (OMe)

$^{119}Sn\{^{1}H\}$-NMR (C_6D_6, 74.6MHz)

δ [ppm] = 48.74

Elemental analysis:

	C	H	N
Found [%]	34.36	8.19	6.96
Calculated [%]	36.12	7.71	7.66

7.14 Synthesis of Ni[(Sn(N*t*Bu)$_2$SiMe$_2$)$_2$μ-O*i*Pr]$_2$ 10

*I*PrOH freshly distilled from CaH_2 (0.38 ml, 4.91 mmol) was slowly added to a stirred solution of Ni[(Sn(N*t*Bu)$_2$SiMe$_2$)]$_4$ (0.82 g, 0.61 mmol) in toluene at room temperature. The solution turned instantaneously from dark red to dark green with the formation of a solid at the bottom of the flask. The reaction mixture was allowed to stir for 2 hours and then the volatiles were removed under reduced pressure. The black residue was extracted with *n*-hexane and the solution was re-concentrated until a solid starts to form at the glass wall. The solution was kept at room temperature and after 7 days, fine yellow needles were isolated (0.50 g, 56 %).

Characterisation:

Formula: $C_{46}H_{110}N_8Si_4O_2Sn_4Ni$

Molecular weight (calculated): 1452.35 g/mol

^{1}H-NMR (C_6D_6, 200.1MHz)

δ [ppm] = 0.44 (12H, s, Si(C**H**$_3$)$_2$)

1.49 (36H, s, C (C**H**$_3$)$_3$)

2.62 (6H, d, CH(C**H**$_3$)$_2$)

3.39 (1H, sep, C**H**(CH$_3$)$_2$)

$^{13}C\{^1H\}$-NMR (C_6D_6, 50.3MHz)

δ [ppm] = 7.25 (SiMe)
37.02 ($C(\mathbf{C}H_3)_3$)
53.41 ($\mathbf{C}(CH_3)_3$)
65.23 ($CH(\mathbf{C}H_3)_2$)
96.59 ($\mathbf{C}H(CH_3)_2$)

$^{119}Sn\{^1H\}$-NMR (C_6D_6, 74.6MHz)

δ [ppm] = -398.46

Elemental analysis:

	C	H	N
Found [%]	39.12	7.89	8.03
Calculated [%]	38.04	7.57	7.72

7.15 Synthesis of [{$Ni_2Ge_2(OtBu)_8$}{$Na_2Ge_2(OtBu)_6$}] 11

$NiBr_2$ (0.10 g, 0.46 mmol) was added in a solution of $[NaGe(OtBu)_3]_2$ (0.29 g, 0.46 mmol) in THF. The suspension was refluxed during 24 hours, during which the colour turned to dark red-brown. After filtration of NaBr, the solvent was removed under reduced pressure until a violet solid starts to form at the glass wall. The solid was re-dissolved and a small amount of *n*-hexane was added. The solution was kept at -10 °C over 3 days and blue violet needles were isolated (0.20 g, 29 %).

Characterisation:
Formula: $C_{56}H_{126}O_{14}Ge_4Ni_2Na_2$
Molecular weight (calculated): 1476.32 g/mol
Elemental analysis:

	C	H	N
Found [%]	44.32	8.01	0.11
Calculated [%]	45.55	8.53	0.00

Chapter 8

References

1 (a) M. Veith, *Z. Naturforsch*., **1978**, *87B*, 1; (b) M Veith, *Z. Naturforsch*., **1978**, *87B*, 7.

2 O. Nefedov, S. Kolesnikov, A. Ioffe, *J. Organomet. Chem.*, **1977**, *5*, 181.

3 W. Neumann, *The Organometallic and Coordination Chemistry of Germanium, Tin and Lead*, Eds. M. Gielen, P. Harrison, Freund, Tel Aviv, **1978**, 51.

4 J. Donaldson, *Prog. Inorg. Chem.*, **1968**, *8*, 287.

5 M. Johnson, D. Shriver, S. Shriver, *J. Am. Chem. Soc.*, **1966**, *88*, 1588.

6 T. Marks, *J. Am. Chem. Soc.*, **1971**, *93*, 7090.

7 E. Fischer, A. Massboel, *Angew. Chem., Int. Ed. Engl.*, **1964**, *3*, 580.

8 W. Hieber, R. Breu, *Chem. Ber.*, **1957**, *90*, 1270.

9 W. Jetz, P. Simons, J. Thompson, W. Graham, *Inorg. Chem.*, **1966**, *5*, 2217.

10 S. Knox, C. Mitchell, F. Stone, *J. Organomet. Chem.*, **1967**, *16*, 67.

11 F. Cloke, K. Cox, M. Green J. Bashkin, K. Prout, *J. Chem. Soc., Chem. Commun.*, **1981**, 117.

12 A. Manning, *Chem. Commun.*, **1966**, 906.

13 E. Gladyshev, V. Ermolaev, N. Vyazankin, Y. Sorokin, *Zh. Obshch. Khim.*, **1968**, *38*, 662.

14 M. Holt, W. Wilson, J. Nelson, *Chem. Rev.*, **1989**, *89*, 11.

15 D. Bradley, *Chem. Rev.*, **1989**, *89*, 1317.

16 R. Mehrotra, A. Singh, S. Sogani, *Chem. Rev.*, **1994**, *94*, 1643.

17 L. Hubert-Pfalzgraf, *New J. Chem.*, **1987**, *11*, 663.

18 D. Bradley, R. Mehrotra, D. Gaur, *Metal Alkoxides*, Academic Press, New York, **1978**.

19 A. Venugopal, J. Aluha, M. Scurell, *Catalysis Letters*, **2003**, *90(1-2)*, 1.

20 M. Kharson, D. Musaev, S. Kiperman, A. Slinkin, *Kinetika in Kataliz*, **1994**, *35(4)*, 616.

21 J. Shabaker, G. Huber, J. Dumesic, *J. of Catalysis*, **2004**, *222(1)*, 180.

22 Q. Dong, C. Wu, M. Jin, Z. Huang, M. Zheng, J. You, Z. Lin, *Solid State ionics*, **2004**, *167(1-2)*, 49.

23 M. Veith, D. Käfer, J. Koch, P. May, L. Stahl, V. Huch, *Chem. Ber.*, **1992**, *125*, 1033.

24 L. Mond, C. Langer, F. Quincke, *J. Chem. Soc.*, **1890**, 749.

25 L. Meriwether, M. Fiene, *J. Am. Chem. Soc*., **1959,** *81(16)*, 4200.

26 D. Adams, *Metal ligand and related vibrations*, Ed. Arnold, **1967**, p 84.

27 M. Veith, L. Stahl, V. Huch, *J. Chem. Soc., Chem. Commun.*, **1990**, 359.

28 T. Al Allaf, C. Eaborn, P. Hitchcock, M. Lappert, A. Pidcock, *J. Chem. Soc., Chem. Commun.*, **1985**, 548.

29 P. Hitchcock, M. Lappert, M. Misra, *J. Chem. Soc., Chem. Commun.*, **1985**, 863.

30 M. Lappert, R. Rowe, *Coord. Chem. Rev.*, **1990**, *100*, 267.

31 P. Davidson, D. Harris, M. Lappert, *J. Chem. Soc., Dalton Trans.*, **1976**, 2268**.**

32 W. Petz, *Chem. Rev*., **1986**, *86*, 1019.

33 J. Schneider, N. Czap, *J. Chem. Soc., Dalton Trans.*,**1999**, 595.

34 K. Klabunde, *Chemistry of Free Atoms and Particles*, Academic Press, New York, **1980.**

35 K. Klabunde, P. Timms, P. Skell, *Inorg. Synth.*, **1979**, *19*, 59.

36 U. Zenneck, *Angew. Chem., Int. Ed. ,Engl.*, **1990**, *29*, 126.

37 C. Pluta, K. Pörschke, R. Mynott, P. Betz, C. Krüger, *Chem. Ber.*, **1991**, *124*, 1321.

38 D. Goldberg, D. Harris, M. Lappert, K. Thomas, *J. Chem. Soc., Chem. Commun.*, **1976**, 21.

39 M. Grenz, W. du Mont, *J. Organomet. Chem.*, **1983**, *C5*, 241.

40 A. Arduengo, III *Acc. Chem. Res.*, **1999**, *32*, 913.

41 M. Driess, H. Grützmacher, *Angew. Chem., Int. Ed. Engl.*, **1996**, *35*, 828.

42 M. Regitz, *Angew. Chem., Int. Ed. Engl.*, **1996**, *35*, 725.

43 P. Bazinet, G. Yap, D. Richeson, *J. Am. Chem. Soc*, **2001**, *123*, 11162.

44 W. Hermann, M. Denk, J. Behm, W. Sherer, F. Klingan, H. Bok, B. Solouki, M. Wagner, *Angew. Chem., Int. Ed. Engl.*, **1992**, *31*, 1485.

45 J. Bender, A. Shusterman, M. Banaszack-Holl, J. Kampf, *Organometallics*, **1999**, *18*, 1547.

46 K. Litz, J. Bender, J. Kampf, M. Banaszack-Holl, *Angew. Chem., Int. Ed. Engl.*, **1997**, *36*, 496.

47 M. Grenz, E. Hahn, W. du Mont, J. Pickardt, *Angew. Chem., Int. Ed. Engl.*, **1984**, *23*, 61.

48 J. Schneider, J. Hagen, D. Bläser, R. Boese, F. Fabrizi de Biani, P. Zanello, C. Krüger, *Eur. J. Inorg. Chem.*, **1999**, 1987.

49 E. Simón-Manson, C. Kubiak, *Angew. Chem.*, **2005**, *117*, 1149.

50 J. Singh, N. Jain, R. Mehrotra, *Synth. React. Inorg, Met.-Org. Chem.*, **1979**, *9(1)*, 79.

51 M. Veith, R. Rösler, *Z. Naturforsch.*, **1986**, *41B*, 1071.

53 J. Singh, B. Baranwal, R. Mehrotra, *Z. anorg. allg. Chem.*, **1981**, *447*, 235.

54 B. Baranwal, R. Mehrotra, *Aust, J. Chem.*, **1980**, *33*, 37.

55 R. Mehrotra, *Adv. Inorg. Chem. Radiochem.*, **1983**, *26*, 269.

56 K. Valtchev, *Dissertation*, Universität des Saarlandes, **2002**.

57 G. Magraf, T. Kretz, F. F. de Biani, F. Laschi, S. Losi, P. Zanello, J. W. Bats, B. Wolf, K. Removic-Langer, M. Lang, A. Prokofiev, W. Assmus, H. W. Lerner, M. Wagner, *Inorg. Chem.*, **2006**, *45*, 1277.

58 X. H. Liu, J. H. Zeng, *Acta Crystallogr*., Sect. E: *Structure Rep. Online*, **2006**, *62*, 1501.

59 J. Koch, *Dissertation*, Universität des Saarlandes, **1990**.

60 Y. Yamamoto, S. Kuwabaram, S. Matsuo, T. Ohno, H. Nishiyama, K. Itoh, *Organometallics*, **2004**, *23(16)*, 3898.

61 S. Klose, U. Floerke, H. Egold, P. Mathur, *Organometallics*, **2003**, *22(17)*, 3360.

62 T. Chivers, D. Eisher, C. Federochuk, G. Schatte, H. Thuononen, R. T. Boere, *Inorg. Chem.*, **2006**, *45(5)*, 2119.

63 G. Binsch, H. Kessler, *Angew. Chem.*, **1980**, *92*, 445. *Angew. Chem. Int. Ed. Engl*., **1980**, *19*, 411.

64 M. Veith, M. Ehses, V. Huch, *New J. Chem.*, **2005**, *29*, 154.

65 P. Braunstein, M. Veith, J. Blin, V. Huch, *Organometallics*, **2001**, *20*, 627.

66 M. Weidenbruch, *Eur. J. Inorg: Chem.*, **1999**, 373.

67 A. R. Rossi, R. Hoffmann, *Inorg. Chem.*, **1975**, *14(2)*, 365.

68 M. Weidenbruch, A. Stilter, K. Peters, H. G. von Schnering, *Chem. Ber*., **1996**, *129*, 1565.

69 V. N. Khrustalev, I. V. Borisova, N. N. Zemlyanskii, Yu. A. Ustynyuk, M. Yu. Antipin, *Kristallografiya*, **2002**, *47*, 672.

70 D. J. Teff, J. C. Huffman, K. G. Caulton, *Inorg. Chem.*, **1997**, *36*, 4372.

71 M. J. Hampden-Smith, D. S. Williams, A. L. Rheingold, *Inorg. Chem.*, **1990**, *29*, 4076.

72 T. J. Boyle, D. C. Bradley, M. J. Hampden-Smith, A. Patel, *Inorg. Chem.*, **1995**, *34*, 5893.

73 T. J. Boyle, T. M. Alam, C. J. Tafoya, E. R. Mechenbier, J. W. Ziller, *Inorg. Chem.*, **1999**, *38*, 2422.

74 A. F. Holleman, E. Wiberg, N.Wiberg, *Lehrbuch der anorganischen Chemie*, *101*, verbesserte und stark erweiterte Aufl., de Gruyter, **1995**.

75 W. Strohmeier, *Angew. Chem.*, **1964**, *76*, 873.

76 W. Strohmeier, *Angew. Chem., Int. Ed. Engl.*, **1964**, *3*, 730.

77 M. Grenz, E. Hahn, W. du Mont, J. Pickardt, *Angew. Chem.*, **1984**, *96*, 69; *Angew. Chem., Int. Ed. Engl.*, **1984**, *23*, 61.

78 P. Hithcock, M. Lappert, S. Thomas, A. Thorne, *J. Organomet. Chem.*, **1986**, *315*, 27.

79 M. Mehring, C. Löw, M. Schürmann, F. Uhlig, K. Jurkschat, *Organometallics*, **2000**, *19*, 4613.

80 S. F. A. Kettle, E. Boccaleri, E. Diana, R. Rossetti, P. L. Stanghellini, M. C. Lapalucci, G. Longoni, *J. Cluster Sci.*, **2001**, *12(1)*, 175.

81 M. Weidenbruch, A. Stiller, *Z. Anorg. Allg. Chem.*, **1996**, *622*, 534.

82 D. Käfer, *Dissertation*, Universität des Saarlandes, **1987**.

83 H. Werner, R. Prinz, *Chem. Ber.*, **1967**, *100*, 265.

84 M. Veith, S. Weidner, K. Kunze, D. Käfer, J. Hans, V. Huch, *Coord. Chem. Rev.*, **1994**, *137*, 297.

85 M. Veith, *Angew. Chem.*, **1975**, *87*, 8, 287.

86 M. Veith, C. Bélot, V. Huch, *personal communication.*

87 T. J. Boyle, T. M. Alam, M. A. Rodriguez, C. A. Zechmann, *Inorg. Chem.*, **2002**, *41*, 2574.

88 M. Veith, F. Toellner, *J. Organomet. Chem.*, **1983**, *246*, 219.

89 M. J. Hampden-Smith, T. A. Wark, A. Rheingold, J. C. Huffman, *Can. J. Chem.*, **1991**, *69*, 121.

90 T. Fjeldberg, P. B. Hitchcock, M. F. Lappert, S. J. Smith, A. J. Thorne, *Chem. Commun.*, **1985**, 939.

91 M. Veith, P. Hobien, R. Rösler, *Z. Naturforsch., B: Chem. Sci.*, **1989**, *44*, 1067.

92 H. Reuter, M. Keßler, *Z. anorg. Allg. Chem.*, **1991**, *598/599*, 259.

93 *Multinuclear NMR*, Ed. J. Mason, Plenum Press, New York, **1987**, 75.

94 W. C. Hsuan, L. F. Dahl, *J. Am. Chem. Soc.*, **1969**, *91(6)*, 1351.

95 P. B. Hitchcock, M. F. Lappert, S. A. Thomas, A. J. Thorne, A. J. Carty, N. J. Taylor, *J. Organomet. Chem.*, **1986**, *315*, 27.

96 P. Braunstein, C. Charles, A. Tiripicchio, F. Ugozzoli, *J. Chem. Soc., Dalton Trans.*, **1996**, 4365.

97 T. J. Boyle, J. M. Segall, T. M. Alam, M. A. Rodriguez, J. M. Santana, *J. Am. Chem. Soc.*, **2002**, *124*, 6904.

98 P. Bazinet, G. Yap, D. Richeson, *J. Am. Chem. Soc*, **2001**, *123*, 11162.

99 W. Hermann, M. Denk, J. Behm, W. Sherer, F. Klingan, H. Bok, B. Solouki, M. Wagner, *Angew. Chem., Int. Ed. Engl.*, **1992**, *31*, 1485.

100 J. Bender, A. Shusterman, M. Banaszack-Holl, J. Kampf, *Organometallics*, **1999**, *18*, 1547.

101 K. Litz, J. Bender, J. Kampf, M. Banaszack-Holl, *Angew. Chem., Int. Ed. Engl.*, **1997**, *36*, 496.

102 L. Sacconi, F. Mani, A. Bencini, *Comprehensive Coordination Chemistry*, Eds G. Wilkinson, R. D. Gillard, J. A. McCleverty, Pergamon Press, Oxford, **1987**.

103 M. Veith, M. Grosser, *Z. Naturforsch.*, **1982**, *37B(11)*, 1375.

104 W. du Mont, H. Kroth, Z. Naturforsch., B: Anorg. Chem. Org. Chem., **1980**, *35*, 700.

105 M. Veith, *Comments Inorg. Chem.*, **1985**, *4(4)*, 179.

106 A. Schmuck, P. Pyykkö, K. Seppelt, *Angew. Chem.*, **1990**, *102*, 211.; *Angew. Chem. Int. Ed. Engl.*, **1990**, *29*, 213.

107 *Metal clusters in Chemistry*, Vol 1: *Molecular Metal Clusters*, Eds P. Braunstein, L. A. Oro, P. R. Raithby, **1999**, p 88.

108 B. Eichler, B. Phillips, P. Power, M. Augustine, *Inorg. Chem.*, **2000**, *39*, 5450.

109 B. Eichler, P. Power, *Inorg. Chem.*, **2000**, *39*, 5444.

110 M. Veith, A. Müller, L. Stahl, M. Nötzel, M. Jarczyk, V. Huch, *Inorg. Chem.*, **1996**, *35*, 3848.

111 M. Veith, L. Stahl, *Angew. Chem.*, **1993**, *105:1*, 123.

112 S. K. Jain, B. S. Garg, Y. K. Bhoon, *Transition Met. Chem.*, **1987**, *12*, 73.

113 L. Sacconi, *Transition Met. Chem.*, **1968**, *4*, 199.

114 A. B. P. Lever, *Inorganic Electronic Spectroscopy*, Elsevier, **1968**.

115 J. C. Bailar, H. J. Hemmeléus, R. Nyholm, A. F. Trotman-Dickenson, *Comprehensive Inorganic Chemistry*, Pergamon Press, **1973**.

116 D. Evans, *J. Chem. Soc.*, **1959**, 2003.

117 A. Escuer, R. Vicente, M. S. El Fallah, X. Solans, M. Font-Bardia, *J. Chem. Soc., Chem. Commun.*, **1996**, 1013.

118 A. Escuer, R. Vicente, B. Mernari, A. El Gueddi, M. Pierrot, *Inorg. Chem.*, **1997**, *36*, 2511.

119 A. Escuer, R. Vicente, M. S. El Fallah, S. B. Kumar, F. A. Mautner, D. Gatteschi, *J. Chem. Soc., Dalton Trans*, **1998**, *23*, 3905.

120 S. S. Massoud, F. A. Mautner, R. Vicente, B. M. Rodrigue, *Inorg. Chem. Acta*, **2006**, *359(10)*, 3321.

121 M. Kurmoo, H. Kumagai, M. Akita, K. Inoue, S. Takagi, *Inorg. Chem.*, **2006**, *45*, 1627.

122 K. F. Purcell, J. C. Kotz, *Inorganic Chemistry*, Holt-Saunders International Editions, **1977**.

123 M. Veith, A. Belo, *Z. Naturforsch.*, **1987**, *42B*, 5, 525.

124 J. M. Shacketford, H. D. Schmertzing, C. H. Heuter, H. Podall, *J. Org. Chem.*, **1963**, *28*, 1700.

125 D. H. Harris, M. F. Lappert, *J. Chem. Soc. Chem. Commun.*, **1974**, *21*, 895.

126 V. G. Kessler, S. Gohil, S. Parola, *Dalton Trans.*, **2003**, 544.

127 E. Fritscher, *Dissertation*, Universität des Saarlandes, **1997**.

128 A. D. Liehr, C. J. Ballhausen, *Ann. Phys.*, **1959**, *6*, 134.

129 D. Reinen, *Ber. Bunsenges. Physik. Chem.*, **1965**, *69*, 82.

130 R. C. Mehrotra, J. Singh, *Can. J. Chem.*, **1984**, *62*, 1003.

131 R. K. Dubey, A. Shah, A. Sing, R. C. Mehrotra, *Recl. Trav. Chim. Pays Bas*, **1988**, *107*, 237.

132 R. C. Haushalter, F. W. Lai, *Inorg. Chem.*, **1989**, *28*, 2904.

133 J. R. Harper, A. L. Rheingold, *J. Am. Chem. Soc.*, **1990**, *112*, 4037.

134 M. Hesse, H. Meier, B. Zeeh, *Spectroscopic Methods in Organic Chemistry*, Georg Thieme Verlag, Stuttgart, New York, **1995**.

135 A. O. Legendre, F. C. Andrade, S. R. Ananias, A. E. Auro, A. V. G. Netto, R. H. A. Santos, J. G. Ferreira, F. R. Martins, *J. Braz. Chem. Soc.*, **2006**, *17(8)*, 1683.

136 L- Xu, L. Zhu, S. Wu, X. Chen, Q. Teng, *Central Eur. J. Chem.*, **2006**, *4(4)*, 732.

137 C. J. Carmalt, J. D. Mileham, A. J. P. White, D. J. Williams, *Dalton Trans.*, **2003**, 4255.

138 J. J. Zuckermann, *J. Chem. Educ*., **1965**, *42*, 315.

139 R. Krishnamurthy, W. P. Shaap, *J. Chem. Educ*., **1969**, *46*, 799.

Appendix

Additional informations on the X-ray crystal structures

Compound 1

Table 1. Crystal data and structure refinement for shelxs2028.

Identification code	shelxs2028	
Empirical formula	C24 H54 Ni O6 Sn2	
Formula weight	734.76	
Temperature	293(2) K	
Wavelength	0.71073 Å	
Crystal system	Monoclinic	
Space group	P2(1)/n	
Unit cell dimensions	a = 16.386(3) Å	α= 90°.
	b = 11.889(2) Å	β= 113.73(3)°.
	c = 19.136(4) Å	γ = 90°.
Volume	3412.8(11) $Å^3$	
Z	4	
Density (calculated)	1.430 Mg/m^3	
Absorption coefficient	2.027 mm^{-1}	
F(000)	1496	
Crystal size	0.4 x 0.25 x 0.2 mm^3	
Theta range for data collection	2.07 to 24.01°.	
Index ranges	-18<=h<=18, -13<=k<=13, -21<=l<=21	
Reflections collected	20470	
Independent reflections	5211 [R(int) = 0.1586]	
Completeness to theta = 24.01°	97.1 %	
Absorption correction	Numerical	
Refinement method	Full-matrix least-squares on F^2	
Data / restraints / parameters	5211 / 0 / 298	
Goodness-of-fit on F^2	1.095	

Final R indices [I>2sigma(I)]	R1 = 0.0633, wR2 = 0.1556
R indices (all data)	R1 = 0.0712, wR2 = 0.1622
Largest diff. peak and hole	1.825 and -1.289 e.Å^{-3}

Table 2. Atomic coordinates (x 10^4) and equivalent isotropic displacement parameters (Å^{2}x 10^3)
for shelxs2028. U(eq) is defined as one third of the trace of the orthogonalized U^{ij} tensor.

	x	y	z	U(eq)
Sn(2)	7383(1)	5920(1)	350(1)	40(1)
Sn(1)	7512(1)	11297(1)	786(1)	38(1)
Ni(1)	7417(1)	8608(1)	552(1)	34(1)
O(1)	7355(3)	9999(4)	-26(3)	42(1)
O(2)	7443(3)	9731(4)	1315(3)	41(1)
O(3)	6562(3)	7372(4)	229(3)	42(1)
O(4)	8239(3)	7349(4)	779(3)	42(1)
O(5)	8843(4)	11213(4)	1175(4)	54(1)
O(6)	7387(5)	6153(5)	-688(3)	60(2)
C(1)	7285(6)	10111(6)	-797(4)	52(2)
C(2)	7294(12)	8978(9)	-1133(7)	111(5)
C(3)	6455(12)	10716(16)	-1249(8)	145(7)
C(4)	8107(12)	10769(15)	-787(8)	137(7)
C(5)	7464(6)	9595(6)	2063(4)	51(2)
C(6)	6636(8)	10135(9)	2110(6)	83(3)
C(7)	8304(8)	10122(8)	2643(5)	83(3)
C(8)	7458(7)	8320(7)	2219(5)	65(3)
C(9)	5599(5)	7386(6)	-53(5)	47(2)
C(10)	5315(6)	8616(8)	-33(8)	86(4)
C(11)	5196(7)	6938(11)	-854(7)	96(4)
C(12)	5303(7)	6687(12)	487(9)	101(4)

C(13)	9206(5)	7353(6)	1078(4)	44(2)
C(14)	9519(9)	6675(17)	531(11)	149(8)
C(15)	9532(9)	8485(12)	1111(16)	194(12)
C(16)	9575(9)	6790(20)	1835(10)	200(12)
C(17)	9504(6)	12069(7)	1407(6)	63(2)
C(18)	9212(8)	13054(10)	841(10)	121(6)
C(19)	10343(7)	11576(10)	1380(9)	94(4)
C(20)	9655(12)	12425(16)	2198(10)	160(9)
C(21)	7322(7)	5340(8)	-1253(6)	69(3)
C(22)	8240(11)	5001(16)	-1172(11)	165(9)
C(23)	6838(15)	5891(12)	-1991(7)	162(9)
C(24)	6844(15)	4299(13)	-1185(10)	170(9)

Table 3. Bond lengths [Å] and angles [°] for shelxs2028.

Sn(2)-O(6)	2.009(6)	C(1)-C(2)	1.49 (1)
Sn(2)-O(3)	2.142(5)	C(1)-C(4)	1.55(2)
Sn(2)-O(4)	2.145(5)	C(5)-C(7)	1.51(1)
Sn(1)-O(5)	2.003(5)	C(5)-C(6)	1.54(1)
Sn(1)-O(1)	2.130(5)	C(5)-C(8)	1.55(1)
Sn(1)-O(2)	2.143(4)	C(9)-C(11)	1.50(1)
Ni(1)-O(4)	1.943(5)	C(9)-C(10)	1.54(1)
Ni(1)-O(3)	1.952(5)	C(9)-C(12)	1.55(1)
Ni(1)-O(2)	1.966(5)	C(13)-C(15)	1.44(2)
Ni(1)-O(1)	1.968(5)	C(13)-C(16)	1.48(2)
O(1)-C(1)	1.441(9)	C(13)-C(14)	1.56(2)
O(2)-C(5)	1.428(9)	C(17)-C(20)	1.49(2)
O(3)-C(9)	1.447(9)	C(17)-C(19)	1.52(1)
O(4)-C(13)	1.452(9)	C(17)-C(18)	1.54(1)
O(5)-C(17)	1.42 (1)	C(21)-C(23)	1.47(2)
O(6)-C(21)	1.42(1)	C(21)-C(24)	1.50(2)
C(1)-C(3)	1.47(2)	C(21)-C(22)	1.50(2)

O(6)-Sn(2)-O(3)	91.9(2)	C(2)-C(1)-C(4)	107.5(1)
O(6)-Sn(2)-O(4)	90.4(2)	O(2)-C(5)-C(7)	109.6(7)
O(3)-Sn(2)-O(4)	71.9(2)	O(2)-C(5)-C(6)	110.2(7)
O(5)-Sn(1)-O(1)	91.7(2)	C(7)-C(5)-C(6)	110.4(8)
O(5)-Sn(1)-O(2)	92.1(2)	O(2)-C(5)-C(8)	107.7(6)
O(1)-Sn(1)-O(2)	73.0(2)	C(7)-C(5)-C(8)	109.8(8)
O(4)-Ni(1)-O(3)	80.5(2)	C(6)-C(5)-C(8)	109.0(7)
O(4)-Ni(1)-O(2)	123.5(2)	O(3)-C(9)-C(11)	110.0(7)
O(3)-Ni(1)-O(2)	123.0(2)	O(3)-C(9)-C(10)	107.3(6)
O(4)-Ni(1)-O(1)	130.4(2)	C(11)-C(9)-C(10)	110.4(9)
O(3)-Ni(1)-O(1)	125.9(2)	O(3)-C(9)-C(12)	109.4(7)
O(2)-Ni(1)-O(1)	80.1(2)	C(11)-C(9)-C(12)	111.3(9)
C(1)-O(1)-Ni(1)	128.2(4)	C(10)-C(9)-C(12)	108.3(9)
C(1)-O(1)-Sn(1)	128.1(4)	C(15)-C(13)-O(4)	110.4(7)
Ni(1)-O(1)-Sn(1)	103.6(2)	C(15)-C(13)-C(16)	112.1(1)
C(5)-O(2)-Ni(1)	130.7(4)	O(4)-C(13)-C(16)	109.5(8)
C(5)-O(2)-Sn(1)	126.0(4)	C(15)-C(13)-C(14)	107.2(1)
Ni(1)-O(2)-Sn(1)	103.2(2)	O(4)-C(13)-C(14)	109.6(7)
C(9)-O(3)-Ni(1)	130.2(4)	C(16)-C(13)-C(14)	108.0(1)
C(9)-O(3)-Sn(2)	126.3(4)	O(5)-C(17)-C(20)	108.4(9)
Ni(1)-O(3)-Sn(2)	103.5(2)	O(5)-C(17)-C(19)	107.5(8)
C(13)-O(4)-Ni(1)	129.3(4)	C(20)-C(17)-C(19)	111.2(1)
C(13)-O(4)-Sn(2)	126.6(4)	O(5)-C(17)-C(18)	110.1(8)
Ni(1)-O(4)-Sn(2)	103.7(2)	C(20)-C(17)-C(18)	112.2(1)
C(17)-O(5)-Sn(1)	131.3(5)	C(19)-C(17)-C(18)	107.4(1)
C(21)-O(6)-Sn(2)	129.0(6)	O(6)-C(21)-C(23)	106.0(8)
O(1)-C(1)-C(3)	108.7(8)	O(6)-C(21)-C(24)	112.2(9)
O(1)-C(1)-C(2)	110.3(7)	C(23)-C(21)-C(24)	110.7(1)
C(3)-C(1)-C(2)	110.7(1)	O(6)-C(21)-C(22)	109.8(9)
O(1)-C(1)-C(4)	108.8(8)	C(23)-C(21)-C(22)	110.4(1)
C(3)-C(1)-C(4)	110.7(1)	C(24)-C(21)-C(22)	107.8(1)

Symmetry transformations used to generate equivalent atoms:

Table 4. Anisotropic displacement parameters ($Å^2 x\ 10^3$) for shelxs2028. The anisotropic

displacement factor exponent takes the form: $-2p^2[\ h^2\ a^{*2}U^{11} + ... + 2\ h\ k\ a^*\ b^*\ U^{12}\ ]$

	U^{11}	U^{22}	U^{33}	U^{23}	U^{13}	U^{12}
Sn(2)	48(1)	24(1)	43(1)	-1(1)	14(1)	3(1)
Sn(1)	42(1)	24(1)	47(1)	1(1)	17(1)	3(1)
Ni(1)	41(1)	23(1)	34(1)	-1(1)	12(1)	1(1)
O(1)	56(3)	32(2)	32(2)	3(2)	12(2)	1(2)
O(2)	59(3)	28(2)	39(3)	-1(2)	23(2)	-2(2)
O(3)	38(3)	30(2)	54(3)	-4(2)	14(2)	-1(2)
O(4)	38(3)	32(2)	45(3)	-6(2)	7(2)	2(2)
O(5)	45(3)	41(3)	69(4)	-1(3)	17(3)	1(2)
O(6)	92(5)	45(3)	46(3)	-13(3)	30(3)	-5(3)
C(1)	78(6)	38(4)	40(4)	11(3)	23(4)	2(4)
C(2)	230(17)	56(6)	68(7)	-10(5)	83(10)	-16(8)
C(3)	169(15)	187(17)	66(8)	49(10)	35(10)	89(14)
C(4)	181(16)	171(15)	80(9)	-16(9)	75(11)	-88(13)
C(5)	82(6)	32(4)	43(4)	-3(3)	29(4)	-5(4)
C(6)	127(10)	67(6)	81(7)	5(5)	70(8)	9(6)
C(7)	122(9)	61(6)	43(5)	-2(4)	10(6)	-20(6)
C(8)	106(8)	39(4)	55(5)	5(4)	39(6)	-9(5)
C(9)	33(4)	37(4)	64(5)	4(3)	13(4)	1(3)
C(10)	41(5)	58(6)	146(11)	-18(6)	23(6)	4(4)
C(11)	51(6)	120(10)	90(8)	-38(7)	-2(6)	3(6)
C(12)	57(7)	116(10)	136(12)	24(9)	45(7)	-9(7)
C(13)	33(4)	43(4)	47(4)	-3(3)	6(3)	3(3)
C(14)	68(8)	213(19)	167(16)	-79(15)	47(10)	7(10)
C(15)	48(7)	78(9)	410(40)	-10(14)	43(13)	-3(6)
C(16)	54(8)	400(30)	113(13)	130(18)	4(8)	-5(14)

C(17)	44(5)	51(5)	91(7)	-5(5)	24(5)	-10(4)
C(18)	83(9)	57(7)	200(17)	23(8)	31(10)	-21(6)
C(19)	66(7)	79(7)	138(11)	15(7)	42(7)	2(6)
C(20)	163(15)	200(18)	142(15)	-118(14)	88(13)	-115(15)
C(21)	89(7)	57(5)	59(6)	-20(4)	29(5)	7(5)
C(22)	124(13)	195(19)	170(17)	-108(15)	54(12)	21(12)
C(23)	290(20)	89(10)	42(6)	-9(6)	1(10)	46(12)
C(24)	290(30)	97(11)	154(16)	-100(12)	119(18)	-85(14)

Compound 2

Table 1. Crystal data and structure refinement for sh2361.

Identification code	sh2361	
Empirical formula	C32 H72 Ni2 O8 Pb2	
Formula weight	1116.70	
Temperature	103(2) K	
Wavelength	0.71073 Å	
Crystal system	Monoclinic	
Space group	P2(1)/n	
Unit cell dimensions	a = 9.742(4) Å	α = 90°.
	b = 14.803(7) Å	β = 97.61(2)°.
	c = 14.717(6) Å	γ = 90°.
Volume	2103.7(16) $Å^3$	
Z	2	
Density (calculated)	1.763 Mg/m^3	
Absorption coefficient	8.900 mm^{-1}	
F(000)	1096	
Crystal size	0.2 x 0.25 x 0.43 mm^3	
Theta range for data collection	1.96 to 23.96°.	
Index ranges	-8<=h<=10, -16<=k<=16, -16<=l<=15	
Reflections collected	12464	
Independent reflections	3024 [R(int) = 0.1416]	
Completeness to theta = 23.96°	92.2 %	
Absorption correction	Semi-empirical from equivalents	
Refinement method	Full-matrix least-squares on F^2	
Data / restraints / parameters	3024 / 0 / 211	
Goodness-of-fit on F^2	1.454	
Final R indices [I>2sigma(I)]	R1 = 0.1118, wR2 = 0.2314	
R indices (all data)	R1 = 0.1567, wR2 = 0.2477	
Largest diff. peak and hole	3.708 and -4.624 e.$Å^{-3}$	

Table 2. Atomic coordinates (x 10^4) and equivalent isotropic displacement parameters ($Å^2$x 10^3)
for sh2361. U(eq) is defined as one third of the trace of the orthogonalized U^{ij} tensor.

	x	y	z	U(eq)
Pb	1981(1)	2626(1)	1551(1)	40(1)
Ni	535(3)	791(2)	595(2)	24(1)
O(1)	1(16)	2009(9)	896(10)	28(4)
O(2)	2240(15)	1141(10)	1387(10)	33(4)
O(3)	2521(18)	2772(11)	204(14)	48(5)
O(4)	549(14)	304(9)	-647(9)	23(4)
C(1)	-1370(30)	2560(19)	730(20)	54(9)
C(2)	-2170(40)	1900(20)	240(30)	150(20)
C(3)	-1560(40)	2860(30)	1560(30)	120(20)
C(4)	-980(30)	3270(30)	170(30)	101(16)
C(5)	3390(20)	623(18)	1797(16)	33(7)
C(6)	4730(20)	1113(16)	1628(19)	45(8)
C(7)	3300(30)	556(17)	2815(18)	54(8)
C(8)	3310(20)	-297(15)	1400(20)	54(9)
C(9)	3210(30)	3500(20)	-117(19)	53(8)
C(10)	4370(40)	3840(20)	660(30)	130(20)
C(11)	2320(30)	4229(19)	-450(20)	68(10)
C(12)	3950(30)	3180(20)	-920(20)	75(12)
C(13)	1220(20)	666(15)	-1392(15)	23(5)
C(14)	2710(20)	788(16)	-1053(18)	38(7)
C(15)	580(20)	1584(17)	-1604(16)	38(7)
C(16)	950(30)	39(17)	-2173(17)	46(7)

Table 3. Bond lengths [Å] and angles [°] for sh2361.

Pb-O(3)	2.13(2)	O(4)#1-Ni-O(4)	78.6(7)
Pb-O(2)	2.23(1)	O(1)-Ni-O(4)	125.9(6)
Pb-O(1)	2.23(2)	O(4)#1-Ni-O(2)	128.1(6)
Pb-Ni	3.288(3)	O(1)-Ni-O(2)	81.4(6)
Ni-O(4)#1	1.94(1)	O(4)-Ni-O(2)	122.5(6)
Ni-O(1)	1.94(1)	O(4)#1-Ni-Pb	151.3(4)
Ni-O(4)	1.97(1)	O(1)-Ni-Pb	41.3(5)
Ni-O(2)	1.97(1)	O(4)-Ni-Pb	130.2(4)
O(1)-C(1)	1.55(2)	O(2)-Ni-Pb	41.3(4)
O(2)-C(5)	1.42(2)	C(1)-O(1)-Ni	135.0(2)
O(3)-C(9)	1.39(3)	C(1)-O(1)-Pb	121.8(1)
O(4)-C(13)	1.45(2)	Ni-O(1)-Pb	103.6(6)
O(4)-Ni#1	1.94(1)	C(5)-O(2)-Ni	131.6(1)
C(1)-C(3)	1.33(4)	C(5)-O(2)-Pb	125.4(1)
C(1)-C(2)	1.39(4)	Ni-O(2)-Pb	103.0(6)
C(1)-C(4)	1.43(4)	C(9)-O(3)-Pb	125.9(1)
C(5)-C(8)	1.48(3)	C(13)-O(4)-Ni#1	129.8(1)
C(5)-C(7)	1.52(3)	C(13)-O(4)-Ni	128.8(1)
C(5)-C(6)	1.54(3)	Ni#1-O(4)-Ni	101.4(7)
C(9)-C(11)	1.43(4)	C(3)-C(1)-C(2)	125(4)
C(9)-C(12)	1.53(4)	C(3)-C(1)-C(4)	112(3)
C(9)-C(10)	1.58(4)	C(2)-C(1)-C(4)	112(4)
C(13)-C(16)	1.47(3)	C(3)-C(1)-O(1)	105(2)
C(13)-C(14)	1.48(3)	C(2)-C(1)-O(1)	97(2)
C(13)-C(15)	1.51(3)	C(4)-C(1)-O(1)	101(2)
O(3)-Pb-O(2)	87.3(6)	O(2)-C(5)-C(8)	109.3(2)
O(3)-Pb-O(1)	86.9(6)	O(2)-C(5)-C(7)	108.0(2)
O(2)-Pb-O(1)	69.8(5)	C(8)-C(5)-C(7)	109(2)
O(3)-Pb-Ni	80.2(4)	O(2)-C(5)-C(6)	108(2)
O(2)-Pb-Ni	35.7(4)	C(8)-C(5)-C(6)	112(2)
O(1)-Pb-Ni	35.1(3)	C(7)-C(5)-C(6)	111(2)
O(4)#1-Ni-O(1)	127.0(6)	O(3)-C(9)-C(11)	114(2)

O(3)-C(9)-C(12)	109(2)	O(4)-C(13)-C(14)	108.1(2)
C(11)-C(9)-C(12)	107(2)	C(16)-C(13)-C(14)	114(2)
O(3)-C(9)-C(10)	109(2)	O(4)-C(13)-C(15)	105.8(2)
C(11)-C(9)-C(10)	111(3)	C(16)-C(13)-C(15)	112(2)
C(12)-C(9)-C(10)	107(3)	C(14)-C(13)-C(15)	108.6(2)
O(4)-C(13)-C(16)	107.7(2)		

Symmetry transformations used to generate equivalent atoms:
#1 -x,-y,-z

Table 4. Anisotropic displacement parameters ($Å^2 x\ 10^3$) for sh2361. The anisotropic displacement factor exponent takes the form: $-2\pi^2[h^2 a^{*2} U^{11} + ... + 2 h k a^* b^* U^{12}]$

	U^{11}	U^{22}	U^{33}	U^{23}	U^{13}	U^{12}
Pb	59(1)	12(1)	49(1)	-12(1)	2(1)	6(1)
Ni	34(2)	16(2)	20(2)	-3(1)	2(1)	4(1)
O(1)	50(10)	0(8)	39(10)	0(7)	30(9)	23(7)
O(2)	50(10)	12(9)	35(10)	-10(7)	-2(9)	6(7)
O(3)	60(12)	10(10)	75(15)	1(9)	12(11)	-6(8)
O(4)	47(9)	15(9)	7(8)	-12(6)	5(8)	0(7)
C(1)	51(17)	40(20)	70(20)	-23(16)	8(16)	65(15)
C(2)	160(40)	20(20)	260(60)	-70(30)	-70(40)	30(20)
C(3)	90(30)	140(40)	120(40)	-100(30)	-40(30)	100(30)
C(4)	90(30)	120(40)	110(30)	80(30)	70(30)	60(20)
C(5)	2(11)	80(20)	19(15)	-4(12)	-9(10)	21(11)
C(6)	32(15)	20(15)	80(20)	-18(14)	-3(15)	8(11)
C(7)	90(20)	31(17)	43(19)	33(14)	24(17)	1(15)
C(8)	30(15)	13(15)	110(30)	-9(15)	-3(16)	1(11)
C(9)	60(20)	60(20)	33(19)	2(15)	8(17)	-13(17)
C(10)	200(40)	40(20)	140(40)	40(20)	-80(30)	-100(30)

C(11)	70(20)	40(20)	110(30)	44(19)	60(20)	17(15)
C(12)	60(20)	40(20)	120(30)	30(20)	-10(20)	-16(15)
C(13)	33(13)	31(15)	11(14)	1(10)	25(11)	-4(10)
C(14)	24(13)	25(15)	60(20)	-24(13)	7(13)	1(10)
C(15)	51(16)	44(18)	25(16)	13(12)	27(14)	2(12)
C(16)	54(17)	41(19)	45(19)	-4(14)	20(15)	-10(13)

Compound 3

Table 1. Crystal data and structure refinement for sh2218.

Identification code	sh2218	
Empirical formula	C40 H72 Fe2 Ni2 O16 Sn2	
Formula weight	1275.48	
Temperature	103(2) K	
Wavelength	0.71073 Å	
Crystal system	Triclinic	
Space group	P-1	
Unit cell dimensions	a = 10.6720(5) Å	α = 86.907(2)°
	b = 10.8659(5) Å	β = 88.002(2)°
	c = 23.6521(11) Å	γ = 80.176(2)°
Volume	2697.6(2) $Å^3$	
Z	2	
Density (calculated)	1.570 Mg/m^3	
Absorption coefficient	2.177 mm^{-1}	
F(000)	1296	
Crystal size	0.25 x 0.1 x 0.05 mm^3	
Theta range for data collection	1.73 to 33.02°.	
Index ranges	-16<=h<=16, -16<=k<=16, -36<=l<=36	
Reflections collected	86330	
Independent reflections	20135 [R(int) = 0.0407]	
Completeness to theta = 33.02°	98.8 %	
Absorption correction	None	
Refinement method	Full-matrix least-squares on F^2	
Data / restraints / parameters	20135 / 0 / 583	
Goodness-of-fit on F^2	1.212	
Final R indices [I>2sigma(I)]	R1 = 0.0419, wR2 = 0.0997	
R indices (all data)	R1 = 0.0516, wR2 = 0.1051	
Largest diff. peak and hole	2.733 and -1.314 $e.Å^{-3}$	

Table 2. Atomic coordinates (x 10^4) and equivalent isotropic displacement parameters ($Å^2$x 10^3)
for sh2218. U(eq) is defined as one third of the trace of the orthogonalized U^{ij} tensor.

	x	y	z	U(eq)
Sn(1)	2379(1)	7215(1)	1271(1)	16(1)
Ni(1)	659(1)	8981(1)	397(1)	13(1)
Fe(1)	2433(1)	5092(1)	1716(1)	18(1)
Sn(2)	7422(1)	2290(1)	3776(1)	15(1)
Ni(2)	5732(1)	3973(1)	4657(1)	14(1)
Fe(2)	8392(1)	85(1)	3655(1)	16(1)
O(1)	694(2)	8437(2)	1210(1)	16(1)
O(2)	2078(2)	7543(2)	419(1)	17(1)
O(3)	776(2)	10658(2)	95(1)	16(1)
O(4)	3395(2)	8554(2)	1309(1)	24(1)
O(5)	2173(3)	6046(3)	2862(1)	32(1)
O(6)	5068(3)	4321(3)	1313(1)	42(1)
O(7)	155(3)	5021(3)	1058(1)	35(1)
O(8)	2239(3)	2552(2)	2141(1)	37(1)
O(9)	5569(2)	2874(2)	4032(1)	16(1)
O(10)	7514(2)	3132(2)	4527(1)	19(1)
O(11)	5201(2)	5775(2)	4636(1)	18(1)
O(12)	7470(2)	3799(2)	3289(1)	27(1)
O(13)	6799(2)	9(3)	2676(1)	33(1)
O(14)	7336(3)	-520(3)	4781(1)	32(1)
O(15)	10899(3)	864(3)	3528(1)	42(1)
O(16)	9620(3)	-2501(3)	3508(1)	36(1)
C(1)	-163(3)	8877(3)	1678(1)	18(1)
C(2)	607(3)	9314(3)	2137(1)	24(1)
C(3)	-1121(3)	9952(3)	1442(1)	24(1)
C(4)	-821(3)	7798(3)	1907(1)	22(1)

C(5)	2835(3)	6924(3)	-41(1)	18(1)
C(6)	2549(3)	5602(3)	-67(1)	24(1)
C(7)	2457(3)	7677(3)	-584(1)	24(1)
C(8)	4236(3)	6902(3)	72(1)	26(1)
C(9)	1702(3)	11430(3)	205(1)	18(1)
C(10)	3029(3)	10715(3)	61(1)	25(1)
C(11)	1412(3)	12628(3)	-167(2)	28(1)
C(12)	1613(3)	11725(3)	828(1)	27(1)
C(13)	4493(3)	8623(4)	1639(2)	31(1)
C(14)	4840(4)	9901(4)	1484(2)	34(1)
C(15)	5593(4)	7613(5)	1456(3)	70(2)
C(16)	4171(6)	8507(8)	2265(2)	82(2)
C(17)	2273(3)	5706(3)	2410(1)	22(1)
C(18)	4034(3)	4650(3)	1463(1)	28(1)
C(19)	1049(3)	5081(3)	1309(1)	24(1)
C(20)	2335(3)	3546(3)	1977(1)	25(1)
C(21)	4450(3)	2590(3)	3759(1)	19(1)
C(22)	3298(3)	3427(3)	4008(2)	29(1)
C(23)	4572(4)	2868(3)	3124(1)	30(1)
C(24)	4371(3)	1223(3)	3888(2)	25(1)
C(25)	8637(3)	3120(3)	4854(1)	25(1)
C(26)	8254(3)	4029(4)	5323(2)	31(1)
C(27)	9076(4)	1809(4)	5109(2)	34(1)
C(28)	9674(3)	3546(4)	4468(2)	40(1)
C(29)	5450(3)	6684(3)	4201(1)	23(1)
C(30)	4826(4)	7967(3)	4390(2)	33(1)
C(31)	6888(4)	6609(3)	4126(2)	33(1)
C(32)	4896(4)	6390(3)	3651(1)	33(1)
C(33)	8132(4)	4020(3)	2763(2)	33(1)
C(34)	7370(5)	5202(4)	2490(2)	52(1)
C(35)	9461(5)	4241(5)	2890(2)	51(1)
C(36)	8206(6)	2935(4)	2378(2)	49(1)
C(37)	7416(3)	73(3)	3059(1)	22(1)
C(38)	7733(3)	-258(3)	4343(1)	21(1)

C(39)	9910(3)	587(3)	3579(1)	26(1)
C(40)	9134(3)	-1492(3)	3568(1)	24(1)

Table 3. Bond lengths [Å] and angles [°] for sh2218.

Sn(1)-O(4)	1.965(2)	O(4)-C(13)	1.445(4)
Sn(1)-O(1)	2.049(2)	O(5)-C(17)	1.145(4)
Sn(1)-O(2)	2.055(2)	O(6)-C(18)	1.151(4)
Sn(1)-Fe(1)	2.4754(5)	O(7)-C(19)	1.154(4)
Ni(1)-O(3)#1	1.931(2)	O(8)-C(20)	1.148(4)
Ni(1)-O(3)	1.943(2)	O(9)-C(21)	1.462(3)
Ni(1)-O(1)	1.981(2)	O(10)-C(25)	1.448(3)
Ni(1)-O(2)	1.981(2)	O(11)-C(29)	1.437(3)
Fe(1)-C(20)	1.776(3)	O(11)-Ni(2)#2	1.924(2)
Fe(1)-C(18)	1.786(3)	O(12)-C(33)	1.439(4)
Fe(1)-C(19)	1.793(3)	O(13)-C(37)	1.151(4)
Fe(1)-C(17)	1.797(3)	O(14)-C(38)	1.147(4)
Sn(2)-O(12)	1.958(2)	O(15)-C(39)	1.147(4)
Sn(2)-O(9)	2.052(2)	O(16)-C(40)	1.144(4)
Sn(2)-O(10)	2.054(2)	C(1)-C(3)	1.512(4)
Sn(2)-Fe(2)	2.4700(5)	C(1)-C(2)	1.527(4)
Ni(2)-O(11)#2	1.924(2)	C(1)-C(4)	1.531(4)
Ni(2)-O(11)	1.942(2)	C(5)-C(7)	1.515(4)
Ni(2)-O(9)	1.982(2)	C(5)-C(6)	1.524(4)
Ni(2)-O(10)	1.986(2)	C(5)-C(8)	1.524(4)
Fe(2)-C(40)	1.780(3)	C(9)-C(12)	1.522(4)
Fe(2)-C(37)	1.784(3)	C(9)-C(11)	1.523(4)
Fe(2)-C(38)	1.795(3)	C(9)-C(10)	1.531(4)
Fe(2)-C(39)	1.795(3)	C(13)-C(16)	1.511(6)
O(1)-C(1)	1.459(3)	C(13)-C(14)	1.520(5)
O(2)-C(5)	1.456(3)	C(13)-C(15)	1.532(7)
O(3)-C(9)	1.439(3)	C(21)-C(24)	1.516(4)
O(3)-Ni(1)#1	1.931(2)	C(21)-C(23)	1.520(4)

C(21)-C(22)	1.521(4)	O(9)-Sn(2)-O(10)	74.37(8)
C(25)-C(27)	1.519(5)	O(12)-Sn(2)-Fe(2)	131.38(7)
C(25)-C(26)	1.524(4)	O(9)-Sn(2)-Fe(2)	124.44(6)
C(25)-C(28)	1.527(5)	O(10)-Sn(2)-Fe(2)	121.58(6)
C(29)-C(32)	1.519(5)	O(11)#2-Ni(2)-O(11)	77.67(9)
C(29)-C(30)	1.522(5)	O(11)#2-Ni(2)-O(9)	131.42(8)
C(29)-C(31)	1.527(5)	O(11)-Ni(2)-O(9)	125.41(9)
C(33)-C(36)	1.519(6)	O(11)#2-Ni(2)-O(10)	128.56(9)
C(33)-C(35)	1.521(6)	O(11)-Ni(2)-O(10)	123.96(9)
C(33)-C(34)	1.524(6)	O(9)-Ni(2)-O(10)	77.45(8)
O(4)-Sn(1)-O(1)	93.52(9)	C(40)-Fe(2)-C(37)	92.01(1)
O(4)-Sn(1)-O(2)	93.66(8)	C(40)-Fe(2)-C(38)	93.46(1)
O(1)-Sn(1)-O(2)	74.27(8)	C(37)-Fe(2)-C(38)	117.62(1)
O(4)-Sn(1)-Fe(1)	136.03(6)	C(40)-Fe(2)-C(39)	90.39(2)
O(1)-Sn(1)-Fe(1)	120.46(5)	C(37)-Fe(2)-C(39)	121.14(2)
O(2)-Sn(1)-Fe(1)	120.43(6)	C(38)-Fe(2)-C(39)	120.90(2)
O(3)#1-Ni(1)-O(3)	77.86(8)	C(40)-Fe(2)-Sn(2)	178.39(1)
O(3)#1-Ni(1)-O(1)	128.84(8)	C(37)-Fe(2)-Sn(2)	88.97(1)
O(3)-Ni(1)-O(1)	125.34(8)	C(38)-Fe(2)-Sn(2)	87.22(1)
O(3)#1-Ni(1)-O(2)	129.78(8)	C(39)-Fe(2)-Sn(2)	88.01(1)
O(3)-Ni(1)-O(2)	125.40(8)	C(1)-O(1)-Ni(1)	130.11(2)
O(1)-Ni(1)-O(2)	77.40(8)	C(1)-O(1)-Sn(1)	126.45(2)
C(20)-Fe(1)-C(18)	92.64(2)	Ni(1)-O(1)-Sn(1)	103.09(8)
C(20)-Fe(1)-C(19)	88.89(1)	C(5)-O(2)-Ni(1)	130.20(2)
C(18)-Fe(1)-C(19)	124.73(2)	C(5)-O(2)-Sn(1)	126.66(2)
C(20)-Fe(1)-C(17)	93.43(1	Ni(1)-O(2)-Sn(1)	102.87(9)
C(18)-Fe(1)-C(17)	114.87(2)	C(9)-O(3)-Ni(1)#1	128.79(2)
C(19)-Fe(1)-C(17)	120.17(2)	C(9)-O(3)-Ni(1)	129.07(2)
C(20)-Fe(1)-Sn(1)	173.24(1)	Ni(1)#1-O(3)-Ni(1)	102.14(8)
C(18)-Fe(1)-Sn(1)	90.09(1)	C(13)-O(4)-Sn(1)	130.7(2)
C(19)-Fe(1)-Sn(1)	84.47(1)	C(21)-O(9)-Ni(2)	131.38(2)
C(17)-Fe(1)-Sn(1)	91.03(1)	C(21)-O(9)-Sn(2)	125.37(2)
O(12)-Sn(2)-O(9)	92.99(9)	Ni(2)-O(9)-Sn(2)	103.04(8)
O(12)-Sn(2)-O(10)	95.75(1)	C(25)-O(10)-Ni(2)	130.35(2)

C(25)-O(10)-Sn(2)	126.80(2)	O(6)-C(18)-Fe(1)	177.2(3)
Ni(2)-O(10)-Sn(2)	102.82(9)	O(7)-C(19)-Fe(1)	176.8(3)
C(29)-O(11)-Ni(2)#2	129.12(2)	O(8)-C(20)-Fe(1)	178.2(3)
C(29)-O(11)-Ni(2)	128.55(2)	O(9)-C(21)-C(24)	108.6(2)
Ni(2)#2-O(11)-Ni(2)	102.33(9)	O(9)-C(21)-C(23)	109.1(2)
C(33)-O(12)-Sn(2)	132.6(2)	C(24)-C(21)-C(23)	110.9(3)
O(1)-C(1)-C(3)	106.9(2)	O(9)-C(21)-C(22)	106.9(2)
O(1)-C(1)-C(2)	108.9(2)	C(24)-C(21)-C(22)	110.7(3)
C(3)-C(1)-C(2)	110.6(3)	C(23)-C(21)-C(22)	110.5(3)
O(1)-C(1)-C(4)	108.4(2)	O(10)-C(25)-C(27)	109.5(3)
C(3)-C(1)-C(4)	110.9(2)	O(10)-C(25)-C(26)	106.7(2)
C(2)-C(1)-C(4)	110.9(2)	C(27)-C(25)-C(26)	110.2(3)
O(2)-C(5)-C(7)	107.4(2)	O(10)-C(25)-C(28)	108.9(3)
O(2)-C(5)-C(6)	109.0(2)	C(27)-C(25)-C(28)	110.9(3)
C(7)-C(5)-C(6)	110.4(2)	C(26)-C(25)-C(28)	110.6(3)
O(2)-C(5)-C(8)	108.5(2)	O(11)-C(29)-C(32)	108.9(2)
C(7)-C(5)-C(8)	110.5(2)	O(11)-C(29)-C(30)	107.7(2)
C(6)-C(5)-C(8)	111.0(3)	C(32)-C(29)-C(30)	110.8(3)
O(3)-C(9)-C(12)	109.1(2)	O(11)-C(29)-C(31)	108.6(3)
O(3)-C(9)-C(11)	108.1(2)	C(32)-C(29)-C(31)	109.8(3)
C(12)-C(9)-C(11)	110.5(3)	C(30)-C(29)-C(31)	110.9(3)
O(3)-C(9)-C(10)	108.7(2)	O(12)-C(33)-C(36)	111.8(3)
C(12)-C(9)-C(10)	109.7(3)	O(12)-C(33)-C(35)	108.9(3)
C(11)-C(9)-C(10)	110.7(2)	C(36)-C(33)-C(35)	110.3(4)
O(4)-C(13)-C(16)	110.4(3)	O(12)-C(33)-C(34)	105.4(3)
O(4)-C(13)-C(14)	105.5(3)	C(36)-C(33)-C(34)	110.4(4)
C(16)-C(13)-C(14)	110.3(4)	C(35)-C(33)-C(34)	109.9(4)
O(4)-C(13)-C(15)	108.9(3)	O(13)-C(37)-Fe(2)	177.0(3)
C(16)-C(13)-C(15)	112.5(5)	O(14)-C(38)-Fe(2)	177.6(3)
C(14)-C(13)-C(15)	108.9(3)	O(15)-C(39)-Fe(2)	177.5(3)
O(5)-C(17)-Fe(1)	177.0(3)	O(16)-C(40)-Fe(2)	179.3(3)

Symmetry transformations used to generate equivalent atoms:

#1 -x,-y+2,-z #2 -x+1,-y+1,-z+1

Table 4. Anisotropic displacement parameters ($Å^2 x\ 10^3$) for sh2218. The anisotropic

displacement factor exponent takes the form: $-2\pi^2[h^2 a^{*2} U^{11} + ... + 2 h k a^* b^* U^{12}]$

	U^{11}	U^{22}	U^{33}	U^{23}	U^{13}	U^{12}
Sn(1)	12(1)	17(1)	18(1)	2(1)	-2(1)	-2(1)
Ni(1)	12(1)	11(1)	15(1)	0(1)	-1(1)	-2(1)
Fe(1)	18(1)	16(1)	18(1)	2(1)	-2(1)	-1(1)
Sn(2)	15(1)	14(1)	19(1)	-2(1)	1(1)	-5(1)
Ni(2)	13(1)	11(1)	19(1)	-1(1)	0(1)	-3(1)
Fe(2)	15(1)	16(1)	18(1)	-4(1)	1(1)	-3(1)
O(1)	14(1)	17(1)	16(1)	0(1)	1(1)	-1(1)
O(2)	15(1)	16(1)	17(1)	-1(1)	2(1)	0(1)
O(3)	14(1)	14(1)	21(1)	1(1)	-4(1)	-7(1)
O(4)	19(1)	27(1)	29(1)	6(1)	-9(1)	-11(1)
O(5)	38(1)	36(1)	24(1)	-4(1)	-2(1)	-7(1)
O(6)	29(1)	43(2)	50(2)	-2(1)	8(1)	9(1)
O(7)	33(1)	29(1)	45(2)	5(1)	-16(1)	-8(1)
O(8)	55(2)	21(1)	36(1)	6(1)	-15(1)	-9(1)
O(9)	12(1)	16(1)	20(1)	-3(1)	-1(1)	-4(1)
O(10)	13(1)	19(1)	25(1)	-7(1)	-2(1)	-4(1)
O(11)	23(1)	12(1)	20(1)	3(1)	2(1)	-5(1)
O(12)	34(1)	17(1)	29(1)	3(1)	12(1)	-6(1)
O(13)	29(1)	44(2)	27(1)	-12(1)	-5(1)	-5(1)
O(14)	41(1)	33(1)	25(1)	-2(1)	6(1)	-9(1)
O(15)	21(1)	46(2)	63(2)	-18(1)	8(1)	-11(1)
O(16)	37(1)	25(1)	44(2)	-9(1)	3(1)	3(1)
C(1)	18(1)	19(1)	16(1)	-2(1)	2(1)	-2(1)
C(2)	28(1)	25(2)	20(1)	-5(1)	0(1)	-9(1)
C(3)	23(1)	22(2)	22(1)	1(1)	4(1)	4(1)
C(4)	21(1)	22(1)	23(1)	1(1)	5(1)	-5(1)

C(5)	17(1)	15(1)	19(1)	0(1)	3(1)	3(1)
C(6)	29(2)	16(1)	26(1)	-3(1)	3(1)	0(1)
C(7)	30(2)	17(1)	21(1)	2(1)	4(1)	3(1)
C(8)	17(1)	25(2)	33(2)	1(1)	5(1)	6(1)
C(9)	19(1)	17(1)	20(1)	0(1)	-3(1)	-9(1)
C(10)	16(1)	26(2)	35(2)	0(1)	0(1)	-9(1)
C(11)	32(2)	19(1)	35(2)	6(1)	-9(1)	-13(1)
C(12)	30(2)	32(2)	23(1)	-6(1)	-3(1)	-14(1)
C(13)	23(1)	38(2)	37(2)	11(1)	-14(1)	-17(1)
C(14)	30(2)	41(2)	35(2)	5(1)	-12(1)	-21(2)
C(15)	30(2)	43(3)	139(6)	10(3)	-43(3)	-7(2)
C(16)	75(4)	158(7)	34(2)	37(3)	-28(2)	-89(4)
C(17)	21(1)	22(1)	24(1)	3(1)	-2(1)	-4(1)
C(18)	27(2)	25(2)	30(2)	0(1)	0(1)	4(1)
C(19)	27(1)	20(1)	26(1)	3(1)	-5(1)	-5(1)
C(20)	30(2)	22(2)	23(1)	1(1)	-7(1)	-3(1)
C(21)	14(1)	17(1)	25(1)	-2(1)	-5(1)	-3(1)
C(22)	16(1)	27(2)	44(2)	-13(1)	-5(1)	0(1)
C(23)	33(2)	29(2)	26(1)	-1(1)	-11(1)	-2(1)
C(24)	20(1)	20(1)	38(2)	-5(1)	1(1)	-9(1)
C(25)	15(1)	26(2)	35(2)	-13(1)	-6(1)	-1(1)
C(26)	25(2)	29(2)	39(2)	-16(1)	-11(1)	-1(1)
C(27)	31(2)	29(2)	40(2)	-12(1)	-19(1)	8(1)
C(28)	17(1)	49(2)	59(2)	-23(2)	3(1)	-14(2)
C(29)	32(2)	15(1)	23(1)	3(1)	3(1)	-8(1)
C(30)	45(2)	12(1)	39(2)	4(1)	6(2)	-4(1)
C(31)	35(2)	26(2)	40(2)	0(1)	14(1)	-14(1)
C(32)	52(2)	26(2)	23(1)	5(1)	-4(1)	-9(2)
C(33)	45(2)	26(2)	28(2)	1(1)	16(1)	-12(2)
C(34)	74(3)	38(2)	40(2)	15(2)	18(2)	-10(2)
C(35)	45(2)	53(3)	57(3)	-2(2)	24(2)	-21(2)
C(36)	86(4)	35(2)	30(2)	-3(2)	21(2)	-22(2)
C(37)	20(1)	21(1)	23(1)	-5(1)	2(1)	-2(1)
C(38)	22(1)	19(1)	23(1)	-4(1)	0(1)	-4(1)

C(39)	20(1)	26(2)	33(2)	-10(1)	3(1)	-4(1)
C(40)	23(1)	23(2)	24(1)	-5(1)	2(1)	-4(1)

Compound 4

Table 1. Crystal data and structure refinement for sh2262.

Identification code	sh2262	
Empirical formula	C54 H94 Fe2 Ge2 Ni2 O18	
Formula weight	1405.59	
Temperature	103(2) K	
Wavelength	0.71073 Å	
Crystal system	Monoclinic	
Space group	P2(1)/n	
Unit cell dimensions	a = 9.8146(12) Å	α= 90°.
	b = 20.943(3) Å	β= 93.092(7)°.
	c = 15.6380(19) Å	γ = 90°.
Volume	3209.7(7) $Å^3$	
Z	2	
Density (calculated)	1.454 Mg/m^3	
Absorption coefficient	2.003 mm^{-1}	
F(000)	1468	
Crystal size	0.45 x 0.33 x 0.1 mm^3	
Theta range for data collection	1.63 to 29.54°.	
Index ranges	-13<=h<=13, -28<=k<=27, -19<=l<=21	
Reflections collected	39642	
Independent reflections	8902 [R(int) = 0.0465]	
Completeness to theta = 29.54°	99.1 %	
Absorption correction	None	
Refinement method	Full-matrix least-squares on F^2	
Data / restraints / parameters	8902 / 0 / 328	
Goodness-of-fit on F^2	1.087	
Final R indices [I>2sigma(I)]	R1 = 0.0470, wR2 = 0.1172	
R indices (all data)	R1 = 0.0769, wR2 = 0.1381	
Largest diff. peak and hole	1.461 and -0.777 $e.Å^{-3}$	

Table 2. Atomic coordinates (x 10^4) and equivalent isotropic displacement parameters ($Å^2$x 10^3)
for sh2262. U(eq) is defined as one third of the trace of the orthogonalized U^{ij} tensor.

	x	y	z	U(eq)
Fe	7118(1)	2821(1)	6175(1)	22(1)
Ge	5526(1)	2071(1)	5665(1)	18(1)
Ni	5381(1)	670(1)	5268(1)	18(1)
O(1)	3849(2)	171(1)	4795(2)	20(1)
O(2)	5327(2)	1289(1)	6230(1)	20(1)
O(3)	5974(2)	1502(1)	4801(1)	20(1)
O(4)	3783(2)	2180(1)	5333(2)	24(1)
O(5)	6928(3)	3563(2)	4584(2)	42(1)
O(6)	9109(3)	1768(2)	6304(2)	40(1)
O(7)	5363(3)	3151(2)	7567(2)	42(1)
O(8)	9134(3)	3739(1)	6863(2)	37(1)
C(1)	2483(3)	388(2)	4585(2)	21(1)
C(2)	1919(3)	703(2)	5372(2)	25(1)
C(3)	2519(4)	869(2)	3853(2)	28(1)
C(4)	1641(3)	-189(2)	4308(3)	28(1)
C(5)	5111(4)	1159(2)	7140(2)	23(1)
C(6)	3914(4)	1554(2)	7422(2)	29(1)
C(7)	4787(4)	453(2)	7193(2)	28(1)
C(8)	6421(4)	1313(2)	7665(2)	29(1)
C(9)	6488(3)	1642(2)	3955(2)	23(1)
C(10)	6373(4)	1021(2)	3458(2)	24(1)
C(11)	7980(4)	1846(2)	4066(2)	28(1)
C(12)	5605(4)	2160(2)	3527(2)	27(1)
C(13)	2850(4)	2713(2)	5294(2)	25(1)
C(14)	1688(4)	2508(2)	4672(3)	36(1)
C(15)	2296(4)	2823(2)	6177(3)	35(1)

C(16)	3511(4)	3315(2)	4967(3)	36(1)
C(17)	6966(4)	3259(2)	5195(2)	30(1)
C(18)	8318(4)	2168(2)	6253(3)	31(1)
C(19)	6018(4)	3003(2)	7017(2)	29(1)
C(20)	8357(4)	3376(2)	6601(2)	27(1)
O(9A)	1227(7)	68(3)	7467(5)	50(1)
O(9B)	1557(12)	203(6)	7797(9)	50(1)
C(21)	488(6)	617(3)	7811(4)	54(1)
C(22A)	-604(10)	297(4)	8284(8)	42(2)
C(22B)	-295(13)	374(6)	8632(10)	42(2)
C(23A)	225(9)	-224(4)	8793(6)	49(2)
C(23B)	-406(13)	-326(6)	8399(9)	49(2)
C(24A)	1359(11)	-386(5)	8189(7)	47(2)
C(24B)	898(16)	-467(7)	7903(10)	47(2)
C(25)	6050(7)	483(4)	9610(5)	76(2)
C(26)	4865(8)	558(4)	9953(5)	79(2)
C(27)	6121(8)	-120(4)	9748(5)	79(2)

Table 3. Bond lengths [Å] and angles [°] for sh2262.

Fe-C(20)	1.785(4)	O(1)-Ni#1	1.921(2)
Fe-C(17)	1.786(4)	O(2)-C(5)	1.475(4)
Fe-C(19)	1.789(4)	O(3)-C(9)	1.470(4)
Fe-C(18)	1.804(4)	O(4)-C(13)	1.443(4)
Fe-Ge	2.325(6)	O(5)-C(17)	1.146(5)
Ge-O(4)	1.776(2)	O(6)-C(18)	1.142(5)
Ge-O(3)	1.871(2)	O(7)-C(19)	1.143(5)
Ge-O(2)	1.876(2)	O(8)-C(20)	1.137(4)
Ni-O(1)#1	1.921(2)	C(1)-C(4)	1.514(5)
Ni-O(1)	1.944(2)	C(1)-C(2)	1.526(5)
Ni-O(3)	1.988(2)	C(1)-C(3)	1.528(5)
Ni-O(2)	1.989(2)	C(5)-C(7)	1.517(5)
O(1)-C(1)	1.437(4)	C(5)-C(6)	1.522(5)

C(5)-C(8)	1.522(5)	O(3)-Ge-O(2)	79.54(1)
C(9)-C(10)	1.516(5)	O(4)-Ge-Fe	129.23(8)
C(9)-C(12)	1.522(5)	O(3)-Ge-Fe	119.87(7)
C(9)-C(11)	1.527(5)	O(2)-Ge-Fe	120.87(7)
C(13)-C(16)	1.519(5)	O(1)#1-Ni-O(1)	77.61(1)
C(13)-C(14)	1.520(5)	O(1)#1-Ni-O(3)	131.35(1)
C(13)-C(15)	1.529(5)	O(1)-Ni-O(3)	124.58(1)
O(9A)-C(21)	1.476(9)	O(1)#1-Ni-O(2)	131.55(1)
O(9A)-C(24A)	1.477(1)	O(1)-Ni-O(2)	125.92(1)
O(9B)-C(21)	1.362(1)	O(3)-Ni-O(2)	74.13(9)
O(9B)-C(24B)	1.557(2)	C(1)-O(1)-Ni#1	130.0(2)
C(21)-C(22A)	1.493(1)	C(1)-O(1)-Ni	127.6(2)
C(21)-C(22B)	1.614(1)	Ni#1-O(1)-Ni	102.39(1)
C(22A)-C(23A)	1.554(1)	C(5)-O(2)-Ge	129.8(2)
C(22B)-C(23B)	1.512(2)	C(5)-O(2)-Ni	128.3(2)
C(23A)-C(24A)	1.535(1)	Ge-O(2)-Ni	101.84(1)
C(23B)-C(24B)	1.561(2)	C(9)-O(3)-Ge	128.9(2)
C(25)-C(27)	1.283(1)	C(9)-O(3)-Ni	128.7(2)
C(25)-C(26)	1.317(1)	Ge-O(3)-Ni	102.03(1)
C(26)-C(27)#2	1.430(1)	C(13)-O(4)-Ge	135.3(2)
C(26)-C(27)	1.918(1)	O(1)-C(1)-C(4)	107.5(3)
C(27)-C(26)#2	1.430(1)	O(1)-C(1)-C(2)	109.1(3)
C(20)-Fe-C(17)	90.51(2)	C(4)-C(1)-C(2)	111.1(3)
C(20)-Fe-C(19)	90.71(2)	O(1)-C(1)-C(3)	108.7(3)
C(17)-Fe-C(19)	119.74(2)	C(4)-C(1)-C(3)	110.3(3)
C(20)-Fe-C(18)	92.26(2)	C(2)-C(1)-C(3)	110.0(3)
C(17)-Fe-C(18)	118.14(2)	O(2)-C(5)-C(7)	105.9(3)
C(19)-Fe-C(18)	121.99(2)	O(2)-C(5)-C(6)	109.4(3)
C(20)-Fe-Ge	177.78(1)	C(7)-C(5)-C(6)	110.3(3)
C(17)-Fe-Ge	91.67(1)	O(2)-C(5)-C(8)	108.7(3)
C(19)-Fe-Ge	88.61(1)	C(7)-C(5)-C(8)	110.5(3)
C(18)-Fe-Ge	86.32(1)	C(6)-C(5)-C(8)	111.8(3)
O(4)-Ge-O(3)	97.53(1)	O(3)-C(9)-C(10)	105.7(3)
O(4)-Ge-O(2)	97.24(1)	O(3)-C(9)-C(12)	108.8(3)

C(10)-C(9)-C(12)	111.2(3)	C(26)#2-C(27)-C(26)	88.2(6)
O(3)-C(9)-C(11)	109.1(3)		
C(10)-C(9)-C(11)	110.0(3)		
C(12)-C(9)-C(11)	111.7(3)		
O(4)-C(13)-C(16)	112.0(3)		
O(4)-C(13)-C(14)	105.2(3)		
C(16)-C(13)-C(14)	109.8(3)		
O(4)-C(13)-C(15)	109.5(3)		
C(16)-C(13)-C(15)	111.0(3)		
C(14)-C(13)-C(15)	109.2(3)		
O(5)-C(17)-Fe	176.1(3)		
O(6)-C(18)-Fe	178.0(3)		
O(7)-C(19)-Fe	175.9(3)		
O(8)-C(20)-Fe	178.7(4)		
C(21)-O(9A)-C(24A)	104.3(6)		
C(21)-O(9B)-C(24B)	104.3(9)		
O(9B)-C(21)-O(9A)	26.4(5)		
O(9B)-C(21)-C(22A)	107.2(7)		
O(9A)-C(21)-C(22A)	102.1(6)		
O(9B)-C(21)-C(22B)	102.3(7)		
O(9A)-C(21)-C(22B)	108.0(6)		
C(22A)-C(21)-C(22B)	23.0(5)		
C(21)-C(22A)-C(23A)	101.5(7)		
C(23B)-C(22B)-C(21)	98.4(9)		
C(24A)-C(23A)-C(22A)	102.5(7)		
C(22B)-C(23B)-C(24B)	104.6(1)		
O(9A)-C(24A)-C(23A)	106.9(7)		
O(9B)-C(24B)-C(23B)	103.8(1)		
C(27)-C(25)-C(26)	95.1(7)		
C(25)-C(26)-C(27)#2	133.2(8)		
C(25)-C(26)-C(27)	41.8(4)		
C(27)#2-C(26)-C(27)	91.8(6)		
C(25)-C(27)-C(26)#2	131.0(7)		
C(25)-C(27)-C(26)	43.1(5)		

Symmetry transformations used to generate equivalent atoms:
#1 -x+1,-y,-z+1 #2 -x+1,-y,-z+2

Table 4. Anisotropic displacement parameters ($Å^2$x 10^3) for sh2262. The anisotropic
displacement factor exponent takes the form: $-2\pi^2[h^2 a^{*2} U^{11} + ... + 2 h k a^* b^* U^{12}]$

	U^{11}	U^{22}	U^{33}	U^{23}	U^{13}	U^{12}
Fe	25(1)	23(1)	18(1)	-2(1)	2(1)	-8(1)
Ge	20(1)	19(1)	16(1)	-1(1)	3(1)	-4(1)
Ni	18(1)	17(1)	17(1)	0(1)	2(1)	-3(1)
O(1)	13(1)	26(1)	21(1)	1(1)	0(1)	-1(1)
O(2)	27(1)	20(1)	14(1)	0(1)	4(1)	-5(1)
O(3)	24(1)	21(1)	17(1)	-1(1)	5(1)	-4(1)
O(4)	20(1)	21(1)	32(1)	-1(1)	2(1)	1(1)
O(5)	58(2)	38(2)	29(2)	9(1)	-7(1)	-19(1)
O(6)	33(2)	36(2)	51(2)	2(1)	4(1)	1(1)
O(7)	40(2)	47(2)	40(2)	-17(1)	17(1)	-15(1)
O(8)	40(2)	38(2)	31(2)	-1(1)	-4(1)	-18(1)
C(1)	17(1)	22(2)	23(2)	2(1)	1(1)	0(1)
C(2)	22(2)	28(2)	27(2)	-1(1)	4(1)	1(1)
C(3)	25(2)	32(2)	27(2)	6(2)	1(1)	2(1)
C(4)	20(2)	29(2)	34(2)	-1(2)	-3(1)	-4(1)
C(5)	31(2)	24(2)	15(2)	1(1)	6(1)	-4(1)
C(6)	34(2)	30(2)	26(2)	-2(2)	11(2)	-1(2)
C(7)	39(2)	25(2)	18(2)	3(1)	3(1)	-6(2)
C(8)	38(2)	30(2)	19(2)	0(1)	-1(1)	-7(2)
C(9)	26(2)	25(2)	18(2)	0(1)	8(1)	-4(1)
C(10)	27(2)	25(2)	21(2)	-2(1)	5(1)	0(1)
C(11)	28(2)	33(2)	26(2)	-2(2)	9(1)	-9(1)

C(12)	38(2)	24(2)	18(2)	2(1)	5(1)	-1(1)
C(13)	26(2)	21(2)	27(2)	1(1)	2(1)	1(1)
C(14)	32(2)	29(2)	45(2)	-2(2)	-12(2)	6(2)
C(15)	34(2)	40(2)	33(2)	-3(2)	6(2)	8(2)
C(16)	35(2)	23(2)	49(2)	6(2)	4(2)	1(2)
C(17)	37(2)	30(2)	24(2)	-1(2)	1(2)	-14(2)
C(18)	27(2)	34(2)	31(2)	0(2)	2(2)	-10(2)
C(19)	33(2)	27(2)	28(2)	-6(2)	1(2)	-11(1)
C(20)	32(2)	30(2)	19(2)	3(1)	2(1)	-6(1)

Compound 5

Table 1. Crystal data and structure refinement for sh2171a.

Identification code	sh2171a	
Empirical formula	C12 H28 O4 Sn2	
Formula weight	473.72	
Temperature	293(2) K	
Wavelength	0.71073 Å	
Crystal system	Monoclinic	
Space group	$P2_1/c$	
Unit cell dimensions	a = 17.823(4) Å	α= 90°.
	b = 7.855(2) Å	β= 99.85(3)°.
	c = 6.3440(10) Å	γ = 90°.
Volume	875.1(3) $Å^3$	
Z	2	
Density (calculated)	1.798 Mg/m^3	
Absorption coefficient	2.858 mm^{-1}	
F(000)	464	
Crystal size	0.793 x 0.302 x 0.278 mm^3	
Theta range for data collection	2.84 to 31.50°.	
Index ranges	-26<=h<=26, -11<=k<=11, -9<=l<=9	
Reflections collected	13163	
Independent reflections	2898 [R(int) = 0.0226]	
Completeness to theta = 31.50°	99.5 %	
Absorption correction	Multi scan	
Refinement method	Full-matrix least-squares on F^2	
Data / restraints / parameters	2898 / 0 / 86	
Goodness-of-fit on F^2	1.103	
Final R indices [I>2sigma(I)]	R1 = 0.0201, wR2 = 0.0509	
R indices (all data)	R1 = 0.0215, wR2 = 0.0519	
Largest diff. peak and hole	0.920 and -1.468 e.$Å^{-3}$	

Table 2. Atomic coordinates (x 10^4) and equivalent isotropic displacement parameters ($Å^2$x 10^3)
for sh2171a. U(eq) is defined as one third of the trace of the orthogonalized U^{ij} tensor.

	x	y	z	U(eq)
Sn(1)	2441(1)	1284(1)	1298(1)	12(1)
O(1)	3064(1)	3238(2)	6(2)	15(1)
O(2)	1789(1)	1941(2)	-2180(2)	13(1)
C(1)	3538(1)	4465(3)	1322(3)	19(1)
C(2)	3643(1)	6098(3)	31(3)	25(1)
C(3)	4317(1)	3690(3)	2224(4)	31(1)
C(4)	1222(1)	784(2)	-3300(3)	15(1)
C(5)	1559(1)	-985(3)	-3612(4)	24(1)
C(6)	546(1)	660(3)	-2076(4)	25(1)

Table 3. Bond lengths [Å] and angles [°] for sh2171a.

Sn(1)-O(1)	2.139(1)	O(1)-Sn(1)-O(2)	71.99(5)
Sn(1)-O(2)#1	2.148(1)	O(2)#1-Sn(1)-O(2)	93.43(4)
Sn(1)-O(2)	2.369(1)	O(1)-Sn(1)-O(1)#1	94.48(4)
Sn(1)-O(1)#1	2.452(1)	O(2)#1-Sn(1)-O(1)#1	70.17(5)
O(1)-C(1)	1.448(2)	O(2)-Sn(1)-O(1)#1	158.41(5)
O(1)-Sn(1)#2	2.452(1)	C(1)-O(1)-Sn(1)	123.1(1)
O(2)-C(4)	1.451(2)	C(1)-O(1)-Sn(1)#2	125.1(1)
O(2)-Sn(1)#2	2.148(1)	Sn(1)-O(1)-Sn(1)#2	107.34(5)
C(1)-C(3)	1.535(3)	C(4)-O(2)-Sn(1)#2	124.9(1)
C(1)-C(2)	1.550(3)	C(4)-O(2)-Sn(1)	120.6(1)
C(4)-C(5)	1.540(3)	Sn(1)#2-O(2)-Sn(1)	110.05(5)
C(4)-C(6)	1.544(3)	O(1)-C(1)-C(3)	110.6(2)
O(1)-Sn(1)-O(2)#1	93.59(6)	O(1)-C(1)-C(2)	110.9(2)

C(3)-C(1)-C(2)	109.9(2)	O(2)-C(4)-C(6)	109.3(1)
O(2)-C(4)-C(5)	112.0(1)	C(5)-C(4)-C(6)	111.3(1)

Symmetry transformations used to generate equivalent atoms:
#1 x,-y+1/2,z+1/2 #2 x,-y+1/2,z-1/2

Table 4. Anisotropic displacement parameters ($Å^2 x\ 10^3$) for sh2171a. The anisotropic
displacement factor exponent takes the form: $-2p^2[\ h^2\ a^{*2}U^{11} + ...\ + 2\ h\ k\ a^*\ b^*\ U^{12}\ ]$

	U^{11}	U^{22}	U^{33}	U^{23}	U^{13}	U^{12}
Sn(1)	14(1)	12(1)	9(1)	0(1)	2(1)	1(1)
O(1)	16(1)	19(1)	10(1)	-1(1)	0(1)	-6(1)
O(2)	15(1)	14(1)	10(1)	0(1)	0(1)	-4(1)
C(1)	18(1)	27(1)	12(1)	-4(1)	3(1)	-8(1)
C(2)	29(1)	24(1)	23(1)	-3(1)	6(1)	-13(1)
C(3)	20(1)	50(1)	21(1)	2(1)	-5(1)	-10(1)
C(4)	16(1)	16(1)	13(1)	0(1)	-1(1)	-5(1)
C(5)	26(1)	18(1)	28(1)	-8(1)	8(1)	-3(1)
C(6)	17(1)	25(1)	33(1)	-8(1)	8(1)	-7(1)

Compound 6

Table 1. Crystal data and structure refinement for sh2388.

Identification code	sh2388	
Empirical formula	C26 H42 Fe2 O14 Sn3	
Formula weight	1046.37	
Temperature	103(2) K	
Wavelength	0.71073 Å	
Crystal system	Monoclinic	
Space group	P2(1)/n	
Unit cell dimensions	a = 13.4599(6) Å	α= 90°.
	b = 16.2430(7) Å	β= 103.866(2)°.
	c = 18.0443(8) Å	γ = 90°.
Volume	3830.0(3) $Å^3$	
Z	4	
Density (calculated)	1.815 Mg/m^3	
Absorption coefficient	2.725 mm^{-1}	
F(000)	2048	
Crystal size	0.6 x 0.48 x 0.2 mm^3	
Theta range for data collection	1.71 to 32.50°.	
Index ranges	-18<=h<=20, -21<=k<=24, -27<=l<=27	
Reflections collected	101285	
Independent reflections	13875 [R(int) = 0.0504]	
Completeness to theta = 32.50°	100.0 %	
Absorption correction	Empirical	
Refinement method	Full-matrix least-squares on F^2	
Data / restraints / parameters	13875 / 0 / 418	
Goodness-of-fit on F^2	1.195	
Final R indices [I>2sigma(I)]	R1 = 0.0266, wR2 = 0.0570	
R indices (all data)	R1 = 0.0375, wR2 = 0.0677	

Largest diff. peak and hole	2.172 and -0.958 e.Å^{-3}

Table 2. Atomic coordinates (x 10^4) and equivalent isotropic displacement parameters (Å^{2}x 10^3)
for sh2388. U(eq) is defined as one third of the trace of the orthogonalized U^{ij} tensor.

	x	y	z	U(eq)
Sn(1)	6202(1)	7992(1)	1234(1)	14(1)
Sn(2)	3612(1)	7979(1)	376(1)	14(1)
Sn(3)	2488(1)	6816(1)	1552(1)	14(1)
Fe(1)	7681(1)	8846(1)	1180(1)	16(1)
Fe(2)	843(1)	6123(1)	1061(1)	18(1)
O(1)	4792(1)	8391(1)	1352(1)	15(1)
O(2)	5230(1)	7608(1)	245(1)	17(1)
O(3)	2520(1)	8007(1)	1193(1)	17(1)
O(4)	3589(1)	6796(1)	922(1)	15(1)
O(5)	6254(1)	6973(1)	1820(1)	22(1)
O(6)	3408(1)	6987(1)	2560(1)	21(1)
O(7)	6233(2)	10040(1)	297(1)	33(1)
O(8)	8439(2)	7494(2)	387(1)	37(1)
O(9)	8339(2)	8828(2)	2856(1)	42(1)
O(10)	9406(2)	9896(2)	1098(2)	48(1)
O(11)	1685(2)	4471(2)	1471(2)	47(1)
O(12)	-50(2)	7153(2)	2069(1)	42(1)
O(13)	1061(2)	6756(2)	-416(1)	38(1)
O(14)	-1192(2)	5465(2)	415(2)	49(1)
C(1)	4643(2)	8875(2)	1999(1)	18(1)
C(2)	5377(2)	8595(2)	2725(2)	30(1)
C(3)	4758(3)	9778(2)	1835(2)	30(1)
C(4)	5585(2)	7563(2)	-453(2)	26(1)

C(5)	4783(3)	7918(3)	-1103(2)	50(1)
C(6)	5874(3)	6699(2)	-588(2)	43(1)
C(7)	1651(2)	8542(2)	1165(2)	22(1)
C(8)	1658(3)	8829(2)	1963(2)	39(1)
C(9)	1681(3)	9245(2)	626(2)	42(1)
C(10)	4151(2)	6058(1)	801(1)	17(1)
C(11)	4325(2)	5515(2)	1505(2)	25(1)
C(12)	3574(2)	5630(2)	81(2)	26(1)
C(13)	7206(2)	6637(2)	2240(2)	25(1)
C(14)	7471(3)	5905(2)	1806(3)	50(1)
C(15)	7080(3)	6401(3)	3022(2)	46(1)
C(16)	3427(2)	6470(2)	3210(1)	22(1)
C(17)	4370(2)	6715(2)	3816(2)	33(1)
C(18)	2466(2)	6569(2)	3493(2)	35(1)
C(19)	6782(2)	9565(2)	646(2)	21(1)
C(20)	8129(2)	8008(2)	698(2)	23(1)
C(21)	8060(2)	8827(2)	2205(2)	25(1)
C(22)	8730(2)	9483(2)	1127(2)	29(1)
C(23)	1384(2)	5124(2)	1330(2)	30(1)
C(24)	326(2)	6750(2)	1691(2)	27(1)
C(25)	976(2)	6510(2)	161(1)	23(1)
C(26)	-395(2)	5722(2)	662(2)	30(1)

Table 3. Bond lengths [Å] and angles [°] for sh2388.

Sn(1)-O(5)	1.958(2)	O(13)-C(25)	1.147(3)
Sn(1)-O(2)	2.041(2)	O(14)-C(26)	1.138(3)
Sn(1)-O(1)	2.063(2)	C(1)-C(2)	1.510(4)
Sn(1)-Fe(1)	2.4477(4)	C(1)-C(3)	1.512(4)
Sn(2)-O(4)	2.164(2)	C(4)-C(6)	1.492(4)
Sn(2)-O(1)	2.175(2)	C(4)-C(5)	1.505(5)
Sn(2)-O(3)	2.317(2)	C(7)-C(9)	1.506(4)
Sn(2)-O(2)	2.326(2)	C(7)-C(8)	1.512(4)
Sn(3)-O(6)	1.959(2)	C(10)-C(12)	1.513(3)
Sn(3)-O(3)	2.044(2)	C(10)-C(11)	1.518(4)
Sn(3)-O(4)	2.074(2)	C(13)-C(15)	1.510(4)
Sn(3)-Fe(2)	2.4526(4)	C(13)-C(14)	1.511(5)
Fe(1)-C(22)	1.772(3)	C(16)-C(18)	1.509(4)
Fe(1)-C(19)	1.788(3)	C(16)-C(17)	1.516(4)
Fe(1)-C(20)	1.796(3)	O(5)-Sn(1)-O(2)	98.42(7)
Fe(1)-C(21)	1.797(3)	O(5)-Sn(1)-O(1)	97.17(7)
Fe(2)-C(26)	1.773(3)	O(2)-Sn(1)-O(1)	76.90(6)
Fe(2)-C(24)	1.786(3)	O(5)-Sn(1)-Fe(1)	125.21(5)
Fe(2)-C(25)	1.791(3)	O(2)-Sn(1)-Fe(1)	119.71(5)
Fe(2)-C(23)	1.796(3)	O(1)-Sn(1)-Fe(1)	127.09(5)
O(1)-C(1)	1.461(3)	O(4)-Sn(2)-O(1)	89.53(6)
O(2)-C(4)	1.453(3)	O(4)-Sn(2)-O(3)	69.37(6)
O(3)-C(7)	1.448(3)	O(1)-Sn(2)-O(3)	86.04(6)
O(4)-C(10)	1.460(3)	O(4)-Sn(2)-O(2)	86.06(6)
O(5)-C(13)	1.430(3)	O(1)-Sn(2)-O(2)	69.00(6)
O(6)-C(16)	1.437(3)	O(3)-Sn(2)-O(2)	145.23(6)
O(7)-C(19)	1.148(3)	O(6)-Sn(3)-O(3)	95.96(7)
O(8)-C(20)	1.140(3)	O(6)-Sn(3)-O(4)	97.81(7)
O(9)-C(21)	1.145(3)	O(3)-Sn(3)-O(4)	76.64(7)
O(10)-C(22)	1.142(3)	O(6)-Sn(3)-Fe(2)	135.64(5)
O(11)-C(23)	1.142(4)	O(3)-Sn(3)-Fe(2)	113.95(5)
O(12)-C(24)	1.147(4)	O(4)-Sn(3)-Fe(2)	119.79(5)

C(22)-Fe(1)-C(19)	92.0(1)	O(1)-C(1)-C(2)	110.2(2)
C(22)-Fe(1)-C(20)	93.0(1)	O(1)-C(1)-C(3)	109.0(2)
C(19)-Fe(1)-C(20)	119.8(1)	C(2)-C(1)-C(3)	112.7(2)
C(22)-Fe(1)-C(21)	91.8(1)	O(2)-C(4)-C(6)	110.0(2)
C(19)-Fe(1)-C(21)	123.7(1)	O(2)-C(4)-C(5)	109.4(2)
C(20)-Fe(1)-C(21)	116.1(1)	C(6)-C(4)-C(5)	113.6(3)
C(22)-Fe(1)-Sn(1)	178.55(9)	O(3)-C(7)-C(9)	109.3(2)
C(19)-Fe(1)-Sn(1)	86.52(8)	O(3)-C(7)-C(8)	109.4(2)
C(20)-Fe(1)-Sn(1)	87.74(9)	C(9)-C(7)-C(8)	112.7(3)
C(21)-Fe(1)-Sn(1)	89.00(9)	O(4)-C(10)-C(12)	109.2(2)
C(26)-Fe(2)-C(24)	89.8(1)	O(4)-C(10)-C(11)	109.5(2)
C(26)-Fe(2)-C(25)	92.8(1)	C(12)-C(10)-C(11)	113.3(2)
C(24)-Fe(2)-C(25)	121.0(1)	O(5)-C(13)-C(15)	107.7(2)
C(26)-Fe(2)-C(23)	93.3(1)	O(5)-C(13)-C(14)	108.6(3)
C(24)-Fe(2)-C(23)	122.6(1)	C(15)-C(13)-C(14)	112.1(3)
C(25)-Fe(2)-C(23)	116.1(1)	O(6)-C(16)-C(18)	111.4(2)
C(26)-Fe(2)-Sn(3)	174.0(1)	O(6)-C(16)-C(17)	106.5(2)
C(24)-Fe(2)-Sn(3)	87.94(9)	C(18)-C(16)-C(17)	111.4(2)
C(25)-Fe(2)-Sn(3)	83.59(8)	O(7)-C(19)-Fe(1)	177.6(2)
C(23)-Fe(2)-Sn(3)	92.59(9)	O(8)-C(20)-Fe(1)	177.6(3)
C(1)-O(1)-Sn(1)	123.9(1)	O(9)-C(21)-Fe(1)	177.3(3)
C(1)-O(1)-Sn(2)	126.8(1)	O(10)-C(22)-Fe(1)	179.5(4)
Sn(1)-O(1)-Sn(2)	109.36(7)	O(11)-C(23)-Fe(2)	176.3(3)
C(4)-O(2)-Sn(1)	119.9(2)	O(12)-C(24)-Fe(2)	176.7(2)
C(4)-O(2)-Sn(2)	127.7 (2)	O(13)-C(25)-Fe(2)	179.8(3)
Sn(1)-O(2)-Sn(2)	104.58(7)	O(14)-C(26)-Fe(2)	179.1(3)
C(7)-O(3)-Sn(3)	120.1(2)		
C(7)-O(3)-Sn(2)	128.3(1)		
Sn(3)-O(3)-Sn(2)	104.38(7)		
C(10)-O(4)-Sn(3)	124.0(1)		
C(10)-O(4)-Sn(2)	126.7(1)		
Sn(3)-O(4)-Sn(2)	108.97(7)		
C(13)-O(5)-Sn(1)	121.3(1)		
C(16)-O(6)-Sn(3)	124.0(1)		

Symmetry transformations used to generate equivalent atoms:

Table 4. Anisotropic displacement parameters ($Å^2 x\ 10^3$) for sh2388. The anisotropic

displacement factor exponent takes the form: $-2p^2[\ h^2\ a^{*2}U^{11} + ... + 2\ h\ k\ a^*\ b^*\ U^{12}\ ]$

	U^{11}	U^{22}	U^{33}	U^{23}	U^{13}	U^{12}
Sn(1)	14(1)	11(1)	17(1)	1(1)	6(1)	-1(1)
Sn(2)	16(1)	14(1)	13(1)	2(1)	2(1)	2(1)
Sn(3)	13(1)	16(1)	14(1)	0(1)	3(1)	-1(1)
Fe(1)	13(1)	13(1)	23(1)	3(1)	5(1)	0(1)
Fe(2)	14(1)	22(1)	17(1)	0(1)	4(1)	-2(1)
O(1)	15(1)	15(1)	15(1)	-3(1)	4(1)	1(1)
O(2)	21(1)	18(1)	14(1)	-1(1)	8(1)	0(1)
O(3)	14(1)	16(1)	21(1)	2(1)	4(1)	4(1)
O(4)	15(1)	13(1)	19(1)	0(1)	6(1)	1(1)
O(5)	16(1)	18(1)	30(1)	10(1)	5(1)	-1(1)
O(6)	22(1)	24(1)	16(1)	1(1)	1(1)	-5(1)
O(7)	23(1)	27(1)	48(1)	15(1)	4(1)	3(1)
O(8)	37(1)	40(1)	35(1)	-2(1)	11(1)	16(1)
O(9)	47(1)	46(1)	27(1)	-5(1)	-2(1)	-4(1)
O(10)	19(1)	40(1)	82(2)	22(1)	10(1)	-5(1)
O(11)	47(2)	33(1)	58(2)	20(1)	3(1)	3(1)
O(12)	32(1)	71(2)	26(1)	-11(1)	11(1)	10(1)
O(13)	43(1)	49(1)	19(1)	8(1)	4(1)	4(1)
O(14)	22(1)	56(2)	70(2)	-34(1)	12(1)	-14(1)
C(1)	18(1)	20(1)	16(1)	-6(1)	5(1)	2(1)
C(2)	37(2)	34(2)	18(1)	-1(1)	5(1)	9(1)
C(3)	45(2)	19(1)	27(1)	-6(1)	7(1)	6(1)
C(4)	35(1)	27(1)	21(1)	-4(1)	14(1)	-3(1)

C(5)	50(2)	84(3)	18(1)	6(2)	11(1)	7(2)
C(6)	56(2)	31(2)	53(2)	-15(1)	36(2)	-2(1)
C(7)	16(1)	21(1)	27(1)	1(1)	4(1)	7(1)
C(8)	37(2)	50(2)	28(1)	-11(1)	2(1)	25(1)
C(9)	33(2)	31(2)	65(2)	21(2)	22(2)	17(1)
C(10)	16(1)	12(1)	24(1)	-3(1)	7(1)	1(1)
C(11)	25(1)	19(1)	33(1)	5(1)	9(1)	4(1)
C(12)	26(1)	19(1)	32(1)	-7(1)	7(1)	-2(1)
C(13)	18(1)	20(1)	34(1)	9(1)	3(1)	1(1)
C(14)	48(2)	38(2)	64(2)	2(2)	14(2)	22(2)
C(15)	40(2)	62(2)	33(2)	19(2)	0(1)	6(2)
C(16)	30(1)	20(1)	17(1)	0(1)	5(1)	2(1)
C(17)	26(1)	49(2)	21(1)	7(1)	0(1)	7(1)
C(18)	29(1)	54(2)	22(1)	7(1)	5(1)	-5(1)
C(19)	17(1)	17(1)	31(1)	5(1)	6(1)	-3(1)
C(20)	20(1)	26(1)	25(1)	4(1)	6(1)	3(1)
C(21)	23(1)	22(1)	29(1)	-3(1)	2(1)	-3(1)
C(22)	18(1)	25(1)	44(2)	10(1)	6(1)	2(1)
C(23)	27(1)	30(1)	31(1)	9(1)	6(1)	-4(1)
C(24)	19(1)	44(2)	18(1)	-2(1)	3(1)	-2(1)
C(25)	20(1)	28(1)	19(1)	-2(1)	-1(1)	2(1)
C(26)	20(1)	31(1)	39(2)	-12(1)	10(1)	-3(1)

Table 5. Hydrogen coordinates (x 10^4) and isotropic displacement parameters ($Å^2$x 10^3)
for sh2388.

	x	y	z	U(eq)
H(1)	3930	8781	2052	21
H(2A)	5295	8002	2791	45
H(2B)	5231	8891	3161	45
H(2C)	6081	8711	2695	45
H(3A)	5467	9890	1816	46
H(3B)	4584	10110	2239	46
H(3C)	4299	9920	1343	46
H(4)	6213	7912	-384	31
H(5A)	4158	7586	-1183	75
H(5B)	5036	7915	-1568	75
H(5C)	4631	8485	-980	75
H(6A)	6413	6512	-153	64
H(6B)	6126	6676	-1054	64
H(6C)	5274	6342	-644	64
H(7)	1011	8219	963	26
H(8A)	1683	8349	2297	59
H(8B)	1036	9146	1952	59
H(8C)	2260	9175	2157	59
H(9A)	2326	9546	798	62
H(9B)	1106	9617	619	62
H(9C)	1631	9029	112	62
H(10)	4833	6232	727	20
H(11A)	4666	5835	1955	38
H(11B)	4756	5046	1444	38
H(11C)	3665	5314	1572	38
H(12A)	2913	5436	151	39
H(12B)	3975	5159	-25	39

H(12C)	3462	6016	-348	39
H(13)	7754	7063	2292	30
H(14A)	6934	5487	1756	75
H(14B)	8126	5673	2085	75
H(14C)	7524	6082	1298	75
H(15A)	6933	6894	3289	69
H(15B)	7713	6145	3314	69
H(15C)	6513	6010	2969	69
H(16)	3494	5882	3064	27
H(17A)	4981	6638	3618	50
H(17B)	4422	6371	4270	50
H(17C)	4315	7295	3952	50
H(18A)	2373	7150	3604	53
H(18B)	2525	6242	3958	53
H(18C)	1876	6377	3099	53

Compound 7

Table 1. Crystal data and structure refinement for sh2256.

Identification code	sh2256	
Empirical formula	C40 H90 Mo2 O16 Sn6	
Formula weight	1731.14	
Temperature	103(2) K	
Wavelength	0.71073 Å	
Crystal system	Monoclinic	
Space group	P2(1)/n	
Unit cell dimensions	a = 10.2169(6) Å	α= 90°.
	b = 26.9659(16) Å	β= 110.298(3)°.
	c = 11.7063(8) Å	γ = 90°.
Volume	3024.9(3) $Å^3$	
Z	2	
Density (calculated)	1.901 Mg/m^3	
Absorption coefficient	2.889 mm^{-1}	
F(000)	1684	
Crystal size	0.2 x 0.3 x 0.45 mm^3	
Theta range for data collection	1.51 to 29.63°.	
Index ranges	-14<=h<=13, -37<=k<=35, -16<=l<=15	
Reflections collected	36193	
Independent reflections	8476 [R(int) = 0.0598]	
Completeness to theta = 29.63°	99.3 %	
Absorption correction	Multi scan	
Refinement method	Full-matrix least-squares on F^2	
Data / restraints / parameters	8476 / 0 / 305	
Goodness-of-fit on F^2	1.131	
Final R indices [I>2sigma(I)]	R1 = 0.1099, wR2 = 0.2804	
R indices (all data)	R1 = 0.1325, wR2 = 0.2940	

Extinction coefficient	0.00020(8)
Largest diff. peak and hole	7.403 and -2.890 e.Å^{-3}

Table 2. Atomic coordinates (x 10^4) and equivalent isotropic displacement parameters (Å^{2}x 10^3)
for sh2256. U(eq) is defined as one third of the trace of the orthogonalized U^{ij} tensor.

	x	y	z	U(eq)
Sn(1)	9264(1)	1540(1)	-79(1)	17(1)
Sn(2)	10134(1)	806(1)	2600(1)	17(1)
Sn(3)	12435(1)	961(1)	1142(1)	19(1)
Mo	9326(1)	351(1)	-715(1)	12(1)
O(1)	10326(12)	860(4)	880(10)	15(2)
O(2)	11670(14)	1690(4)	744(10)	19(2)
O(3)	9306(13)	1515(4)	1989(11)	20(2)
O(4)	7788(12)	851(5)	-738(12)	21(2)
O(5)	10044(13)	1018(4)	-1281(11)	18(2)
O(6)	12327(12)	1007(5)	3008(12)	22(2)
O(7)	8578(13)	71(4)	-2104(11)	20(2)
O(8)	11252(12)	101(4)	-307(10)	16(2)
C(1)	12390(30)	2164(9)	1080(20)	38(5)
C(2)	13840(20)	2086(7)	940(20)	35(5)
C(3)	11560(30)	2554(7)	180(20)	41(6)
C(4)	12540(30)	2283(9)	2330(20)	47(6)
C(5)	8695(19)	1843(7)	2638(18)	25(4)
C(6)	7400(30)	1581(11)	2800(30)	50(7)
C(7)	8280(30)	2332(10)	1920(20)	56(9)
C(8)	9740(30)	1937(8)	3894(18)	34(5)
C(9)	6345(17)	783(6)	-826(16)	20(3)
C(10)	6290(20)	574(8)	332(18)	29(4)

C(11)	5600(20)	443(7)	-1947(18)	28(4)
C(12)	5650(20)	1291(8)	-1060(20)	32(4)
C(13)	10110(20)	1121(6)	-2473(17)	24(4)
C(14)	8572(16)	1140(6)	-3360(13)	15(3)
C(15)	10800(20)	1622(7)	-2401(17)	27(4)
C(16)	10880(20)	717(8)	-2859(19)	31(4)
C(17)	13406(18)	929(8)	4148(17)	26(4)
C(18)	13240(20)	1298(8)	5050(20)	38(5)
C(19)	13330(30)	403(7)	4590(20)	54(8)
C(20)	14800(20)	989(12)	4000(20)	51(7)

Table 3. Bond lengths [Å] and angles [°] for sh2256.

Sn(1)-O(1)	2.23(1)	O(5)-C(13)	1.45(2)
Sn(1)-O(5)	2.32(1)	O(6)-C(17)	1.42(2)
Sn(1)-O(2)	2.34(1)	O(8)-Mo#1	1.94(1)
Sn(1)-O(4)	2.35(1)	C(1)-C(4)	1.45(3)
Sn(1)-O(3)	2.41(1)	C(1)-C(3)	1.52(3)
Sn(2)-O(1)	2.10(1)	C(1)-C(2)	1.57(3)
Sn(2)-O(3)	2.11(1)	C(5)-C(8)	1.51(3)
Sn(2)-O(6)	2.19(1)	C(5)-C(7)	1.54(3)
Sn(3)-O(1)	2.09(1)	C(5)-C(6)	1.57(3)
Sn(3)-O(2)	2.11(1)	C(9)-C(10)	1.49(3)
Sn(3)-O(6)	2.23(1)	C(9)-C(12)	1.52(2)
Mo-O(7)	1.71(1)	C(9)-C(11)	1.56(2)
Mo-O(8)#1	1.94(1)	C(13)-C(16)	1.51(3)
Mo-O(8)	1.98(1)	C(13)-C(15)	1.51(2)
Mo-O(4)	2.06(1)	C(13)-C(14)	1.55(2)
Mo-O(5)	2.13(1)	C(17)-C(20)	1.50(3)
Mo-O(1)	2.26(1)	C(17)-C(18)	1.50(3)
Mo-Mo#1	2.584(3)	C(17)-C(19)	1.52(3)
O(2)-C(1)	1.46(3)	O(1)-Sn(1)-O(5)	66.2(4)
O(3)-C(5)	1.44(2)	O(1)-Sn(1)-O(2)	71.1(4)
O(4)-C(9)	1.45(2)	O(5)-Sn(1)-O(2)	79.7(4)

O(1)-Sn(1)-O(4)	70.1(4)	Sn(3)-O(1)-Sn(2)	107.7(5)
O(5)-Sn(1)-O(4)	68.7(4)	Sn(3)-O(1)-Sn(1)	105.3(4)
O(2)-Sn(1)-O(4)	137.2(4)	Sn(2)-O(1)-Sn(1)	110.5(5)
O(1)-Sn(1)-O(3)	68.6(4)	Sn(3)-O(1)-Mo	110.4(5)
O(5)-Sn(1)-O(3)	134.7(4)	Sn(2)-O(1)-Mo	125.9(5)
O(2)-Sn(1)-O(3)	86.7(4)	Sn(1)-O(1)-Mo	94.8(4)
O(4)-Sn(1)-O(3)	95.4(4)	C(1)-O(2)-Sn(3)	130.2(1)
O(1)-Sn(2)-O(3)	76.8(4)	C(1)-O(2)-Sn(1)	128.3(1)
O(1)-Sn(2)-O(6)	76.3(5)	Sn(3)-O(2)-Sn(1)	100.7(5)
O(3)-Sn(2)-O(6)	96.2(5)	C(5)-O(3)-Sn(2)	124.9(1)
O(1)-Sn(3)-O(2)	78.7(4)	C(5)-O(3)-Sn(1)	130.8(1)
O(1)-Sn(3)-O(6)	75.6(4)	Sn(2)-O(3)-Sn(1)	103.4(5)
O(2)-Sn(3)-O(6)	91.4(5)	C(9)-O(4)-Mo	131.9(1)
O(7)-Mo-O(8)#1	100.2(5)	C(9)-O(4)-Sn(1)	130.0(1)
O(7)-Mo-O(8)	99.1(5)	Mo-O(4)-Sn(1)	96.5(5)
O(8)#1-Mo-O(8)	97.3(4)	C(13)-O(5)-Mo	126.6(1)
O(7)-Mo-O(4)	100.9(5)	C(13)-O(5)-Sn(1)	127.5(10)
O(8)#1-Mo-O(4)	91.4(5)	Mo-O(5)-Sn(1)	95.5(4)
O(8)-Mo-O(4)	156.4(5)	C(17)-O(6)-Sn(2)	124.7(1)
O(7)-Mo-O(5)	99.5(5)	C(17)-O(6)-Sn(3)	128.7(1)
O(8)#1-Mo-O(5)	158.9(5)	Sn(2)-O(6)-Sn(3)	99.6(5)
O(8)-Mo-O(5)	86.7(4)	Mo#1-O(8)-Mo	82.7(4)
O(4)-Mo-O(5)	77.7(5)	C(4)-C(1)-O(2)	109.5(2)
O(7)-Mo-O(1)	168.0(5)	C(4)-C(1)-C(3)	113(2)
O(8)#1-Mo-O(1)	91.1(4)	O(2)-C(1)-C(3)	108.1(2)
O(8)-Mo-O(1)	83.1(4)	C(4)-C(1)-C(2)	111(2)
O(4)-Mo-O(1)	74.8(4)	O(2)-C(1)-C(2)	105.0(2)
O(5)-Mo-O(1)	68.8(4)	C(3)-C(1)-C(2)	109.7(2)
O(7)-Mo-Mo#1	104.7(4)	O(3)-C(5)-C(8)	109.1(2)
O(8)#1-Mo-Mo#1	49.3(3)	O(3)-C(5)-C(7)	108.7(2)
O(8)-Mo-Mo#1	48.1(3)	C(8)-C(5)-C(7)	110.8(2)
O(4)-Mo-Mo#1	136.0(4)	O(3)-C(5)-C(6)	109.1(2)
O(5)-Mo-Mo#1	131.0(3)	C(8)-C(5)-C(6)	107.4(2)
O(1)-Mo-Mo#1	85.6(3)	C(7)-C(5)-C(6)	112(2)

O(4)-C(9)-C(10)	110.2(1)	O(5)-C(13)-C(14)	106.3(1)
O(4)-C(9)-C(12)	107.3(2)	C(16)-C(13)-C(14)	109.7(2)
C(10)-C(9)-C(12)	109.9(2)	C(15)-C(13)-C(14)	110.7(2)
O(4)-C(9)-C(11)	108.7(1)	O(6)-C(17)-C(20)	109.5(2)
C(10)-C(9)-C(11)	112.4(2)	O(6)-C(17)-C(18)	108.8(2)
C(12)-C(9)-C(11)	108.3(2)	C(20)-C(17)-C(18)	110.6(29)
O(5)-C(13)-C(16)	110.7(2)	O(6)-C(17)-C(19)	110.1(2)
O(5)-C(13)-C(15)	107.1(1)	C(20)-C(17)-C(19)	108.0(2)
C(16)-C(13)-C(15)	112.2(2)	C(18)-C(17)-C(19)	110.2(2)

Symmetry transformations used to generate equivalent atoms:
#1 -x+2,-y,-z

Table 4. Anisotropic displacement parameters ($Å^2$x 10^3) for sh2256. The anisotropic
displacement factor exponent takes the form: $-2\pi^2[h^2 a^{*2}U^{11} + ... + 2 h k a^* b^* U^{12}]$

	U^{11}	U^{22}	U^{33}	U^{23}	U^{13}	U^{12}
Sn(1)	21(1)	12(1)	16(1)	1(1)	3(1)	2(1)
Sn(2)	19(1)	20(1)	14(1)	1(1)	6(1)	1(1)
Sn(3)	15(1)	18(1)	24(1)	-2(1)	8(1)	-2(1)
Mo	14(1)	10(1)	11(1)	0(1)	4(1)	0(1)
O(1)	16(5)	4(4)	17(5)	3(4)	-3(4)	-5(4)
O(2)	33(7)	10(5)	14(5)	-4(4)	9(5)	-5(4)
O(3)	29(6)	13(5)	25(6)	3(4)	15(5)	10(5)
O(4)	10(5)	22(6)	27(6)	-3(5)	0(5)	2(4)
O(5)	23(6)	14(5)	19(6)	2(4)	10(5)	3(4)
O(6)	13(5)	26(6)	25(6)	-3(5)	5(5)	-3(5)
O(7)	20(6)	17(6)	17(6)	2(4)	0(5)	3(4)
O(8)	18(5)	10(5)	17(5)	3(4)	3(4)	-1(4)
C(1)	44(12)	46(13)	27(10)	4(9)	17(9)	-10(10)

C(2)	38(11)	17(9)	55(14)	-8(8)	21(10)	-16(8)
C(3)	54(14)	15(9)	43(13)	6(8)	5(11)	-6(9)
C(4)	75(18)	33(12)	40(13)	4(10)	31(13)	-18(12)
C(5)	23(9)	29(9)	26(9)	-2(7)	13(7)	10(7)
C(6)	33(12)	69(18)	50(15)	-23(13)	18(11)	4(11)
C(7)	100(20)	47(14)	25(11)	7(10)	23(13)	50(15)
C(8)	53(13)	41(12)	18(9)	-12(8)	23(9)	5(10)
C(9)	15(7)	18(7)	22(8)	-1(6)	0(6)	3(6)
C(10)	24(9)	43(11)	27(10)	4(8)	17(8)	5(8)
C(11)	25(9)	28(9)	28(9)	-13(7)	6(7)	-2(7)
C(12)	22(9)	30(10)	36(11)	4(8)	1(8)	19(8)
C(13)	36(10)	14(7)	24(9)	-2(6)	13(8)	-6(7)
C(14)	19(7)	14(7)	5(6)	7(5)	-3(5)	1(5)
C(15)	46(12)	25(9)	19(8)	3(7)	21(8)	0(8)
C(16)	43(12)	31(10)	24(9)	-3(8)	16(9)	-6(9)
C(17)	16(8)	34(10)	20(8)	-1(7)	-3(6)	-1(7)
C(18)	40(12)	25(10)	34(11)	-15(8)	-3(9)	0(8)
C(19)	90(20)	13(9)	28(11)	-3(8)	-21(12)	10(10)
C(20)	14(9)	100(20)	30(12)	-14(13)	-7(8)	0(11)

Compound 8

Table 1. Crystal data and structure refinement for sh2152a.

Identification code	sh2152a	
Empirical formula	C40 H96 Ge4 N8 Ni Si4	
Formula weight	1150.68	
Temperature	293(2) K	
Wavelength	0.71073 Å	
Crystal system	Monoclinic	
Space group	P2/c	
Unit cell dimensions	a = 40.342(8) Å	α= 90°.
	b = 13.351(3) Å	β= 90.01(3)°.
	c = 22.723(5) Å	γ = 90°.
Volume	12239(5) $Å^3$	
Z	8	
Density (calculated)	1.249 Mg/m^3	
Absorption coefficient	2.354 mm^{-1}	
F(000)	4832	
Crystal size	0.8 x 0.49 x 0.36 mm^3	
Theta range for data collection	1.51 to 30.51°.	
Index ranges	-56<=h<=56, -18<=k<=18, -32<=l<=31	
Reflections collected	158806	
Independent reflections	36589 [R(int) = 0.0354]	
Completeness to theta = 30.51°	97.9 %	
Absorption correction	Multiscan	
Refinement method	Full-matrix least-squares on F^2	
Data / restraints / parameters	36589 / 0 / 1122	
Goodness-of-fit on F^2	1.081	
Final R indices [I>2sigma(I)]	R1 = 0.0355, wR2 = 0.0754	
R indices (all data)	R1 = 0.0490, wR2 = 0.0797	
Largest diff. peak and hole	1.112 and -0.819 $e.Å^{-3}$	

Table 2. Atomic coordinates (x 10^4) and equivalent isotropic displacement parameters (Å^{2}x 10^3)
for sh2152a. U(eq) is defined as one third of the trace of the orthogonalized U^{ij} tensor.

	x	y	z	U(eq)
Ni(1)	5000	6011(1)	2500	12(1)
Ge(1)	4576(1)	4898(1)	2514(1)	14(1)
Ge(2)	4882(1)	7119(1)	1785(1)	13(1)
Si(2)	4696(1)	8549(1)	1027(1)	21(1)
Si(1)	4175(1)	3294(1)	2430(1)	23(1)
N(1)	4241(1)	4381(1)	2012(1)	19(1)
N(2)	4475(1)	3716(1)	2927(1)	21(1)
N(3)	4561(1)	8146(1)	1715(1)	18(1)
N(4)	5005(1)	7621(1)	1051(1)	19(1)
C(1)	4075(1)	4734(2)	1467(1)	23(1)
C(2)	3717(1)	5099(2)	1607(1)	38(1)
C(3)	4270(1)	5599(2)	1184(1)	29(1)
C(4)	4054(1)	3859(2)	1023(1)	37(1)
C(5)	4577(1)	3355(2)	3516(1)	25(1)
C(6)	4938(1)	3674(2)	3644(1)	29(1)
C(7)	4343(1)	3797(2)	3985(1)	40(1)
C(8)	4558(1)	2192(2)	3533(1)	44(1)
C(9)	4283(1)	2070(2)	2064(1)	38(1)
C(10)	3743(1)	3146(3)	2730(1)	43(1)
C(11)	5248(1)	7225(2)	621(1)	22(1)
C(12)	5126(1)	6208(2)	375(1)	30(1)
C(13)	5277(1)	7975(2)	106(1)	33(1)
C(14)	5589(1)	7092(3)	915(1)	40(1)
C(15)	4322(1)	8568(2)	2145(1)	21(1)
C(16)	4060(1)	9214(2)	1816(1)	29(1)

C(17)	4508(1)	9234(2)	2595(1)	31(1)
C(18)	4138(1)	7712(2)	2464(1)	31(1)
C(19)	4859(1)	9873(2)	1005(1)	38(1)
C(20)	4381(1)	8394(2)	420(1)	36(1)
Ni(2)	2495(1)	8985(1)	145(1)	14(1)
Ge(3)	2952(1)	9966(1)	135(1)	15(1)
Ge(4)	2388(1)	7856(1)	851(1)	15(1)
Ge(5)	2102(1)	10194(1)	168(1)	16(1)
Ge(6)	2531(1)	7905(1)	-602(1)	18(1)
Si(3)	3438(1)	11341(1)	93(1)	20(1)
Si(4)	2218(1)	6424(1)	1614(1)	24(1)
Si(5)	1738(1)	11866(1)	291(1)	26(1)
Si(6)	2580(1)	6514(1)	-1436(1)	34(1)
N(5)	3113(1)	11058(1)	573(1)	19(1)
N(6)	3298(1)	10376(1)	-370(1)	19(1)
C(21)	3026(1)	11451(2)	1162(1)	22(1)
C(22)	3245(1)	10952(2)	1637(1)	36(1)
C(23)	3081(1)	12599(2)	1176(1)	39(1)
C(24)	2656(1)	11241(2)	1286(1)	33(1)
C(25)	3423(1)	10033(2)	-947(1)	26(1)
C(26)	3180(1)	9290(2)	-1237(1)	32(1)
C(27)	3463(1)	10941(3)	-1360(1)	61(1)
C(28)	3765(1)	9509(3)	-870(2)	59(1)
C(29)	3866(1)	11121(2)	408(1)	35(1)
C(30)	3430(1)	12646(2)	-229(1)	37(1)
N(7)	2058(1)	6863(1)	946(1)	20(1)
N(8)	2544(1)	7290(1)	1553(1)	24(1)
C(31)	1790(1)	6493(2)	549(1)	21(1)
C(32)	1542(1)	5849(2)	904(1)	30(1)
C(33)	1940(1)	5844(2)	57(1)	31(1)
C(34)	1599(1)	7382(2)	279(1)	32(1)
C(35)	2808(1)	7656(2)	1959(1)	30(1)
C(36)	1577(1)	10323(2)	1163(1)	24(1)
C(37)	2690(1)	8621(2)	2268(1)	42(1)

C(38)	3129(1)	7861(2)	1614(1)	40(1)
C(39)	2354(1)	5074(2)	1620(1)	39(1)
C(40)	1933(1)	6636(2)	2256(1)	40(1)
N(9)	2032(1)	11431(1)	-211(1)	24(1)
N(10)	1773(1)	10725(1)	666(1)	21(1)
C(41)	2183(1)	11917(2)	-722(2)	49(1)
C(42A)	2499(1)	12583(4)	-418(2)	26(1)
C(43A)	1953(1)	12731(4)	-967(2)	28(1)
C(44A)	2312(1)	11234(4)	-1127(2)	32(1)
C(42B)	1902(2)	11483(6)	-1305(3)	62(2)
C(43B)	2169(2)	12922(6)	-802(4)	69(2)
C(44B)	2489(1)	11354(4)	-979(3)	36(1)
C(45)	2880(1)	6838(3)	2426(2)	59(1)
C(46)	1240(1)	9913(2)	942(1)	35(1)
C(47)	1771(1)	9486(2)	1479(1)	29(1)
C(48)	1511(1)	11177(2)	1606(1)	41(1)
C(49)	1876(1)	13003(2)	721(2)	44(1)
C(50)	1314(1)	12148(2)	-24(2)	48(1)
N(11)	2790(1)	6767(2)	-773(1)	29(1)
N(12)	2321(1)	7548(2)	-1305(1)	30(1)
C(51)	3041(1)	6201(2)	-426(1)	33(1)
C(52)	2871(1)	5530(2)	33(2)	49(1)
C(53)	3277(1)	6930(2)	-101(2)	52(1)
C(54)	3253(1)	5540(3)	-836(2)	62(1)
C(55)	2073(1)	8091(2)	-1671(1)	37(1)
C(56)	1895(1)	7345(3)	-2077(1)	53(1)
C(57)	1805(1)	8589(3)	-1278(1)	50(1)
C(58)	2250(1)	8909(2)	-2036(1)	41(1)
C(59)	2361(1)	5264(2)	-1465(1)	52(1)
C(60)	2835(1)	6641(3)	-2121(1)	50(1)
Ni(3)	0	6334(1)	2500	14(1)
Ge(7)	425(1)	5238(1)	2494(1)	17(1)
Ge(8)	94(1)	7461(1)	3212(1)	18(1)
Si(7)	886(1)	3793(1)	2488(1)	26(1)

Si(8)	225(1)	8977(1)	3943(1)	32(1)
N(13)	553(1)	4134(2)	2036(1)	27(1)
N(14)	771(1)	4749(1)	2977(1)	22(1)
C(61)	418(1)	3713(2)	1483(1)	39(1)
C(62A)	510(2)	2576(5)	1457(4)	60(2)
C(63A)	90(2)	3977(8)	1376(3)	68(3)
C(64A)	670(2)	4189(6)	990(3)	57(2)
C(62B)	648(2)	3084(5)	1146(3)	44(2)
C(63B)	94(2)	3037(4)	1682(3)	42(1)
C(64B)	263(2)	4549(4)	1071(3)	40(1)
C(65)	912(1)	5037(2)	3557(1)	29(1)
C(66)	704(1)	5872(2)	3842(1)	32(1)
C(67)	1274(1)	5427(3)	3487(2)	53(1)
C(68)	913(1)	4118(3)	3968(2)	63(1)
C(69)	870(1)	2479(2)	2788(2)	49(1)
C(70)	1300(1)	4014(2)	2122(1)	35(1)
N(15)	-83(1)	8051(2)	3887(1)	28(1)
N(16)	412(1)	8492(1)	3314(1)	26(1)
C(71)	-337(1)	7674(2)	4300(1)	37(1)
C(72)	-466(1)	8565(3)	4674(2)	65(1)
C(73)	-636(1)	7235(2)	3960(1)	37(1)
C(74)	-183(1)	6873(3)	4706(1)	60(1)
C(75)	677(1)	8897(2)	2929(1)	31(1)
C(76)	923(1)	9530(3)	3300(2)	49(1)
C(77)	869(1)	8040(2)	2638(1)	39(1)
C(78)	520(1)	9580(2)	2451(1)	42(1)
C(79)	69(1)	10306(2)	3860(2)	52(1)
C(80)	488(1)	8887(3)	4628(1)	44(1)

Table 3. Bond lengths [Å] and angles [°] for sh2152a.

Ni(1)-Ge(2)	2.2483(5)	Ni(2)-Ge(6)	2.2317(5)
Ni(1)-Ge(2)#1	2.2483(5)	Ni(2)-Ge(4)	2.2433(5)
Ni(1)-Ge(1)	2.2673(4)	Ni(2)-Ge(3)	2.2625(5)
Ni(1)-Ge(1)#1	2.2675(4)	Ni(2)-Ge(5)	2.2635(5)
Ge(1)-N(2)	1.880(2)	Ge(3)-N(5)	1.881(2)
Ge(1)-N(1)	1.897(2)	Ge(3)-N(6)	1.887(2)
Ge(1)-Si(1)	2.6901(8)	Ge(3)-Si(3)	2.6868(7)
Ge(2)-N(4)	1.865(2)	Ge(4)-N(8)	1.873(2)
Ge(2)-N(3)	1.890(2)	Ge(4)-N(7)	1.893(2)
Ge(2)-Si(2)	2.6784(8)	Ge(4)-Si(4)	2.6709(8)
Si(2)-N(3)	1.742(2)	Ge(5)-N(10)	1.883(2)
Si(2)-N(4)	1.758(2)	Ge(5)-N(9)	1.884(2)
Si(2)-C(19)	1.886(3)	Ge(5)-Si(5)	2.6871(8)
Si(2)-C(20)	1.888(3)	Ge(6)-N(12)	1.867(2)
Si(1)-N(2)	1.749(2)	Ge(6)-N(11)	1.885(2)
Si(1)-N(1)	1.755(2)	Ge(6)-Si(6)	2.6599(8)
Si(1)-C(10)	1.884(3)	Si(3)-N(5)	1.747(2)
Si(1)-C(9)	1.884(3)	Si(3)-N(6)	1.757(2)
N(1)-C(1)	1.485(3)	Si(3)-C(30)	1.889(3)
N(2)-C(5)	1.482(3)	Si(3)-C(29)	1.893(3)
N(3)-C(15)	1.484(3)	Si(4)-N(7)	1.750(2)
N(4)-C(11)	1.482(3)	Si(4)-N(8)	1.757(2)
C(1)-C(3)	1.538(3)	Si(4)-C(40)	1.879(3)
C(1)-C(4)	1.546(3)	Si(4)-C(39)	1.885(3)
C(1)-C(2)	1.556(3)	Si(5)-N(9)	1.744(2)
C(5)-C(7)	1.542(4)	Si(5)-N(10)	1.752(2)
C(5)-C(6)	1.545(3)	Si(5)-C(49)	1.889(3)
C(5)-C(8)	1.554(4)	Si(5)-C(50)	1.892(3)
C(11)-C(14)	1.539(4)	Si(6)-N(12)	1.756(3)
C(11)-C(13)	1.545(3)	Si(6)-N(11)	1.760(2)
C(11)-C(12)	1.549(3)	Si(6)-C(60)	1.873(3)
C(15)-C(18)	1.543(3)	Si(6)-C(59)	1.891(3)
C(15)-C(17)	1.551(3)	N(5)-C(21)	1.480(3)
C(15)-C(16)	1.555(3)	N(6)-C(25)	1.478(3)

C(21)-C(22)	1.545(4)	Ni(3)-Ge(8)#2	2.2412(5)
C(21)-C(24)	1.547(3)	Ni(3)-Ge(7)#2	2.2552(5)
C(21)-C(23)	1.549(3)	Ni(3)-Ge(7)	2.2553(5)
C(25)-C(27)	1.541(4)	Ge(7)-N(13)	1.876(2)
C(25)-C(26)	1.542(3)	Ge(7)-N(14)	1.891(2)
C(25)-C(28)	1.556(4)	Ge(7)-Si(7)	2.6782(8)
N(7)-C(31)	1.492(3)	Ge(8)-N(15)	1.867(2)
N(8)-C(35)	1.491(3)	Ge(8)-N(16)	1.895(2)
C(31)-C(33)	1.539(3)	Ge(8)-Si(8)	2.6714(8)
C(31)-C(34)	1.543(3)	Si(7)-N(13)	1.749(2)
C(31)-C(32)	1.546(3)	Si(7)-N(14)	1.754(2)
C(35)-C(37)	1.542(4)	Si(7)-C(69)	1.883(3)
C(35)-C(38)	1.541(4)	Si(7)-C(70)	1.891(3)
C(35)-C(45)	1.550(4)	Si(8)-N(16)	1.742(2)
C(36)-N(10)	1.479(3)	Si(8)-N(15)	1.757(2)
C(36)-C(47)	1.543(3)	Si(8)-C(80)	1.887(3)
C(36)-C(48)	1.544(3)	Si(8)-C(79)	1.892(3)
C(36)-C(46)	1.551(3)	N(13)-C(61)	1.481(3)
N(9)-C(41)	1.463(3)	N(14)-C(65)	1.486(3)
C(41)-C(43B)	1.355(9)	C(61)-C(63A)	1.389(7)
C(41)-C(44A)	1.397(6)	C(61)-C(62B)	1.468(6)
C(41)-C(43A)	1.533(6)	C(61)-C(62A)	1.564(7)
C(41)-C(44B)	1.561(6)	C(61)-C(64B)	1.584(7)
C(41)-C(42A)	1.701(6)	C(61)-C(64A)	1.643(7)
C(41)-C(42B)	1.838(9)	C(61)-C(63B)	1.651(6)
N(11)-C(51)	1.490(4)	C(65)-C(66)	1.538(4)
N(12)-C(55)	1.489(4)	C(65)-C(68)	1.543(4)
C(51)-C(52)	1.538(4)	C(65)-C(67)	1.556(4)
C(51)-C(54)	1.541(4)	N(15)-C(71)	1.479(3)
C(51)-C(53)	1.549(4)	N(16)-C(75)	1.482(3)
C(55)-C(56)	1.536(4)	C(71)-C(73)	1.544(4)
C(55)-C(58)	1.545(4)	C(71)-C(74)	1.545(4)
C(55)-C(57)	1.551(4)	C(71)-C(72)	1.552(4)
Ni(3)-Ge(8)	2.2411(5)	C(75)-C(77)	1.534(4)

C(75)-C(78)	1.551(4)	N(1)-Si(1)-C(9)	116.3(1)
C(75)-C(76)	1.554(4)	C(10)-Si(1)-C(9)	106.5(1)
Ge(2)-Ni(1)-Ge(2)#1	97.72(3)	N(2)-Si(1)-Ge(1)	44.06(6)
Ge(2)-Ni(1)-Ge(1)	106.32(2)	N(1)-Si(1)-Ge(1)	44.63(6)
Ge(2)#1-Ni(1)-Ge(1)	125.55(2)	C(10)-Si(1)-Ge(1)	127.9(1)
Ge(2)-Ni(1)-Ge(1)#1	125.55(2)	C(9)-Si(1)-Ge(1)	125.7(1)
Ge(2)#1-Ni(1)-Ge(1)#1	106.32(2)	C(1)-N(1)-Si(1)	130.2(1)
Ge(1)-Ni(1)-Ge(1)#1	98.09(2)	C(1)-N(1)-Ge(1)	135.0(1)
N(2)-Ge(1)-N(1)	80.83(8)	Si(1)-N(1)-Ge(1)	94.84(9)
N(2)-Ge(1)-Ni(1)	136.08(6)	C(5)-N(2)-Si(1)	132.1(1)
N(1)-Ge(1)-Ni(1)	140.10(6)	C(5)-N(2)-Ge(1)	131.7(1)
N(2)-Ge(1)-Si(1)	40.30(6)	Si(1)-N(2)-Ge(1)	95.64(9)
N(1)-Ge(1)-Si(1)	40.54(6)	C(15)-N(3)-Si(2)	132.6(1)
Ni(1)-Ge(1)-Si(1)	167.04(2)	C(15)-N(3)-Ge(2)	131.7(1)
N(4)-Ge(2)-N(3)	81.22(8)	Si(2)-N(3)-Ge(2)	94.92(8)
N(4)-Ge(2)-Ni(1)	145.65(6)	C(11)-N(4)-Si(2)	134.4(1)
N(3)-Ge(2)-Ni(1)	133.07(6)	C(11)-N(4)-Ge(2)	129.7(1)
N(4)-Ge(2)-Si(2)	40.81(6)	Si(2)-N(4)-Ge(2)	95.29(9)
N(3)-Ge(2)-Si(2)	40.40(6)	N(1)-C(1)-C(3)	110.9(2)
Ni(1)-Ge(2)-Si(2)	173.29(2)	N(1)-C(1)-C(4)	109.2(2)
N(3)-Si(2)-N(4)	88.58(8)	C(3)-C(1)-C(4)	108.8(2)
N(3)-Si(2)-C(19)	114.9(1)	N(1)-C(1)-C(2)	110.3(2)
N(4)-Si(2)-C(19)	114.5(1)	C(3)-C(1)-C(2)	108.9(2)
N(3)-Si(2)-C(20)	114.3(1)	C(4)-C(1)-C(2)	108.6(2)
N(4)-Si(2)-C(20)	115.0(1)	N(2)-C(5)-C(7)	109.3(2)
C(19)-Si(2)-C(20)	108.6(1)	N(2)-C(5)-C(6)	110.0(2)
N(3)-Si(2)-Ge(2)	44.68(6)	C(7)-C(5)-C(6)	109.9(2)
N(4)-Si(2)-Ge(2)	43.90(6)	N(2)-C(5)-C(8)	109.5(2)
C(19)-Si(2)-Ge(2)	1236.0(1)	C(7)-C(5)-C(8)	109.6(2)
C(20)-Si(2)-Ge(2)	125.42(9)	C(6)-C(5)-C(8)	108.5(2)
N(2)-Si(1)-N(1)	88.68(9)	N(4)-C(11)-C(14)	110.3(2)
N(2)-Si(1)-C(10)	116.1(1)	N(4)-C(11)-C(13)	108.6(2)
N(1)-Si(1)-C(10)	115.1(1)	C(14)-C(11)-C(13)	109.7(2)
N(2)-Si(1)-C(9)	113.9(1)	N(4)-C(11)-C(12)	109.8(2)

C(14)-C(11)-C(12)	109.8(2)	N(11)-Ge(6)-Ni(2)	135.49(7)
C(13)-C(11)-C(12)	108.6(2)	N(12)-Ge(6)-Si(6)	41.15(8)
N(3)-C(15)-C(18)	110.0(2)	N(11)-Ge(6)-Si(6)	41.34(7)
N(3)-C(15)-C(17)	109.6(2)	Ni(2)-Ge(6)-Si(6)	175.87(2)
C(18)-C(15)-C(17)	110.4(2)	N(5)-Si(3)-N(6)	88.52(8)
N(3)-C(15)-C(16)	109.7(2)	N(5)-Si(3)-C(30)	115.4(1)
C(18)-C(15)-C(16)	108.1(2)	N(6)-Si(3)-C(30)	116.1(1)
C(17)-C(15)-C(16)	109.2(2)	N(5)-Si(3)-C(29)	114.5(1)
Ge(6)-Ni(2)-Ge(4)	97.06(2)	N(6)-Si(3)-C(29)	114.0(1)
Ge(6)-Ni(2)-Ge(3)	108.28(3)	C(30)-Si(3)-C(29)	107.7(1)
Ge(4)-Ni(2)-Ge(3)	123.53(2)	N(5)-Si(3)-Ge(3)	44.19(6)
Ge(6)-Ni(2)-Ge(5)	121.57(2)	N(6)-Si(3)-Ge(3)	44.39(6)
Ge(4)-Ni(2)-Ge(5)	109.17(2)	C(30)-Si(3)-Ge(3)	129.2(1)
Ge(3)-Ni(2)-Ge(5)	99.10(2)	C(29)-Si(3)-Ge(3)	123.12(9)
N(5)-Ge(3)-N(6)	80.95(8)	N(7)-Si(4)-N(8)	89.25(9)
N(5)-Ge(3)-Ni(2)	136.44(5)	N(7)-Si(4)-C(40)	113.5(1)
N(6)-Ge(3)-Ni(2)	140.92(6)	N(8)-Si(4)-C(40)	114.8(1)
N(5)-Ge(3)-Si(3)	40.35(5)	N(7)-Si(4)-C(39)	115.8(1)
N(6)-Ge(3)-Si(3)	40.66(6)	N(8)-Si(4)-C(39)	114.3(1)
Ni(2)-Ge(3)-Si(3)	172.13(2)	C(40)-Si(4)-C(39)	108.4(1)
N(8)-Ge(4)-N(7)	81.73(8)	N(7)-Si(4)-Ge(4)	44.96(6)
N(8)-Ge(4)-Ni(2)	144.75(6)	N(8)-Si(4)-Ge(4)	44.33(6)
N(7)-Ge(4)-Ni(2)	133.37(6)	C(40)-Si(4)-Ge(4)	123.6(1)
N(8)-Ge(4)-Si(4)	40.97(6)	C(39)-Si(4)-Ge(4)	127.9(1)
N(7)-Ge(4)-Si(4)	40.79(6)	N(9)-Si(5)-N(10)	88.47(9)
Ni(2)-Ge(4)-Si(4)	174.01(2)	N(9)-Si(5)-C(49)	113.9(1)
N(10)-Ge(5)-N(9)	80.70(8)	N(10)-Si(5)-C(49)	115.0(1)
N(10)-Ge(5)-Ni(2)	140.92(6)	N(9)-Si(5)-C(50)	115.7(1)
N(9)-Ge(5)-Ni(2)	136.09(6)	N(10)-Si(5)-C(50)	115.4(1)
N(10)-Ge(5)-Si(5)	40.48(6)	C(49)-Si(5)-C(50)	107.6(2)
N(9)-Ge(5)-Si(5)	40.24(6)	N(9)-Si(5)-Ge(5)	44.25(6)
Ni(2)-Ge(5)-Si(5)	167.97(2)	N(10)-Si(5)-Ge(5)	44.25(6)
N(12)-Ge(6)-N(11)	82.5(1)	C(49)-Si(5)-Ge(5)	124.0(1)
N(12)-Ge(6)-Ni(2)	141.80(7)	C(50)-Si(5)-Ge(5)	128.4(1)

N(12)-Si(6)-N(11)	89.4(1)	N(7)-C(31)-C(33)	109.9(2)
N(12)-Si(6)-C(60)	113.4(2)	N(7)-C(31)-C(34)	110.4(2)
N(11)-Si(6)-C(60)	115.4(1)	C(33)-C(31)-C(34)	109.9(2)
N(12)-Si(6)-C(59)	115.0(1)	N(7)-C(31)-C(32)	109.8(2)
N(11)-Si(6)-C(59)	115.1(1)	C(33)-C(31)-C(32)	108.7(2)
C(60)-Si(6)-C(59)	107.9(1)	C(34)-C(31)-C(32)	108.1(2)
N(12)-Si(6)-Ge(6)	44.43(7)	N(8)-C(35)-C(37)	109.5(2)
N(11)-Si(6)-Ge(6)	45.02(7)	N(8)-C(35)-C(38)	110.1(2)
C(60)-Si(6)-Ge(6)	124.8(1)	C(37)-C(35)-C(38)	110.1(2)
C(59)-Si(6)-Ge(6)	127.31(9)	N(8)-C(35)-C(45)	109.1(2)
C(21)-N(5)-Si(3)	131.8(1)	C(37)-C(35)-C(45)	109.6(2)
C(21)-N(5)-Ge(3)	132.2(1)	C(38)-C(35)-C(45)	108.4(3)
Si(3)-N(5)-Ge(3)	95.46(8)	N(10)-C(36)-C(47)	110.4(2)
C(25)-N(6)-Si(3)	130.4(1)	N(10)-C(36)-C(48)	108.8(2)
C(25)-N(6)-Ge(3)	134.7(1)	C(47)-C(36)-C(48)	108.5(2)
Si(3)-N(6)-Ge(3)	94.95(8)	N(10)-C(36)-C(46)	110.4(2)
N(5)-C(21)-C(22)	110.1(2)	C(47)-C(36)-C(46)	109.9(2)
N(5)-C(21)-C(24)	109.2(2)	C(48)-C(36)-C(46)	108.7(2)
C(22)-C(21)-C(24)	110.2(2)	C(41)-N(9)-Si(5)	130.9(2)
N(5)-C(21)-C(23)	109.6(2)	C(41)-N(9)-Ge(5)	133.5(2)
C(22)-C(21)-C(23)	109.3(2)	Si(5)-N(9)-Ge(5)	95.51(9)
C(24)-C(21)-C(23)	108.3(2)	C(36)-N(10)-Si(5)	130.1(1)
N(6)-C(25)-C(27)	109.4(2)	C(36)-N(10)-Ge(5)	134.4(1)
N(6)-C(25)-C(26)	111.1(2)	Si(5)-N(10)-Ge(5)	95.26(9)
C(27)-C(25)-C(26)	108.2(2)	C(43B)-C(41)-C(44A)	124.9(5)
N(6)-C(25)-C(28)	110.0(2)	C(43B)-C(41)-N(9)	121.9(5)
C(27)-C(25)-C(28)	109.3(3)	C(44A)-C(41)-N(9)	113.0(3)
C(26)-C(25)-C(28)	108.8(2)	C(43B)-C(41)-C(43A)	39.2(4)
C(31)-N(7)-Si(4)	132.8(1)	C(44A)-C(41)-C(43A)	116.7(4)
C(31)-N(7)-Ge(4)	132.4(1)	N(9)-C(41)-C(43A)	110.5(3)
Si(4)-N(7)-Ge(4)	94.25(9)	C(43B)-C(41)-C(44B)	117.3(5)
C(35)-N(8)-Si(4)	134.6(2)	C(44A)-C(41)-C(44B)	31.0(3)
C(35)-N(8)-Ge(4)	129.3(2)	N(9)-C(41)-C(44B)	114.5(3)
Si(4)-N(8)-Ge(4)	94.70(9)	C(43A)-C(41)-C(44B)	133.2(3)

C(43B)-C(41)-C(42A)	64.3(4)	Ge(7)#2-Ni(3)-Ge(7)	99.08(2)
C(44A)-C(41)-C(42A)	109.1(3)	N(13)-Ge(7)-N(14)	81.23(9)
N(9)-C(41)-C(42A)	102.9(3)	N(13)-Ge(7)-Ni(3)	136.29(7)
C(43A)-C(41)-C(42A)	103.3(3)	N(14)-Ge(7)-Ni(3)	141.37(6)
C(44B)-C(41)-C(42A)	79.0(3)	N(13)-Ge(7)-Si(7)	40.58(7)
C(43B)-C(41)-C(42B)	101.0(5)	N(14)-Ge(7)-Si(7)	40.77(6)
C(44A)-C(41)-C(42B)	63.2(4)	Ni(3)-Ge(7)-Si(7)	174.38(2)
N(9)-C(41)-C(42B)	100.1(3)	N(15)-Ge(8)-N(16)	81.47(9)
C(43A)-C(41)-C(42B)	65.7(3)	N(15)-Ge(8)-Ni(3)	144.23(7)
C(44B)-C(41)-C(42B)	93.9(4)	N(16)-Ge(8)-Ni(3)	133.69(6)
C(42A)-C(41)-C(42B)	156.9(3)	N(15)-Ge(8)-Si(8)	40.93(7)
C(51)-N(11)-Si(6)	133.0(2)	N(16)-Ge(8)-Si(8)	40.55(7)
C(51)-N(11)-Ge(6)	132.7(2)	Ni(3)-Ge(8)-Si(8)	172.29(2)
Si(6)-N(11)-Ge(6)	93.6(1)	N(13)-Si(7)-N(14)	88.83(9)
C(55)-N(12)-Si(6)	133.42(2)	N(13)-Si(7)-C(69)	115.4(1)
C(55)-N(12)-Ge(6)	131.0(2)	N(14)-Si(7)-C(69)	116.0(1)
Si(6)-N(12)-Ge(6)	94.4(1)	N(13)-Si(7)-C(70)	112.3(1)
N(11)-C(51)-C(52)	110.5(2)	N(14)-Si(7)-C(70)	113.5(1)
N(11)-C(51)-C(54)	110.4(2)	C(69)-Si(7)-C(70)	109.6(1)
C(52)-C(51)-C(54)	108.9(2)	N(13)-Si(7)-Ge(7)	44.22(6)
N(11)-C(51)-C(53)	110.6(2)	N(14)-Si(7)-Ge(7)	44.74(6)
C(52)-C(51)-C(53)	108.4(3)	C(69)-Si(7)-Ge(7)	130.2(1)
C(54)-C(51)-C(53)	108.0(3)	C(70)-Si(7)-Ge(7)	120.21(9)
N(12)-C(55)-C(56)	109.5(3)	N(16)-Si(8)-N(15)	89.2(1)
N(12)-C(55)-C(58)	109.5(2)	N(16)-Si(8)-C(80)	114.1(1)
C(56)-C(55)-C(58)	110.6(2)	N(15)-Si(8)-C(80)	114.3(1)
N(12)-C(55)-C(57)	110.9(2)	N(16)-Si(8)-C(79)	114.2(1)
C(56)-C(55)-C(57)	107.3(3)	N(15)-Si(8)-C(79)	114.8(1)
C(58)-C(55)-C(57)	109.2(3)	C(80)-Si(8)-C(79)	109.3(1)
Ge(8)-Ni(3)-Ge(8)#2	95.65(3)	N(16)-Si(8)-Ge(8)	45.02(7)
Ge(8)-Ni(3)-Ge(7)#2	124.06(2)	N(15)-Si(8)-Ge(8)	44.13(6)
Ge(8)#2-Ni(3)-Ge(7)#2	108.14(2)	C(80)-Si(8)-Ge(8)	125.1(1)
Ge(8)-Ni(3)-Ge(7)	108.14(2)	C(79)-Si(8)-Ge(8)	125.7(1)
Ge(8)#2-Ni(3)-Ge(7)	124.05(2)	C(61)-N(13)-Si(7)	133.0(2)

C(61)-N(13)-Ge(7)	131.8(2)	C(64A)-C(61)-C(63B)	152.7(4)
Si(7)-N(13)-Ge(7)	95.2(1)	N(14)-C(65)-C(66)	110.6(2)
C(65)-N(14)-Si(7)	130.4(2)	N(14)-C(65)-C(68)	109.3(2)
C(65)-N(14)-Ge(7)	135.1(2)	C(66)-C(65)-C(68)	108.8(3)
Si(7)-N(14)-Ge(7)	94.5(1)	N(14)-C(65)-C(67)	110.8(2)
C(63A)-C(61)-C(62B)	130.9(4)	C(66)-C(65)-C(67)	108.2(2)
C(63A)-C(61)-N(13)	113.8(3)	C(68)-C(65)-C(67)	109.1(3)
C(62B)-C(61)-N(13)	115.3(3)	C(71)-N(15)-Si(8)	134.0(2)
C(63A)-C(61)-C(62A)	117.8(5)	C(71)-N(15)-Ge(8)	130.0(2)
C(62B)-C(61)-C(62A)	43.4(4)	Si(8)-N(15)-Ge(8)	94.9(1)
N(13)-C(61)-C(62A)	108.2(4)	C(75)-N(16)-Si(8)	131.4(2)
C(63A)-C(61)-C(64B)	48.9(5)	C(75)-N(16)-Ge(8)	132.8(1)
C(62B)-C(61)-C(64B)	110.0(4)	Si(8)-N(16)-Ge(8)	94.4(1)
N(13)-C(61)-C(64B)	112.3(3)	N(15)-C(71)-C(73)	110.7(2)
C(62A)-C(61)-C(64B)	139.0(4)	N(15)-C(71)-C(74)	109.5(2)
C(63A)-C(61)-C(64A)	111.8(6)	C(73)-C(71)-C(74)	110.6(3)
C(62B)-C(61)-C(64A)	58.2(4)	N(15)-C(71)-C(72)	108.6(3)
N(13)-C(61)-C(64A)	101.8(3)	C(73)-C(71)-C(72)	107.7(2)
C(62A)-C(61)-C(64A)	101.6(4)	C(74)-C(71)-C(72)	109.8(3)
C(64B)-C(61)-C(64A)	64.4(4)	N(16)-C(75)-C(77)	110.3(2)
C(63A)-C(61)-C(63B)	55.5(5)	N(16)-C(75)-C(78)	109.6(2)
C(62B)-C(61)-C(63B)	109.3(4)	C(77)-C(75)-C(78)	110.0(2)
N(13)-C(61)-C(63B)	105.5(3)	N(16)-C(75)-C(76)	109.8(2)
C(62A)-C(61)-C(63B)	70.7(4)	C(77)-C(75)-C(76)	108.3(2)
C(64B)-C(61)-C(63B)	103.6(4)	C(78)-C(75)-C(76)	108.7(2)

Symmetry transformations used to generate equivalent atoms:

#1 -x+1,y,-z+1/2 #2 -x,y,-z+1/2

Table 4. Anisotropic displacement parameters ($Å^2 x\ 10^3$) for sh2152a. The anisotropic

displacement factor exponent takes the form: $-2p^2[\ h^2\ a^{*2}U^{11} + ... + 2\ h\ k\ a^*\ b^*\ U^{12}\ ]$

	U^{11}	U^{22}	U^{33}	U^{23}	U^{13}	U^{12}
Ni(1)	15(1)	10(1)	11(1)	0	-1(1)	0
Ge(1)	16(1)	13(1)	14(1)	0(1)	-1(1)	-2(1)
Ge(2)	17(1)	12(1)	11(1)	1(1)	-1(1)	0(1)
Si(2)	33(1)	16(1)	14(1)	4(1)	-3(1)	3(1)
Si(1)	24(1)	20(1)	25(1)	0(1)	-1(1)	-10(1)
N(1)	19(1)	18(1)	20(1)	-1(1)	-3(1)	-4(1)
N(2)	26(1)	17(1)	21(1)	4(1)	-1(1)	-8(1)
N(3)	24(1)	15(1)	14(1)	1(1)	-2(1)	4(1)
N(4)	26(1)	18(1)	13(1)	3(1)	1(1)	0(1)
C(1)	22(1)	22(1)	24(1)	-2(1)	-9(1)	-3(1)
C(2)	24(1)	41(2)	50(2)	4(1)	-8(1)	3(1)
C(3)	34(1)	28(1)	26(1)	5(1)	-11(1)	-7(1)
C(4)	52(2)	31(1)	29(1)	-7(1)	-15(1)	-6(1)
C(5)	28(1)	26(1)	20(1)	6(1)	0(1)	-7(1)
C(6)	31(1)	34(1)	21(1)	8(1)	-4(1)	-3(1)
C(7)	34(1)	59(2)	26(1)	7(1)	7(1)	-5(1)
C(8)	63(2)	28(1)	40(2)	17(1)	-11(1)	-12(1)
C(9)	57(2)	17(1)	42(2)	-1(1)	-8(1)	-9(1)
C(10)	32(1)	56(2)	42(2)	5(1)	3(1)	-21(1)
C(11)	27(1)	24(1)	15(1)	2(1)	4(1)	-3(1)
C(12)	43(1)	23(1)	25(1)	-2(1)	10(1)	-4(1)
C(13)	44(1)	30(1)	25(1)	6(1)	12(1)	-6(1)
C(14)	27(1)	65(2)	27(1)	-6(1)	3(1)	4(1)
C(15)	26(1)	17(1)	20(1)	-2(1)	-2(1)	8(1)
C(16)	30(1)	27(1)	32(1)	0(1)	-6(1)	12(1)
C(17)	37(1)	28(1)	27(1)	-11(1)	-9(1)	12(1)

C(18)	36(1)	26(1)	31(1)	2(1)	11(1)	8(1)
C(19)	65(2)	19(1)	30(1)	8(1)	2(1)	1(1)
C(20)	48(2)	39(1)	21(1)	-1(1)	-11(1)	15(1)
Ni(2)	15(1)	14(1)	12(1)	1(1)	1(1)	-2(1)
Ge(3)	15(1)	17(1)	13(1)	-1(1)	1(1)	-3(1)
Ge(4)	19(1)	15(1)	12(1)	2(1)	1(1)	-2(1)
Ge(5)	16(1)	15(1)	18(1)	3(1)	1(1)	-1(1)
Ge(6)	23(1)	19(1)	12(1)	-1(1)	0(1)	-6(1)
Si(3)	17(1)	20(1)	24(1)	-2(1)	3(1)	-5(1)
Si(4)	37(1)	19(1)	16(1)	5(1)	1(1)	-5(1)
Si(5)	21(1)	18(1)	40(1)	3(1)	0(1)	3(1)
Si(6)	47(1)	34(1)	21(1)	-12(1)	13(1)	-19(1)
N(5)	17(1)	19(1)	20(1)	-5(1)	1(1)	-4(1)
N(6)	18(1)	22(1)	18(1)	-2(1)	4(1)	-5(1)
C(21)	24(1)	24(1)	19(1)	-8(1)	2(1)	-5(1)
C(22)	38(1)	47(2)	23(1)	-7(1)	-6(1)	-3(1)
C(23)	51(2)	29(1)	38(2)	-14(1)	11(1)	-8(1)
C(24)	25(1)	48(2)	26(1)	-12(1)	8(1)	-7(1)
C(25)	23(1)	35(1)	20(1)	-5(1)	9(1)	-10(1)
C(26)	34(1)	39(1)	23(1)	-9(1)	9(1)	-12(1)
C(27)	104(3)	53(2)	25(1)	-2(1)	23(2)	-38(2)
C(28)	26(1)	93(3)	57(2)	-42(2)	6(1)	7(2)
C(29)	19(1)	45(2)	40(2)	-13(1)	-1(1)	-6(1)
C(30)	45(2)	25(1)	43(2)	5(1)	11(1)	-8(1)
N(7)	26(1)	18(1)	16(1)	3(1)	1(1)	-6(1)
N(8)	31(1)	24(1)	16(1)	7(1)	-5(1)	-4(1)
C(31)	25(1)	17(1)	22(1)	0(1)	2(1)	-7(1)
C(32)	30(1)	27(1)	33(1)	1(1)	8(1)	-9(1)
C(33)	36(1)	31(1)	26(1)	-11(1)	7(1)	-12(1)
C(34)	33(1)	25(1)	37(1)	4(1)	-10(1)	-8(1)
C(35)	36(1)	33(1)	20(1)	9(1)	-11(1)	-6(1)
C(36)	24(1)	22(1)	26(1)	-4(1)	8(1)	0(1)
C(37)	53(2)	47(2)	25(1)	-8(1)	-5(1)	-12(1)
C(38)	30(1)	51(2)	38(2)	1(1)	-9(1)	-3(1)

C(39)	60(2)	24(1)	34(1)	10(1)	-8(1)	-2(1)
C(40)	57(2)	42(2)	22(1)	4(1)	10(1)	-12(1)
N(9)	25(1)	18(1)	28(1)	8(1)	0(1)	-1(1)
N(10)	17(1)	17(1)	27(1)	0(1)	4(1)	1(1)
C(41)	40(2)	45(2)	64(2)	39(2)	23(1)	17(1)
C(45)	78(2)	52(2)	46(2)	27(2)	-37(2)	-17(2)
C(46)	23(1)	35(1)	48(2)	1(1)	6(1)	-5(1)
C(47)	32(1)	29(1)	25(1)	1(1)	8(1)	1(1)
C(48)	52(2)	32(1)	38(2)	-10(1)	14(1)	6(1)
C(49)	49(2)	17(1)	65(2)	-6(1)	9(2)	-2(1)
C(50)	27(1)	46(2)	71(2)	15(2)	-2(1)	12(1)
N(11)	41(1)	23(1)	23(1)	-7(1)	9(1)	-3(1)
N(12)	39(1)	35(1)	15(1)	-2(1)	-4(1)	-15(1)
C(51)	36(1)	26(1)	37(1)	0(1)	13(1)	6(1)
C(52)	52(2)	45(2)	50(2)	19(1)	15(1)	12(1)
C(53)	47(2)	39(2)	69(2)	5(2)	-14(2)	7(1)
C(54)	71(2)	56(2)	60(2)	-2(2)	30(2)	28(2)
C(55)	45(2)	46(2)	18(1)	6(1)	-13(1)	-21(1)
C(56)	66(2)	56(2)	37(2)	5(2)	-22(2)	-28(2)
C(57)	34(2)	82(2)	35(2)	13(2)	-9(1)	2(2)
C(58)	56(2)	40(2)	28(1)	1(1)	-2(1)	-16(1)
C(59)	71(2)	41(2)	45(2)	-25(1)	25(2)	-28(2)
C(60)	60(2)	64(2)	27(1)	-17(1)	18(1)	-28(2)
Ni(3)	16(1)	14(1)	11(1)	0	0(1)	0
Ge(7)	16(1)	16(1)	18(1)	-3(1)	1(1)	1(1)
Ge(8)	21(1)	18(1)	14(1)	-3(1)	-2(1)	4(1)
Si(7)	23(1)	19(1)	37(1)	1(1)	7(1)	5(1)
Si(8)	37(1)	30(1)	28(1)	-15(1)	-14(1)	12(1)
N(13)	23(1)	22(1)	36(1)	-13(1)	2(1)	3(1)
N(14)	20(1)	19(1)	26(1)	2(1)	-1(1)	3(1)
C(61)	51(2)	31(1)	35(1)	-19(1)	-1(1)	3(1)
C(62A)	75(5)	39(4)	65(5)	-29(3)	-3(4)	-5(3)
C(63A)	43(4)	112(7)	51(4)	-51(5)	-16(3)	15(4)
C(64A)	67(5)	67(5)	36(3)	-13(3)	9(3)	-3(4)

C(62B)	40(3)	47(4)	46(4)	-26(3)	0(3)	10(3)
C(63B)	44(3)	34(3)	48(3)	-26(3)	-3(3)	-9(2)
C(64B)	51(3)	38(3)	30(3)	-19(2)	-8(2)	10(3)
C(65)	25(1)	29(1)	31(1)	2(1)	-11(1)	3(1)
C(66)	29(1)	44(2)	22(1)	-3(1)	-7(1)	7(1)
C(67)	22(1)	66(2)	71(2)	-30(2)	-7(1)	1(1)
C(68)	103(3)	41(2)	46(2)	13(2)	-35(2)	1(2)
C(69)	56(2)	22(1)	68(2)	5(1)	21(2)	7(1)
C(70)	24(1)	40(1)	43(2)	3(1)	9(1)	9(1)
N(15)	29(1)	35(1)	19(1)	-10(1)	-4(1)	12(1)
N(16)	35(1)	19(1)	25(1)	-5(1)	-8(1)	-1(1)
C(71)	26(1)	67(2)	18(1)	-11(1)	-1(1)	15(1)
C(72)	35(2)	113(3)	48(2)	-50(2)	-1(1)	17(2)
C(73)	31(1)	54(2)	26(1)	-6(1)	3(1)	8(1)
C(74)	39(2)	112(3)	30(2)	27(2)	7(1)	15(2)
C(75)	34(1)	26(1)	34(1)	1(1)	-12(1)	-9(1)
C(76)	51(2)	47(2)	48(2)	-1(1)	-18(1)	-22(1)
C(77)	37(1)	38(2)	42(2)	2(1)	7(1)	-8(1)
C(78)	53(2)	33(1)	42(2)	10(1)	-16(1)	-12(1)
C(79)	65(2)	33(2)	58(2)	-25(1)	-25(2)	20(1)
C(80)	43(2)	57(2)	32(1)	-21(1)	-15(1)	16(1)

Compound 9-H

Table 1. Crystal data and structure refinement for sh614.

Identification code	sh614	
Empirical formula	C44 H112 N8 Ni O4 Si4 Sn4	
Formula weight	1463.25	
Temperature	293(2) K	
Wavelength	0.71073 Å	
Crystal system	Tetragonal	
Space group	P4(2)/n	
Unit cell dimensions	a = 17.235(9) Å	α= 90°.
	b = 17.235(9) Å	β= 90°.
	c = 11.253(6) Å	γ = 90°.
Volume	3343(3) $Å^3$	
Z	2	
Density (calculated)	1.454 Mg/m^3	
Absorption coefficient	1.862 mm^{-1}	
F(000)	1496	
Crystal size	0.45 x 0.30 x 0.25 mm^3	
Theta range for data collection	1.67 to 22.50°.	
Index ranges	0<=h<=18, 0<=k<=18, 0<=l<=6	
Reflections collected	1624	
Independent reflections	1521 [R(int) = 0.0244]	
Completeness to theta = 22.50°	69.5 %	
Absorption correction	Empirical	
Refinement method	Full-matrix least-squares on F^2	
Data / restraints / parameters	1521 / 0 / 137	
Goodness-of-fit on F^2	0.947	
Final R indices [I>2sigma(I)]	R1 = 0.0317, wR2 = 0.1024	
R indices (all data)	R1 = 0.0438, wR2 = 0.1117	

Largest diff. peak and hole	0.514 and -0.476 e.Å^{-3}

Table 2. Atomic coordinates (x 10^4) and equivalent isotropic displacement parameters (Å^{2}x 10^3)
for sh614. U(eq) is defined as one third of the trace of the orthogonalized U^{ij} tensor.

	x	y	z	U(eq)
Sn	7693(1)	6249(1)	1581(1)	30(1)
Ni	7500	7500	2500	26(1)
Si	6858(1)	4738(1)	1259(2)	38(1)
O	8819(2)	5879(2)	1589(4)	47(2)
N(1)	7133(3)	5196(3)	2629(6)	30(2)
N(2)	7234(3)	5442(3)	405(8)	34(2)
C(1)	9132(4)	5259(4)	923(8)	60(2)
C(2)	7459(4)	4816(4)	3714(8)	45(2)
C(3)	8240(5)	4446(5)	3442(9)	73(3)
C(4)	6873(5)	4219(5)	4210(9)	73(2)
C(5)	7589(5)	5445(6)	4651(9)	81(3)
C(6)	7197(4)	5525(4)	-881(13)	54(3)
C(7)	7562(7)	6285(6)	-1249(14)	99(4)
C(8)	6363(5)	5532(6)	-1351(9)	89(3)
C(9)	7558(8)	4874(8)	-1555(11)	129(5)
C(10)	5787(4)	4651(4)	1286(9)	56(2)
C(11)	7263(4)	3740(4)	1025(8)	59(2)

Table 3. Bond lengths [Å] and angles [°] for sh614.

Sn-O	2.043(4)	Sn-Ni	2.415(1)
Sn-N(2)	2.076(7)	Sn-Si	2.996(2)
Sn-N(1)	2.370(5)	Ni-Sn#1	2.415(1)

Ni-Sn#2	2.415(1)	Sn#2-Ni-Sn#3	100.57(2)
Ni-Sn#3	2.415(1)	N(2)-Si-N(1)	94.2(3)
Si-N(2)	1.677(7)	N(2)-Si-C(10)	116.9(3)
Si-N(1)	1.796(6)	N(1)-Si-C(10)	106.5(4)
Si-C(10)	1.853(7)	N(2)-Si-C(11)	116.1(3)
Si-C(11)	1.875(7)	N(1)-Si-C(11)	115.1(3)
O-C(1)	1.413(8)	C(10)-Si-C(11)	107.4(3)
N(1)-C(2)	1.494(9)	N(2)-Si-Sn	41.9(3)
N(2)-C(6)	1.46(1)	N(1)-Si-Sn	52.3(2)
C(2)-C(3)	1.52(1)	C(10)-Si-Sn	123.2(3)
C(2)-C(5)	1.53(1)	C(11)-Si-Sn	129.4(2)
C(2)-C(4)	1.55(1)	C(1)-O-Sn	126.6(4)
C(6)-C(9)	1.49(1)	C(2)-N(1)-Si	127.5(4)
C(6)-C(7)	1.51(1)	C(2)-N(1)-Sn	126.1(4)
C(6)-C(8)	1.53(1)	Si-N(1)-Sn	90.9(3)
O-Sn-N(2)	98.9(2)	C(6)-N(2)-Si	128.6(5)
O-Sn-N(1)	98.4(2)	C(6)-N(2)-Sn	125.8(4)
N(2)-Sn-N(1)	69.5(3)	Si-N(2)-Sn	105.5(4)
O-Sn-Ni	114.03(1)	N(1)-C(2)-C(3)	110.6(7)
N(2)-Sn-Ni	145.0(1)	N(1)-C(2)-C(5)	108.0(6)
N(1)-Sn-Ni	114.5(2)	C(3)-C(2)-C(5)	107.8(7)
O-Sn-Si	100.7(1)	N(1)-C(2)-C(4)	109.9(6)
N(2)-Sn-Si	32.7(2)	C(3)-C(2)-C(4)	111.8(6)
N(1)-Sn-Si	36.82(1)	C(5)-C(2)-C(4)	108.6(8)
Ni-Sn-Si	139.62(4)	N(2)-C(6)-C(9)	114.4(8)
Sn-Ni-Sn#1	100.58(2)	N(2)-C(6)-C(7)	109.8(8)
Sn-Ni-Sn#2	129.27(4)	C(9)-C(6)-C(7)	110.0(1)
Sn#1-Ni-Sn#2	100.58(2)	N(2)-C(6)-C(8)	112.7(7)
Sn-Ni-Sn#3	100.58(2)	C(9)-C(6)-C(8)	102.8(9)
Sn#1-Ni-Sn#3	129.27(4)	C(7)-C(6)-C(8)	106.8(8)

Symmetry transformations used to generate equivalent atoms:

#1 y,-x+3/2,-z+1/2 #2 -x+3/2,-y+3/2,z #3 -y+3/2,x,-z+1/2

Table 4. Anisotropic displacement parameters ($Å^2 x\ 10^3$) for sh614. The anisotropic

displacement factor exponent takes the form: $-2\pi^2[\ h^2\ a^{*2}U^{11} + ...\ + 2\ h\ k\ a^*\ b^*\ U^{12}\ ]$

	U^{11}	U^{22}	U^{33}	U^{23}	U^{13}	U^{12}
Sn	29(1)	27(1)	35(1)	-4(1)	-1(1)	0(1)
Ni	25(1)	25(1)	30(2)	0	0	0
Si	36(1)	30(1)	48(2)	-8(1)	-4(1)	-2(1)
O	30(2)	44(3)	67(5)	-22(2)	-1(2)	10(2)
N(1)	37(3)	35(3)	17(6)	5(3)	-3(3)	0(2)
N(2)	46(3)	41(3)	15(7)	0(3)	-5(3)	-1(2)
C(2)	57(4)	45(4)	34(7)	15(4)	-13(4)	-3(3)
C(6)	41(4)	44(4)	77(11)	-4(5)	3(5)	0(3)

Compound 10

Table 1. Crystal data and structure refinement for sh2313.

Identification code	sh2313	
Empirical formula	C46 H110 N8 Ni O2 Si4 Sn4	
Formula weight	1453.25	
Temperature	103(2) K	
Wavelength	0.71073 Å	
Crystal system	Monoclinic	
Space group	I2	
Unit cell dimensions	a = 16.195(3) Å	α= 90°.
	b = 10.774(2) Å	β= 94.774(13)°.
	c = 18.863(4) Å	γ = 90°.
Volume	3279.6(11) $Å^3$	
Z	2	
Density (calculated)	1.472 Mg/m^3	
Absorption coefficient	1.895 mm^{-1}	
F(000)	1484	
Crystal size	0.2 x 0.3 x 0.42 mm^3	
Theta range for data collection	1.59 to 28.84°.	
Index ranges	-21<=h<=21, -14<=k<=14, -25<=l<=25	
Reflections collected	38281	
Independent reflections	8499 [R(int) = 0.0539]	
Completeness to theta = 28.84°	99.5 %	
Absorption correction	Empirical	
Refinement method	Full-matrix least-squares on F^2	
Data / restraints / parameters	8499 / 1 / 313	
Goodness-of-fit on F^2	1.282	
Final R indices [I>2sigma(I)]	R1 = 0.0444, wR2 = 0.1099	
R indices (all data)	R1 = 0.0490, wR2 = 0.1126	
Absolute structure parameter	0.23(3)	

Largest diff. peak and hole	3.988 and -2.717 e.Å^{-3}

Table 2. Atomic coordinates (x 10^4) and equivalent isotropic displacement parameters (Å^{2}x 10^3)
for sh2313. U(eq) is defined as one third of the trace of the orthogonalized U^{ij} tensor.

	x	y	z	U(eq)
Ni(1)	0	3161(1)	0	13(1)
Sn(1)	-61(1)	3015(1)	-1303(1)	13(1)
Sn(2)	-1509(1)	3319(1)	-240(1)	13(1)
Si(1)	546(1)	2566(2)	-2636(1)	19(1)
Si(2)	-3165(1)	3764(2)	32(1)	19(1)
O(1)	-1429(2)	3171(4)	-1400(2)	21(1)
N(1)	295(3)	3900(5)	-2186(3)	19(1)
N(2)	226(3)	1603(5)	-1973(3)	20(1)
N(3)	-2598(3)	2431(5)	-81(3)	20(1)
N(4)	-2339(3)	4726(5)	-125(3)	20(1)
C(1)	486(4)	5220(6)	-2277(4)	25(1)
C(2)	-55(5)	5985(6)	-1802(4)	33(2)
C(3)	1401(5)	5493(8)	-2058(5)	38(2)
C(4)	273(6)	5583(8)	-3050(4)	42(2)
C(5)	98(4)	261(6)	-1926(3)	21(1)
C(6)	176(5)	-143(7)	-1144(4)	32(2)
C(7)	761(5)	-419(7)	-2316(5)	39(2)
C(8)	-761(5)	-96(8)	-2257(5)	39(2)
C(9)	1678(4)	2437(7)	-2772(4)	31(2)
C(10)	-40(5)	2362(7)	-3530(4)	35(2)
C(11)	-2724(4)	1126(6)	103(4)	26(1)
C(12)	-2119(5)	317(7)	-287(5)	36(2)
C(13)	-2569(5)	907(8)	899(4)	39(2)

C(14)	-3634(5)	749(8)	-157(6)	46(2)
C(15)	-2276(4)	6071(6)	-232(4)	23(1)
C(16)	-1375(5)	6495(7)	-7(4)	31(2)
C(17)	-2868(5)	6733(7)	244(4)	38(2)
C(18)	-2487(5)	6422(7)	-1010(4)	37(2)
C(19)	-3535(4)	3934(7)	937(4)	31(2)
C(20)	-4091(4)	3928(8)	-628(4)	34(2)
C(21)	-2022(7)	3245(15)	-1973(5)	79(4)
C(22)	-2641(6)	2258(11)	-2009(5)	57(3)
C(23)	-1705(5)	3163(16)	-2833(6)	153(9)

Table 3. Bond lengths [Å] and angles [°] for sh2313.

Ni(1)-Sn(2)	2.4533(6)	Si(2)-C(20)	1.877(7)
Ni(1)-Sn(2)#1	2.4533(6)	O(1)-C(21)	1.387(8)
Ni(1)-Sn(1)#1	2.4571(6)	N(1)-C(1)	1.468(8)
Ni(1)-Sn(1)	2.4572(6)	N(2)-C(5)	1.464(8)
Sn(1)-N(1)	2.044(5)	N(3)-C(11)	1.466(8)
Sn(1)-N(2)	2.055(5)	N(4)-C(15)	1.467(8)
Sn(1)-O(1)	2.214(4)	C(1)-C(4)	1.52(1)
Sn(1)-Si(1)	2.816(2)	C(1)-C(3)	1.53(1)
Sn(1)-Sn(2)	3.2259(7)	C(1)-C(2)	1.54(1)
Sn(2)-N(4)	2.050(5)	C(5)-C(8)	1.52(1)
Sn(2)-N(3)	2.052(5)	C(5)-C(6)	1.53(1)
Sn(2)-O(1)	2.208(4)	C(5)-C(7)	1.537(9)
Sn(2)-Si(2)	2.814(2)	C(11)-C(13)	1.52(1)
Si(1)-N(1)	1.734(5)	C(11)-C(12)	1.54(1)
Si(1)-N(2)	1.737(5)	C(11)-C(14)	1.57(1)
Si(1)-C(10)	1.878(8)	C(15)-C(18)	1.53(1)
Si(1)-C(9)	1.878(7)	C(15)-C(17)	1.54(1)
Si(2)-N(3)	1.727(5)	C(15)-C(16)	1.56(1)
Si(2)-N(4)	1.737(6)	C(21)-C(22)	1.46(2)
Si(2)-C(19)	1.865(7)	C(21)-C(23)	1.74(2)

Sn(2)-Ni(1)-Sn(2)#1	172.06(5)	Ni(1)-Sn(2)-Sn(1)	48.99(2)
Sn(2)-Ni(1)-Sn(1)#1	98.38(2)	Si(2)-Sn(2)-Sn(1)	152.12(4)
Sn(2)#1-Ni(1)-Sn(1)#1	82.13(2)	N(1)-Si(1)-N(2)	92.7(2)
Sn(2)-Ni(1)-Sn(1)	82.14(2)	N(1)-Si(1)-C(10)	114.5(3)
Sn(2)#1-Ni(1)-Sn(1)	98.38(2)	N(2)-Si(1)-C(10)	114.7(3)
Sn(1)#1-Ni(1)-Sn(1)	172.63(5)	N(1)-Si(1)-C(9)	113.5(3)
N(1)-Sn(1)-N(2)	75.6(2)	N(2)-Si(1)-C(9)	114.0(3)
N(1)-Sn(1)-O(1)	104.2(2)	C(10)-Si(1)-C(9)	107.1(3)
N(2)-Sn(1)-O(1)	106.4(2)	N(1)-Si(1)-Sn(1)	46.3(2)
N(1)-Sn(1)-Ni(1)	142.6(2)	N(2)-Si(1)-Sn(1)	46.6(2)
N(2)-Sn(1)-Ni(1)	132.1(2)	C(10)-Si(1)-Sn(1)	129.4(3)
O(1)-Sn(1)-Ni(1)	92.0(1)	C(9)-Si(1)-Sn(1)	123.5(2)
N(1)-Sn(1)-Si(1)	37.8(2)	N(3)-Si(2)-N(4)	92.9(2)
N(2)-Sn(1)-Si(1)	37.9(2)	N(3)-Si(2)-C(19)	114.2(3)
O(1)-Sn(1)-Si(1)	111.1(1)	N(4)-Si(2)-C(19)	114.1(3)
Ni(1)-Sn(1)-Si(1)	156.37(4)	N(3)-Si(2)-C(20)	113.5(3)
N(1)-Sn(1)-Sn(2)	136.7(2)	N(4)-Si(2)-C(20)	114.5(3)
N(2)-Sn(1)-Sn(2)	132.1(2)	C(19)-Si(2)-C(20)	107.4(3)
O(1)-Sn(1)-Sn(2)	43.1(1)	N(3)-Si(2)-Sn(2)	46.5(2)
Ni(1)-Sn(1)-Sn(2)	48.88(1)	N(4)-Si(2)-Sn(2)	46.5(2)
Si(1)-Sn(1)-Sn(2)	153.89(4)	C(19)-Si(2)-Sn(2)	124.6(2)
N(4)-Sn(2)-N(3)	75.5(2)	C(20)-Si(2)-Sn(2)	128.0(3)
N(4)-Sn(2)-O(1)	104.5(2)	C(21)-O(1)-Sn(2)	132.4(6)
N(3)-Sn(2)-O(1)	103.5(2)	C(21)-O(1)-Sn(1)	133.7(6)
N(4)-Sn(2)-Ni(1)	133.1(2)	Sn(2)-O(1)-Sn(1)	93.7(2)
N(3)-Sn(2)-Ni(1)	142.8(2)	C(1)-N(1)-Si(1)	133.3(4)
O(1)-Sn(2)-Ni(1)	92.2(1)	C(1)-N(1)-Sn(1)	128.6(4)
N(4)-Sn(2)-Si(2)	37.9(2)	Si(1)-N(1)-Sn(1)	96.0(2)
N(3)-Sn(2)-Si(2)	37.6(2)	C(5)-N(2)-Si(1)	133.2(4)
O(1)-Sn(2)-Si(2)	109.2(1)	C(5)-N(2)-Sn(1)	130.8(4)
Ni(1)-Sn(2)-Si(2)	158.10(4)	Si(1)-N(2)-Sn(1)	95.5(2)
N(4)-Sn(2)-Sn(1)	131.1(2)	C(11)-N(3)-Si(2)	133.0(4)
N(3)-Sn(2)-Sn(1)	136.2(2)	C(11)-N(3)-Sn(2)	128.3(4)
O(1)-Sn(2)-Sn(1)	43.2(1)	Si(2)-N(3)-Sn(2)	95.9(2)

C(15)-N(4)-Si(2)	132.5(4)	N(3)-C(11)-C(13)	111.5(6)
C(15)-N(4)-Sn(2)	131.5(4)	N(3)-C(11)-C(12)	108.8(5)
Si(2)-N(4)-Sn(2)	95.6(2)	C(13)-C(11)-C(12)	108.9(6)
N(1)-C(1)-C(4)	109.1(6)	N(3)-C(11)-C(14)	108.7(6)
N(1)-C(1)-C(3)	111.2(6)	C(13)-C(11)-C(14)	110.1(6)
C(4)-C(1)-C(3)	110.3(6)	C(12)-C(11)-C(14)	108.8(7)
N(1)-C(1)-C(2)	108.3(5)	N(4)-C(15)-C(18)	111.4(6)
C(4)-C(1)-C(2)	108.9(6)	N(4)-C(15)-C(17)	108.9(6)
C(3)-C(1)-C(2)	108.9(6)	C(18)-C(15)-C(17)	110.2(6)
N(2)-C(5)-C(8)	110.7(6)	N(4)-C(15)-C(16)	109.1(5)
N(2)-C(5)-C(6)	109.7(5)	C(18)-C(15)-C(16)	108.6(6)
C(8)-C(5)-C(6)	108.8(6)	C(17)-C(15)-C(16)	108.6(6)
N(2)-C(5)-C(7)	109.5(5)	O(1)-C(21)-C(22)	115.0(9)
C(8)-C(5)-C(7)	109.5(6)	O(1)-C(21)-C(23)	119.0(9)
C(6)-C(5)-C(7)	108.7(6)	C(22)-C(21)-C(23)	100.0(9)

Symmetry transformations used to generate equivalent atoms:
#1 -x,y,-z

Table 4. Anisotropic displacement parameters ($Å^2 x\ 10^3$) for sh2313. The anisotropic displacement factor exponent takes the form: $-2p^2[\ h^2\ a^{*2}U^{11} + ... + 2\ h\ k\ a^*\ b^*\ U^{12}\ ]$

	U^{11}	U^{22}	U^{33}	U^{23}	U^{13}	U^{12}
Ni(1)	12(1)	15(1)	14(1)	0	5(1)	0
Sn(1)	12(1)	17(1)	11(1)	-4(1)	5(1)	-4(1)
Sn(2)	10(1)	15(1)	15(1)	3(1)	4(1)	3(1)
Si(1)	20(1)	22(1)	16(1)	-3(1)	6(1)	-1(1)
Si(2)	14(1)	25(1)	19(1)	3(1)	5(1)	2(1)
O(1)	21(2)	12(2)	33(2)	2(2)	19(2)	-6(2)
N(1)	23(3)	19(2)	17(2)	1(2)	9(2)	-3(2)

N(2)	25(3)	16(2)	20(3)	-2(2)	7(2)	0(2)
N(3)	14(2)	18(2)	30(3)	1(2)	6(2)	-2(2)
N(4)	21(3)	17(2)	23(3)	0(2)	6(2)	4(2)
C(1)	31(3)	20(3)	24(3)	3(2)	8(3)	-5(3)
C(2)	38(4)	19(3)	43(4)	0(3)	12(3)	0(3)
C(3)	32(4)	35(4)	49(5)	-12(3)	19(3)	-16(3)
C(4)	63(6)	35(4)	28(4)	15(3)	7(4)	-10(4)
C(5)	28(3)	14(3)	23(3)	-6(2)	10(3)	-3(2)
C(6)	49(4)	18(3)	30(4)	1(3)	10(3)	-5(3)
C(7)	48(5)	26(4)	48(5)	-9(3)	27(4)	4(3)
C(8)	35(4)	30(4)	50(5)	-5(3)	-7(4)	-7(3)
C(9)	26(3)	32(4)	36(4)	-1(3)	17(3)	3(3)
C(10)	49(5)	33(4)	23(3)	-6(3)	8(3)	3(3)
C(11)	21(3)	21(3)	36(4)	9(3)	6(3)	-4(2)
C(12)	42(4)	21(3)	46(5)	2(3)	10(4)	-2(3)
C(13)	38(4)	39(4)	41(4)	18(3)	10(3)	1(3)
C(14)	29(4)	34(4)	78(7)	5(4)	6(4)	-10(3)
C(15)	26(3)	18(3)	26(3)	0(2)	4(3)	1(2)
C(16)	33(4)	22(3)	38(4)	2(3)	1(3)	-4(3)
C(17)	50(5)	25(3)	43(4)	-3(3)	24(4)	11(3)
C(18)	44(4)	30(4)	36(4)	6(3)	-4(3)	4(3)
C(19)	28(3)	38(4)	29(3)	3(3)	7(3)	6(3)
C(20)	14(3)	44(4)	42(4)	5(3)	-4(3)	3(3)
C(21)	72(6)	105(9)	52(5)	34(7)	-48(5)	-42(7)
C(22)	41(5)	84(8)	44(5)	-10(5)	-6(4)	-10(5)
C(23)	48(5)	280(18)	114(9)	186(12)	-82(6)	-130(9)

Compound 11

Table 1. Crystal data and structure refinement for sh2261.

Identification code	sh2261	
Empirical formula	C28 H63 Ge2 Na Ni O7	
Formula weight	738.66	
Temperature	203(2) K	
Wavelength	0.71073 Å	
Crystal system	Monoclinic	
Space group	P2(1)	
Unit cell dimensions	a = 9.4667(7) Å	α= 90°.
	b = 15.6903(12) Å	β= 93.040(4)°.
	c = 25.7362(19) Å	γ = 90°.
Volume	3817.4(5) $Å^3$	
Z	4	
Density (calculated)	1.285 Mg/m^3	
Absorption coefficient	2.099 mm^{-1}	
F(000)	1560	
Crystal size	0.22 x 0.4 x 0.56 mm^3	
Theta range for data collection	0.79 to 24.18°.	
Index ranges	-10<=h<=10, -17<=k<=17, -29<=l<=29	
Reflections collected	33158	
Independent reflections	11966 [R(int) = 0.0736]	
Completeness to theta = 24.18°	99.2 %	
Absorption correction	Empirical	
Refinement method	Full-matrix least-squares on F^2	
Data / restraints / parameters	11966 / 1 / 745	
Goodness-of-fit on F^2	1.002	
Final R indices [I>2sigma(I)]	R1 = 0.0534, wR2 = 0.1139	
R indices (all data)	R1 = 0.0838, wR2 = 0.1270	
Absolute structure parameter	0.00	

Largest diff. peak and hole 1.968 and -0.514 e.Å^{-3}

Table 2. Atomic coordinates (x 10^4) and equivalent isotropic displacement parameters (Å^{2}x 10^3)
for sh2261. U(eq) is defined as one third of the trace of the orthogonalized U^{ij} tensor.

	x	y	z	U(eq)
Ge(1)	9259(1)	5679(1)	7207(1)	25(1)
Ge(2)	8314(1)	8168(1)	10357(1)	24(1)
Ge(3)	2737(1)	6689(1)	4793(1)	23(1)
Ge(4)	4899(1)	6706(1)	2708(1)	24(1)
Ni(1)	8882(1)	6486(1)	8272(1)	20(1)
Ni(2)	8715(1)	7450(1)	9271(1)	18(1)
Na(1)	2671(3)	7291(2)	3578(1)	27(1)
Na(2)	5012(3)	6118(2)	3926(1)	24(1)
O(1)	7989(5)	6419(3)	7575(2)	24(1)
O(2)	10053(5)	5679(3)	7925(2)	25(1)
O(3)	8028(5)	6407(3)	8938(2)	22(1)
O(4)	9552(5)	7540(3)	8598(2)	22(1)
O(5)	9621(5)	7484(3)	9975(2)	24(1)
O(6)	7514(5)	8225(4)	9641(2)	27(1)
O(7)	10386(6)	6552(4)	7011(2)	40(2)
O(8)	7166(6)	7267(4)	10504(2)	31(2)
O(9)	5131(5)	5703(3)	3105(2)	25(1)
O(10)	5106(5)	7300(3)	3360(2)	25(1)
O(11)	2937(5)	6778(4)	2776(2)	29(1)
O(12)	2571(5)	6095(4)	4137(2)	26(1)
O(13)	2518(6)	7710(4)	4410(2)	30(1)
O(14)	4707(5)	6612(4)	4729(2)	26(1)
C(1)	6602(8)	6689(6)	7368(3)	29(2)

C(2)	6787(9)	7277(7)	6901(4)	44(3)
C(3)	5884(10)	7152(6)	7801(4)	39(2)
C(4)	5759(8)	5878(6)	7201(4)	36(2)
C(5)	11206(9)	5131(5)	8102(3)	26(2)
C(6)	10710(10)	4197(6)	8045(4)	47(3)
C(7)	11513(9)	5341(6)	8678(3)	35(2)
C(8)	12500(10)	5293(7)	7801(4)	53(3)
C(9)	10397(8)	8197(6)	8370(3)	29(2)
C(10)	10686(10)	8876(6)	8779(4)	42(3)
C(11)	9542(10)	8555(6)	7907(4)	46(3)
C(12)	11743(9)	7792(6)	8192(4)	40(2)
C(13)	7169(8)	5739(5)	9168(3)	27(2)
C(14)	6980(10)	5026(6)	8763(4)	42(2)
C(15)	7981(9)	5417(6)	9654(3)	36(2)
C(16)	5775(9)	6120(6)	9304(4)	40(2)
C(17)	11002(8)	7239(6)	10171(3)	25(2)
C(18)	11734(8)	6766(6)	9742(3)	30(2)
C(19)	10853(9)	6634(7)	10635(3)	40(2)
C(20)	11838(9)	8026(6)	10341(4)	46(3)
C(21)	6447(8)	8823(5)	9468(3)	25(2)
C(22)	6134(14)	8697(11)	8900(4)	102(6)
C(23)	6971(16)	9678(8)	9561(8)	138(8)
C(24)	5145(12)	8701(10)	9759(5)	102(6)
C(25)	10923(9)	6646(10)	6498(4)	64(4)
C(26)	12192(13)	7132(8)	6542(5)	78(4)
C(27)	11681(13)	5717(8)	6335(4)	72(4)
C(28)	9907(12)	6630(11)	6087(4)	87(5)
C(29)	6587(8)	7117(6)	10995(3)	31(2)
C(30)	7712(9)	6880(6)	11410(3)	39(3)
C(31)	5519(9)	6417(6)	10924(4)	42(3)
C(32)	5847(9)	7956(6)	11190(4)	39(2)
C(33)	5902(9)	4952(6)	2916(4)	32(2)
C(34)	5904(11)	4321(6)	3346(4)	54(3)
C(35)	7421(10)	5231(7)	2801(4)	51(3)

C(36)	5112(11)	4628(7)	2431(4)	56(3)
C(37)	5939(9)	8078(6)	3396(3)	30(2)
C(38)	5938(9)	8399(5)	3944(3)	32(2)
C(39)	5210(11)	8761(6)	3025(4)	50(3)
C(40)	7433(9)	7915(7)	3237(4)	49(3)
C(41)	1898(8)	6851(5)	2347(3)	25(2)
C(42)	494(9)	7048(6)	2594(4)	44(3)
C(43)	1800(10)	5993(7)	2064(4)	47(3)
C(44)	2280(9)	7564(6)	1981(3)	35(2)
C(45)	1721(9)	5336(5)	4096(3)	30(2)
C(46)	1741(9)	5023(6)	3538(4)	36(2)
C(47)	2337(13)	4677(6)	4465(4)	60(3)
C(48)	190(9)	5533(7)	4212(4)	61(3)
C(49)	1715(9)	8420(5)	4594(3)	29(2)
C(50)	1693(10)	9094(6)	4165(4)	46(3)
C(51)	172(9)	8142(7)	4663(4)	55(3)
C(52)	2346(11)	8753(7)	5100(4)	57(3)
C(53)	5731(8)	6609(6)	5159(3)	29(2)
C(54)	7136(9)	6375(7)	4926(3)	43(3)
C(55)	5359(10)	5936(7)	5558(3)	42(3)
C(56)	5829(10)	7483(6)	5404(3)	42(2)

Table 3. Bond lengths [Å] and angles [°] for sh2261.

Ge(1)-O(7)	1.823(6)	Ge(3)-Na(1)	3.264(3)
Ge(1)-O(1)	1.952(5)	Ge(3)-Na(2)	3.306(3)
Ge(1)-O(2)	1.958(5)	Ge(4)-O(11)	1.878(5)
Ge(2)-O(8)	1.835(6)	Ge(4)-O(9)	1.883(6)
Ge(2)-O(5)	1.944(5)	Ge(4)-O(10)	1.920(5)
Ge(2)-O(6)	1.956(5)	Ge(4)-Na(2)	3.263(3)
Ge(3)-O(14)	1.885(5)	Ge(4)-Na(1)	3.286(3)
Ge(3)-O(13)	1.887(5)	Ni(1)-O(2)	1.933(5)
Ge(3)-O(12)	1.927(6)	Ni(1)-O(3)	1.937(5)

Ni(1)-O(1)	1.946(5)	C(5)-C(7)	1.53(1)
Ni(1)-O(4)	1.946(5)	C(5)-C(6)	1.54(1)
Ni(1)-Ni(2)	2.993(1)	C(9)-C(11)	1.51(1)
Ni(2)-O(3)	1.943(5)	C(9)-C(10)	1.51(1)
Ni(2)-O(4)	1.947(5)	C(9)-C(12)	1.52(1)
Ni(2)-O(6)	1.949(5)	C(13)-C(16)	1.51(1)
Ni(2)-O(5)	1.965(5)	C(13)-C(15)	1.52(1)
Na(1)-O(11)	2.241(6)	C(13)-C(14)	1.53(1)
Na(1)-O(13)	2.253(6)	C(17)-C(20)	1.52(1)
Na(1)-O(12)	2.370(6)	C(17)-C(18)	1.53(1)
Na(1)-O(10)	2.401(6)	C(17)-C(19)	1.53(1)
Na(1)-Na(2)	2.982(4)	C(21)-C(23)	1.44(1)
Na(2)-O(9)	2.219(6)	C(21)-C(22)	1.49(1)
Na(2)-O(14)	2.242(6)	C(21)-C(24)	1.49(1)
Na(2)-O(10)	2.363(6)	C(25)-C(28)	1.39(1)
Na(2)-O(12)	2.402(6)	C(25)-C(26)	1.42(1)
O(1)-C(1)	1.453(9)	C(25)-C(27)	1.68(2)
O(2)-C(5)	1.444(9)	C(29)-C(31)	1.50(1)
O(3)-C(13)	1.470(9)	C(29)-C(30)	1.52(1)
O(4)-C(9)	1.45(1)	C(29)-C(32)	1.59(1)
O(5)-C(17)	1.428(9)	C(33)-C(34)	1.49(1)
O(6)-C(21)	1.432(9)	C(33)-C(36)	1.51(1)
O(7)-C(25)	1.45(1)	C(33)-C(35)	1.55(1)
O(8)-C(29)	1.42(1)	C(37)-C(38)	1.50(1)
O(9)-C(33)	1.48(1)	C(37)-C(40)	1.51(1)
O(10)-C(37)	1.45(1)	C(37)-C(39)	1.57(1)
O(11)-C(41)	1.442(9)	C(41)-C(44)	1.52(1)
O(12)-C(45)	1.44(1)	C(41)-C(43)	1.53(1)
O(13)-C(49)	1.442(9)	C(41)-C(42)	1.53(1)
O(14)-C(53)	1.432(8)	C(45)-C(47)	1.50(1)
C(1)-C(3)	1.52(1)	C(45)-C(46)	1.52(1)
C(1)-C(2)	1.53(1)	C(45)-C(48)	1.53(1)
C(1)-C(4)	1.55(1)	C(49)-C(52)	1.50(1)
C(5)-C(8)	1.51(1)	C(49)-C(50)	1.53(1)

C(49)-C(51)	1.54(1)	O(3)-Ni(1)-O(4)	79.3(2)
C(53)-C(56)	1.51(1)	O(1)-Ni(1)-O(4)	124.0(2)
C(53)-C(55)	1.53(1)	O(2)-Ni(1)-Ni(2)	141.8(2)
C(53)-C(54)	1.53(1)	O(3)-Ni(1)-Ni(2)	39.6(1)
O(7)-Ge(1)-O(1)	94.2(3)	O(1)-Ni(1)-Ni(2)	141.2(2)
O(7)-Ge(1)-O(2)	93.4(2)	O(4)-Ni(1)-Ni(2)	39.8(2)
O(1)-Ge(1)-O(2)	76.0(2)	O(3)-Ni(2)-O(4)	79.2(2)
O(8)-Ge(2)-O(5)	94.5(2)	O(3)-Ni(2)-O(6)	123.5(2)
O(8)-Ge(2)-O(6)	91.4(2)	O(4)-Ni(2)-O(6)	131.7(2)
O(5)-Ge(2)-O(6)	76.9(2)	O(3)-Ni(2)-O(5)	123.3(2)
O(14)-Ge(3)-O(13)	95.2(2)	O(4)-Ni(2)-O(5)	129.8(2)
O(14)-Ge(3)-O(12)	85.9(2)	O(6)-Ni(2)-O(5)	76.6(2)
O(13)-Ge(3)-O(12)	87.2(3)	O(3)-Ni(2)-Ni(1)	39.4(2)
O(14)-Ge(3)-Na(1)	84.5(2)	O(4)-Ni(2)-Ni(1)	39.7(2)
O(13)-Ge(3)-Na(1)	42.1(2)	O(6)-Ni(2)-Ni(1)	142.6(2)
O(12)-Ge(3)-Na(1)	45.9(2)	O(5)-Ni(2)-Ni(1)	140.0(2)
O(14)-Ge(3)-Na(2)	40.7(2)	O(11)-Na(1)-O(13)	175.0(2)
O(13)-Ge(3)-Na(2)	86.3(2)	O(11)-Na(1)-O(12)	106.6(2)
O(12)-Ge(3)-Na(2)	45.9(2)	O(13)-Na(1)-O(12)	69.3(2)
Na(1)-Ge(3)-Na(2)	53.98(7)	O(11)-Na(1)-O(10)	68.4(2)
O(11)-Ge(4)-O(9)	95.0(2)	O(13)-Na(1)-O(10)	109.3(2)
O(11)-Ge(4)-O(10)	86.9(2)	O(12)-Na(1)-O(10)	102.5(2)
O(9)-Ge(4)-O(10)	85.9(2)	O(11)-Na(1)-Na(2)	86.4(2)
O(11)-Ge(4)-Na(2)	84.8(2)	O(13)-Na(1)-Na(2)	88.8(2)
O(9)-Ge(4)-Na(2)	41.0(2)	O(12)-Na(1)-Na(2)	51.8(2)
O(10)-Ge(4)-Na(2)	45.7(2)	O(10)-Na(1)-Na(2)	50.7(2)
O(11)-Ge(4)-Na(1)	41.1(2)	O(11)-Na(1)-Ge(3)	141.3(2)
O(9)-Ge(4)-Na(1)	85.7(2)	O(13)-Na(1)-Ge(3)	34.2(1)
O(10)-Ge(4)-Na(1)	46.3(2)	O(12)-Na(1)-Ge(3)	35.7(1)
Na(2)-Ge(4)-Na(1)	54.17(7)	O(10)-Na(1)-Ge(3)	104.8(2)
O(2)-Ni(1)-O(3)	130.0(2)	Na(2)-Na(1)-Ge(3)	63.73(8)
O(2)-Ni(1)-O(1)	76.7(2)	O(11)-Na(1)-Ge(4)	33.4(1)
O(3)-Ni(1)-O(1)	129.1(2)	O(13)-Na(1)-Ge(4)	143.6(2)
O(2)-Ni(1)-O(4)	125.1(2)	O(12)-Na(1)-Ge(4)	103.9(2)

O(10)-Na(1)-Ge(4)	35.3(1)	C(9)-O(4)-Ni(2)	132.2(5)
Na(2)-Na(1)-Ge(4)	62.53(8)	Ni(1)-O(4)-Ni(2)	100.5(2)
Ge(3)-Na(1)-Ge(4)	126.3(1)	C(17)-O(5)-Ge(2)	124.5(5)
O(9)-Na(2)-O(14)	174.4(2)	C(17)-O(5)-Ni(2)	131.6(5)
O(9)-Na(2)-O(10)	68.8(2)	Ge(2)-O(5)-Ni(2)	102.9(2)
O(14)-Na(2)-O(10)	108.0(2)	C(21)-O(6)-Ni(2)	132.6(5)
O(9)-Na(2)-O(12)	108.0(2)	C(21)-O(6)-Ge(2)	123.7(5)
O(14)-Na(2)-O(12)	67.9(2)	Ni(2)-O(6)-Ge(2)	103.1(2)
O(10)-Na(2)-O(12)	102.7(2)	C(25)-O(7)-Ge(1)	124.6(7)
O(9)-Na(2)-Na(1)	88.3(2)	C(29)-O(8)-Ge(2)	124.8(5)
O(14)-Na(2)-Na(1)	86.2(2)	C(33)-O(9)-Ge(4)	122.1(5)
O(10)-Na(2)-Na(1)	51.8(2)	C(33)-O(9)-Na(2)	126.6(5)
O(12)-Na(2)-Na(1)	50.8(2)	Ge(4)-O(9)-Na(2)	105.1(3)
O(9)-Na(2)-Ge(4)	33.9(2)	C(37)-O(10)-Ge(4)	119.6(5)
O(14)-Na(2)-Ge(4)	142.1(2)	C(37)-O(10)-Na(2)	131.1(5)
O(10)-Na(2)-Ge(4)	35.6(1)	Ge(4)-O(10)-Na(2)	98.7(2)
O(12)-Na(2)-Ge(4)	103.8(2)	C(37)-O(10)-Na(1)	121.0(5)
Na(1)-Na(2)-Ge(4)	63.31(8)	Ge(4)-O(10)-Na(1)	98.4(2)
O(9)-Na(2)-Ge(3)	142.2(2)	Na(2)-O(10)-Na(1)	77.5(2)
O(14)-Na(2)-Ge(3)	33.2(1)	C(41)-O(11)-Ge(4)	124.8(5)
O(10)-Na(2)-Ge(3)	104.5(2)	C(41)-O(11)-Na(1)	124.8(4)
O(12)-Na(2)-Ge(3)	35.2(1)	Ge(4)-O(11)-Na(1)	105.5(2)
Na(1)-Na(2)-Ge(3)	62.29(8)	C(45)-O(12)-Ge(3)	118.9(5)
Ge(4)-Na(2)-Ge(3)	125.59(9)	C(45)-O(12)-Na(1)	130.7(5)
C(1)-O(1)-Ni(1)	131.4(4)	Ge(3)-O(12)-Na(1)	98.3(2)
C(1)-O(1)-Ge(1)	124.3(4)	C(45)-O(12)-Na(2)	122.5(5)
Ni(1)-O(1)-Ge(1)	103.4(2)	Ge(3)-O(12)-Na(2)	99.0(2)
C(5)-O(2)-Ni(1)	133.3(5)	Na(1)-O(12)-Na(2)	77.3(2)
C(5)-O(2)-Ge(1)	123.0(4)	C(49)-O(13)-Ge(3)	122.0(5)
Ni(1)-O(2)-Ge(1)	103.6(2)	C(49)-O(13)-Na(1)	126.8(5)
C(13)-O(3)-Ni(1)	132.0(4)	Ge(3)-O(13)-Na(1)	103.7(3)
C(13)-O(3)-Ni(2)	127.0(5)	C(53)-O(14)-Ge(3)	124.5(4)
Ni(1)-O(3)-Ni(2)	101.0(2)	C(53)-O(14)-Na(2)	126.6(4)
C(9)-O(4)-Ni(1)	127.2(5)	Ge(3)-O(14)-Na(2)	106.2(2)

O(1)-C(1)-C(3)	107.5(6)	C(23)-C(21)-C(24)	108.8(1)
O(1)-C(1)-C(2)	108.9(6)	C(22)-C(21)-C(24)	110.5(1)
C(3)-C(1)-C(2)	111.2(8)	C(28)-C(25)-C(26)	128.2(1)
O(1)-C(1)-C(4)	107.7(7)	C(28)-C(25)-O(7)	115.4(8)
C(3)-C(1)-C(4)	110.7(7)	C(26)-C(25)-O(7)	108.5(9)
C(2)-C(1)-C(4)	110.8(7)	C(28)-C(25)-C(27)	94.7(1)
O(2)-C(5)-C(8)	111.0(7)	C(26)-C(25)-C(27)	96.6(1)
O(2)-C(5)-C(7)	106.2(6)	O(7)-C(25)-C(27)	108.2(1)
C(8)-C(5)-C(7)	110.1(8)	O(8)-C(29)-C(31)	107.6(7)
O(2)-C(5)-C(6)	108.3(7)	O(8)-C(29)-C(30)	112.2(7)
C(8)-C(5)-C(6)	111.3(7)	C(31)-C(29)-C(30)	110.6(8)
C(7)-C(5)-C(6)	109.7(7)	O(8)-C(29)-C(32)	109.9(7)
O(4)-C(9)-C(11)	107.4(7)	C(31)-C(29)-C(32)	109.9(7)
O(4)-C(9)-C(10)	107.7(7)	C(30)-C(29)-C(32)	106.6(7)
C(11)-C(9)-C(10)	110.9(8)	O(9)-C(33)-C(34)	105.4(7)
O(4)-C(9)-C(12)	108.4(7)	O(9)-C(33)-C(36)	107.9(7)
C(11)-C(9)-C(12)	109.9(8)	C(34)-C(33)-C(36)	111.9(9)
C(10)-C(9)-C(12)	112.4(7)	O(9)-C(33)-C(35)	108.5(7)
O(3)-C(13)-C(16)	108.7(7)	C(34)-C(33)-C(35)	111.5(8)
O(3)-C(13)-C(15)	107.7(6)	C(36)-C(33)-C(35)	111.2(8)
C(16)-C(13)-C(15)	110.6(7)	O(10)-C(37)-C(38)	108.3(6)
O(3)-C(13)-C(14)	107.0(6)	O(10)-C(37)-C(40)	110.7(7)
C(16)-C(13)-C(14)	112.0(7)	C(38)-C(37)-C(40)	110.9(7)
C(15)-C(13)-C(14)	110.6(8)	O(10)-C(37)-C(39)	108.3(7)
O(5)-C(17)-C(20)	109.6(7)	C(38)-C(37)-C(39)	108.7(8)
O(5)-C(17)-C(18)	108.6(6)	C(40)-C(37)-C(39)	109.8(8)
C(20)-C(17)-C(18)	110.8(7)	O(11)-C(41)-C(44)	110.9(7)
O(5)-C(17)-C(19)	108.6(6)	O(11)-C(41)-C(43)	108.4(7)
C(20)-C(17)-C(19)	110.2(7)	C(44)-C(41)-C(43)	111.2(7)
C(18)-C(17)-C(19)	109.0(7)	O(11)-C(41)-C(42)	105.7(7)
O(6)-C(21)-C(23)	109.1(8)	C(44)-C(41)-C(42)	110.4(7)
O(6)-C(21)-C(22)	108.6(7)	C(43)-C(41)-C(42)	110.0(7)
C(23)-C(21)-C(22)	109.4(1)	O(12)-C(45)-C(47)	109.1(7)
O(6)-C(21)-C(24)	110.4(8)	O(12)-C(45)-C(46)	107.5(6)

C(47)-C(45)-C(46)	110.6(8)	C(52)-C(49)-C(51)	109.5(8)
O(12)-C(45)-C(48)	110.6(7)	C(50)-C(49)-C(51)	107.6(8)
C(47)-C(45)-C(48)	111.0(8)	O(14)-C(53)-C(56)	110.2(7)
C(46)-C(45)-C(48)	108.1(7)	O(14)-C(53)-C(55)	110.5(7)
O(13)-C(49)-C(52)	111.2(7)	C(56)-C(53)-C(55)	111.0(7)
O(13)-C(49)-C(50)	106.5(6)	O(14)-C(53)-C(54)	105.4(6)
C(52)-C(49)-C(50)	112.1(8)	C(56)-C(53)-C(54)	110.3(8)
O(13)-C(49)-C(51)	109.8(7)	C(55)-C(53)-C(54)	109.4(7)

Symmetry transformations used to generate equivalent atoms:

Table 4. Anisotropic displacement parameters ($Å^2 x\ 10^3$) for sh2261. The anisotropic displacement factor exponent takes the form: $-2p^2[\ h^2\ a^{*2}U^{11} + ...\ + 2\ h\ k\ a^*\ b^*\ U^{12}\ ]$

	U^{11}	U^{22}	U^{33}	U^{23}	U^{13}	U^{12}
Ge(1)	24(1)	31(1)	20(1)	-5(1)	4(1)	-2(1)
Ge(2)	25(1)	23(1)	24(1)	-6(1)	2(1)	0(1)
Ge(3)	24(1)	25(1)	21(1)	5(1)	7(1)	4(1)
Ge(4)	23(1)	29(1)	20(1)	1(1)	6(1)	4(1)
Ni(1)	23(1)	19(1)	18(1)	-2(1)	3(1)	-1(1)
Ni(2)	20(1)	17(1)	18(1)	-1(1)	3(1)	0(1)
Na(1)	26(2)	31(2)	23(2)	1(2)	6(1)	3(1)
Na(2)	27(2)	25(2)	21(2)	1(1)	8(1)	3(1)
O(1)	24(3)	24(3)	23(3)	1(3)	3(2)	0(2)
O(2)	29(3)	21(3)	26(3)	-7(3)	5(2)	2(3)
O(3)	28(3)	11(3)	26(3)	-5(2)	2(2)	-12(2)
O(4)	33(3)	11(3)	23(3)	3(2)	1(2)	-2(2)
O(5)	25(3)	27(3)	21(3)	-7(3)	1(2)	0(3)
O(6)	30(3)	27(3)	25(3)	-1(3)	9(2)	11(3)
O(7)	38(3)	54(5)	26(3)	6(3)	-5(3)	-16(3)

O(8)	37(3)	40(4)	17(3)	-8(3)	5(3)	-9(3)
O(9)	33(3)	20(3)	23(3)	-5(3)	14(2)	2(3)
O(10)	28(3)	21(3)	26(3)	-2(3)	3(2)	-2(2)
O(11)	17(3)	47(4)	22(3)	2(3)	2(2)	0(3)
O(12)	20(3)	27(3)	32(4)	2(3)	8(2)	-5(2)
O(13)	38(3)	22(3)	29(4)	8(3)	4(3)	4(3)
O(14)	21(3)	42(4)	14(3)	2(3)	-2(2)	3(3)
C(1)	17(4)	43(5)	26(5)	-6(5)	-5(3)	3(4)
C(2)	34(5)	67(8)	32(6)	7(5)	-3(4)	14(5)
C(3)	42(6)	39(6)	37(6)	2(5)	0(4)	0(5)
C(4)	18(5)	46(6)	43(6)	1(5)	-1(4)	-1(4)
C(5)	35(5)	16(5)	27(5)	-3(4)	2(4)	9(4)
C(6)	52(6)	28(6)	60(7)	-1(5)	-18(5)	3(5)
C(7)	31(5)	37(6)	35(6)	1(4)	-5(4)	5(4)
C(8)	35(6)	56(7)	71(8)	7(6)	23(5)	15(5)
C(9)	20(5)	27(5)	39(6)	2(5)	7(4)	-5(4)
C(10)	53(6)	29(6)	47(7)	-6(5)	16(5)	-15(5)
C(11)	51(6)	41(6)	47(7)	23(5)	15(5)	-8(5)
C(12)	32(5)	36(6)	52(7)	16(5)	6(4)	-12(4)
C(13)	24(5)	25(5)	31(5)	0(4)	4(4)	-11(4)
C(14)	50(6)	26(6)	48(7)	3(5)	0(5)	-16(5)
C(15)	46(6)	28(6)	34(6)	15(4)	5(4)	-10(4)
C(16)	39(6)	48(6)	35(6)	5(5)	26(4)	-15(4)
C(17)	16(4)	35(5)	24(5)	-5(4)	-5(3)	7(4)
C(18)	26(5)	37(5)	28(5)	-1(5)	5(4)	10(4)
C(19)	34(5)	58(7)	29(5)	0(6)	2(4)	12(5)
C(20)	29(5)	53(7)	54(7)	-12(5)	-10(4)	4(5)
C(21)	24(5)	15(5)	36(6)	-2(4)	4(4)	4(3)
C(22)	90(10)	171(16)	44(8)	25(9)	-1(7)	96(10)
C(23)	123(13)	33(8)	250(20)	-21(10)	-100(14)	37(8)
C(24)	47(8)	146(15)	115(13)	74(11)	24(8)	50(8)
C(25)	29(5)	133(11)	31(6)	22(8)	3(4)	-41(7)
C(26)	77(9)	104(11)	55(8)	-2(7)	15(7)	-63(8)
C(27)	106(10)	57(8)	54(8)	-11(7)	4(7)	9(8)

C(28)	66(8)	173(14)	22(6)	20(8)	2(5)	-68(9)
C(29)	19(5)	51(6)	24(5)	11(4)	9(4)	-5(4)
C(30)	26(5)	66(8)	26(5)	12(5)	3(4)	2(4)
C(31)	42(6)	51(7)	33(6)	-5(5)	8(4)	-17(5)
C(32)	34(5)	45(7)	40(6)	-8(5)	12(4)	6(4)
C(33)	39(5)	19(5)	39(6)	-5(4)	3(4)	14(4)
C(34)	60(7)	33(6)	70(8)	-8(6)	8(6)	18(5)
C(35)	42(6)	56(7)	59(8)	2(6)	16(5)	21(5)
C(36)	69(7)	44(7)	54(8)	-31(6)	-2(6)	11(5)
C(37)	36(5)	23(5)	30(5)	3(4)	1(4)	-1(4)
C(38)	39(5)	23(5)	34(6)	-11(4)	9(4)	-14(4)
C(39)	59(7)	37(7)	53(7)	16(5)	-8(5)	-16(5)
C(40)	28(5)	58(7)	64(8)	-13(6)	13(5)	-4(5)
C(41)	25(5)	32(6)	18(5)	-3(4)	-3(3)	3(4)
C(42)	28(5)	55(7)	48(7)	13(5)	0(4)	2(4)
C(43)	52(6)	58(7)	30(6)	1(5)	-5(5)	4(5)
C(44)	28(5)	51(6)	26(5)	11(5)	2(4)	10(4)
C(45)	29(5)	27(5)	37(6)	9(4)	11(4)	1(4)
C(46)	38(5)	25(5)	44(6)	-8(5)	-6(4)	-10(4)
C(47)	106(10)	21(6)	55(8)	4(5)	3(7)	-18(6)
C(48)	33(6)	76(9)	76(9)	-35(7)	30(5)	-16(5)
C(49)	42(5)	18(5)	28(5)	-1(4)	16(4)	6(4)
C(50)	59(7)	25(6)	55(7)	7(5)	13(5)	17(5)
C(51)	30(6)	64(8)	73(8)	7(6)	13(5)	19(5)
C(52)	74(8)	52(8)	45(7)	-24(6)	3(6)	15(6)
C(53)	29(4)	39(6)	20(5)	4(5)	-3(3)	6(4)
C(54)	26(5)	74(8)	28(5)	4(5)	-4(4)	0(5)
C(55)	41(6)	58(7)	26(5)	5(5)	-4(4)	12(5)
C(56)	54(6)	44(6)	25(5)	-5(5)	-12(4)	3(5)